ABSTRACT

Title of Dissertation:	ZOOPLANKTON, LARVAL FISH, AND INVESTIGATIVE METHODS IN THE CHOPTANK RIVER
	Catherine L. Fitzgerald, Doctor of Philosophy, 2025
Dissertation directed by:	Professor Jamie Pierson Marine, Estuarine, and Environmental Science

Accurate predictions of recruitment are vital for stock assessments and fisheries management, however recruitment of fish larvae to adult populations is highly variable and the driving forces underlying it are complex. Physical environmental conditions such as temperature, salinity, and dissolved oxygen indirectly impact fish recruitment by altering the distribution of zooplankton prey. Studies of zooplankton and larval fish ecology have previously relied mainly on taxonomic identification via morphological features. This method comes with drawbacks that tissue metabarcoding of the gene cytochrome oxidase 1 (CO1) shows promise in overcoming. This dissertation will investigate the use of a powerful genetic tool, use it to characterize larval fish diets, and from that knowledge examine abundances of important prey species and zooplankton community structure across three decades. The study location is the Choptank River, a tidal tributary of the Chesapeake Bay and an important spawning and nursery ground for striped bass

(*Morone saxatilis*), white perch (*Morone americana*), and bay anchovy (*Anchoa mitchilli*). The Choptank has a long history of monitoring for physical conditions, zooplankton, and juvenile fish, making it an ideal study site.

Metabarcoding of the CO1 gene shows promise in detecting rare organisms and expanding our knowledge of zooplankton diversity; it is hindered by a lack of standardization and metrics directly comparable to counts. CO1 metabarcoding also shows promise as a tool to investigate larval fish diets, revealing a higher diversity of prey and ontogenetic changes in feeding strategy. The abundance of zooplankton taxa found to be important as prey for larval fish was significantly different in the study years (2018-2019) from that expected based on the decadal trends revealed in the Chesapeake Bay Program zooplankton monitoring data (1984-2002). This makes a strong case for continued monitoring to capture changes in zooplankton abundance and determine factors driving the observed patterns. Changes in the abundance of key zooplankton prey, associated with changes in environmental conditions, may contribute to observed declines in recruitment of larval fish.

ZOOPLANKTON, LARVAL FISH, AND INVESTIGATIVE METHODS IN THE CHOPTANK RIVER

by

Catherine L. Fitzgerald

Dissertation submitted to the Faculty of the Graduate School of the
University of Maryland, College Park, in partial fulfillment
of the requirements for the degree of
Doctor of Philosophy
2025

Advisory Committee:
Professor Jamie Pierson, Chair
Dr. Louis Plough
Professor Mike Roman
Professor Ann Bucklin
Professor Ryan Woodland
Dr. Dave Richardson

Dedication

To you, dear reader: stay curious.

Acknowledgements

First and foremost, I would like to thank my advisor Jamie Pierson, without whom none of this would be possible. He is an outstanding scientist with a near-encyclopedic knowledge of everything to do with zooplankton (and many other topics besides!). As a mentor, he continually demonstrated an enormous capacity for empathy, adaptability to situations as they arose, optimism tempered by an equal measure of pragmatism, and a sense of humor which always left me feeling confident and motivated after our meetings. I am incredibly fortunate to have worked with him. Thanks also to my co-advisor, Louis Plough, who continued working with me through arguably some of the most challenging aspects of this research while he was taking the next steps in his own career. And of course I would like to thank my other committee members Ann Bucklin, Mike Roman, Ryan Woodland, and Dave Richardson, and my Dean's representative Alexandra Bely, who have provided excellent advice and guidance on both my dissertation and on my career pathway. Thanks in particular to Ann for introducing me to exciting international opportunities in marine science!

I am enormously grateful to everyone at Horn Point Laboratory, many across UMCES, and my colleagues around the word for all of their support throughout this process. From directly assisting with labwork and presentation design to general advice, conversation, and community events, the support of this geographically distant but close-knit community was a vital part of my research process. I would need an entire chapter just to list the names of everyone who has helped shape my graduate experience so in lieu of that, know that your kindness and generosity have made this an experience I will treasure for the rest of my life.

I would also like to thank all the organizations which have graciously funded this research through fellowships and grants: Maryland Sea Grant, Horn Point, UMCES, the National

Science Foundation, the Ratcliffe Environmental Entrepreneurs Fellowship, the Izaak Walton League of America Midshore Chapter, the Ryan Saba Memorial Fellowship, the Mid-Shore Fishing Club, and the Debbie Morrin-Norlund Memorial Fellowship.

Finally, I would like to thank my family and friends. You have always been so supportive and interested throughout my graduate career, even when I disappeared into my research and wasn't good at explaining exactly what it was I was so occupied doing. Thank you for encouraging me onward when I had doubts, and for also telling me it's ok to take breaks (and for so often being the best part of those breaks!).

An enormous and heartfelt thank you to everyone who has helped make this possible; I am eternally grateful for your support and understanding.

Table of Contents

Dedication ii
Acknowledgements iii
Table of Contents v
List of Tables viii
Chapter 2 viii
Chapter 3 ix
Chapter 4 xi
Supplemental tables xii
List of Figures xiv
Chapter 2 xiv
Chapter 3 xv
Chapter 4 xx
Supplemental figures xxiii
Chapter 1: Introduction 1
References 6
Chapter 2: Comparing metabarcoding and morphological identification for use in zooplankton monitoring and ecological studies 11
Introduction 11
Methods 14
Fieldwork 14
Sample Processing 15
Additional Environmental Data 17
Data Analysis 18
Results 24
Error estimation 24
Number of organisms processed by each method 26
Taxonomic resolution 27
Species richness and community composition 27
Diversity patterns 28
Abundance 29
Time 34
Cost 35
Discussion 35
Number of organisms processed by each method 35
Taxonomic resolution 36
Species richness and community composition 37
Diversity patterns 38
Abundance 41
Time and cost 46
Conclusions 46
Acknowledgements 47
References 48
Tables 54

Figures 61
Chapter 3: Characterization of the zooplankton diets of larval striped bass (*Morone saxatilis*), white perch (*Morone americana*), and bay anchovy (*Anchoa mitchilli*) 72
Introduction 72
Methods 75
Fieldwork 75
Sample processing 76
Data analysis 81
Results 81
Blocking primer efficacy 82
Feeding incidence 83
Off-target detections 84
Fish length classes 85
Length vs. gape width 85
Diets 86
Diet ontogeny 88
Spatiotemporal distribution of larvae 90
Analysis of potential feeding selectivity 90
Discussion 96
Blocking primer efficacy 96
Feeding incidence 97
Off-target detections 99
Length vs. gape width 100
Diets 101
Diet ontogeny 105
Spatiotemporal distribution of larvae 107
Analysis of potential feeding selectivity 109
Conclusions 113
Acknowledgements 114
References 114
Tables 123
Figures 131
Chapter 4: Zooplankton ecology in the Choptank River: then and now 154
Introduction 154
Methods 157
2018-2019 data 157
Historical and additional environmental data 157
Data analysis 158
Results 161
Zooplankton abundance over time 161
Rank-dominance over time 164
Drivers of abundance 165
Community structure over time 167
Discussion 169
Zooplankton abundance over time 169
Drivers of abundance 170

Community structure over time 172
Conclusions 177
Acknowledgements 178
References 178
Tables 183
Figures 189
Chapter 5: Conclusion 206
References 209
Appendices: Supplemental figures 210
List of combined references 224

List of Tables

Chapter 2

Table 2.1: Tables showing species richness and results of Jaccard testing on all samples in common between A) morphological and inclusive data sets, and B) morphological and exclusive data sets. 54

Table 2.2: Table showing species richness and results of Jaccard testing on all samples in common between A) morphological and inclusive data sets, and B) morphological and exclusive data sets, split into size fractions. 64 indicates microzooplankton (64-200 μm), 200 indicates mesozooplankton (> 200 μm). 54

Table 2.3: Table showing significant results of linear regression models on Shannon diversity scores for biomass (mg) and concentration (individuals/m^3) data vs. continuous environmental parameters for each data set. 55

Table 2.4: Spearman correlation coefficients showing the relationship between total zooplankton abundance per sample in morphological vs. inclusive and morphological vs. exclusive data with each abundance measure. * indicates significant results. 55

Table 2.5: Linear regression results showing the relationship between total zooplankton abundance per sample in morphological vs. inclusive or morphological vs. exclusive data with each abundance measure. * indicates significant results, x indicates the model failed a homoscedasticity test. 56

Table 2.6: Table showing significant results of linear regression models on total zooplankton abundance measures vs. continuous environmental parameters for each data set. 57

Table 2.7: Table showing significant results of linear regression models on *Acartia tonsa* abundance measures vs. continuous environmental parameters for each data set. 58

Table 2.8: Table showing significant results of linear regression models on Bivalvia abundance measures vs. continuous environmental parameters for each data set. 59
Table 2.9: Table showing significant results of linear regression models on Annelida abundance measures vs. continuous environmental parameters for each data set. 60

Chapter 3

Table 3.1: Table showing primer sequences used in the fish gut amplifications. Bold areas in the blocking primer sequences indicate areas of overlap with the universal primer. Blocking primer sequences are an exact pairing for each fish species; this greater affinity and concentration compared to the universal primer ensure more complete annealing to the larval fish DNA. A C3 spacer at the 3' end of each blocking primer prevents elongation. Each zooplankton sequence has five or more mismatches with the blocking primer sequence, ensuring low annealing efficacy with the blocking primer and allowing the universal primer to bind instead. 123
Table 3.2: Table with the total sequence reads detected in each of two groups: "empty" gut larvae (larvae with no PCR amplification or inhibition) and their peers (same species, same length class, normal amplification). "Empty gut" indicates the total reads detected for each larva with an empty gut (n= 1 *M. americana*, n= 1 *A. mitchilli*), "Full gut 95% CI" indicates the 95% confidence interval range of the total reads detected for peers (n= 24 *M. americana*, n= 7 *A. mitchilli*). Values which fall outside confidence intervals and are therefore significantly different are in bold. 123
Table 3.3: Table comparing the percentages of total sequence reads divided into classifications between groups of fish larvae. Larvae are divided into two groups: "Empty gut" indicates the reads detected for each larva with an empty gut (larvae with no PCR amplification or inhibition;

n= 1 *M. americana*, n= 1 *A. mitchilli*), "Full gut 95% CI" indicates the 95% confidence interval range of the reads detected for peers (same species, same length class, normal amplification; n= 24 *M. americana*, n= 7 *A. mitchilli*). Sequence reads for each group are divided into classifications: predator (sequence reads matching the larval fish species being tested), unknown (sequence reads with no taxonomic identification), and other (sequence reads with a taxonomic identification other than that of the larva being tested). Values which fall outside confidence intervals and are therefore significantly different are in bold. 124

Table 3.4: Table showing linear regression and Spearman's correlation results for average relative abundance of prey taxa vs. size classes (TL, mm) of larvae for all three fish species. Significant relationships only. 125

Table 3.5: Table showing only the taxa with a significant difference between their relative abundance in the water column vs *M. americana* gut contents. "*" denotes which abundance is significantly higher than the other. 126

Table 3.6: Table showing only the taxa without a significant difference in their relative abundance in the water column vs *M. americana* gut contents. 127

Table 3.7: Table showing only the taxa with a significant difference in their relative abundance in the water column vs *M. saxatilis* gut contents. "*" denotes which abundance is significantly higher than the other. 128

Table 3.8: Table showing only the taxa without a significant difference in their abundance in the water column vs *M. saxatilis* gut contents. 129

Table 3.9: Table showing only the taxa with a significant difference in their relative abundance in the water column vs *A. mitchilli* gut contents. "*" denotes which abundance is significantly higher than the other. 130

Table 3.10: Table showing only the taxa without a significant difference in their abundance in the water column vs *A. mitchilli* gut contents. 130

Chapter 4

Table 4.1: Linear regression results on CBP historic data. Log10 transformed total zooplankton abundance vs. time; significant results only. Results shown for the entire Choptank River, and with the river separated into salinity zones (1= 0-4 psu, 2= 8-10 psu, and 3= 10-14 psu). Slope units are individuals/m³/year. 183

Table 4.2: Linear regression and Spearman-rank correlation results on CBP historic data. 12-month running means of select taxa abundance vs. time; significant results only. Results shown for the entire Choptank River, and with the river separated into salinity zones (1= 0-4 psu, 2= 8-10 psu, and 3= 10-14 psu). Slope units are individuals/m³/year. 184

Table 4.3: Table of simple linear regression results for concentration (individuals/m³) of select taxa vs environmental parameters. Significant results only. 185

Table 4.4: Table of multiple linear regression results for concentration (individuals/m³) of select taxa vs environmental parameters. Significant results only. 186

Table 4.5: Results of SIMPER pairwise testing on mesozooplankton community data from three year-pairs: 1984-1985, 2000-2001, and 2018-2019. Only significant pairwise test results are shown. Average indicates the average contribution of each taxon to the dissimilarity, * indicates taxa with significant permutation p values. 187

Table 4.6: Results of SIMPER pairwise testing on microzooplankton community data from three year-pairs: 1984-1985, 2000-2001, and 2018-2019. Only significant pairwise test results are

shown. Average indicates the average contribution of each taxon to the dissimilarity, * indicates taxa with significant permutation p values. 188

Supplemental tables

Table S2.2: Table of forward barcode and primer sequences for metabarcoding of zooplankton samples. 211

Table S2.3: Table of reverse barcode and primer sequences for metabarcoding of zooplankton samples. 212

Table S2.4: Table of taxa identified in the morphological data set, listed in alphabetical order by phylum. Full taxonomic identification is written out in the format: phylum,class,order,family,genus,species. Where a taxonomic level was unknown, “Unknown” is substituted. 213

Table S2.5: Table of taxa identified in the inclusive data set, listed in alphabetical order by phylum. Full taxonomic identification is written out in the format: phylum,class,order,family,genus,species. Where a taxonomic level was unknown, “Unknown” is substituted. Continued on next two pages. 214

Table S2.6: Table of taxa identified in the exclusive data set, listed in alphabetical order by phylum. Full taxonomic identification is written out in the format: phylum,class,order,family,genus,species. Where a taxonomic level was unknown, “Unknown” is substituted. Continued on next page. 217

Table S3.2: Table describing which taxa were classified as hard-bodied and soft-bodied prey. Bryozoans were classified as soft bodied on the assumption that fish larvae were consuming free-

swimming bryozoan larvae (generally without shells) rather than feeding from benthic bryozoan colonies (generally with encrusting type shells). 221
Table S4.1: List of taxa and life stages excluded from each data set, and why they were omitted. 223

List of Figures

Chapter 2

Fig. 2.1: Map of the Choptank River with station locations. 61

Fig. 2.2: Boxplot depicting the number of organisms processed from each sample across all shared samples for morphological and metabarcoding data sets. Y-axis log10 transformed. 62

Fig. 2.3: Boxplot depicting the number of organisms processed in each sample across all shared samples for morphological and metabarcoding data sets, shown by size fraction. Whole, unfractionated samples excluded. Y-axis log10 transformed. 63

Fig. 2.4: Taxonomic resolution in each of the three data sets. Percent positive identifications are the number of identifications made to each taxonomic level, across the entirety of each data set. E.g. almost 100% of organisms in each data set were identified at the Phylum level, but the morphological data set had about 79% of organisms identified at the Phylum level and at the Class level; 21% of organisms were classified as "Unknown" at Class level and below. 64

Fig. 2.5: Boxplots showing results of ANOVA testing on per-sample Shannon scores, grouped by data set and plotted for biomass (mg) and concentration (individuals/m^3) measures. Post-hoc pairwise Wilcoxon testing results reflected in a, b, c groupings; members of different groups are significantly different. 65

Fig. 2.6: Heatmap showing only significant results of Spearman correlation testing on per-sample Shannon scores vs environmental parameters for each data set. X-axis shows diversity scores calculated from concentration (individuals/m^3) and biomass (mg) for each data set. 66

Fig. 2.7: Paired scatter plots of morphological vs. inclusive (left, dark purple) and morphological vs exclusive (right, light purple) data across five abundance measures for the total zooplankton in each sample. 67

Fig. 2.8: Heatmap showing only significant results of Spearman correlation testing on total zooplankton abundance vs environmental parameters for all three data sets. 68

Fig. 2.9: Scatter plots showing log10+1 transformed abundance (ind./m²) data for *Acartia tonsa*, plotted for each combination of data set. 69

Fig. 2.10: Scatter plots showing log10+1 transformed abundance (ind./m²) data for Bivalvia, plotted for each combination of data set. 69

Fig. 2.11: Scatter plots showing log10+1 transformed abundance (ind./m²) data for Annelida, plotted for each combination of data set. 69

Fig. 2.12: Bar graph showing the processing time per sample for each method. Active processing time: time a worker spends actively handling the sample; passive processing time- likely paid: time a worker spends not actively handling the sample (e.g. waiting for a centrifuge cycle to complete), but still engaged with the task; passive processing time- likely unpaid; time a worker spends not actively handling the sample, and not engaged in the task (e.g. an overnight incubation). 70

Fig. 2.13: Bar graph showing the cost per sample for each method in USD. 71

Chapter 3

Fig. 3.1: Scatter plots demonstrating the species specificity of the blocking primers for A) *Morone americana* and B) *Morone saxatilis*. X-axes list the combinations of amplified DNA and primers in each test, y-axes list the Cq fluorescence value detected by qPCR. Error bars show standard error of Cq values; most testing did not produce enough error to appear beyond the margins of the points themselves. 131

Fig. 3.2: Scatter plots demonstrating the coblocking capacity of the blocking primers for A) *Morone americana*, B) *Morone saxatilis*, C) *Anchoa mitchilli*. X-axes list the combinations of amplified DNA and primers in each test, y-axes list the Cq fluorescence value detected by qPCR. Error bars show standard error of Cq values; most testing did not produce enough error to appear beyond the margins of the points themselves. 132

Fig. 3.3: Bar graph showing the total number of sequence reads for each fish species. Colors indicate reads from the same fish species (red: presumably predator reads), and all other species (blue: presumably prey and off-target reads). The data used were post-bioinformatics and filtering but included all taxa regardless of whether they were discarded from downstream analyses as off-target..... 133

Fig. 3.4: Gel showing no amplification of 4 uL DNA from an *A. mitchilli* larva (lanes labeled 386), but successful amplification of 4 uL fish larva DNA plus 2 uL zooplankton DNA to test for inhibition (lane labeled 386i). 134

Fig. 3.5: Bar graph showing the total number of sequence reads for the fish with "empty" guts and their peers. Colors indicate reads from the same fish species (red: presumably predator reads), reads without a taxonomic identification (grey), and all other taxonomic identifications (blue: prey and off-target reads). The data used were post-processing but included all taxa, regardless of whether they were discarded from downstream analyses. Each empty fish is a single individual; peers are fish of the same species and length class as the "empty" larvae (3-3.99 mm TL for both species) which amplified and were sequenced as expected. 135

Fig. 3.6: Heatmaps showing retained and discarded taxa detected in *Morone americana* larval gut samples. Each column pair has percent presence on the left (number of larvae with these taxa in their gut, expressed as a percent), average relative abundance (average proportion of gut

contents made up by each taxon) on the right. Column pairs are sorted vertically by decreasing average relative abundance; taxa having <0.01 average relative abundance greyed out..... 136
Fig. 3.7: Heatmaps showing retained and discarded taxa detected in *Morone saxatilis* larval gut samples. Each column pair has percent presence on the left (number of larvae with these taxa in their gut, expressed as a percent), average relative abundance (average proportion of gut contents made up by each taxon) on the right. Column pairs are sorted vertically by decreasing average relative abundance; taxa having <0.01 average relative abundance greyed out. 137
Fig. 3.8: Heatmaps showing retained and discarded taxa detected in *Anchoa mitchilli* larval gut samples. Each column pair has percent presence on the left (number of larvae with these taxa in their gut, expressed as a percent), average relative abundance (average proportion of gut contents made up by each taxon) on the right. Column pairs are sorted vertically by decreasing average relative abundance; taxa having <0.01 average relative abundance greyed out. 138
Fig. 3.9: Histograms depicting the frequency of body lengths (total length, in mm) recorded for each larval fish species..... 139
Fig. 3.10: Total length (mm) vs. gape width (mm) for each species of fish larvae measured in this study, with regression lines where possible (not possible for *A. mitchilli*)..... 140
Fig. 3.11: Relative abundance (percent of sequences from all sequences retained for each species of fish larvae surveyed) of each major prey group associated with each species of fish larvae. Data square root transformed for ease of viewing (note that the relative abundances no longer sum to 1 due to transformation). 141
Fig. 3.12: Amundsen plots of *M. americana*, *M. saxatilis*, and *A. mitchilli* overall diets. 142
Fig. 3.13: Composite graph showing the average relative abundance of the top five prey taxa in *M. americana* larvae stomachs. Each sub-plot represents a larval size-class in increasing order

(e.g. Size bin 3 represents larvae with TL 3-3.99 mm long, Size bin 4 represents larvae with TL 4-4.99 mm long, etc.). The colors identifying prey are consistent identifiers across all such graphs. 143
Fig. 3.14: Composite graph showing the average relative abundance of the top five prey taxa in *M. saxatilis* larvae stomachs. Each sub-plot represents a larval size-class in increasing order (e.g. Size bin 3 represents larvae with TL 3-3.99 mm long, Size bin 4 represents larvae with TL 4-4.99 mm long, etc.). The colors identifying prey are consistent identifiers across all such graphs. .. 144
Fig. 3.15: Composite graph showing the average relative abundance of the top five prey taxa in *A. mitchilli* larvae stomachs. Each sub-plot represents a larval size-class in increasing order (e.g. Size bin 3 represents larvae with TL 3-3.99 mm long, Size bin 4 represents larvae with TL 4-4.99 mm long, etc.). The colors identifying prey are consistent identifiers across all such graphs. .. 145
Fig. 3.16: Line graph showing the average relative abundance (square root transformed) of all of the prey taxa in the diets of *M. americana*, vs. the size classes of *M. americana* larvae surveyed (note that the relative abundances will no longer sum to 1 due to transformation). All prey displayed here had a significant ($p < 0.05$ for linear regression and/or Spearman's correlation) increase or decrease across the size classes of larvae; prey taxa without a trend across size classes are not shown. 146
Fig. 3.17: Line graph showing the average relative abundance (square root transformed) of all of the prey taxa in the diets of *M. saxatilis*, vs. the size classes of *M. saxatilis* larvae surveyed (note that the relative abundances will no longer sum to 1 due to transformation). All prey displayed here showed a significant ($p < 0.05$ for linear regression and/or Spearman's correlation) increase or decrease across the size classes of larvae; prey taxa without a trend across size classes are not shown. 147

Fig. 3.18: Line graph showing the average relative abundance (square root transformed) of all of the prey taxa in the diets of *A. mitchilli*, vs. the size classes of *A. mitchilli* larvae surveyed (note that the relative abundances will no longer sum to 1 due to transformation). All prey displayed here showed a significant ($p < 0.05$ for linear regression and/or Spearman's correlation) increase or decrease across the size classes of larvae; prey taxa without a trend across size classes are not shown. 148

Fig. 3.19: Amundsen plots of *M. americana* by size class, showing the number of larvae in each class (n= xx). 149

Fig. 3.20: Amundsen plots of *M. saxatilis* by size class, showing the number of larvae in each class (n= xx). 150

Fig. 3.21: Amundsen plots of *A. mitchilli* by size class, showing the number of larvae in each class (n= xx). 151

Fig. 3.22: Diagram showing spatiotemporal distribution of moronid (*M. americana, M. saxatilis*) size classes. Study year 2018 in the left column, 2019 in the right column. Within each year column, data for *M. saxatilis* is shown on the left in purple, *M. americana* on the right in pink. The central blue column shows the arrangement of stations from the headwaters of the Choptank (top, dark blue) to the mouth (bottom, light blue). Shades of blue indicate salinity zones: darkest blue= zone 1 (0-4 psu), mid blue= zone 2 (8-10 psu), light blue= zone 3 (10-14 psu). Each histogram lists the total number of larvae (n= xx) from the respective fish species sampled at that site and time, and shows the number of larvae within each 1 mm TL size bin. 152

Fig. 3.23: Diagram showing spatiotemporal distribution of *A. mitchilli* size classes (data in blue histograms). Lefthand blue column shows the arrangement of stations from the headwaters of the Choptank (top, dark blue) to the mouth (bottom, light blue). Shades of blue indicate salinity

zones: darkest blue= zone 1 (0-4 psu), mid blue= zone 2 (8-10 psu), light blue= zone 3 (10-14 psu). Each histogram lists the total number of larvae (n= xx) from the respective fish species sampled at that site and time, and shows the number of larvae within each 1 mm TL size bin. 153

Chapter 4

Fig. 4.1: Map of the Choptank River with all sites used to examine zooplankton ecology. Hues of blue represent salinity zones: dark blue= fresh (zone 1, 0-4 psu), blue= median (zone 2, 6-10 psu), and light blue= salt (zone 3, 10-14 psu). 189

Fig. 4.2: Abundance (individuals/m³) of select mesozooplankton taxa over time. *Bosmina* scaled for clarity; dedicated y-axis on the right. 190

Fig. 4.4: 12-month running mean of abundance (individuals/m³) (solid lines) and raw abundance (dotted lines) of select mesozooplankton taxa over time. *Bosmina* scaled for clarity; dedicated y-axis on the right. 191

Fig. 4.5: 12-month running mean of abundance (individuals/m³) (solid lines) and raw abundance (dotted lines) of select microzooplankton taxa over time. 191

Fig. 4.6: 12-month running mean of abundance (individuals/m³) (solid lines) and raw abundance (dotted lines) of select mesozooplankton taxa over time in salinity zones zone 1 (0-4 psu), 2 (8-10 psu), and 3 (10-14 psu). 192

Fig. 4.7: 12-month running mean of abundance (individuals/m³) (solid lines) and raw abundance (dotted lines) of select microzooplankton taxa over time in salinity zones zone 1 (0-4 psu), 2 (8-10 psu), and 3 (10-14 psu). 193

Fig. 4.8: *A. tonsa* mesozooplankton (adults) abundance over time as predicted by CBP data vs SG study measures. Abundance shown is the 12-month running mean of CBP data (1984-2001)

and SG data (2018-2019). The black line is a linear regression generated by modeling CBP *A. tonsa* running mean abundance over time, extrapolated across the full timeline. The shaded area represents 95% confidence intervals of CBP data as measured (1984-2001), and as predicted based on the regression (2018-2019). 194
Fig. 4.9: *E. carolleeae* mesozooplankton (adults) abundance over time as predicted by CBP data vs SG study measures. Abundance shown is the 12-month running mean of CBP data (1984-2001) and SG data (2018-2019). The black line is a linear regression generated by modeling CBP *E. carolleeae* running mean abundance over time, extrapolated across the full timeline. The shaded area represents 95% confidence intervals of CBP data as measured (1984-2001), and as predicted based on the regression (2018-2019). 195
Fig. 4.10: *Bosmina* mesozooplankton abundance over time as predicted by CBP data vs SG study measures. Abundance shown is the 12-month running mean of CBP data (1984-2001) and SG data (2018-2019). The black line is a linear regression generated by modeling CBP *Bosmina* running mean abundance over time, extrapolated across the full timeline. The shaded area represents 95% confidence intervals of CBP data as measured (1984-2001), and as predicted based on the regression (2018-2019). 196
Fig. 4.11: *Diaphanosoma* mesozooplankton abundance over time as predicted by CBP data vs SG study measures. Abundance shown is the 12-month running mean of CBP data (1984-2001) and SG data (2018-2019). The black line is a linear regression generated by modeling CBP *Diaphanosoma* running mean abundance over time, extrapolated across the full timeline. The shaded area represents 95% confidence intervals of CBP data as measured (1984-2001), and as predicted based on the regression (2018-2019). 197

Fig 4.12: *A. tonsa* microzooplankton (nauplii) abundance over time as predicted by CBP data vs our study measures. Abundance shown is the 12-month running mean of CBP data (1984-2002) and our study (2018-2019). The black line is a linear regression generated by modeling CBP *A. tonsa* running mean abundance over time, extrapolated across the full timeline. The shaded area represents 95% confidence intervals of CBP data as measured (1984-2002), and as predicted based on the regression (2018-2019). 198
Fig. 4.13: *Synchaeta* microzooplankton abundance over time as predicted by CBP data vs our study measures. Abundance shown is the 12-month running mean of CBP data (1984-2002) and our study (2018-2019; here appearing as a single point due to limited data). The black line is a linear regression generated by modeling CBP *Synchaeta* running mean abundance over time, extrapolated across the full timeline. The shaded area represents 95% confidence intervals of CBP data as measured (1984-2002), and as predicted based on the regression (2018-2019; here appearing as a line due to limited data). 199
Fig. 4.14: Relative abundance of select mesozooplankton taxa at four time points and three salinity zones. The beginning (1984-1985) and end (2000-2001) of the CBP zooplankton monitoring data, two years which were most like SG study years in terms of environmental conditions (1999-2000), and SG study years (2018-2019). Fresh (zone 1, 0-4 psu), Median (zone 2, 6-10 psu), and Salt (zone 3, 10-14 psu). 200
Fig. 4.15: Relative abundance of select microzooplankton taxa at four time points and three salinity zones. The beginning (1984-1985) and end (2000-2001) of the CBP zooplankton monitoring data, two years which were most like SG study years in terms of environmental conditions (1999-2000), and SG study years (2018-2019). Fresh (zone 1, 0-4 psu), Median (zone 2, 6-10 psu), and Salt (zone 3, 10-14 psu). 201

Fig. 4.16: Rank-dominance of select mesozooplankton taxa at four time points and three salinity zones. The beginning (1984-1985) and end (2000-2001) of the CBP zooplankton monitoring data, two years which were most like our study years in terms of environmental conditions (1999-2000), and our study years (2018-2019). Fresh (zone 1, 0-4 psu), Median (zone 2, 6-10 psu), and Salt (zone 3, 10-14 psu)..... 202
Fig. 4.17: Rank dominance of select microzooplankton taxa at four time points and three salinity zones. The beginning (1984-1985) and end (2000-2001) of the CBP zooplankton monitoring data, two years which were most like our study years in terms of environmental conditions (1999-2000), and our study years (2018-2019). Fresh (zone 1, 0-4 psu), Median (zone 2, 6-10 psu), and Salt (zone 3, 10-14 psu)..... 203
Fig. 4.18: NMDS on mesozooplankton community data from three year-pairs: 1984-1985, 2000-2001, and 2018-2019. Significant differences between 1984-1985 and 2018-2019, and 2000-2001 and 2018-2019 only. 204
Fig. 4.19: NMDS on microzooplankton community data from three year-pairs: 1984-1985, 2000-2001, and 2018-2019. All year-pairs were significantly different from one another. 205

Supplemental figures

Fig. S2.1: Modified steps of Qiagen DNeasy blood and tissue DNA extraction kit. All other steps were followed as written in the kit protocol. 210
Fig S2.7: Grids of line graphs showing water column profiles from surface to within 1m of the bottom for select hydrographic data at all stations sampled in 2018 (left grid) and 2019 (right grid). Each row represents data from a station, in order top to bottom from the headwaters to the

mouth of the Choptank River. Each column represents Dissolved oxygen (mg/L, red), Salinity (ppt, blue), or Temperature (°C, green). Line textures indicate the month of sampling..... 219
Fig S3.1: Modified steps of Omega EZNA tissue DNA extraction kit. All other steps were followed as written in the kit protocol. 220
Fig S3.3: Photographs of empty (left column) and full (right column) larvae of *Morone americana*. 222
Fig S3.4: Photographs of empty (left column) and full (right column) larvae of *Anchoa mitchilli*. 222

Chapter 1: Introduction

The Chesapeake Bay is home to the iconic striped bass (*Morone saxatilis*), white perch (*Morone americana*), and bay anchovy (*Anchoa mitchilli*) fisheries. These fisheries are vital to the local economy. In 2016 the striped bass commercial fishery was worth $7.7 billion and recreational fishery was worth $103 million; in 2014 the white perch fishery was estimated at $1.04 million (Butowski and Morin 2015, Southwick Associates 2019). Although the exact dollar value of the bay anchovy fishery has not been calculated, they are a vital food source for the moronid fisheries, making up 60-90% of the diets of striped bass and white perch in the Chesapeake Bay (Hartman and Brandt 1995). In addition to their economic value, these fish species are ecologically valuable as high trophic level consumers (striped bass) and forage fishes (white perch, bay anchovy) (Setzler et al. 1980, Hartman and Brandt 1995, Pagenkopp Lohan et al. 2023).

The Choptank River is a tributary of the Chesapeake Bay and an important spawning and nursery ground for striped bass, white perch, and bay anchovy (Smithsonian Environmental Research Center 2005, Dorfman et al. 2016). It is a tidal, fresh-to-brackish river and as such it is subject to change on a variety of temporal and spatial scales which results in a dynamic, complex estuary (Kimmel et al. 2009, Favier and Winkler 2014). The sensitive larvae of these key fish species are exposed to a physically and biologically complex environment at the time in their life cycle when they are most vulnerable. As weather patterns become increasingly variable in a changing climate, changes in the typical seasonal hydrology of the Choptank River will likely affect the distribution of the organisms living in the ecosystem (Kimmel et al. 2009).

The Choptank has a long history of monitoring for physical conditions, zooplankton, and juvenile fish, making it an ideal study site to investigate the use of a powerful genetic tool, use it to characterize larval fish diets, and from that knowledge examine abundances of important prey species and zooplankton community structure across three decades.

The striped bass, white perch, and bay anchovy fisheries rely on strong recruitment to maintain their populations under pressure from fishing. Accurate predictions of recruitment are vital for stock assessment and fisheries management, as recruitment determines the size of the contribution to the adult population. However, recruitment of fish larvae to adult populations is highly variable from year to year and within years during successive fish spawns (Shideler and Houde 2014a). Physical environmental conditions such as temperature, salinity, and dissolved oxygen exert large, direct, bottom-up effects on the growth and survival of fish larvae to recruitment, and are relatively easy to monitor and incorporate into fisheries models. However, the remaining variability in larval fish survival and recruitment may be due to their trophic relationships with zooplankton, as mediated by the environmental conditions of the estuary (Houde 1987, 2008, Siddon et al. 2013, Hare 2014).

Larval striped bass, bay anchovy, and white perch feed on zooplankton prey (Sheridan 1978, Limburg et al. 1997). The timing of zooplankton blooms in the Choptank River is largely determined by seasonal temperature and spatiotemporal alignment with phytoplankton blooms (Kimmel et al. 2009), but the species composition of an assemblage is determined by the physical tolerances and phenology of each zooplankton species. The river has a salinity gradient from the headwaters (fresh) to the mouth (mesohaline); the position of this gradient and associated zooplankton taxa changes daily with the tidal cycle, monthly with seasonal inputs of

fresh water, and likely on interannual and decadal timescales with the North Atlantic Oscillation (Kimmel and Roman 2004, Nye et al. 2014).

Zooplankton taxa vary in their biochemical content, life histories, growth rates, and sizes, and so offer differing suitability as prey for larval fish. The zooplankton which larval fish favor as prey provide calorie- and nutrient-dense meals that encourage a faster growth rate, allowing larvae to quickly outgrow size-selective predation and recruit to the adult population (Harding 1999, Beaugrand et al. 2003, Martino and Houde 2010, Robert et al. 2014). Recruitment of striped bass larvae to adult populations is generally high during periods of high freshwater discharge in the Chesapeake due in part to improved spatiotemporal overlap with their zooplankton prey (Kimmel et al. 2009, Martino and Houde 2010).

Studies of zooplankton biodiversity and larval fish diet have previously relied mainly on taxonomic identification via morphological features. This is the standard method for each field, but it comes with drawbacks, including heavy reliance on broad, high-resolution morphological knowledge, inability to account for cryptic species, and inability to identify partially- or fully-digested remains. The relatively new genetic method of tissue metabarcoding shows promise in overcoming these obstacles, so long as the correct genetic marker and database are chosen for the study (Bucklin et al. 2019, Schroeder et al. 2020, Questel et al. 2021). Other studies have compared morphological and metabarcoding methods for investigating zooplankton biodiversity and fish diets, however larvae of first-feeding size (2-20 mm TL) remain understudied (Lindeque et al. 2013, Bucklin et al. 2019, Pan et al. 2021, Pagenkopp Lohan et al. 2023). Based on these prior studies, metabarcoding may both widen and specify our knowledge of larval fish diets, giving us more accurate insight into their feeding ecology and which zooplankton prey species

are the most important to monitor. Equipped with the knowledge from dietary studies, we can examine patterns of key zooplankton taxa abundance from historical data sets to understand how the prey field has changed over time in response to environmental variables, and what effect that has had, and may yet have on larval fish survival to recruitment.

Significance

This study expands our knowledge of larval fish diets by revealing both a greater taxonomic breadth and resolution of prey than was previously determined by traditional methods. This knowledge is important for maintaining the accuracy of recruitment predictions, particularly in a changing climate as fish species face unprecedented pressures. By focusing on the understudied larval life stages (2-20 mm TL) of three fish with different life history patterns (bay anchovy, striped bass, white perch), this study helps close a critical gap in our understanding of fish feeding ecology.

Despite its clear importance, the Chesapeake Bay Program's zooplankton monitoring program was shuttered in 2002, and zooplankton were removed from the Chesapeake Bay Water Quality model as of 2019 due in part to a lack of monitoring efforts to keep the model parameters up to date and relevant (Cerco and Noel 2019). This study solidifies the utility of long-term zooplankton monitoring and provides valuable information on the changing zooplankton ecology of the Choptank River – a river deemed a Habitat Focus Area by NOAA for its role as a critical nursery habitat for vulnerable life stages of key fish species.

In addition to furthering our scientific knowledge, this study is also useful for scientists, managers, and the local community. It assesses the use of a genetic tool in both zooplankton ecology and fish dietary studies, and clarifies which method is best suited for the various operational scales and questions posed by scientists and managers. This will help pave the way for future zooplankton monitoring and trophic studies conducted here and in other critical locations with other important fish species. Managers and the local community will gain greater insight into the mechanisms that can cause variability in fish populations that are not only economically and ecologically valuable, but also important cultural symbols of the waterman lifestyle and the Chesapeake Bay. Better knowledge of the ecology of the Choptank River and these key species will help balance our economic, conservation, and social goals.

Structure

As previously stated, the goal of this dissertation is to investigate the use of a powerful genetic tool, use it to characterize larval fish diets, and from that knowledge examine abundances of important prey species and zooplankton community structure across three decades. To that end, this dissertation is divided into three data chapters and a conclusion.

In Chapter 2, I examine the efficacy of CO1 metabarcoding for studying zooplankton ecology. I derived three data sets from paired zooplankton samples taken from the Choptank River in 2018-2019: one set from morphological identification and two from CO1 metabarcoding (one strictly filtered and one broadly filtered). Common ecological analyses were run on each data set and the results were compared to determine the differences in conclusions produced. Processing time and cost of each method were compared to determine how each method balances efficiency with information gained.

In Chapter 3, I use the set of zooplankton samples processed with CO1 metabarcoding and fish larvae samples taken as part of the same 2018-2019 study to describe the feeding ecology of three fish species: striped bass (*Morone saxatilis*), white perch (*Morone americana*), and bay anchovy (*Anchoa mitchilli*). Overall diets and diet ontogeny were described, and comparisons of diet to the zooplankton community clarified predator-prey relationships.

In Chapter 4, I use the set of the zooplankton samples processed with morphological identification to examine patterns between modern and historical zooplankton communities in the Choptank River. Historical zooplankton communities were derived from the Chesapeake Bay Program's zooplankton monitoring data (1984-2002). Zooplankton species identified as key prey for larval fishes were examined for predicted vs. actual abundances, three time points were examined for changes in the overall community structure, and potential environmental drivers of observed changes were investigated across all time points.

References

Beaugrand, G., K. M. Brander, J. Alistair Lindley, S. Souissi, and P. C. Reid. 2003. Plankton effect on cod recruitment in the North Sea. Nature 426:661–664.

Bucklin, A., H. D. Yeh, J. M. Questel, D. E. Richardson, B. Reese, N. J. Copley, and P. H. Wiebe. 2019. Time-series metabarcoding analysis of zooplankton diversity of the NW Atlantic continental shelf. ICES Journal of Marine Science 76:1162–1176.

Butowski, N., and R. Morin. 2015. 2014 Fishery Managemant Plans. Report to the Legislative Committees, Maryland Department of Natural Resources Fisheries Service, Annapolis, MD.

Cerco, C. F., and M. R. Noel. 2019. 2017 Chesapeake Bay Water Quality and Sediment Transport Model:580.

Dorfman, D., A. Mabrouk, L. Bauer, C. Clement, D. M. Nelson, and L. Claflin. 2016. Choptank Ecological Assessment: Digital Atlas- Baseline Status Report.

Favier, J.-B., and G. Winkler. 2014. Coexistence, distribution patterns and habitat utilization of the sibling species complex Eurytemora affinis in the St Lawrence estuarine transition zone. Journal of Plankton Research 36:1247–1261.

Harding, J. 1999. Selective feeding behavior of larval naked gobies Gobiosoma bosc and blennies Chasmodes bosquianus and Hypsoblennius hentzi:preferences for bivalve veligers. Marine Ecology Progress Series 179:145–153.

Hare, J. A. 2014. The future of fisheries oceanography lies in the pursuit of multiple hypotheses. ICES Journal of Marine Science 71:2343–2356.

Hartman, K. J., and S. B. Brandt. 1995. Predatory demand and impact of striped bass, bluefish, and weakfish in the Chesapeake Bay: applications of bioenergetics models. Canadian Journal of Fisheries and Aquatic Sciences 52:1667–1687.

Houde, E. D. 1987. Fish Early Life Dynamics and Recruitment Variability. American Fisheries Society Symposium 2:17–29.

Houde, E. D. 2008. Emerging from Hjort's Shadow. Journal of Northwest Atlantic Fishery Science 41:53–70.

Kimmel, D. G., W. D. Miller, L. W. Harding, E. D. Houde, and M. R. Roman. 2009. Estuarine Ecosystem Response Captured Using a Synoptic Climatology. Estuaries and Coasts 32:403–409.

Kimmel, D., and M. Roman. 2004. Long-term trends in mesozooplankton abundance in Chesapeake Bay, USA: influence of freshwater input. Marine Ecology Progress Series 267:71–83.

Limburg, K. E., M. L. Pace, D. Fischer, and K. K. Arend. 1997. Consumption, Selectivity, and Use of Zooplankton by Larval Striped Bass and White Perch in a Seasonally Pulsed Estuary:15.

Lindeque, P. K., H. E. Parry, R. A. Harmer, P. J. Somerfield, and A. Atkinson. 2013. Next Generation Sequencing Reveals the Hidden Diversity of Zooplankton Assemblages. PLoS ONE 8:e81327.

Martino, E. J., and E. D. Houde. 2010. Recruitment of striped bass in Chesapeake Bay: Spatial and temporal environmental variability and availability of zooplankton prey. Marine Ecology Progress Series 409:213–228.

Nye, J. A., M. R. Baker, R. Bell, A. Kenny, K. H. Kilbourne, K. D. Friedland, E. Martino, M. M. Stachura, K. S. Van Houtan, and R. Wood. 2014. Ecosystem effects of the Atlantic Multidecadal Oscillation. Journal of Marine Systems 133:103–116.

Pagenkopp Lohan, K. M., R. Aguilar, R. DiMaria, K. Heggie, T. D. Tuckey, M. C. Fabrizio, and M. B. Ogburn. 2023. Juvenile Striped Bass consume diverse prey in Chesapeake Bay tributaries. Marine and Coastal Fisheries 15:e210259.

Pan, W., C. Qin, T. Zuo, G. Yu, W. Zhu, H. Ma, and S. Xi. 2021. Is Metagenomic Analysis an Effective Way to Analyze Fish Feeding Habits? A Case of the Yellowfin Sea Bream Acanthopagrus latus (Houttuyn) in Daya Bay. Frontiers in Marine Science 8:634651.

Questel, J. M., R. R. Hopcroft, H. M. DeHart, C. A. Smoot, K. N. Kosobokova, and A. Bucklin. 2021. Metabarcoding of zooplankton diversity within the Chukchi Borderland, Arctic

Ocean: improved resolution from multi-gene markers and region-specific DNA databases. Marine Biodiversity 51:4.

Robert, D., H. M. Murphy, G. P. Jenkins, and L. Fortier. 2014. Poor taxonomical knowledge of larval fish prey preference is impeding our ability to assess the existence of a "critical period" driving year-class strength. ICES Journal of Marine Science 71:2042–2052.

Schroeder, A., D. Stanković, A. Pallavicini, F. Gionechetti, M. Pansera, and E. Camatti. 2020. DNA metabarcoding and morphological analysis - Assessment of zooplankton biodiversity in transitional waters. Marine Environmental Research 160:104946.

Setzler, E. M., W. R. Boynton, K. V. Wood, H. H. Zion, L. Lubbers, N. K. Mountford, P. Frere, L. Tucker, and J. A. Mihursky. 1980. Synopsis of Biological Data on Striped Bass, Morone saxatilis (Walbaum). NOAA technical report NMFS circular, National Oceanic and Atmospheric Administration.

Sheridan, P. F. 1978. Food Habits of the Bay Anchovy, Anchoa mitchilli, in Apalachicola Bay, Florida. Northeast Gulf Science 2.

Shideler, A. C., and E. D. Houde. 2014. Spatio-temporal variability in larval-stage feeding and nutritional sources as factors influencing striped bass (Morone saxatilis) recruitment success. Estuaries and Coasts 37:561–575.

Siddon, E. C., T. Kristiansen, F. J. Mueter, K. K. Holsman, R. A. Heintz, and E. V. Farley. 2013. Spatial match-mismatch between juvenile fish and prey provides a mechanism for recruitment variability across contrasting climate conditions in the eastern Bering Sea. PLoS ONE 8.

Smithsonian Environmental Research Center. 2005. Zooplankton / Food-Web Monitoring for Adaptive Multi Species Management. Chesapeake Research Consortium.

Southwick Associates. 2019. The Economic Contributions of Recreational and Commercial Striped Bass Fishing. McGraw Center for Conservation Leadership, Fernandina Beach, FL.

Chapter 2: Comparing metabarcoding and morphological identification for use in zooplankton monitoring and ecological studies

Introduction

Studies of zooplankton ecology and biodiversity have relied mainly on morphological taxonomic identification. This method is considered the standard because the original taxonomic descriptions of species have been made based on morphological characteristics. These data are in the form of direct counts and abundance for each taxon present, which can be used in any kind of downstream analyses (Bucklin et al. 2016, Hirai et al. 2021). Morphological identification can also provide information on life cycle stage, age, sex, and size of the organisms present in the sample; these data are sometimes needed to answer ecological questions.

However, morphological taxonomic identification relies heavily on morphological taxonomy expertise which is both broad (covers all taxa which may be observed) and specific (can use morphology to identify organisms to species level and stage). Training for this takes time and is generally geographically specific, limiting a worker to a particular location or taxonomic specialty where they are most effective (Schroeder et al. 2020). Such training relies on taxonomic keys, which frequently only exist for adult life stages, and limits identifications to well-studied organisms (Bucklin et al. 2021, Machida et al. 2021). Morphological identification is also labor-intensive, sometimes taking years to process zooplankton samples by hand under a microscope, and it can be expensive to pay for the expert time and knowledge required (Schroeder et al. 2020). Morphological methods also cannot account for cryptic species complexes: organisms which are likely two or more different species, but which appear so morphologically similar that they have previously been classified as a single species (Bucklin et

al. 2016, Machida et al. 2021). Zooplankton are particularly challenging to identify via morphological taxonomy because they are an extremely diverse, multiphyletic group including 15 phyla and 41 functional groups (orders and classes) (Bucklin et al. 2021). Further complicating matters, some species are only members of the plankton for part of their lives (meroplankton), impeding the creation of identification keys for their planktonic stage.

In an attempt to overcome some of these obstacles, zooplankton ecologists have turned to DNA metabarcoding: a high throughput method which uses a universal, diagnostic gene sequence to identify multiple species in a mixed environmental sample. Because this method targets a single gene, both trace environmental DNA (eDNA) and tissue samples can be used for zooplankton identification. Processing samples via metabarcoding is faster, allowing for studies with higher spatial and temporal resolution (Schroeder et al. 2020). Metabarcoding can provide more taxonomic identifications to species level, detects cryptic species, and can accurately identify taxonomy of young stages of organisms (Hirai et al. 2021, Machida et al. 2021).

However, metabarcoding performance varies. Application of this method is not yet standardized, so different studies use differing methods and sometimes generate conflicting results (Compson et al. 2020). The marker chosen determines whether taxonomic identifications are broad or specific, and the markers which allow accurate identifications to the species level tend to have taxonomic biases (Bucklin et al. 2019, Schroeder et al. 2020). For example, there is an extensive database for mitochondrial marker cytochrome oxidase 1 (CO1) which can be used to accurately identify zooplankton to species; however, the primers for CO1 are biased against cnidarians, sponges, and ctenophores (Bucklin et al. 2011, Questel et al. 2021). The bioinformatics process (particularly the sequence cleanup and clustering protocols) and completeness of the taxonomic reference database used both play large parts in determining how

many taxa are identified, and if they are identified correctly (Bucklin et al. 2016, Porter and Hajibabaei 2020, Schroeder et al. 2020). No matter which processing methods are used, metabarcoding results are semi-quantitative at best, offering measures of relative abundance which correlate best with morphological methods for only the most abundant taxa in a sample (Bucklin et al. 2019, Schroeder et al. 2020). Metabarcoding also cannot offer any information about life stage, sizes, age, or sex of zooplankton or prey present; this information is frequently important in zooplankton ecology (Bucklin et al. 2016).

Each method has its own strengths and weaknesses; as with any emerging technique, metabarcoding should be tested alongside morphological identification in order to determine if the methods offer fundamentally different (and potentially misleading) conclusions about a study system's biodiversity and ecology. Identifying differences in the results produced by the two methods will assist other investigators and managers in choosing which method is appropriate in answering their own questions.

In this study, we examined the zooplankton of the Choptank River, a tributary of the Chesapeake Bay on the Mid-Atlantic coast of the USA. The Choptank River is rich in zooplankton, which support a major spawning ground of predatory fishes such as striped bass and white perch (Dorfman et al. 2016). As such, it is important economically and ecologically to the Chesapeake Bay and Mid-Atlantic coast. The Choptank River is also a well-documented and dynamic system with pronounced seasonality and a strong salinity gradient. These attributes present a natural zooplankton community which changes in a predictable way with time and environmental conditions, thus offering a range of *in-situ* conditions under which to compare the performance of the two methods.

Zooplankton samples were collected with net tows and processed for both morphological identification under stereo dissecting microscope and for genetic identification using metabarcoding with CO1. The data were divided into three data sets and then all three data sets were compared quantitatively to determine where and how their conclusions about the system agreed or differed among the methods and data sets. In addition, the methods were assessed for differences in time investment, cost, and taxonomic resolution. The results of this study will help pave the way for aquatic monitoring programs and scientific investigations to come.

Methods

Fieldwork

Samples were collected from the Choptank River in Maryland, USA once a month from late spring through early fall (April-September) in 2018 and 2019 as part of the Maryland Sea Grant (MDSG) project: "*Novel Genomic Tools to Assess Fish Diet and Prey Quality in the Choptank River*" (https://www.mdsg.umd.edu/research-projects/2018/rfish-109). Five sites were sampled; three of the five were chosen to correspond to the Chesapeake Bay Program's Water Quality Monitoring Stations, while the other two stations were selected based on the location of the leading edge of the salinity front (Fig. 2.1). A small craft equipped with a port-deploying winch mounted on a davit was used courtesy of Horn Point Laboratory, University of Maryland Center for Environmental Science (UMCES).

At each site the water column salinity, temperature, and dissolved oxygen were collected at 1 m intervals from the surface to 1 m above the bottom with a YSI sonde probe (Pro2030 https://www.ysi.com/pro2030). Zooplankton were collected with a plankton net tow (0.5 m

diameter opening, 64 μm mesh net), equipped with a flow meter. Nets were deployed to half the station depth to avoid underwater obstacles, towed there for 2.5-10 minutes, then brought to just under the surface and towed there for 2.5-10 minutes for a total tow time of 5-20 min. Zooplankton samples were split in half using a Folsom plankton splitter into two equal samples. Each half-sample was filtered through a 200 μm sieve, creating size-fractionated samples: one with animals 200 μm or larger, and one with animals larger than 64 μm but smaller than 200 μm. One set of size-fractionated samples was preserved in 4% pH-buffered formalin for morphological identification, the other set was preserved in 95% ethanol for metabarcoding identification. Complete ethanol changes were performed for zooplankton samples preserved in 95% ethanol within a week of the sampling date.

Sample Processing

Zooplankton morphological identification

Zooplankton samples for morphological identification were split with a Folsom plankton splitter and diluted as-needed for ease of sub-sampling. A 5 mL stempel pipette subsample containing at least 200 animals was quantified on a Ward counting wheel under dissecting scope (Leica M60) (Hensen 1887). Individual plankters were identified to the lowest taxonomic level possible (DeBoyd 1977, Johnson and Allen 2012, Pennak 1953, Thorp and Covich 2001), and processed subsamples were preserved and stored separately. After waiting for at least one year for zooplankton to cease shrinking (Ahlstrom and Thrailkill 1963), the remaining whole zooplankton sample (minus the subsample removed for quantification) was measured for settled biovolume via Imhoff cone.

Zooplankton metabarcoding

Zooplankton samples for metabarcoding identification were diluted as-needed for sub-sampling, then a 1 or 2 mL stempel pipette was used to take a 1-4 mL subsample, aiming for about 1 cm^3 of zooplankton tissue. Each subsample was wet-weighed and then DNA was extracted using a modified Qiagen DNeasy blood and tissue kit protocol. Kit instructions were followed as written except for steps as listed in supplementary materials (S2.1). Each sample was eluted twice into the same catch tube to capture the maximum amount of DNA: first with an aliquot of 40 µL, then 30 µL.

CO1 amplicon libraries were generated with a two-round PCR protocol: in round one, Leray primers amplified a 313 bp length of the CO1 gene, followed by a second PCR where 6 bp barcodes were annealed to the amplicons to allow for multiplexing (O'Donnell et al. 2016).

Specifically, the PCR process was conducted as follows. Extracted DNA was amplified with a custom master mix (11.5 µL PCR-safe water, 5 µL 5x buffer, 1.5 µL $MgCl_2$, 0.5 µL dNTPs, 1.25 µL primer M1COlintF (Leray et al. 2013b), 1.25 µL primer jgHCO21198 (Leray et al. 2013b), 0.7 µL BSA, 0.25 µL Taq; 22 µL master mix and 3 µL extracted DNA per reaction well, run in triplicate) using a modified Leray protocol (denature at 95°C for 3 min; 30 cycles of: 95°C for 30 s, 48°C for 45 s, 72°C for 50 s; extension at 72°C for 10 min; hold at 8°C). Amplified products were pooled, amplification was confirmed via gel electrophoresis, and products were diluted 1:5 for barcode addition. The master mix was the same for barcode addition as for amplification except that barcode primers were used (supplemental, Fig. S2.2 and S2.3). PCR for barcode addition followed the Leray protocol as detailed above. Amplification was confirmed on a representative subsample using gel electrophoresis and DNA concentration of each sample was quantified on Qubit. Barcoded products were pooled into libraries using 50

ng DNA from each sample. The concentration of DNA in each pool was quantified, visual confirmation of DNA size fragment was performed on agarose gel, and the pools were sent to Genewiz for library preparation and sequencing. Sequencing was performed on the Illumina MiSeq using paired-end sequencing with 300 bp fragments to cover the amplicon size.

Raw sequence data were processed through a bioinformatics pipeline designed by Dr. Louis Plough. Reads were trimmed and demultiplexed with cutadapt, processed with DADA2 to produce preliminary OTUs (Callahan et al. 2016), and then clustered at 97% similarity with VSEARCH (Frøslev et al. 2017). OTUs with < 100 reads were excluded from the final data set. Taxonomic assignment was performed with a Bayesian Lowest Common Ancestor (BCLA) algorithm (Gao et al. 2017). This algorithm matched OTU sequences to sequences in a custom CO1 database which was downloaded from MIDORI2 (GB version 258, longest) and formatted for BLCA (Leray et al. 2022). BCLA assignments were verified with remote-BLAST to the entire NCBI nt database. Non-animal and terrestrial taxa were removed from the data set prior to analyses.

Additional Environmental Data

Chlorophyll and Secchi depth data included in this study were provided by the Maryland Department of Natural Resources Tidewater Ecosystem Assessment Division, Eyes on the Bay program (www.eyesonthebay.net). This monitoring program takes monthly measures from stations in the Choptank River and other locations around the Chesapeake Bay. Chlorophyll and Secchi depth data from Eyes on the Bay were supplemented with data collected and provided by ShoreRivers Inc (https://www.shorerivers.org/). Choptank River flow data was provided by the U.S. Geological Survey, 2016, National Water Information System data available on the World

Wide Web (USGS Water Data for the Nation), accessed November 11, 2022, at URL [http://waterdata.usgs.gov/nwis/]. Flow data were retrieved using R package dataRetrieval (De Cicco et al. 2022).

Missing values for chlorophyll a and Secchi depth at stations Jamaica Point and Buoy 45 were interpolated with inverse distance weighting, performed in R using function idw from the gstat package.

Data Analysis

All samples from sites and dates in common between the morphological and metabarcoding data sets were used for all analyses (n= 45). Samples in common between the data sets spanned all months (April-September), both years (2018, 2019), and all five stations sampled.

The environmental parameters considered in this study were: river mile, day of year, maximum cast depth, temperature, salinity, dissolved oxygen, chlorophyll a, Secchi depth, river flow on the day of sampling, average river flow for the month of sampling, and average river flow for the month prior to sampling. River mile was used as a proxy for station location in analyses which required continuous variables (e.g. multiple linear regression). Day of year was used as a proxy for season. Maximum cast depth was used as a rough estimate of zooplankton vertical position in the water column; e.g. a significant, negative correlation between the abundance of a particular species and cast depth would indicate that species was distributed mainly at the surface during our daytime sampling. Chlorophyll a was used as a proxy for phytoplankton abundance. Average river flow for the month prior to sampling was used to account for time-lagged effects of river flow rate on zooplankton.

All analyses were completed in R and Excel. Code for select R analyses was written with drafting support from Perplexity.ai (Perplexity).

Creation of data sets

Data from the two methods were split into three data sets. One data set for morphological data (morphological), and two for metabarcoding data (metabarcoding). The two metabarcoding data sets were derived from the same data, but different filters were applied to the post-bioinformatics taxonomic assignments which resulted in a strictly filtered data set (exclusive) and a generously filtered data set (inclusive).

The filters are as follows. All unclassified OTUs (referred to as "Unknown" taxa) which had 100 reads or fewer across all samples were removed from the exclusive set; unclassified OTUs were only excluded from the inclusive set if they had fewer than 100 reads and those reads were in fewer than five samples. BLCA taxonomy assignment was modified in each data set based on the confidence of the assignment at each taxonomic level; assignments with confidence <95% were marked "Unknown" in exclusive, confidence <80% were marked as "Unknown" in inclusive. This did not remove taxa from the data sets, but rather changed the taxonomic resolution of the OTU assignments. BLAST taxonomic assignments were used to trim taxa in each data set. BLAST assignments with 95% confidence or greater and at least a 240 bp match length were retained in the exclusive data set; all others were removed. BLAST assignments with 80% confidence or greater and 157 bp match length were retained in the inclusive data set; all others were removed.

Off-target taxa were removed from all three data sets. For the sake of simplicity, "off-target taxa" were organisms that would not be reasonably classified as zooplankton e.g. fungi,

terrestrial insects, and phytoplankton. Animals which are known to have an aquatic, planktonic stage were retained in the data sets e.g. midges and mosquitoes.

Abundance measure calculations

Raw counts and reads were converted into data types relevant to ecological study. Relative abundance, biovolume, biomass, and biomass concentrations were calculated for all three data sets. Relative abundance was calculated for each taxon within each sample (such that the relative abundance of all taxa within each sample summed is equal to 1). Then, biomass (mg) was calculated for each taxon in each sample of the inclusive and exclusive data sets by multiplying the taxon's relative abundance by the total biomass of that sample.

Total biomass of each metabarcoding sample was calculated like so:

total biomass of zooplankton sample (mg)= mass of subsample (mg)/ volume of subsample (mL) * total volume of zooplankton sample (mL)

Biomass concentration was calculated for each taxon within each sample for the inclusive and exclusive metabarcoding data sets like so[1]:

relative abundance of taxon * (total biomass of zooplankton sample (mg) / (volume filtered by the plankton net (m^3)/2))

[1] The volume filtered by the plankton net was divided in half because each net catch was divided in half: one half of the sample for processing by metabarcoding, one half for morphological.

Biovolume was calculated for each taxon within each sample for the inclusive and exclusive metabarcoding data sets according to Balvay 1987. The relationship for bulk zooplankton samples was used:

$$\text{biovolume (mL)} = 10^{((\log(\text{biomass (mg)})-2.290)/0.948)}$$

For the two metabarcoding data sets, abundance and concentration measures were calculated for each taxon within each sample using counts derived from a technique used by microbiologists to convert sequence reads to counts (Vandeputte et al. 2017):

$$\text{count} = \text{relative abundance} * \text{total number of organisms counted in each sample}$$

$$\text{concentration } (m^3) = \text{count} * (\text{volume filtered by the plankton net } (m^3)/2)$$

$$\text{abundance } (m^2) = \text{concentration } (m^3) * \text{range of sampling depth (m)}$$

For the morphological data set, biovolume for each taxon within each sample was calculated by multiplying the whole sample biovolume by the relative abundance of the taxon. Biomass and biomass concentration were calculated based on Balvay 1987, again using the relationship for bulk samples:

$$\text{biomass (mg)} = 10^{(0.948 * \log(\text{biovolume (mL)})+2.290)}$$

Biomass concentration was calculated the same way for the morphological data set as it was for the two metabarcoding data sets.

The number of organisms processed in each aliquot by morphological identification was calculated like so:

organisms processed in morphological aliquot= sum of all counts for each taxon in the sample

In order to calculate the number of organisms processed by metabarcoding, the number of organisms in the entire half-sample needed to be calculated first. This was done using the counts, dilution, and Folsom split data of the morphological half-sample sample. Half-sample is used here because each net tow was split in half, with one half-sample processed by each method. That equation follows:

organisms in each half-sample= ((organisms processed in morphological aliquot/morphological aliquot volume (mL)) * morphological sample dilution (mL)) * (number of Folsom splits^2)

The number of organisms processed in each metabarcoding aliquot was then calculated like so:

organisms processed in metabarcoding aliquot = (organisms in each half-sample/metabarcoding sample dilution (mL)) * metabarcoding aliquot volume (mL)

Handling of data

Time investment and costs were recorded throughout sample processing and divided on a per-sample basis. For taxonomic resolution, lists of all unique organisms from each data set were compared for the percent of organisms positively identified to each of six taxonomic levels: phylum, class, order, family, genus, species.

Quantitative assessment explored the relationships between the three data sets across measures commonly used by ecologists. Measures for consideration included: species richness, diversity, and abundance. For all quantitative assessment investigations, absolute values of results between the three data sets were expected to differ so patterns were compared instead (e.g.: did all three data sets show a significant, positive linear relationship between total zooplankton abundance and chlorophyll, regardless of the slope or intercept values?).

Stations Jamaica Point (JP) and ET 5.1 (51) and the month of July were omitted from analyses where samples were examined by station and month; these were only sampled once and lacked statistical power. For aggregations of samples not grouped by station and month the data were left intact.

The morphological data set included information on the life stages of each organism identified; these are non-comparable with metabarcoding data so the stage-specific information was summed into one measure per taxon, per sample. Likewise, in the metabarcoding data sets the same taxonomic identification was sometimes assigned to several different OTUs. This is likely due to crypsis in the species complex, but as that is beyond the scope of this study to ascertain, the OTUs with identical taxonomy were summed together into one measure per taxon, per sample.

Comparisons between the three data sets across measures of abundance needed to be direct, without differences in taxonomic resolution. For each taxon, the taxonomic assignment was reduced to the lowest common resolution between all three data sets, then the abundance data were summed across the new identification within each sample where applicable. For example, the morphological data set identified several rotifers to the species level but the metabarcoding data sets only identified these organisms to the Phylum "Rotifera". All rotifers in all data sets were therefore reclassified as "Rotifera" and where more than one "Rotifera" was present in a sample, their abundances were summed.

Results

Error estimation

Select samples were processed in duplicate to quantify differences (error) in species quantifications. For the morphological data set, a second aliquot was enumerated for two samples, both size fractions (n= 4). For the metabarcoding data set (the inclusive data set), extracted DNA was amplified, sequenced, and processed in duplicate for one sample, both size fractions (n= 2). Percent difference in enumeration (PDE), coefficient of variation (CV), standard deviation (SD), and percent taxonomic disagreement (PTD) were calculated for the replicates as outlined in Stribling et al. 2003.

Among the replicates of the morphological data, the taxa which were present in both replicates (n= 14 out of 27 total unique taxa identified among morphological replicates) had PDE ranging from 2.79-88.16%. 10% of these shared taxa were below the 5% cutoff used by the EPA (U.S. EPA 2017), so 90% of taxa had a large difference in enumeration between replicates. CV

ranged from 3.95-124.68%; 77% of taxa had CV <50%. Those taxa with CV <50% had a difference in enumeration which was between the 1st and 3rd quantiles of the distribution. PTD for the replicates ranged from 9.74-41.99%. Two out of four samples were below the 15% PTD cutoff used by the EPA ("National Lakes Assessment 2017 Laboratory Operations Manual" 2017), so half the tested samples had acceptably similar taxonomic assignments between replicates.

Errors appeared to stem largely from sample degradation. 27% of the taxa which were not shared between replicates were identified as "degraded" and placed at a higher taxonomic level than would otherwise be assigned. Several years had passed between initial enumeration and replicate enumeration; had the replicate enumeration been completed closer to the time of initial enumeration the error between them would likely be much smaller. The liquid volume of the samples was noticeably smaller for some sample jars; improper sealing post-enumeration may also be responsible for sample degradation.

Replicates of the metabarcoding data had larger errors by every metric. Among the replicates of the metabarcoding data, the taxa which were present in both replicates (n= 29 out of 68 total unique taxa identified among metabarcoding replicates) had PDE ranging from 0.98-99.26%. Only 3.45% of taxa were below the 5% cutoff; 96% of taxa had a large difference in enumeration between replicates. CV ranged from 1.39-140.37 %; 55% of taxa had CV <50% and were within the 1st and 3rd quantiles. PTD for the replicates ranged from 85.5-90.88%; all of the samples were above the 15% cutoff and did not have acceptably similar taxonomic assignments between replicates.

Several years also passed between initial and replicate amplification and sequencing for the metabarcoding data; sample degradation likely also played a part in the error between replicates.

Number of organisms processed by each method

All samples processed by each method were considered for this analysis (n= 54 morphological; n= 50 metabarcoding).

Overall, significantly more individual plankton were processed in each aliquot by the metabarcoding method ($p= 3.3e^{-6}$, Welch's t-test); only three metabarcoding samples had the same or fewer organisms compared to morphological samples (Fig. 2.2). For the remaining samples, there were 0.7-82.3 times more organisms processed by metabarcoding than morphological.

There was a significant difference in the mean number of organisms counted per size fraction (64 and 200 only; whole samples not considered as they are not part of downstream analyses) in both the morphological (p= 0.002306; Welch's t-test) and metabarcoding methods ($p= 1.0*e^{-6}$, student's two sided t-test). However, opposite trends were observed: more organisms were processed in the 200 fraction than the 64 for the morphological method (2.07:1), but more organisms were processed in the 64 fraction than the 200 for the metabarcoding method (3.22:1) (Fig 2.3). There was a singular high outlier in the metabarcoding data (> 50,000 organisms) which was the result of an aliquot processed from a whole sample; it does not appear in Fig. 2.3.

There was no significant difference in the number of organisms processed between years (Student's t-test morphological p= 0.27, metabarcoding p= 0.14), months (Kruskal-Wallis test morphological p= 0.65, metabarcoding p= 0.044; subsequent pairwise Wilcox tests showed no

differences between groups [Bonferroni and Benjamini & Hochberg p adjust]), or stations (Kruskal-Wallis test morphological p= 0.7, metabarcoding p= 0.16) within each method.

Taxonomic resolution

Taxonomic resolution was higher in both metabarcoding data sets than morphological, but higher in the exclusive set than the inclusive (Fig. 2.4). Only 31% of organisms were identified to the species level in the morphological data set, whereas 79% and 91% were identified to species in the inclusive and exclusive metabarcoding data sets, respectively.

Species richness and community composition

Species richness in the morphological data set was the lowest of the three at 37 taxa, exclusive next highest at 74 taxa, and inclusive highest at 127 taxa. Jaccard indices were calculated on raw community data to determine the percent of shared taxa between morphological vs. inclusive, and morphological vs. exclusive data sets. The values were low: 5.8% for morphological vs. inclusive, and 3.7% for morphological vs. exclusive (Table 2.1). The samples were sorted by size fraction and tested again to determine shared taxa for the microzooplankton and mesozooplankton separately. Microzooplankton communities had only 2.3-4.9% overlap, whereas mesozooplankton communities had 4.7-6.5% overlap (Table 2.2). Jaccard indices calculated for just the 13 most abundant taxa from each data set showed 8.3% overlap between morphological and inclusive taxa and 4.0% overlap between morphological and exclusive taxa.

Diversity patterns

Stations Jamaica Point and ET5.1, and the month of July were omitted from diversity analyses because they were only sampled once. Shannon scores were calculated for each sample, in each data set, based on both the concentration (individuals/m^3) and biomass (mg) data.

Overall diversity patterns between data sets show significantly lower diversity in the morphological data set compared to the metabarcoding data sets, and exclusive diversity significantly lower than inclusive (Fig. 2.5).

Spearman rank correlation tests were run between the diversity scores and a variety of continuous environmental variables: river mile, day of year, maximum cast depth, temperature, salinity, dissolved oxygen, chlorophyll a, Secchi depth, river flow on the day of sampling, average river flow for the month of sampling, and average river flow for the month prior to sampling. The morphological data set and inclusive data set identified a significant positive correlation between river mile and diversity as measured by both biomass and concentration. The inclusive and exclusive data sets both identified a significant negative correlation between chlorophyll a and diversity as measured by both biomass and biomass concentration. It is important to note that where different data sets identified the same environmental variable as significant, the direction of the correlation was consistent.

For the morphological data set, there were additional significant correlations between diversity and temperature, salinity, and mean monthly river flow (Fig. 2.6). The inclusive data set identified diversity significantly correlated with dissolved oxygen. In the metabarcoding data sets, there was no difference in significant correlation coefficients between diversity scores and environmental variables for biomass and concentration. Day of year, Secchi depth, river flow on

the day of sampling, and average river flow for the month prior to sampling were not significantly correlated with diversity scores in any data set.

Linear regressions were run between Shannon scores and each continuous environmental parameter to determine which drivers of diversity were identified by each method (Table 2.3). Simple linear regression models showed that dissolved oxygen, chlorophyll a, and river mile drove diversity in the inclusive data; no other data set had a significant driver of diversity. There was no difference in slopes and p-values of the models for biomass and concentration. All data sets showed no significant linear relationship between diversity and day of year, maximum cast depth, temperature, salinity, Secchi depth, or river flow. Multiple linear regression models were run to examine interactive effects of environmental parameters on diversity using a subset of environmental variables to avoid collinearity as measured by variance inflation factor (maximum cast depth, temperature, salinity, dissolved oxygen, chlorophyll a, Secchi depth, average river flow for the month of sampling, and average river flow for the month prior to sampling). However, all models from each data set failed regression assumptions.

Abundance

Directly comparing across data sets: total zooplankton

Patterns of total zooplankton abundance were examined across five measures: abundance (ind./m^2), concentration (ind./m^3), biovolume (mL), biomass (mg), and biomass concentration (mg/m^3). Relative abundance data were excluded from these analyses; analysis of a total is redundant as this measure sums to 1 in each sample.

Plots of the total zooplankton per sample in each data set, displayed against each other in morphological vs inclusive and morphological vs exclusive scatter plots, show how the

abundance data in each set relate to each other (Fig. 2.7). For some measures, total abundance is overestimated by metabarcoding data (biovolume, concentration), but most measures of total abundance are larger for morphological data than for metabarcoding.

Biovolume, biomass, and biomass concentration all had significant Spearman correlations between morphological and inclusive data sets (0.71, 0.68, 0.64, respectively), and morphological and exclusive data sets (0.71, 0.68, 0.64, respectively) (Table 2.4). The significant coefficients were positive and greater than 0.5, indicating a strong correlation between morphological and metabarcoding data across these measures of abundance when considering the total number of zooplankton in each sample.

Linear regressions of total zooplankton abundance between morphological and metabarcoding data sets were likewise significant only for biomass, biomass concentration, and biovolume measures, however they failed the homoscedasticity regression assumption (Table 2.5). R^2 values were relatively low (< 0.5), indicating linear models have little explanatory power.

Comparing patterns within data sets, between data sets

Total zooplankton

Spearman rank correlation tests were run between the total zooplankton abundance measures and continuous environmental variables (Fig. 2.8). For the morphological data set, dissolved oxygen significantly, negatively, correlated with all five measures of total zooplankton abundance. Dissolved oxygen also correlated significantly and negatively with biomass concentration in the exclusive and inclusive data. All other significant correlations were in just the morphological data set. Within these, only dissolved oxygen was identified as a significant

correlate across all measures of abundance; the rest of the correlates were only significant across two to three measures of abundance. Where multiple measures identified significant drivers, the strength of the correlation varied but the direction of the relationship was consistent.

Linear regressions were run between log10+1 transformed total zooplankton abundance measures and each continuous environmental parameter to examine which drivers of abundance were identified by each method (Table 2.6). Simple linear regression models showed significant drivers of abundance in all three data sets: temperature and day of year drove biomass and biomass concentration in morphological data, dissolved oxygen drove biomass in inclusive and exclusive data. The direction of the relationship was the same for inclusive and exclusive (negative slope). All data sets showed no significant linear relationship between total zooplankton abundance and river mile, day of year, maximum cast depth, salinity, Secchi depth, or river flow. A multiple linear regression model with the following environmental parameters was run for each measure of abundance in each data set: day of year, maximum cast depth, temperature, salinity, dissolved oxygen, chlorophyll a, Secchi depth, and average river flow for the month of sampling. This subset of parameters was chosen to reduce the collinearity of the predictors in the model as determined by the variance inflation factor. The inclusive and exclusive data sets both showed a significant model for biomass concentration and had the same significant parameters within the model (temperature and dissolved oxygen), with the same slope direction (negative).

Specific taxa

Abundance patterns for specific taxa were investigated to compare the results of each method for a specific species (the copepod *Acartia tonsa*) and for species grouped by class

(Bivalvia) and phylum (Annelida). The taxa selected are also the dominant zooplankter in the system (*Acartia tonsa*), abundant but non-dominant zooplankton (Bivalvia), and relatively rare zooplankton (Annelida). Abundances were log10+1 transformed prior to analyses.

Scatter plots of abundance (ind./m²) between data sets were very similar among the abundant shared taxa- *A. tonsa* and Bivalvia- but differed with more rare taxa (Annelida) (Fig.s 2.15, 2.17, 2.19).

Specific taxa: *Acartia tonsa*

Scatter plots of *A. tonsa* abundance (ind./m²) between morphological vs. inclusive and morphological vs. exclusive were almost identical for this dominant taxa; data points fell just shy of the 1:1 line in a plot of inclusive vs. exclusive *A. tonsa* abundance, indicating the abundance data were similar between the metabarcoding data sets but that exclusive data slightly overestimated their abundance (Fig. 2.9).

Linear regressions were run between *A. tonsa* abundance measures and each continuous environmental parameter to examine how drivers of abundance were reported by each method. Simple linear regression models showed significant drivers of abundance in all three data sets, but the data sets had no combinations of drivers and abundance measures in common (Table 2.7). A multiple linear regression model with the following environmental parameters was run for each measure of *A. tonsa* abundance in each data set: day of year, maximum cast depth, temperature, salinity, dissolved oxygen, chlorophyll a, Secchi depth, and average river flow for the month of sampling. All three data sets had significant models for biomass, and identified salinity as a significant driver with a consistent slope direction between data sets. Inclusive and exclusive data sets also identified salinity as a significant driver of *A. tonsa* biovolume.

Specific taxa: Bivalvia

Scatter plots of Bivalvia abundance (ind./m²) between morphological vs. inclusive and morphological vs. exclusive were almost identical for this abundant taxa, but had notable zero values in morphological data compared to metabarcoding (Fig. 2.10). Again, data points fell just shy of the 1:1 line in a plot of inclusive vs. exclusive Bivalvia abundance.

Linear regressions were run between Bivalvia abundance measures and each continuous environmental parameter to examine how drivers of abundance were reported by each method (Table 2.8). Simple linear regression models showed significant drivers of abundance in just the inclusive and exclusive data sets. In both data sets, temperature, day of year, and mean monthly river flow for the month prior to sampling drove Bivalvia abundance, concentration, and biomass. Biomass was also driven by dissolved oxygen in both data sets, and biovolume was driven by temperature and dissolved oxygen in both data sets. The direction of the slope for each of these relationships was consistent between data sets. Multiple linear regression models were run in the same fashion as for *A. tonsa* abundance. Only inclusive and exclusive data sets had significant models, and both identified the same parameter driving Bivalvia biovolume, biomass, and biomass concentration: day of year.

Specific taxa: Annelida

Scatter plots of Annelida abundance (ind./m²) between morphological vs. inclusive and morphological vs. exclusive had noticeably different distributions and had notable zero values in morphological data compared to metabarcoding (Fig. 2.11). Data points were scattered off the 1:1 line in a plot of inclusive vs. exclusive Annelid abundance; the exclusive data generally

overestimated their abundance but in a few samples the inclusive data overestimated their abundance instead.

Linear regressions were run between Annelida abundance measures and each continuous environmental parameter to examine how drivers of abundance were reported by each method (Table 2.9). Simple linear regression models showed significant drivers of multiple measures of abundance in all three data sets, however the only driver shared between data sets was salinity driving biomass concentration in inclusive and exclusive data. Multiple linear regression models were run in the same fashion as for *A. tonsa* abundance. Only inclusive and exclusive data sets had significant models, and both identified similar drivers of Annelida abundance (temperature and maximum cast depth), biovolume (dissolved oxygen and salinity), and biomass (salinity and dissolved oxygen). Where they identified the same driver of abundance, the direction of the relationship was consistent between data sets. Both identified additional drivers of these abundance measures which they did not have in common, and the exclusive data set additionally identified significant drivers of Annelida concentration.

Time

The time required to process samples was divided into three categories: “active processing time” (time a worker spends actively handling the sample), “passive processing time- likely paid” (time a worker spends not actively handling the sample, but still engaged with the task e.g. waiting for a centrifuge cycle to complete), and “passive processing time- likely unpaid” (time a worker spends not actively handling the sample, and not engaged in the task e.g. an overnight incubation) (Fig. 2.12). Morphological identification was entirely active processing time, at 3.73 hrs per sample on average. While metabarcoding required almost the same amount

of time per sample, the bulk of that time was unpaid processing time from an overnight incubation step.

Cost

The cost to process samples was also divided into three categories: the cost of paid expertise to actively process the sample, passively process the sample (calculated from "passive processing time- likely paid"), and the cost of disposables (e.g. reagents, pipette tips). Morphological identification cost slightly less than metabarcoding per sample ($64.45 vs. $72.02 USD respectively), however nearly all of the cost of morphological identification is in paid expertise to process the sample, whereas the cost of metabarcoding is made up largely of the cost of disposable materials (Fig. 2.13).

Discussion

Number of organisms processed by each method

The overall difference in the number of organisms processed by each method naturally followed from the size of the subsample required for each: metabarcoding required about a cubic centimeter of tissue for DNA extraction, whereas morphological identification required only about 200 organisms. The combined volume of 200 organisms would be only a fraction of a cubic centimeter, so it was no surprise that there were thousands more plankters in the metabarcoding subsample.

The magnitude of the difference between organisms tallied in each method was larger for metabarcoding than for morphological, and because it ran in opposite directions there appeared

to be a size bias in each method towards different size fractions. This was likely also due to the need for a tissue sample of a certain size for the metabarcoding; each aliquot for metabarcoding represented about a cubic centimeter of tissue, and because the zooplankton in the 64 size fraction were physically smaller, it followed that there were more organisms per cubic centimeter for the 64 than for the 200.

Why then were more organisms processed in the 200 fraction than the 64 fraction for the morphological method? Paradoxically, it appears that the estimation of the number of organisms in a given aliquot prior to processing was overestimating with larger organisms, and underestimating with smaller organisms. Perhaps in the smaller size fraction, debris or eggs were erroneously considered to be an organism when the aliquot was "skimmed" to determine the appropriate number of organisms were present, whereas it was easier to distinguish organisms from debris in the larger size fraction.

Taxonomic resolution

These results followed expectations. Morphological identification had a reduced taxonomic resolution in part because the technique relies on both broad and specific knowledge of morphology and taxonomy for a given region; a single worker often specializes in specific phyla or the plankters of particular regions. The range of zooplankton taxa in this study were particularly diverse and therefore challenging to identify because the study area spanned a strong salinity gradient and encompassed three seasons. While the morphological taxonomist had experience in the region and with a range of plankters, that knowledge base was pitted against a much larger knowledge base: the NCBI database of gene sequences paired with a taxonomic identification assigned by experts in each phylum. It is no surprise that the exclusive data set also

had the highest taxonomic resolution; only high-confidence identifications were retained by the strict filters, and it is the nature of high-confidence BLAST identifications to assign taxonomy at the species level.

Species richness and community composition

Taxa lists from each data set showed that 70.27% and 57.48% of taxa in the exclusive and inclusive data sets, respectively, were meroplankton: larval or egg stages of benthic organisms and nekton (supplemental, Figures S2.4-S2.6). Meroplankton are notoriously difficult to resolve with morphology, due in part to a lack of reference materials to identify larvae and eggs to a taxonomic level lower than class. Accordingly, meroplankton taxa appear mostly at the genus and species level in the metabarcoding data sets, but where they appear in the morphological data they are only resolved to order or class, resulting in a mismatch.

29.73% of taxa in the morphological data set appear to be taxa not well detected by CO1 or present in the reference database e.g. rotifer species. This could be due to primer or amplification bias for this group, or perhaps a lack of references in the database.

14.86% and 17.32% of taxa in the exclusive and inclusive data sets, respectively, were holoplankton which were present in the morphological data set but not resolved to the same taxonomic level. This is likely because the larvae and eggs of holoplankton, like benthic organisms, have very few species-level identification keys. This is supported by the lowest community overlap being found in the microzooplankton (64 size fraction): this size fraction is largely composed of zooplankton larvae.

Lower overlap between the morphological and exclusive community data vs the morphological and inclusive community data was likely due to a higher proportion of

identifications to the species level in the exclusive data set compared to the inclusive; mismatches due to differential taxonomic resolution made up the bulk of the "unique" identifications in each data set. The Jaccard indices for just the most dominant taxa were not much better than for the entire community, indicating the taxa agreed upon by all methods are not isolated to the most abundant taxa and lending further support to the idea that the low community overlap observed here has more to do with how taxonomy is assigned than the abundances of individual community taxa.

Diversity patterns

In addition to the greater taxonomic resolution and the identification of meroplankton and holoplankton larvae, the much higher number of organisms processed in metabarcoding allowed for the detection of relatively rare organisms which were absent from the much smaller subsamples of the morphological process. These factors led to a much more diverse community in the metabarcoding vs the morphological data. Similarly, it follows that the exclusive data was less diverse than the inclusive due to strict filtering removing some of the more uncertain identifications.

Throughout the diversity and abundance testing, most of the agreements between data sets were on non-significant associations or groupings. This confirmed that there were consistent groupings or variables which were legitimately uninvolved in forming any diversity or abundance patterns, however we will focus most on the patterns in significant findings.

Only the inclusive data set identified any significant drivers of diversity. It was also the most diverse data set overall, although morphological data had the largest range of diversity and

could be reasonably expected to have shown similar results. Encouragingly, the slope of the inclusive diversity relationship with river mile was as expected, and was consistent with both measures of abundance (Jung and Houde 2003, Whitfield et al. 2012). The negative slopes for diversity vs. dissolved oxygen and chlorophyll a were unusual, and break from prior literature on the subject (Childress and Seibel 1998, Campfield and Houde 2011, Verberk et al. 2011, Elliott et al. 2012, Hirai et al. 2021, Downie et al. 2024).

Because the negative slopes with dissolved oxygen and chlorophyll a appeared in correlation tests of both the inclusive and exclusive data sets but not the morphological data set, they could be an artifact of using genetic data or real results hidden from traditional techniques but revealed by the genetic data. Further muddying the waters, the study years were unusually wet years with anomalously high rainfall, possibly contributing to unusual relationships between diversity and environmental variables in this specific data set. However, where the relationship was significant, dissolved oxygen consistently had a negative slope with measures of diversity and abundance throughout this study. Water column profiles show declines in benthic dissolved oxygen in the late spring (May) through late summer (August) of both 2018 and 2019 at the mouth of the Choptank (ET 5.2 and EE 2.1), though oxygen only dropped below 3 mg/L once, in August of 2019 at ET 5.2 (lowest reading 2.6 mg/L; see Fig. S2.7). Bottom water low oxygen may have created a concentrating effect where zooplankton avoiding both the daylight from above and the low oxygen layer from below gathered above the oxycline at those stations. This would have increased zooplankton concentrations (abundance) and diversity at the lowest water column oxygen concentrations, producing the negative correlation between abundance and diversity and dissolved oxygen.

The negative correlation between diversity and dissolved oxygen could also be due to a seasonal effect in the system. In the summer, dissolved oxygen is at its lowest, zooplankton abundance is highest, and benthic organisms spawn, contributing meroplankton to the Chesapeake Bay system and increasing planktonic diversity. While the oxygen levels themselves likely are not causing benthic contributions to the zooplankton community (spawning of benthic organisms is likely driven by tide, day length, or lunar phase (Andries 2001, Mercier and Hamel 2010, Bernard et al. 2016)), they do coincide in time, resulting in a pattern where oxygen could appear to be driving patterns of zooplankton abundance and diversity. It was beyond the scope of this study to tease out these effects, but further testing can ascertain whether this hypothesis is true.

Chlorophyll also consistently had a negative relationship with zooplankton diversity throughout this study which may have been a seasonal effect. In this system, chlorophyll a peaks first and highest in spring and secondarily in fall, just before and after the peak zooplankton diversity. Thus chlorophyll a is at its highest when zooplankton diversity is at its lowest, creating the negative relationship seen here. Further testing will be required to determine whether this holds true.

There was more agreement between data sets on Spearman correlations between diversity and environmental variables. However, we expected to see better agreement between data sets on salinity, as river mile and salinity are intrinsically linked: salinity decreases as river mile increases due to the arrangement of the stations, so we should see diversity decreasing with salinity and increasing with river mile. This pattern appeared in the morphological data, but not in either metabarcoding data set. This is particularly surprising for the inclusive data set because

it identified river mile as not just a correlation with but a driver of diversity; with that strong a relationship, salinity should have appeared as well.

Morphological data also identified monthly river flow and temperature as having significant correlations with diversity derived from biomass only.

These results in isolation would be misleading, particularly without further testing to understand the relationships between diversity and environmental variables in this system, but they would be incomplete rather than in opposition of prior findings. Exclusive data was more incomplete than inclusive, with very limited significant patterns.

Abundance

Directly comparing across data sets: total zooplankton

After taxonomy was backed out to lowest common taxa, the exclusive data set did not include several taxa which were part of the morphological and inclusive data sets. This indicates that while there were more taxa identified overall in the exclusive data than the morphological, whole categories of taxa were missing from the exclusive data set. Some of the taxa which were removed were dominant in the system and highly ecologically relevant, e.g. *Eurytemora carolleeae*. These taxa were excluded not because they were unimportant, but because their read sequence matches with the reference database were too low to pass the strict filtering protocols. This demonstrates that strict filtering artificially removes identifications of taxa which are present in the system.

The strong relationship between methods for total zooplankton biovolume, biomass, and biomass concentration per sample is encouraging. Though not linear and therefore not predictive, a strong, positive monotonic relationship indicates they at least correspond with one another.

Though not significant, the negative slopes and correlations between methods for abundance and concentration were surprising; the data should not be so contradictory.

Comparing patterns within data sets, between data sets

Total zooplankton

As with diversity, the metabarcoding data detected fewer significant relationships between abundance variables and environmental variables than were detected by morphological data. All three data sets showed negative correlations between dissolved oxygen and biomass concentration, which is in alignment with prior research.

Temperature had significant linear relationships with abundance measures in all three data sets, but only appeared in the metabarcoding data when it was part of a multiple linear regression and the effects of other variables were controlled, and the slope was negative instead of positive: contradicting the relationship between temperature and abundance in the morphological data set.

Morphological data identified additional significant correlations and drivers, and all with the same direction of relationship across abundance measures but not the same strength. With the exception of dissolved oxygen and chlorophyll as previously discussed, these relationships were also in alignment with prior research. Inclusive and exclusive data sets had the exact same linear regression model results (both simple and multiple) for drivers of total zooplankton biomass and biomass concentration. This is expected, as the data distributions were very similar between them for these measures as seen in Fig. 2.7.

Specific taxa

Inclusive vs exclusive data

Abundance data were only slightly different for *Acartia tonsa* between inclusive and exclusive data sets because *A. tonsa* had the same number of reads per sample in both data sets. However, differences remained in the results offered by each metabarcoding data set for simple regressions of environmental variables due to the calculation of the abundance measures. Relative abundance is a function of read number and the number of taxa (species richness) in the sample. Exclusive data slightly overestimated abundance compared to inclusive because with fewer taxa per sample, the relative proportions assigned to the taxa which remained were higher. The other abundance measures followed this same pattern of overestimation in exclusive data compared to inclusive because they were all calculated in part based on the relative abundance measure.

Bivalvia, which were also abundant in the system and had only slightly different abundance data between inclusive and exclusive, also exhibited the same pattern where inclusive and exclusive data show nearly the same drivers of abundance. Curiously, the ecological conclusions drawn by the metabarcoding data sets were actually more similar for Bivalvia than *A. tonsa*. This could be due to Bivalvia being aggregate data at the class level as opposed to the species level, therefore having less variation. The data do appear to fall more closely along the 1:1 line of Fig. 2.10.

Annelida, which were also abundant in the system and aggregated at an even higher taxonomic level appeared to contradict this pattern. The ecology of Annelida was even more different between these two data sets than it was for *A. tonsa* and Bivalvia, and the Annelida abundance data scattered further from the 1:1 line between inclusive and exclusive in Fig. 2.11.

As an aggregate at the phylum level, the variation between the data sets should have been reduced. However, variation was introduced by the differential filters applied to each metabarcoding data set: OTUs identified as Annelida but with lower confidence scores were excluded from the exclusive set, unevenly reducing the number of reads in each sample and producing artificially high and low proportions of relative abundance, resulting in more data scatter and less agreement on ecological drivers of abundance between data sets.

For taxa which are abundant in the system being studied, aggregation of metabarcoding data at low taxonomic levels may lead to more robust results, but aggregation at a higher level may have the opposite effect, particularly when using strictly filtered data.

Morphological vs. metabarcoding data

Abundance data for A. tonsa were not consistently over- or under- estimated by either morphological or metabarcoding methods. While none of the environmental drivers were contradictory between data sets for *A. tonsa*, each data set only consistently identified salinity as a driver of *A. tonsa* abundance. They each identified different additional drivers, including the expected relationships between *A. tonsa* abundance, river mile, and salinity in simple regressions of the inclusive data. The amount of disagreement between methods about the drivers of *A. tonsa* abundance is surprising given that it was the dominant species in the system; with ample data the patterns should be more clear.

The spread of data in the Bivalvia abundance scatter plots of Fig. 2.10 indicated there were samples for which Bivalvia existed in the metabarcoding data, but not in the morphological. Accordingly, there were no significant drivers of Bivalvia identified in the morphological data. However, the inclusive and exclusive data sets both identified an array of significant drivers, in

good agreement with each other and in the patterns we expect to see for Bivalvia. CO1 metabarcoding was likely able to detect the presence of Bivalvia more reliably than the morphological method due to the overall larger aliquots processed; Bivalvia were abundant but not dominant in the system, and the likelihood of their appearing in a random aliquot of 200 animals was low. The greater detection capability of metabarcoding allowed for the detection of drivers of abundance which would otherwise have gone unseen.

Annelida data had a similar spread to that of Bivalvia, but with more zero-abundance data points in the morphological data set. Unsurprisingly, there was only one significant driver found for abundance of Annelida in the morphological data set: salinity. As discussed previously, the inclusive and exclusive data sets were also generally unaligned as to the drivers, except for dissolved oxygen which was consistently significant and had the same slope direction. In this case, metabarcoding was able to detect Annelida more reliably than the morphological method, however the differential filtering applied to each data set produced different patterns of abundance which pointed to differing drivers of said abundance in the system. Given the amount of disagreement between all three data sets, it is difficult to say what the correct drivers of Annelida abundance actually were.

Morphological data performed well only for dominant taxa which were likely to appear in a 200-organism aliquot. Metabarcoding performed well for the abundant taxa tested here, except for those with uncertain taxonomic identifications. The shortcomings of morphological data could be easily circumvented by processing more than one aliquot per sample, perhaps simultaneously with two or more workers, however this would not affect the cost or efficiency of the method.

Time and cost

Identification of zooplankton by metabarcoding required less time per sample overall, and less active handling time per sample than morphological identification, making the process far more efficient. In addition to the lower processing time per-sample, samples are frequently processed simultaneously, further increasing the efficiency of this method as noted in prior work (Ershova et al. 2021). Although the cost per sample was about the same between methods, the simultaneous processing of metabarcoding samples also drives down the overall cost of sample processing as the number of samples increases (Ershova et al. 2021).

Conclusions

Although we can identify underlying causes of community mismatches and differences in ecological drivers of zooplankton abundance, it is clear that when these methods are performed in isolation, the communities revealed have a different resolution, a different structure, and the drivers of zooplankton abundance are potentially misleading. Integrated approaches which make use of both morphological and metabarcoding data are likely the best way forward for ecological investigations.

Metabarcoding is undeniably cheaper and faster when samples are processed in bulk. The larger sample size, higher diversity, and greater species richness captured by metabarcoding is useful, particularly when a body of work is primarily concerned with such questions. However, when answering ecological questions the quality of this data remains uncertain. When considering species or phyla level identifications, conclusions to ecological questions can be entirely different in metabarcoding data; morphological data remains relatively consistent, particularly if larger sample size or replicates are used. However, when taxa are aggregated at

low taxonomic levels such as class, metabarcoding data could potentially outperform traditional methods; further testing is required with larger sample sizes for the morphological data to ascertain whether the drivers of class-level abundance identified by metabarcoding are reflected in the morphological data.

When using metabarcoding data, strict filtering led to fewer significant results and possibly more results which ran counter to prior research. Therefore, inclusive filtering should be used as opposed to strict filtering. Such filtering inconsistencies could also be amended by expansion of reference databases to include estuarine zooplankton species, particularly understudied species such as annelids, so that matches between reference databases and study data are strong enough to pass strict filtering.

Acknowledgements

Particular thanks to Ben Lee, who performed the zooplankton metabarcoding and kept track of the associated time and costs. Special thanks also to Courtney Atkinson for coordinating safety procedures for sample processing during COVID, to Richie Long for fieldwork support and rescue, and to Dr. Jamie Pierson, Dr. Louis Plough, and Ben Lee for being my constant companions in the field- from beautiful spring mornings to battling jelly swarms and everything in between. This project was supported by the Maryland Sea Grant "*Novel Genomic Tools to Assess Fish Diet and Prey Quality in the Choptank River*" (https://www.mdsg.umd.edu/research-projects/2018/rfish-109).

References

Ahlstrom, E. H., and J. R. Thrailkill. 1963. Plankton volume loss with time of preservation. Pages 57–73.

Andries, J.-C. 2001. Endocrine and environmental control of reproduction in Polychaeta. Canadian Journal of Zoology 79:254–270.

Balvay, P. G. 1987. Equivalence parameters to estimate total abundance of zooplankton 49.

Bernard, I., J.-C. Massabuau, P. Ciret, M. Sow, A. Sottolichio, S. Pouvreau, and D. Tran. 2016. In situ spawning in a marine broadcast spawner, the Pacific oyster *C rassostrea gigas* : Timing and environmental triggers: Spawning in Oysters. Limnology and Oceanography 61:635–647.

Bucklin, A., P. K. Lindeque, N. Rodriguez-Ezpeleta, A. Albaina, and M. Lehtiniemi. 2016. Metabarcoding of marine zooplankton: prospects, progress and pitfalls. Journal of Plankton Research 38:393–400.

Bucklin, A., K. T. C. A. Peijnenburg, K. N. Kosobokova, T. D. O'Brien, L. Blanco-Bercial, A. Cornils, T. Falkenhaug, R. R. Hopcroft, A. Hosia, S. Laakmann, C. Li, L. Martell, J. M. Questel, D. Wall-Palmer, M. Wang, P. H. Wiebe, and A. Weydmann-Zwolicka. 2021. Toward a global reference database of COI barcodes for marine zooplankton. Marine Biology 168:78.

Bucklin, A., D. Steinke, and L. Blanco-Bercial. 2011. DNA Barcoding of Marine Metazoa. Annual Review of Marine Science 3:471–508.

Bucklin, A., H. D. Yeh, J. M. Questel, D. E. Richardson, B. Reese, N. J. Copley, and P. H. Wiebe. 2019. Time-series metabarcoding analysis of zooplankton diversity of the NW Atlantic continental shelf. ICES Journal of Marine Science 76:1162–1176.

Callahan, B. J., P. J. McMurdie, M. J. Rosen, A. W. Han, A. J. A. Johnson, and S. P. Holmes. 2016. DADA2: High-resolution sample inference from Illumina amplicon data. Nature Methods 13:581–583.

Campfield, P. A., and E. D. Houde. 2011. Ichthyoplankton community structure and comparative trophodynamics in an estuarine transition zone. Fishery Bulletin 109:1–19.

Childress, J. J., and B. A. Seibel. 1998. Life at Stable low Oxygen Levels: Adaptations of Animals to Oceanic Oxygen Minimum Layers. Journal of Experimental Biology 201:1223–1232.

Compson, Z. G., B. McClenaghan, G. A. C. Singer, N. A. Fahner, and M. Hajibabaei. 2020. Metabarcoding From Microbes to Mammals: Comprehensive Bioassessment on a Global Scale. Frontiers in Ecology and Evolution 8:581835.

DeBoyd, S. L. 1977. A guide to marine coastal plankton and marine invertebrate larvae. Kendall/Hunt Publishing Company, Dubuque, Iowa, USA.

Dorfman, D., A. Mabrouk, L. Bauer, C. Clement, D. M. Nelson, and L. Claflin. 2016. Choptank Ecological Assessment: Digital Atlas- Baseline Status Report.

Downie, A. T., W. W. Bennett, S. Wilkinson, M. De Bruyn, and J. D. DiBattista. 2024. From land to sea: Environmental DNA is correlated with long-term water quality indicators in an urbanized estuary. Marine Pollution Bulletin 207:116887.

Elliott, D. T., J. J. Pierson, and M. R. Roman. 2012. Relationship between environmental conditions and zooplankton community structure during summer hypoxia in the northern Gulf of Mexico. Journal of Plankton Research 34:602–613.

Ershova, E. A., O. S. Wangensteen, R. Descoteaux, C. Barth-Jensen, and K. Præbel. 2021. Metabarcoding as a quantitative tool for estimating biodiversity and relative biomass of marine zooplankton. ICES Journal of Marine Science.

Folmer, O., M. Black, W. Hoeh, R. Lutz, and R. Vrijenhoek. 1994. DNA primers for amplification of mitochondrial cytochrome c oxidase subunit I from diverse metazoan invertebrates. Molecular Marine Biology and Biotechnology:6.

Frøslev, T. G., R. Kjøller, H. H. Bruun, R. Ejrnæs, A. K. Brunbjerg, C. Pietroni, and A. J. Hansen. 2017. Algorithm for post-clustering curation of DNA amplicon data yields reliable biodiversity estimates. Nature Communications 8:1188.

Gao, X., H. Lin, K. Revanna, and Q. Dong. 2017. A Bayesian taxonomic classification method for 16S rRNA gene sequences with improved species-level accuracy. BMC Bioinformatics 18:247.

Hensen. (n.d.). First reference to stempel pipette.

Hirai, J., K. Hidaka, S. Nagai, and Y. Shimizu. 2021. DNA/RNA metabarcoding and morphological analysis of epipelagic copepod communities in the Izu Ridge off the southern coast of Japan. ICES Journal of Marine Science:fsab064.

Johnson, W. S., and D. M. Allen. 2012. Zooplankton of the Atlantic and Gulf coasts: a guide to their identification and ecology, second edition. Johns Hopkins University Press, Baltimore, Maryland USA.

Jung, S., and E. D. Houde. 2003. Spatial and temporal variabilities of pelagic fish community structure and distribution in Chesapeake Bay, USA. Estuarine, Coastal and Shelf Science 58:335–351.

Leray, M., N. Knowlton, and R. J. Machida. 2022. MIDORI2: A collection of quality controlled, preformatted, and regularly updated reference databases for taxonomic assignment of eukaryotic mitochondrial sequences. Environmental DNA 4:894–907.

Leray, M., J. Y. Yang, C. P. Meyer, S. C. Mills, N. Agudelo, V. Ranwez, J. T. Boehm, and R. J. Machida. 2013. A new versatile primer set targeting a short fragment of the mitochondrial COI region for metabarcoding metazoan diversity: Application for characterizing coral reef fish gut contents. Frontiers in Zoology 10:1–14.

Machida, R. J., H. Kurihara, R. Nakajima, T. Sakamaki, Y.-Y. Lin, and K. Furusawa. 2021. Comparative analysis of zooplankton diversities and compositions estimated from complement DNA and genomic DNA amplicons, metatranscriptomics, and morphological identifications. ICES Journal of Marine Science:fsab084.

Mercier, A., and J.-F. Hamel. 2010. Synchronized breeding events in sympatric marine invertebrates: role of behavior and fine temporal windows in maintaining reproductive isolation. Behavioral Ecology and Sociobiology 64:1749–1765.

O'Donnell, J. L., R. P. Kelly, N. C. Lowell, and J. A. Port. 2016. Indexed PCR primers induce template- Specific bias in Large-Scale DNA sequencing studies. PLoS ONE 11:1–11.

Pennak, R. W. 1953. Fresh-water invertebrates of the United States. The Ronald Press Company, New York, New York, USA.

Perplexity. 2024. Perplexity.ai (versions from January 2024 until January 2025) [Large language model]. https://www.perplexity.ai/

Porter, T. M., and M. Hajibabaei. 2020. Putting COI Metabarcoding in Context: The Utility of Exact Sequence Variants (ESVs) in Biodiversity Analysis. Frontiers in Ecology and Evolution 8:248.

Questel, J. M., R. R. Hopcroft, H. M. DeHart, C. A. Smoot, K. N. Kosobokova, and A. Bucklin. 2021. Metabarcoding of zooplankton diversity within the Chukchi Borderland, Arctic Ocean: improved resolution from multi-gene markers and region-specific DNA databases. Marine Biodiversity 51:4.

Schroeder, A., D. Stanković, A. Pallavicini, F. Gionechetti, M. Pansera, and E. Camatti. 2020. DNA metabarcoding and morphological analysis - Assessment of zooplankton biodiversity in transitional waters. Marine Environmental Research 160:104946.

Stribling, J. B., S. R. Moulton, and G. T. Lester. 2003. Determining the quality of taxonomic data. Journal of the North American Benthological Society 22:621–631.

The Maryland Department of Natural Resources, Tidewater Ecosystem Assessment Division. Eyes on the Bay (www.eyesonthebay.net)

Thorp, J. H. and A. P. Covich. 2001. Ecology and classification of North American freshwater invertebrates, second edition. Academic Press, San Diego, California, USA.

U.S. EPA. 2017. National Lakes Assessment 2017. Laboratory Operations Manual. V.1.1. EPA 841-B-16-004. U.S. Environmental Protection Agency, Washington, DC.

U.S. Geological Survey, 2016, National Water Information System data available on the World Wide Web (USGS Water Data for the Nation), accessed June 24, 2023, at http://waterdata.usgs.gov/nwis/

Vandeputte, D., G. Kathagen, K. D'hoe, S. Vieira-Silva, M. Valles-Colomer, J. Sabino, J. Wang, R. Y. Tito, L. De Commer, Y. Darzi, S. Vermeire, G. Falony, and J. Raes. 2017. Quantitative microbiome profiling links gut community variation to microbial load. Nature 551:507–511.

Verberk, W. C. E. P., D. T. Bilton, P. Calosi, and J. I. Spicer. 2011. Oxygen supply in aquatic ectotherms: Partial pressure and solubility together explain biodiversity and size patterns 92:1565–1572.

Whitfield, A. K., M. Elliott, A. Basset, S. J. M. Blaber, and R. J. West. 2012. Paradigms in estuarine ecology – A review of the Remane diagram with a suggested revised model for estuaries. Estuarine, Coastal and Shelf Science 97:78–90.

Tables

A)

	All samples	
	Morphological	*Inclusive*
Total taxa (species richness)	37	127
Unique taxa	28	118
Shared taxa	9	
Jaccard index	5.8	

B)

	All samples	
	Morphological	*Exclusive*
Total taxa (species richness)	37	74
Unique taxa	33	70
Shared taxa	4	
Jaccard index	3.7	

Table 2.1: Tables showing species richness and results of Jaccard testing on all samples in common between A) morphological and inclusive data sets, and B) morphological and exclusive data sets.

A)

	64		200	
	Morphological	*Inclusive*	*Morphological*	*Inclusive*
Total taxa	28	100	30	102
Unique taxa	22	94	22	94
Shared taxa	6		8	
Jaccard index	4.9		6.5	

B)

	64		200	
	Morphological	*Exclusive*	*Morphological*	*Exclusive*
Total taxa	28	62	30	60
Unique taxa	26	94	56	60
Shared taxa	2		4	
Jaccard index	2.3		4.7	

Table 2.2: Table showing species richness and results of Jaccard testing on all samples in common between A) morphological and inclusive data sets, and B) morphological and exclusive data sets, split into size fractions. 64 indicates microzooplankton (64-200 μm), 200 indicates mesozooplankton (> 200 μm).

Dataset	Model type	Abundance measure	Environmental parameter	Linear regression		Type of dis/agreement	Patterns match?
				p	slope		
Inclusive	simple	Concentration (ind./m³)	Dissolved oxygen (mg/L)	0.0324	-0.0802	no; inclusive only	
			Chlorophyll a (µg/L)	0.0219	-0.0167		
			River mile	0.0024	0.0166		
		Biomass (mg)	Dissolved oxygen (mg/L)	0.0324	-0.0802		
			Chlorophyll a (µg/L)	0.0219	-0.0167		
			River mile	0.0024	0.0166		

Table 2.3: Table showing significant results of linear regression models on Shannon diversity scores for biomass (mg) and concentration (individuals/m³) data vs. continuous environmental parameters for each data set.

Comparison	Abundance measure	coefficient	p	
Morphological vs Inclusive	Abundance (ind./m²)	-0.085	5.93E-01	
	Concentration (ind./m³)	-0.110	4.88E-01	
	Biovolume (mL)	0.706	1.80E-07	*
	Biomass (mg)	0.671	2.37E-06	*
	Biomass concentration (mg/m³)	0.642	7.73E-06	*
Morphological vs Exclusive	Abundance (ind./m²)	-0.067	6.73E-01	
	Concentration (ind./m³)	-0.095	5.48E-01	
	Biovolume (mL)	0.707	1.66E-07	*
	Biomass (mg)	0.671	2.37E-06	*
	Biomass concentration (mg/m³)	0.642	7.73E-06	*

Table 2.4: Spearman correlation coefficients showing the relationship between total zooplankton abundance per sample in morphological vs. inclusive and morphological vs. exclusive data with each abundance measure. * indicates significant results.

Comparison	Abundance measure	slope	r^2	p		
Morphological vs Inclusive	Abundance (ind./m²)	-0.0872	0.0093	0.544		
	Concentration (ind./m³)	-0.0491	0.0073	0.591		
	Biovolume (mL)	1.12E-06	0.26	5.88E-04	*	x
	Biomass (mg)	3.61	0.27	3.77E-04	*	x
	Biomass concentration (mg/m³)	2.31	0.41	4.61E-06	*	x
Morphological vs Exclusive	Abundance (ind./m²)	-0.0626	0.0081	0.570		
	Concentration (ind./m³)	-0.0351	0.0064	0.614		
	Biovolume (mL)	8.70E-07	0.37	2.17E-05	*	x
	Biomass (mg)	3.61	0.27	3.77E-04	*	x
	Biomass concentration (mg/m³)	2.31	0.41	4.61E-06	*	x

Table 2.5: Linear regression results showing the relationship between total zooplankton abundance per sample in morphological vs. inclusive or morphological vs. exclusive data with each abundance measure. * indicates significant results, x indicates the model failed a homoscedasticity test.

Model type	Dataset	Abundance measure	Environmental parameter	Linear regression					Type of dis/agreement	Patterns match?
				p	slope	parameters	parameter p	parameter slope		
multiple	Inclusive	Biomass concentration	all except river mile, daily river flow, and average river flow for the month prior to sampling	0.033		Temperature	0.033	-0.15	no; inclusive and exclusive only	yes
						Dissolved oxygen	0.047	-0.33		
	Exclusive	Biomass concentration (mg/m^3)		0.033		Temperature	0.033	-0.15		
						Dissolved oxygen	0.047	-0.33		
simple	Morphological	Biomass (mg)	Temperature (C°)	7.46E-04	0.15				no; inclusive and exclusive only	yes
			Day of year	0.0203	9.56E-03					
		Biomass concentration	Temperature (C°)	4.69E-03	0.12					
			Day of year	0.0213	8.76E-03					
	Inclusive	Biomass (mg)	Dissolved oxygen (mg/L)	0.0326	-0.090					
	Exclusive	Biomass (mg)	Dissolved oxygen (mg/L)	0.0326	-0.090					

Table 2.6: Table showing significant results of linear regression models on total zooplankton abundance measures vs. continuous environmental parameters for each data set.

Model type	Dataset	Abundance measure	Environmental parameter	Linear regression					Type of dis/agreement	Patterns match?
				p	slope	parameters	parameter p	parameter slope		
multiple	Morphological	Biomass (mg)	all except river mile, daily river flow, and average river flow for the month prior to sampling	4.71E-03		Temperatur	4.70E-03	0.32	no	
						Salinity	0.033	0.24	yes; all	yes
	Inclusive	Biovolume (mL)		4.76E-03		Salinity	4.80E-03	0.29	no; inclusive and exclusive only	yes
		Biomass (mg)		0.0159		Salinity	0.016	0.10	yes; all	yes
	Exclusive	Biovolume (mL)		9.53E-03		Salinity	9.50E-03	0.25	no; inclusive and exclusive only	yes
		Biomass (mg)		0.0306		Salinity	0.031	0.087	yes; all	yes
simple	Morphological	Abundance (ind./m²)	Temperature (C°)	5.84E-04	0.10				no	
			Dissolved oxygen (mg/L)	8.56E-04	-0.26					
		Concentration (ind./m³)	Temperature (C°)	5.89E-04	0.10					
			Dissolved oxygen (mg/L)	8.57E-04	-0.26					
		Biovolume (mL)	Day of year	0.0130	3.25E-03					
		Biomass (mg)	Temperature (C°)	2.47E-05	0.22					
			Day of year	3.60E-03	0.014					
		Biomass concentration	Temperature (C°)	3.59E-04	0.15					
			Day of year	4.80E-03	0.011					
	Inclusive	Biovolume (mL)	Salinity	0.0296	0.12					
			River mile	0.0341	-0.035					
	Exclusive	Biomass (mg)	Dissolved oxygen (mg/L)	0.0361	-0.090					

Table 2.7: Table showing significant results of linear regression models on *Acartia tonsa* abundance measures vs. continuous environmental parameters for each data set.

Model type	Dataset	Abundance measure	Environmental parameter	Linear regression					Type of dis/agreement	Patterns match?
				p	slope	parameters	parameter p	parameter slope		
multiple	Inclusive	Biovolume	all except river mile, daily river flow, and average river flow for the month prior to sampling	0.0100		Day of year	0.01	0.025	no; inclusive and exclusive only	yes
		Biomass (mg)		0.0132		Day of year	0.013	0.013		
		Biomass concentration (mg/m³)		4.32E-03		Day of year	0.0043	0.013		
	Exclusive	Biovolume (mL)		6.53E-03		Day of year	0.0065	0.028		
		Biomass (mg)		9.32E-03		Day of year	0.0093	0.013		
		Biomass concentration (mg/m³)		3.14E-03		Day of year	0.0031	0.013		
simple	Inclusive	Abundance (ind./m²)	Temperature (C°)	0.0420	0.109				no; inclusive and exclusive only	yes
			Day of year	0.0131	0.0115				no; inclusive and exclusive only	yes
			Monthly mean river flow; prior month (ft³/s)	0.0299	-0.0049				no; inclusive and exclusive only	yes
		Concentration (ind./m³)	Temperature (C°)	0.0276	0.107				no; inclusive and exclusive only	yes
			Day of year	9.65E-03	0.0110				no; inclusive and exclusive only	yes
			Monthly mean river flow; prior month (ft³/s)	0.0425	-0.0042				no; inclusive and exclusive only	yes
		Biovolume (mL)	Temperature (C°)	0.0155	0.175				no; inclusive and exclusive only	yes
			Dissolved oxygen (mg/L)	0.0103	-0.468				no; inclusive and exclusive only	yes
		Biomass (mg)	Temperature (C°)	3.41E-03	0.110				no; inclusive and exclusive only	yes
			Dissolved oxygen (mg/L)	4.01E-03	-0.2751				no; inclusive and exclusive only	yes
			Day of year	3.13E-05	0.0129				no; inclusive and exclusive only	yes
			Monthly mean river flow; prior month (ft³/s)	0.0169	-0.0039				no; inclusive and exclusive only	yes
	Exclusive	Abundance (ind./m²)	Temperature (C°)	0.0427	0.110				no; inclusive and exclusive only	yes
			Day of year	0.0109	0.0120				no; inclusive and exclusive only	yes
			Monthly mean river flow; prior month (ft³/s)	0.0236	-0.0052				no; inclusive and exclusive only	yes
		Concentration (ind./m³)	Temperature (C°)	0.0282	0.108				no; inclusive and exclusive only	yes
			Day of year	7.82E-03	0.0114				no; inclusive and exclusive only	yes
			Monthly mean river flow; prior month (ft³/s)	0.0330	-0.0045				no; inclusive and exclusive only	yes
		Biovolume (mL)	Temperature (C°)	0.0134	0.186				no; inclusive and exclusive only	yes
			Dissolved oxygen (mg/L)	9.62E-03	-0.493				no; inclusive and exclusive only	yes
			Day of year	3.18E-05	0.0254				no; exclusive only	
		Biomass (mg)	Temperature (C°)	3.22E-03	0.113				no; inclusive and exclusive only	yes
			Dissolved oxygen (mg/L)	3.74E-03	-0.284				no; inclusive and exclusive only	yes
			Day of year	2.08E-05	0.0135				no; inclusive and exclusive only	yes
			Monthly mean river flow; prior month (ft³/s)	0.0122	-0.0041				no; inclusive and exclusive only	yes

Table 2.8: Table showing significant results of linear regression models on Bivalvia abundance measures vs. continuous environmental parameters for each data set.

Model type	Dataset	Abundance measure	Environmental parameter	Linear regression					Type of dis/agreement	Patterns match?
				p	slope	parameters	parameter p	parameter slope		
multiple	Inclusive	Abundance (ind./m²)	all except river mile, daily river flow, and average river flow for the month prior to sampling	0.0250		Temperatur	0.049	0.23	no; inclusive and	yes
						Max. cast depth	0.025	0.28	no; inclusive and exclusive only	yes
		Biovolume (mL)		5.16E-04		Temperatur e	0.046	-0.23		
						Salinity	5.00E-04	0.430	no; inclusive and exclusive only	yes
						Dissolved oxygen	0.0016	-0.90	no; inclusive and exclusive only	yes
		Biomass (mg)		1.08E-03		Salinity	0.0011	0.20	no; inclusive and exclusive only	yes
						Dissolved oxygen	0.0051	-0.40	no; inclusive and exclusive only	yes
	Exclusive	Abundance (ind./m²)		6.26E-05		Temperatur e	1.00E-04	0.44	no; inclusive and exclusive only	yes
						Salinity	0.0085	0.26		
						Max. cast depth	0.0067	0.29	no; inclusive and exclusive only	yes
		Concentration (ind./m³)		6.84E-05		Temperatur e	1.00E-04	0.41		
						Salinity	0.011	0.24		
						Max. cast depth	0.045	0.20		
		Biovolume (mL)		1.64E-04		Salinity	2.00E-04	0.51	no; inclusive and exclusive only	yes
						Dissolved oxygen	0.0015	-0.98	no; inclusive and exclusive only	yes
						Day of year	2.00E-04	-0.030		
						Monthly river flow	0.010	-0.010		
		Biomass (mg)		5.35E-05		Salinity	1.00E-04	0.26	no; inclusive and exclusive only	yes
						Dissolved oxygen	0.0025	-0.42	no; inclusive and exclusive only	yes
						Day of year	3.00E-04	-0.013		
						Monthly river flow	0.027	-0.004		
simple	Morphological	Concentration (ind./m³)	Salinity	1.61E-04	0.23					
	Inclusive	Abundance (ind./m²)	Max. cast depth (m)	3.93E-02	0.24					
		Biovolume (mL)	Salinity	4.36E-06	0.38					
		Biomass (mg)	Salinity	1.70E-05	0.17					
		Biomass concentration (mg/m³)	Salinity	1.43E-03	0.14				no; inclusive and exclusive only	yes
			Secchi depth (m)	4.44E-03	1.42					
	Exclusive	Abundance (ind./m²)	Temperature (C°)	7.40E-03	0.13					
		Concentration (ind./m³)	Temperature (C°)	5.95E-03	0.13					
		Biomass concentration (mg/m³)	Salinity	2.74E-04	0.15				no; inclusive and exclusive only	yes

Table 2.9: Table showing significant results of linear regression models on Annelida abundance measures vs. continuous environmental parameters for each data set.

Figures

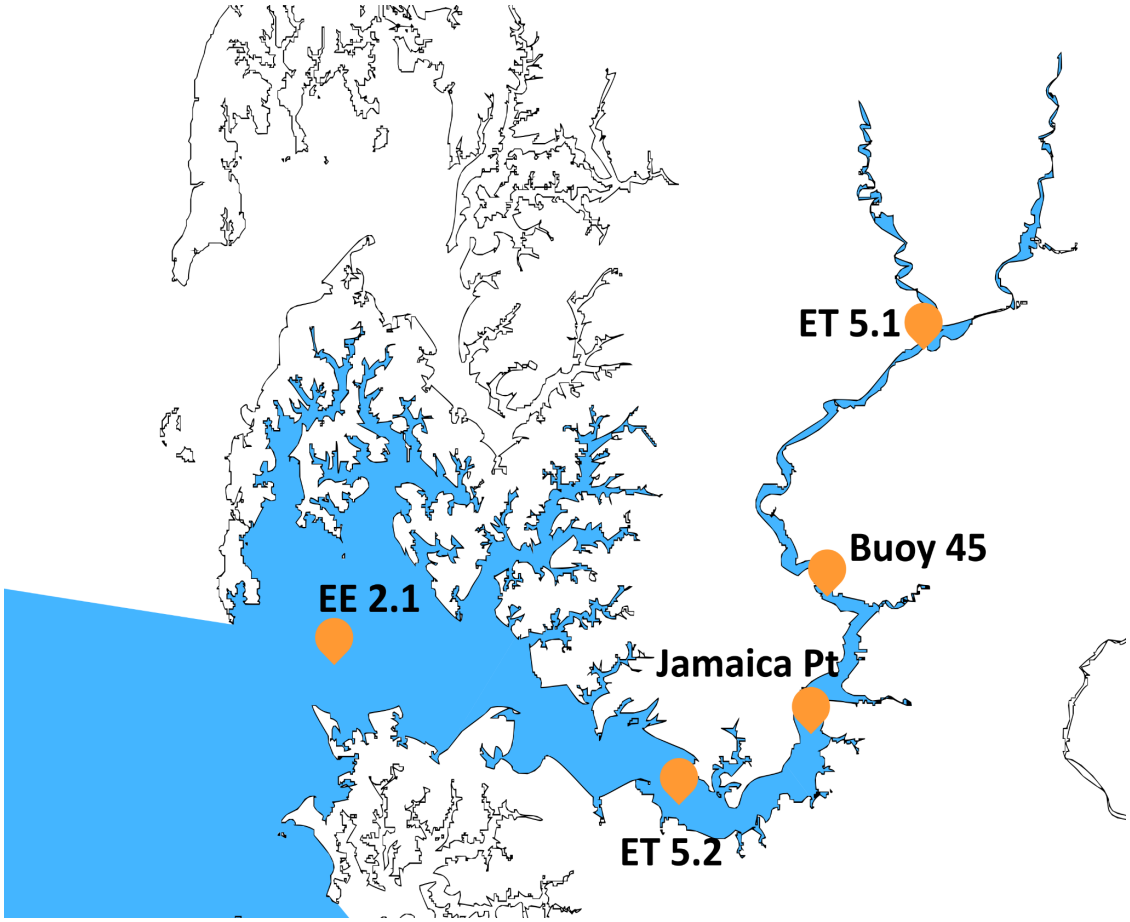

Fig. 2.1: Map of the Choptank River with station locations.

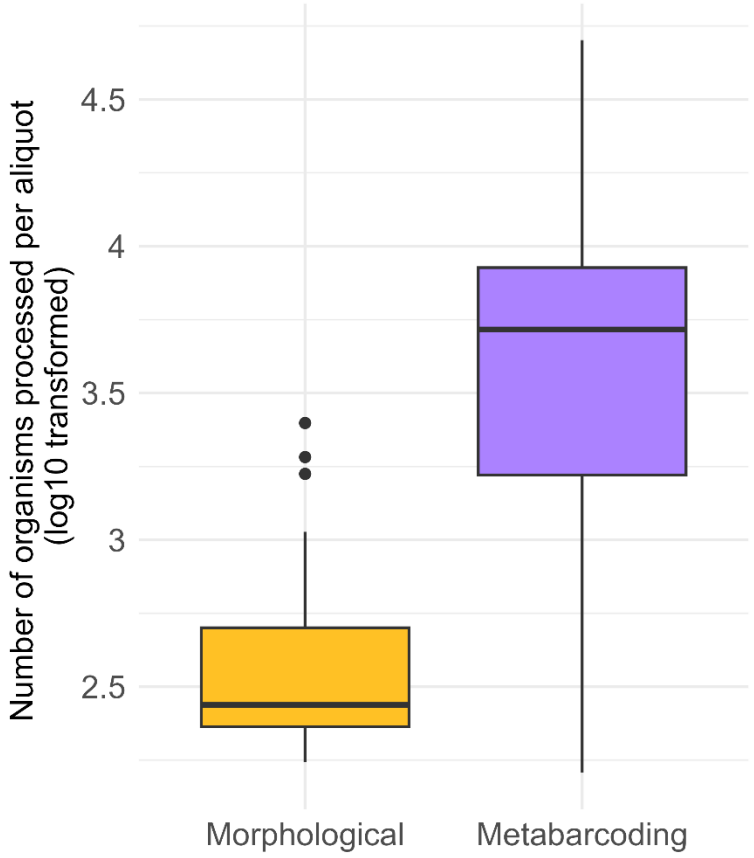

Fig. 2.2: Boxplot depicting the number of organisms processed from each sample across all shared samples for morphological and metabarcoding data sets. Y-axis log10 transformed.

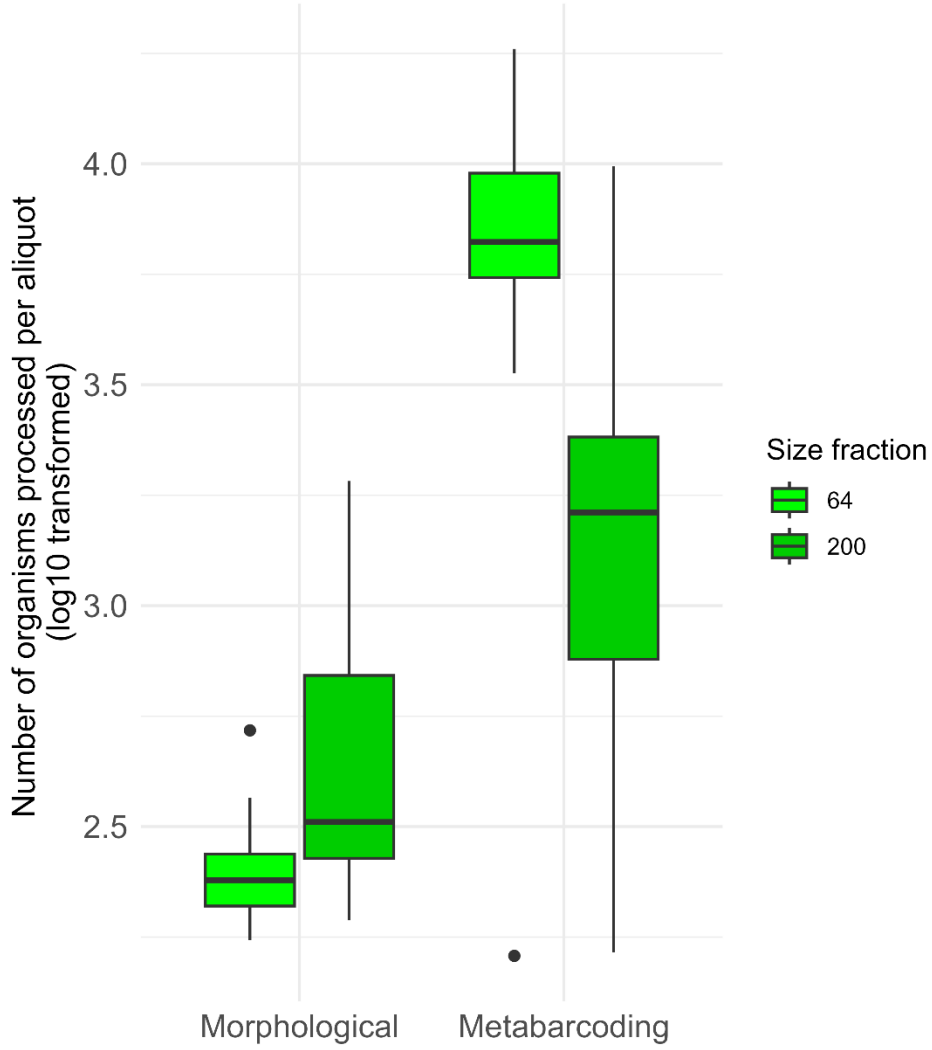

Fig. 2.3: Boxplot depicting the number of organisms processed in each sample across all shared samples for morphological and metabarcoding data sets, shown by size fraction. Whole, unfractionated samples excluded. Y-axis log10 transformed.

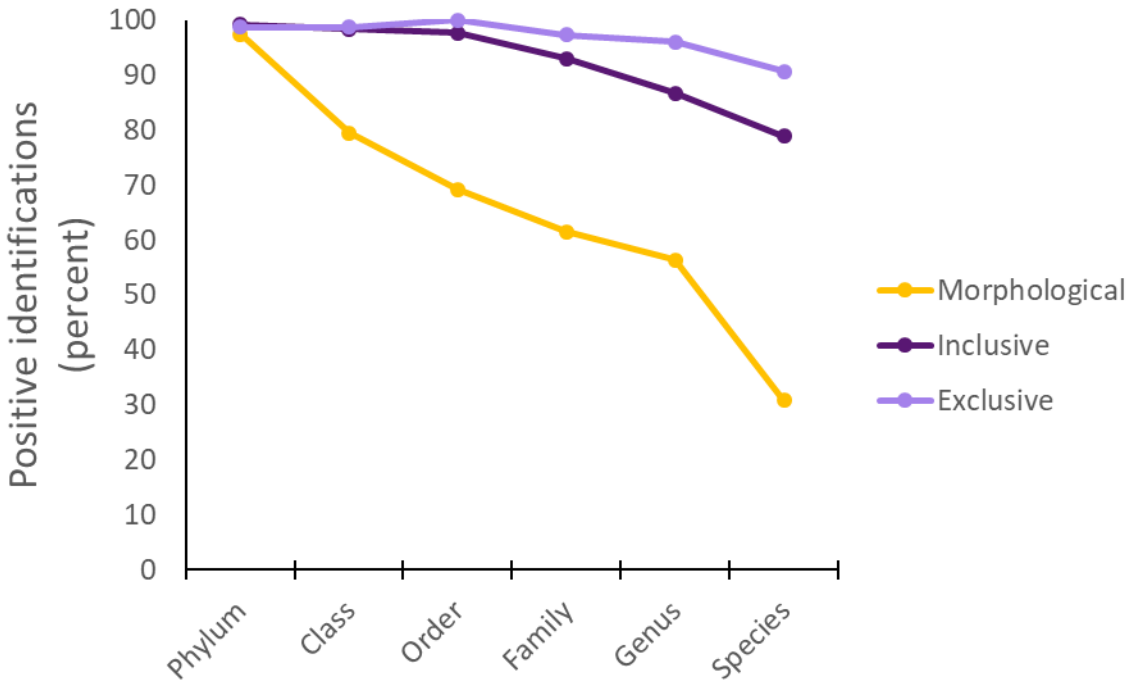

Fig. 2.4: Taxonomic resolution in each of the three data sets. Percent positive identifications are the number of identifications made to each taxonomic level, across the entirety of each data set. E.g. almost 100% of organisms in each data set were identified at the Phylum level, but the morphological data set had about 79% of organisms identified at the Phylum level and at the Class level; 21% of organisms were classified as "Unknown" at Class level and below.

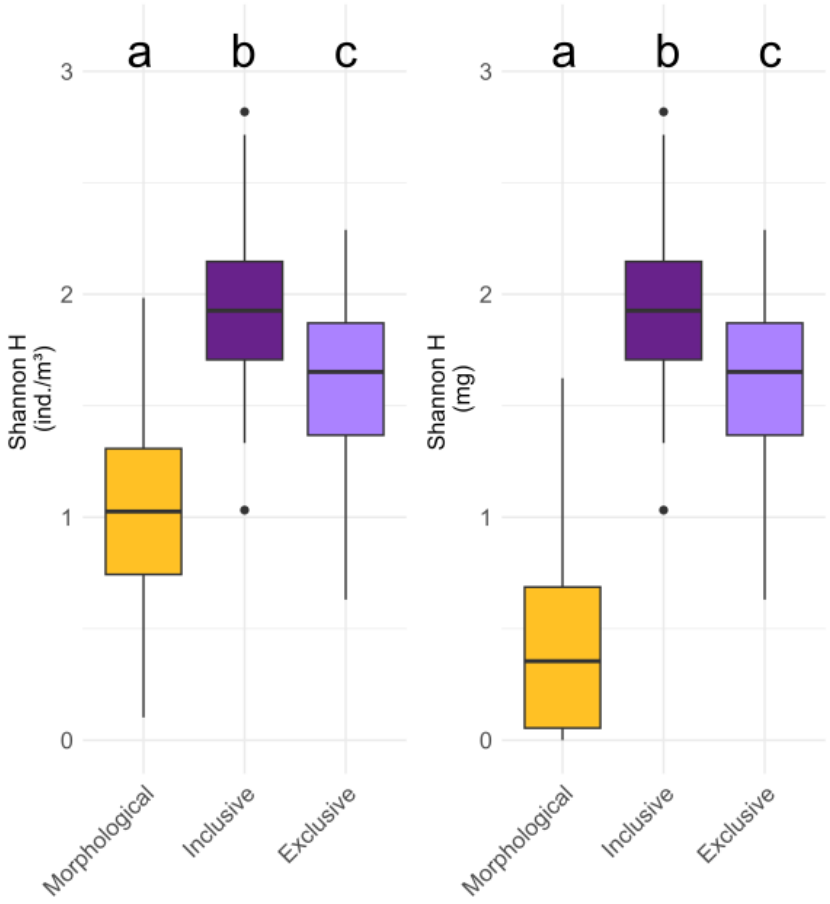

Fig. 2.5: Boxplots showing results of ANOVA testing on per-sample Shannon scores, grouped by data set and plotted for biomass (mg) and concentration (individuals/m³) measures. Post-hoc pairwise Wilcoxon testing results reflected in a, b, c groupings; members of different groups are significantly different.

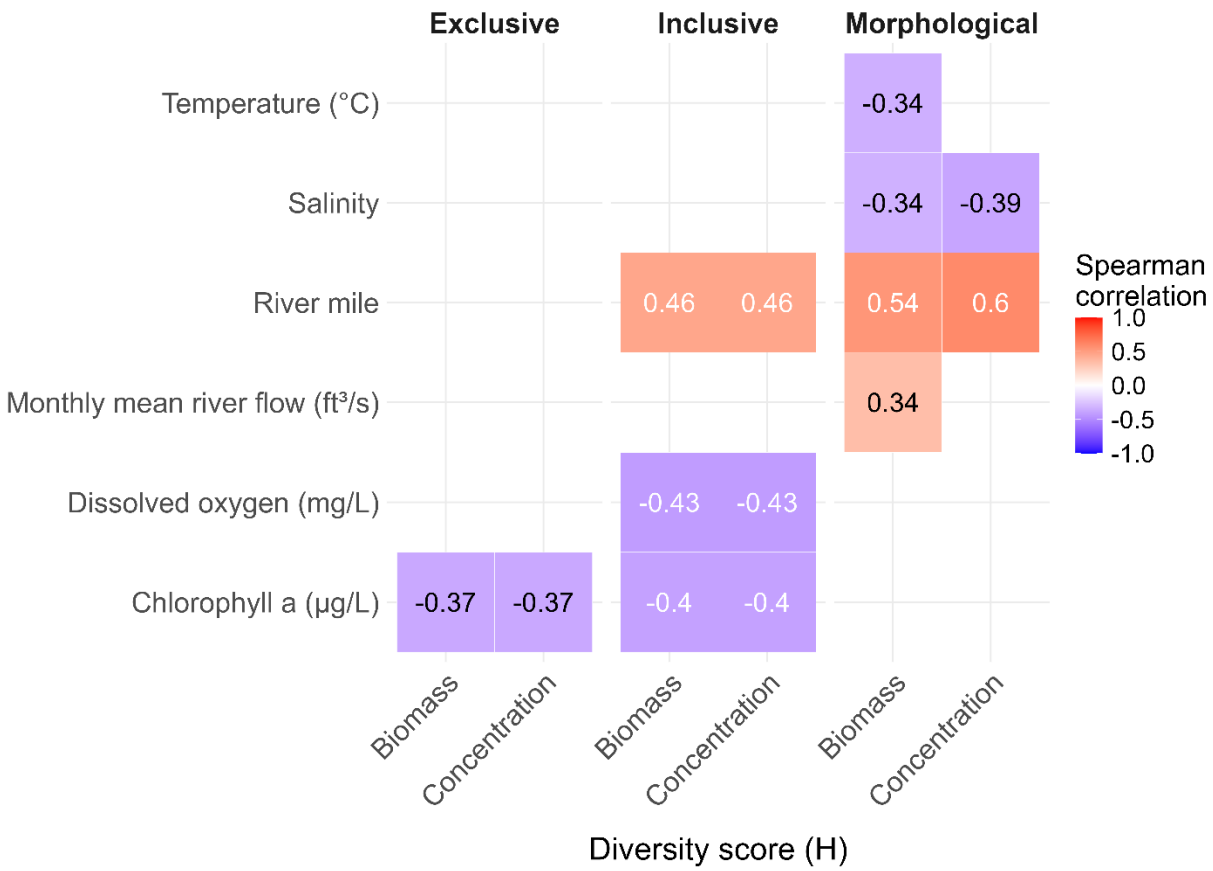

Fig. 2.6: Heatmap showing only significant results of Spearman correlation testing on per-sample Shannon scores vs environmental parameters for each data set. X-axis shows diversity scores calculated from concentration (individuals/m³) and biomass (mg) for each data set.

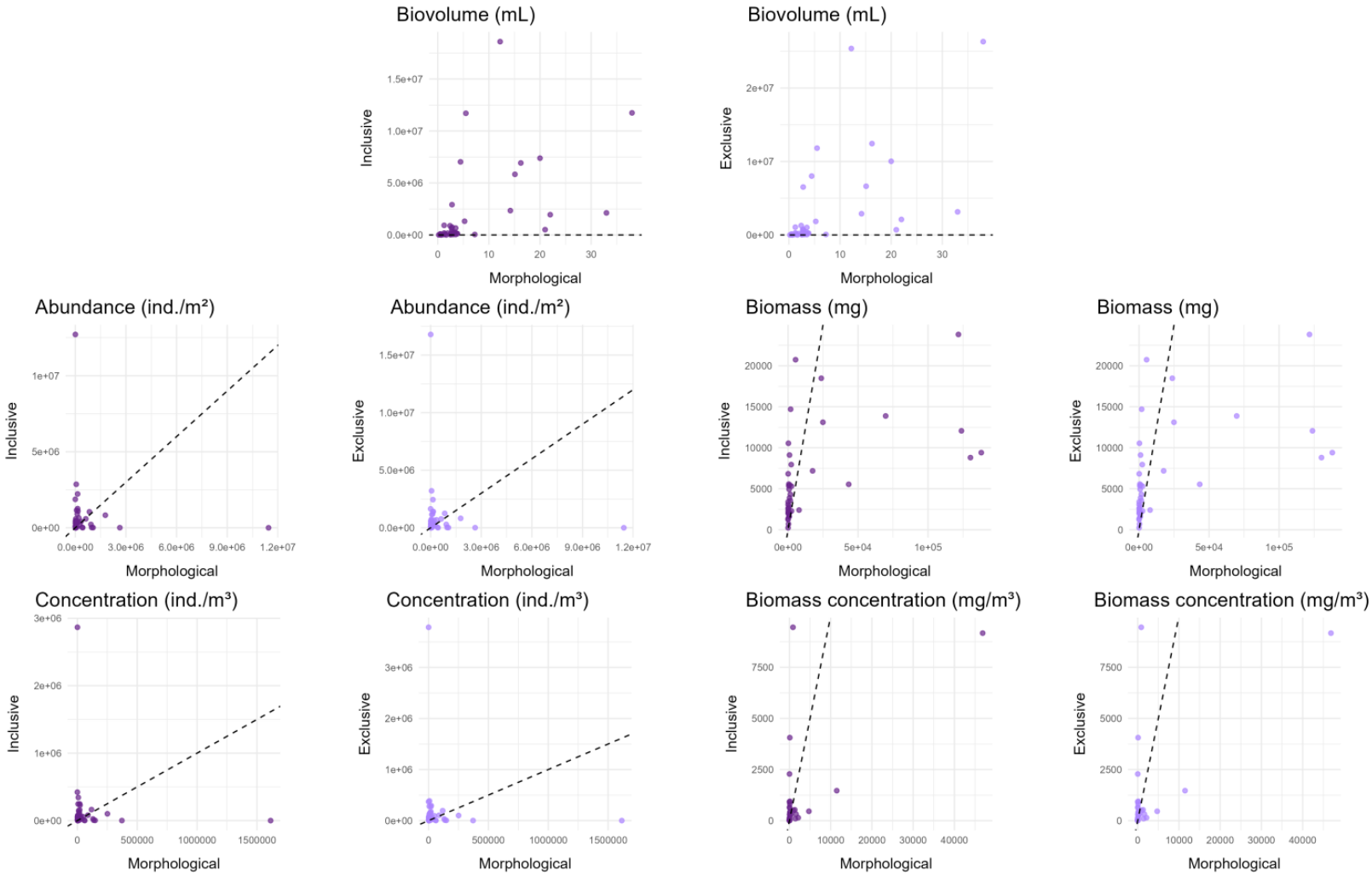

Fig. 2.7: Paired scatter plots of morphological vs. inclusive (left, dark purple) and morphological vs exclusive (right, light purple) data across five abundance measures for the total zooplankton in each sample.

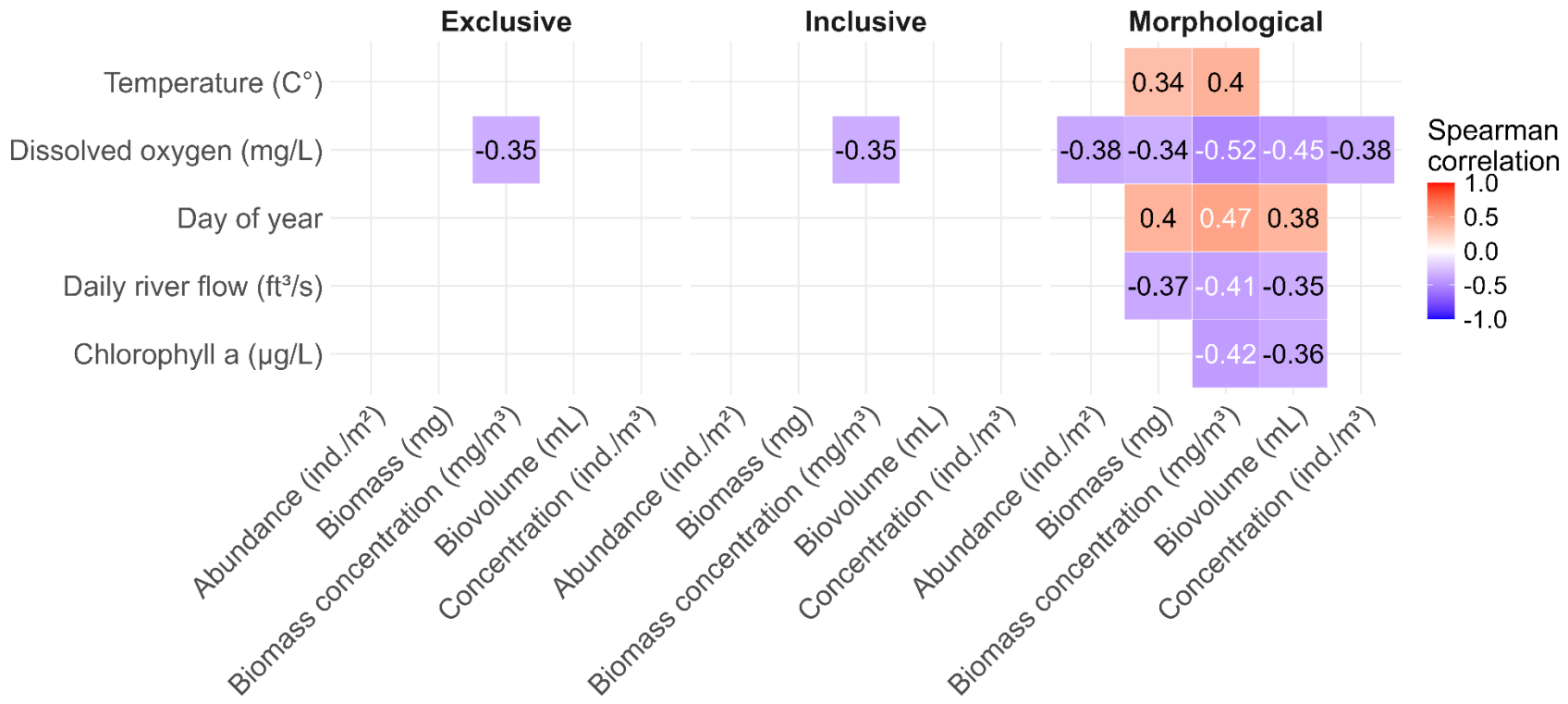

Fig. 2.8: Heatmap showing only significant results of Spearman correlation testing on total zooplankton abundance vs environmental parameters for all three data sets.

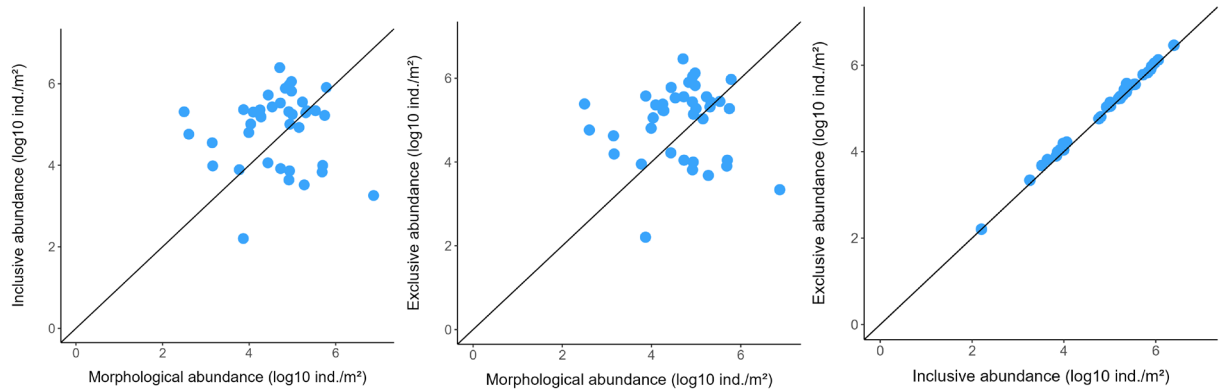

Fig. 2.9: Scatter plots showing log10+1 transformed abundance (ind./m²) data for *Acartia tonsa*, plotted for each combination of data set.

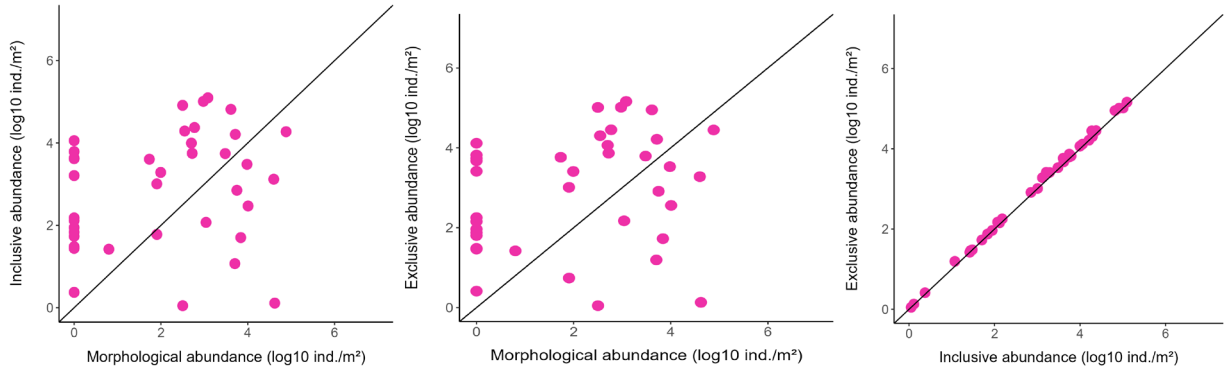

Fig. 2.10: Scatter plots showing log10+1 transformed abundance (ind./m²) data for Bivalvia, plotted for each combination of data set.

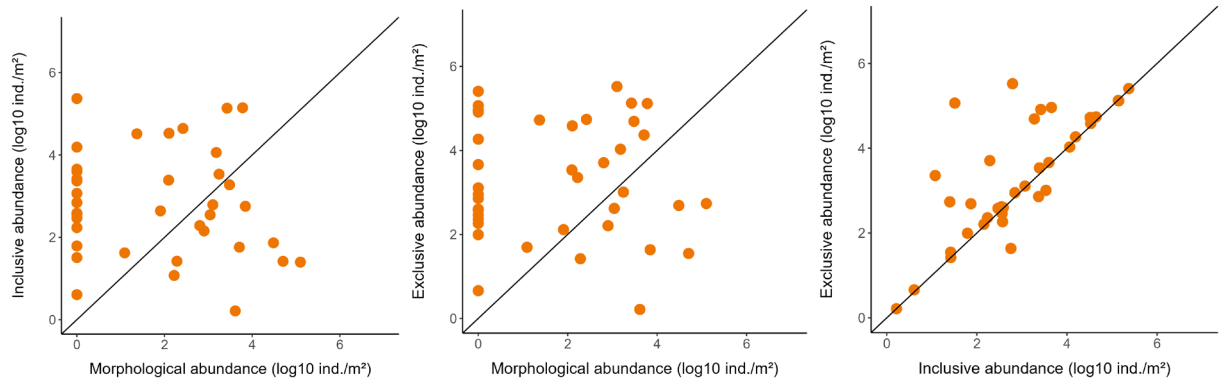

Fig. 2.11: Scatter plots showing log10+1 transformed abundance (ind./m²) data for Annelida, plotted for each combination of data set.

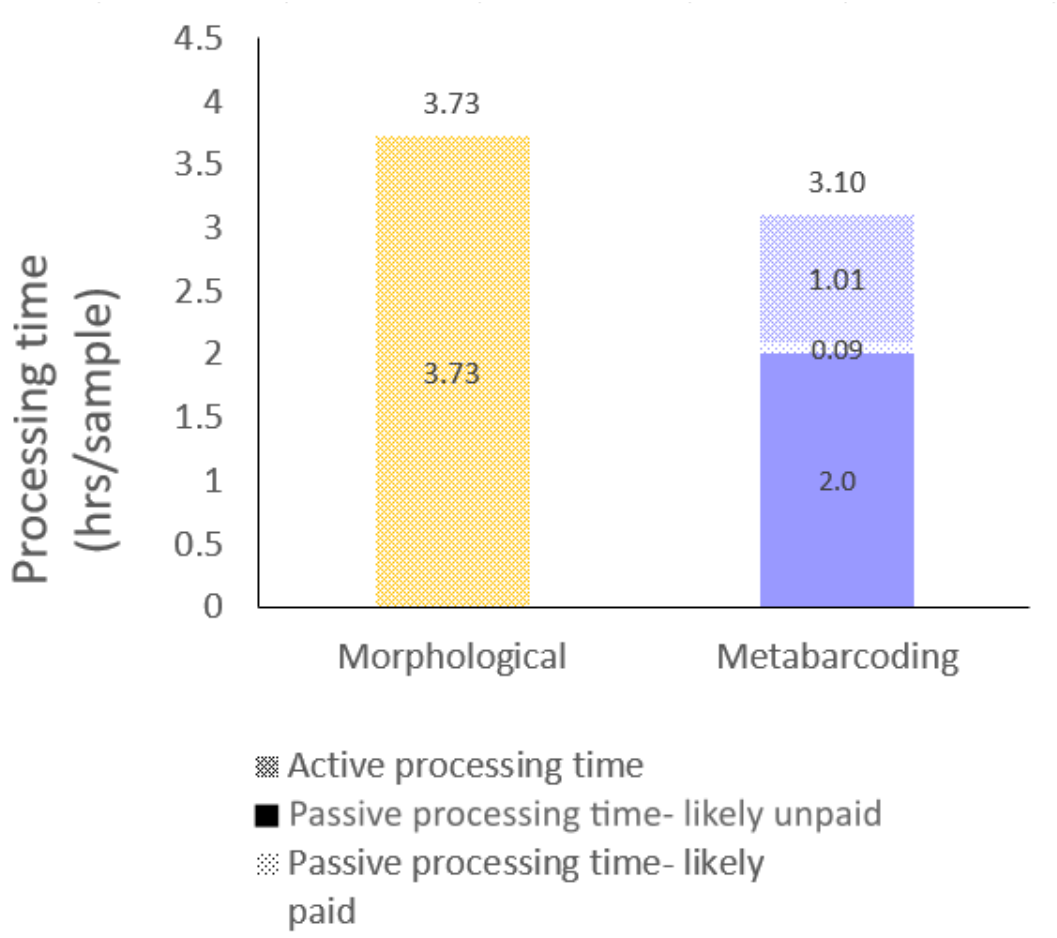

Fig. 2.12: Bar graph showing the processing time per sample for each method. Active processing time: time a worker spends actively handling the sample; passive processing time- likely paid: time a worker spends not actively handling the sample (e.g. waiting for a centrifuge cycle to complete), but still engaged with the task; passive processing time- likely unpaid; time a worker spends not actively handling the sample, and not engaged in the task (e.g. an overnight incubation).

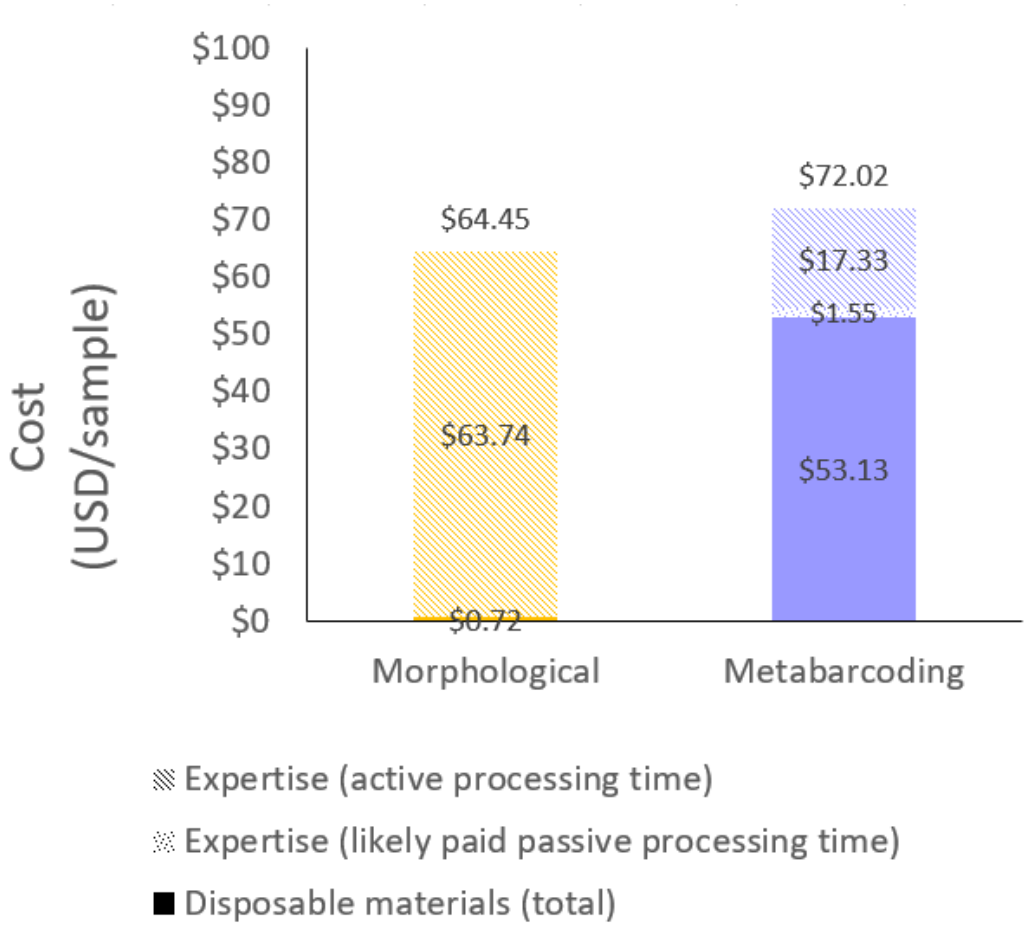

Fig. 2.13: Bar graph showing the cost per sample for each method in USD.

Chapter 3: Characterization of the zooplankton diets of larval striped bass (*Morone saxatilis*), white perch (*Morone americana*), and bay anchovy (*Anchoa mitchilli*)

Introduction

One of the largest remaining challenges in fisheries management is predicting recruitment to the adult population from a cohort of fish. Recruitment is influenced by many factors and so is famously difficult to predict; while estimates have improved over time they remain more accurate on decadal rather than annual timescales (Govoni 2005). For sensitive fisheries with high recruitment variability such as striped bass (> 30 fold fluctuations in annual recruitment; Shideler and Houde 2014a), annual predictions are necessary in order to implement management measures which accurately balance economic and conservation goals.

Recruitment, and hence contribution to adult population size, varies largely based on early life mortality (Hjort 1914, Hunt et al. 2011, Murphy et al. 2012, Hare 2014). Other studies suggest that migration and spawning-stock biomass also, and possibly to a greater degree, explain fluctuations in fishery abundances (Hare 2014), however cohorts consistently experience their highest and most variable mortality in the early life stages from egg to juvenile (Hjort 1914, Hunt et al. 2011, Murphy et al. 2012, Hare 2014). This mortality is driven both by physical conditions of the environment and by trophic relationships between the larvae, their predators, and their prey.

A complete lack of zooplankton prey can cause larval mortality by starvation, however this seems to be uncommon. Nursery grounds are generally rich in food resources and larval fish

do not have any top-down effects on their prey (Houde 1987, 2008), indicating they aren't consuming enough zooplankton to compete with each other or experience food limitation. Thus, in a prey-dense environment like the Choptank river, larval fish are unlikely to succumb to direct starvation. However, low quantity and quality of available prey could create a growth penalty for the larval fish; a penalty which increases the likelihood of mortality due to predation (Hjort 1914, Houde 2008).

The growth-mortality hypothesis states that slow-growing larvae remain smaller for longer periods of time, thus increasing the probability of being preyed upon by size-selective predators (Hjort 1914, Houde 2008). Larval fish predators in the Chesapeake Bay are generally gelatinous predators such as *Chrysaora chesapeakei* and piscivorous fishes (Rilling and Houde 1999). Fish tend to capture prey whole and therefore select prey on a size-limited basis determined by their mouth size (gape)(Setzler-Hamilton et al. 1982). This size-limited predation pressure is ontogenetic: piscivorous fish consume larvae until they outgrow the gape size of their predators. As per the growth-mortality hypothesis, ontogenetic predation pressure means that smaller larvae, and larvae which remain smaller for a longer portion of their early life relative to other members of their cohort, are expected to experience higher predation mortality (Robert et al. 2014). A lower growth rate due to prey quantity or quality will therefore increase the probability of mortality, which accounts for Houde's (1987) observation.

Indicators of prey quality such as size, elemental composition, and lipid quantity differ between zooplankton species and life stages (Sargent et al. 1985, Fraser et al. 1989, Kattner et al. 1989, Graeve et al. 1994, Cabrol et al. 2015). *M. americana* and *M. saxatilis* larvae were found

to have higher proportions of particular species and stages of zooplankton in their stomachs compared to the relative abundance of those zooplankton amongst the assemblage in the water column, indicating selective pressures for particular species (Setzler-Hamilton et al. 1982). Fish larvae are also known to shift their diets from one zooplankton species to another when a preferentially consumed zooplankton species is depleted beyond a given threshold (Robert et al. 2014). Preferentially consuming one or more species of zooplankton might be an indication of attempted optimal foraging: consuming prey which maximizes energy or nutrients gained relative to the energy spent in prey capture. Such optimization attempts could allow fish larvae to maximize their growth rate based on available prey; indeed, as the availability of favored prey increases, the growth rates of larvae increase as well(Harding 1999, Beaugrand et al. 2003, Martino and Houde 2010, Robert et al. 2014). However, if all available prey is of low quality, larvae are likely to grow slower and succumb to predation.

In this chapter, we examined the diets and feeding ecology of the larvae of three economically and ecologically important fish species which spawn in the Choptank River: striped bass (*Morone saxatilis*), white perch (*Morone americana*), and bay anchovy (*Anchoa mitchilli*). Larval fish samples were collected with net tows as part of the same 2018-2019 study outlined in Chapter 2. Fish were processed for gut contents using CO1 metabarcoding, their diets and ontogeny examined, and then their gut contents were compared to the set of water-column zooplankton samples processed with CO1 metabarcoding from Chapter 2 to clarify predator-prey relationships.

Methods

Fieldwork

Samples were collected from the Choptank River in Maryland, USA once a month from late spring through early fall (April-September) in 2018 and 2019 as part of the Maryland Sea Grant (MDSG) project: "*Novel Genomic Tools to Assess Fish Diet and Prey Quality in the Choptank River*". Five sites were sampled; three of the five were chosen to correspond to the Chesapeake Bay Program's Water Quality Monitoring Stations, while the other two stations were selected based on the location of the leading edge of the salinity front. A small craft equipped with a port-deploying winch was used courtesy of Horn Point Laboratory, University of Maryland Center for Environmental Science (UMCES).

At each site the water column salinity, temperature, and dissolved oxygen were collected at 1 m intervals from the surface to 1 m from the bottom with a YSI sonde probe, followed by a Tucker trawl tow (0.5 m^2 opening, 280 µm mesh net; towed for 5-20 min; equipped with flow meter) for fish larvae, and a plankton net tow (0.5 m diameter opening, 64 µm mesh net; towed for 5-20 min; equipped with flow meter) to collect zooplankton. Tucker trawl catches were anesthetized in pH-buffered MS-222 and preserved in 95% ethanol. Zooplankton catches were split using a Folsom plankton splitter into two samples, then each was filtered through a 200 µm sieve to create size-fractionated samples (≥ 200 µm; > 64 µm and < 200 µm). One set was preserved in 4% pH-buffered formalin for morphological identification, the other set was preserved in 95% ethanol for metabarcoding identification. Complete ethanol changes were performed for fish and zooplankton samples preserved in 95% ethanol within a week of sampling date.

Sample processing

Zooplankton metabarcoding

Zooplankton samples for metabarcoding identification were processed as described in Chapter 2. Zooplankton raw sequence reads from that effort were processed through the bioinformatics pipeline alongside the raw sequence reads from the larval fish gut samples. This was done to ensure that zooplankton sequences from the Choptank River community and from the fish gut contents received the exact same quality control and taxonomic assignment.

Larval fish gut metabarcoding

Larval fish identification

Each fish was placed under dissecting scope (Leica M60, Leica S6D) for preliminary morphological identification, photographed, and the tail was clipped off posterior to the anus. Tails were preserved in 95% ethanol at -20°C; the rest of the body was preserved in 95% ethanol at -80°C. Total length (tip of snout to tip of longest caudal fin lobe; or as much of the fish as was available) of each fish was determined either via calibrated dissecting scope micrometer (n=3), or in ImageJ with calibration photographs (n= 133).

Fish tails were extracted and Sanger sequenced to confirm species following a modified Omega E.Z.N.A. Tissue DNA kit protocol. Kit instructions were followed as written except for steps as listed in supplementary materials (S3.1). Extracted DNA was quantified via Qubit and stored at -20°C until amplification. Amplification of CO1 regions was performed with BCL and BCH primers according to Baldwin, Carole C. et al. 2009: 16 µL master mix (6.6 µL PCR-safe water, 10 µL Sybrgreen, 0.7 µL BCL primer, 0.7 µL BCH primer) and 2 µL extracted DNA per well. Extracted DNA was amplified using the following PCR protocol: denature at 95°C for 3 min; 30 cycles of: 95°C for 45 s, 53°C for 30 s, 72°C for 50 s; extension at 72°C for 10 min; hold

at 10°C. Amplified products were sent to Genewiz or McLAB for Sanger sequencing. Sequences were manually trimmed in Chromas (Technelysium Pty Ltd, version 2.6.6). The resulting sequences were compared to the NCBI nt BLAST database to confirm identification down to species.

For dietary analysis, all fish larvae of the appropriate species were extracted following the same protocol as tail extractions and stored at -80°C until ready for amplification. Fish bodies were left largely intact in order to preserve the contents of the entire digestive tract for sequencing; guts were not dissected. Where possible, larger larvae were trimmed of excess dorsal musculoskeletal tissue under dissecting scope to reduce the predator signal in the resulting data; fish too delicate to manipulate were extracted in their entirety.

Blocking primer design

Species specific blocking primers were designed to prevent amplification of predator DNA (DNA from the larval fish themselves) following the procedures of Vestheim and Jarman 2008, Leray et al. 2013, Piñol et al. 2015, and Su et al. 2018. Blocking primers were aligned internally to the universal primers so that they overlapped the 3' end of the forward CO1 Leray primer (m1CO1intF) by 9-10 bp and extended into the fish DNA sequence by an additional 12-15 bp (Table 3.1). The 3' ends of the blocking primers were capped with a C3 spacer to halt elongation.

To ensure blocking was specific to each fish species and to reduce potential coblocking of prey sequences, alignments were made between the universal primer, blocking primer, CO1 sequences of the predator, and CO1 sequences of zooplankton species detected in the water column to ensure complete matches with the predator and 5 or more mismatches between each

zooplankton sequence and the blocking primer. Tm was kept as close to the universal primer set as possible, and self-dimers and hairpins were avoided as determined by primer3plus (https://dev.primer3plus.com/index.html), OligoCalc (https://www.biosyn.com/gizmo/tools/oligo/oligonucleotide%20properties%20calculator.htm), and Thermo Primer Analyzer (https://www.thermofisher.com/us/en/home/brands/thermo-scientific/molecular-biology/molecular-biology-learning-center/molecular-biology-resource-library/thermo-scientific-web-tools/multiple-primer-analyzer.html).

Blocking primer designs were tested for efficacy and coblocking via qPCR of extracted fish and zooplankton DNA. Tests of blocking primers against congeners were performed with *M. americana* and *M. saxatilis* extracted DNA. *M. americana* DNA was amplified with universal primers ("Leray" master mix: 10 µL Sybrgreen, 4.6 µL PCR-safe water, 0.7 µL 10µM M1COlintF primer (Leray et al. 2013), 0.7 µL 10µM primer jgHCO21198 (Folmer et al. 1994), plus 4 µL DNA per well), universal primers plus *M. americana* blocking primer ("blocking" master mix: 10 µL Sybrgreen, 3.9 µL PCR-safe water, 0.7 µL 10µM M1COlintF primer, 0.7 µL 10µM jgHCO21198 primer, 0.7 µL 100µM *M. americana* blocking primer, plus 4 µL DNA per well), and universal primers plus *M. saxatilis* blocking primer (master mix: 10 µL Sybrgreen, 3.9 µL PCR-safe water, 0.7 µL 10µM M1COlintF primer, 0.7 µL 10µM jgHCO21198 primer, 0.7 µL 100µM *M. saxatilis* blocking primer, plus 4 µL DNA per well). Wells were run in duplicate. The same test was performed for *M. saxatilis*. Amplification was performed on a BioRad thermocycler equipped with a fluorescence detection camera, using a modified Leray PCR protocol set to run for 50 cycles (denature at 95°C for 3 min; 50 cycles of: 95°C for 30 s, 48°C for 45 s, 72°C for 50 s; extension at 72°C for 10 min; hold at 8°C).

Coblocking assessments were performed with DNA extractions from all three species of fish and from two zooplankton samples also used in zooplankton metabarcoding. Tests were amplified in duplicate wells: 4 µL fish DNA with universal primers (fish control, "Leray" master mix), 4 µL zooplankton DNA with universal primers (zooplankton control, "Leray" master mix), 4 µL fish DNA with universal primers plus corresponding blocking primer (test of blocking primer against fish, "blocking" master mix), 4 µL zooplankton DNA with universal primers plus each fish-specific blocking primer (test of blocking primer against zooplankton, "blocking" master mix). The amplification protocol was the same used in congener primer testing. Once all blocking primers were confirmed to block amplification for only their respective fish, they were used in library building.

Library building

Amplification, library preparation, and sequencing of extracted fish DNA followed as closely as possible the protocol as outlined for metabarcoding of zooplankton.

CO1 amplicon libraries were generated with a two-round PCR protocol: in round one, Leray primers (Leray et al. 2013b) amplified a 313 bp length of the CO1 gene and blocking primers prevented amplification of predator DNA, followed by a second PCR where 6 bp barcodes were annealed to the amplicons to allow for multiplexing (O'Donnell et al. 2016). For round one: extracted DNA was amplified with a custom master mix (10 µL OneTaq buffer, 3.2 µL PCR-safe water, 0.7 µL 10µM primer M1COlintF (Leray et al. 2013b), 0.7 µL 10µM primer jgHCO21198 (Folmer et al. 1994), 0.7 µL 100µM species-specific blocking primer, 0.7 µL BSA; 16 µL master mix and 4 µL extracted DNA per reaction well, run in triplicate) using a modified Leray protocol (denature at 95°C for 3 min; 38 cycles of: 95°C for 30 s, 48°C for 45 s, 72°C for

50 s; extension at 72°C for 10 min; hold at 8°C). Amplified products were pooled, amplification was confirmed via agarose gel electrophoresis, and products were diluted 1:5 for barcode addition.

The master mix was the same for barcode addition as for amplification except that barcode primers were used and blocking primers were omitted. PCR for barcode addition followed the Leray protocol as detailed above except with 20 cycles instead of 38. Amplification was confirmed using agarose gel electrophoresis and products were quantified on Qbit. Barcoded products were pooled into libraries using 50 ng DNA from each sample. The concentration of DNA in each pool was quantified, visual confirmation of DNA size fragment was performed on agarose gel, and the pools were sent to Genewiz for library preparation and sequencing on the Illumina MiSeq (2x300 bp sequencing to cover the amplicon size).

Raw sequence reads were processed through the same bioinformatics pipeline designed for metabarcoding of the zooplankton samples. Reads were trimmed and demultiplexed with cutadapt, processed with DADA2 to produce preliminary OTUs (Callahan et al. 2016), and then clustered at 97% similarity with VSEARCH (Frøslev et al. 2017). Taxonomic assignment was performed with a Bayesian Lowest Common Ancestor (BCLA) algorithm (Gao et al. 2017). This algorithm matched OTU sequences to sequences in a custom CO1 database which was downloaded from MIDORI2 (GB version 258, longest) and formatted for BLCA (Leray et al. 2022). BCLA assignments were verified with remote-BLAST to the entire NCBI nt database.

Basic filters similar to the inclusive filters employed in chapter 2 were applied prior to analyses: OTUs with taxonomic assignments which had both less than 80% confidence and < 157 bp match with the BLAST assignment were removed, as were OTUs with no taxonomic

assignment which had both fewer than 100 reads and occurred in fewer than 5 samples. These filters were applied in an attempt to preserve the most taxa possible, while removing low-quality OTUs which were likely amplification artefacts.

Data analysis

All data curation and analyses were performed in R and Excel. Code for select R analyses was written with drafting support from Perplexity.ai (Perplexity).

Fish larvae were sorted into 1 mm length classes to account for ontogenetic diet shifts (Setzler-Hamilton et al. 1982). Gape width was determined in ImageJ using calibrated photographs taken during sorting to measure the horizontal distance between the left and right halves of the maxilla (Fernando et al. 2018). These measures were confirmed based on values in the literature (Detwyler and Houde 1970, Shoji et al. 2005, Campfield and Houde 2011, Sullivan et al. 2016).

Species presence/absence and relative proportion of zooplankton taxa consumed were examined to clarify size- and species-specific larval diets. This dietary data was compared to zooplankton community data from the metabarcoding data set used in Chapter 2. Zooplankton community here refers to the zooplankton samples collected in tandem with the fish larvae samples, limited to the applicable zooplankton size fraction(s) as determined by the gape width of each length class.

Results

As we outline the results of this study, it is worth noting the timeline of sample processing and the handling of samples. Fish larvae samples were collected in 2018-2019; fish

larvae catches were placed into 95% ethanol, then the ethanol was changed within a week of the sampling date. There is a concern that low ethanol permeability of tissues after capture may have caused sample degradation prior to processing by not efficiently halting biological processes. Furthermore, fish samples were not extracted for dietary data until 2022. They were stored in 95% ethanol at room temperature for the duration; some degradation and perhaps skewing of results can be expected.

Blocking primer efficacy

Results of cross-species testing on DNA extractions from fish larvae within the same genus show that the blocking primers selectively blocked just the species they were designed for. DNA samples amplified with universal primers and congener blocking primers consistently crossed the fluorescence threshold during the same, low cycle number (Cq= 23 for *M. americana*, 26 for *M. saxatilis*) indicating amplification after only a few cycles, whereas DNA samples amplified with the species-specific blocking primer consistently appeared 10 cycles later (35 for *M. americana*, 36 for *M. saxatilis*) (Fig. 3.1).

The coblocking testing indicated that the blocking primers did not coblock zooplankton. All of the zooplankton samples amplified earliest in the PCR protocol regardless of the combination of blocking primers they were exposed to (Cq= 24-25 in *M. americana* test, 24 in *M. saxatilis* test, 24-26 in *A. mitchilli* test). By contrast, the fish samples all amplified about 10 cycles later with their species-specific blocking primers (Cq= 35 in *M. americana* test, 36 in *M. saxatilis* test, 32 in *A. mitchilli* test) (Fig. 3.2). This indicates that the blocking primers do not affect amplification of the zooplankton community as a whole, just the individual fish species.

After filtering to remove low-quality OTUs as outlined in the methods but prior to removal of off-target taxa for dietary analyses, all sequence reads for each fish species were summed and the percentage of total reads belonging to the predator vs. all other reads examined. *Morone americana* had 5% of reads from predator, 95% all others; *Morone saxatilis* 49% from predator, 51% all others, and *Anchoa mitchilli* 20% from predator, 80% all others (Fig. 3.3).

Feeding incidence

For *M. americana* and *A. mitchilli*, 14.6 and 13.8% of larvae amplified for sequencing did not appear on gels run on the products of the two rounds of PCR, but, when tested, also did not have inhibition preventing the PCR from succeeding; zooplankton DNA added to the amplification well with the extracted fish DNA successfully amplified in both cases (Fig. 3.4). One such individual from each species was sequenced to determine if this lack of amplification was due to the digestive tract being empty of zooplankton, thereby representing a possible measure of feeding incidence.

Post initial filtering but prior to removal of off-target taxa, sequence reads for *M. americana* and *A. mitchilli* were grouped into three classes: predator reads, reads classified as Unknown (OTUs not assigned any taxonomic classification), and all other reads (putatively prey). The proportions of these groups were compared between the individual larva with "empty" guts and their peers i.e. larvae of the same species and size class which amplified as normal (3-3.99 mm TL for both *M. americana* and *A. mitchilli*) (Fig. 3.5). For both species, the "empty" larvae which didn't amplify had significantly fewer total reads overall compared to their peers (Table 3.2), a significantly greater proportion of Unknown sequences than their peers, and in the case of *M. americana*, a significantly lower proportion of other sequences (Table 3.3). The

proportion of predator reads did not change significantly between full and empty larvae of either species. Significance was determined by calculating the 95% confidence intervals of the aggregated data for the peers and comparing the values of the individual larvae to see whether they fell within (nonsignificant difference) or outside (significant difference) the confidence interval range.

Off-target detections

Gut content data were filtered to exclude detections of off-target taxa before downstream analyses. Taxa were considered off-target if they fell into any of these categories: unknown (no taxonomic identification), predator sequences (i.e. sequences matching the fish larvae the sample came from), likely secondary predation (likely detections of prey within the stomachs of prey), parasites, and likely mis-classifications. We retained only zooplankton (holoplankton and meroplankton), fish for the moronids (fish were excluded for *A. mitchilli*, and predator signal was excluded for all three larvae species), diatoms, and insects with planktonic life stages; all other taxa were discarded.

Off-target detections made up 24-51% of total reads from all taxa detected with each larval species (24.31% in *M. americana*, 28.11% in *A. mitchilli*, 51.75% in *M. saxatilis*, see figures 3.6-3.9). The majority of these taxa were fungi for all three fish species, but the discarded taxa most abundant in the larvae stomachs differed. For *M. americana*, the discarded taxa were mostly Unknown sequences (17% of total reads detected in gut), predator signal (5%), human (0.6%), parasites (0.4%), algae (0.2%), fungi (0.1%), and terrestrial animals (0.01%). For *M. saxatilis*, the discarded taxa were mostly predator signal (49% of total reads) and Unknown sequences (2.7%); all other discarded taxa were exceedingly rare: < 0.01 average relative

abundance across all *M. saxatilis* larvae. For *A. mitchilli*, the discarded taxa were mostly predator signal (20% of total reads), other fish (5%), Unknown sequences (2%), terrestrial animals (0.5%), and fungi (0.02%).

Fish length classes

Total length (TL) ranged from 2-18 mm across our larval fish species. Most larvae were 3-11 mm long; driven by *M. americana* length distribution and abundance. Both body length extremes were almost entirely represented by *A. mitchilli* (Fig. 3.9).

Length vs. gape width

Gape size is generally considered to constrain the maximum prey size (Contreras et al. 2019), so linear regression models from the gape widths and body lengths measured in this study were used to determine the maximum zooplankton size fraction from which larvae of a given body length could feed. Only one measure of gape width (GW) for *A. mitchilli* was possible, so no relationship was established. Instead, values from Detwyler and Houde (1970) were used; these values indicate *A. mitchilli* larvae in our study could only feed from the 64-200 μm size fraction of zooplankton in our samples. *M. americana* and *M. saxatilis* larvae from our study each had a highly significant, linear relationship between TL and GW ($p= 0.00076$, $r^2= 0.44$; $p= 0.027$, $r^2= 0.48$, respectively; Fig. 3.10). For both species, even the smallest larvae sampled in this study were able to consume prey larger than 200 μm, so were assumed to feed from the full size range of zooplankton captured in our samples.

Diets

For all three fish larvae species, the most abundant prey class in the diet was the same: crustaceans, specifically copepods (Fig. 3.11). Beyond this, the moronids diets were more similar to one another but *A. mitchilli* diet differed.

Morone americana

To determine dietary gut content, 81 individual larvae were sampled. When viewed by prey class, Crustaceans made up the bulk of *M. americana* larval diets (84%). Eleven percent of their diets were fish, 3% diatoms, 0.8% cnidarians (hydra, hydrozoans), 0.7% benthic taxa (annelid worms, aquatic snails, bivalves, etc.), and 0.2% rotifers (Fig. 3.11). In descending order of their average relative abundance in the gut, the top individual prey taxa of *M.americana* were: *Eurytemora carolleeae* (copepod), *Bosmina liederi* (cladoceran)*, M. saxatilis*, *Acartia tonsa* (copepod), and *Dorosoma cepedianum* (fish).

To assess the efficacy of metabarcoding in detecting quickly-digested prey items which traditional methods may miss, individual prey taxa were classified into two groups: soft-bodied and hard-bodied (see supplemental Table S3.1). Of the total retained reads for *M. americana*, 12.75% were from soft-bodied prey, 87.25% were from hard-bodied prey.

Morone americana had a more diverse diet than the other two larval species (Shannon index of mean relative abundance= 2.73). Accordingly, when dietary data were plotted by frequency of occurrence vs. prey-specific abundance (Amundsen et al. 1996), their diets were generalist with an emphasis on *E. carolleeae* (Fig. 3.12). Despite having the most diverse diet of the three fish larvae species, *M. americana* had a limited dietary niche breadth (Levin's measure, standardized= 0.32; calculated using frequency of occurrence).

Morone saxatilis

Twenty-nine individual larvae were sampled for dietary data. Crustaceans also made up the bulk of *M. saxatilis* diets at 65% of the diet, followed by fish at 33%, diatoms at 1%, cnidarians at 0.4% (hydra), benthic taxa at 0.4% (annelid worms, bivalves, etc.), and rotifers at 0.1% (Fig. 3. 11). In descending order of their average relative abundance, the top individual prey taxa consumed by *M. saxatilis* were: *E. carolleeae*, *A. tonsa*, *M. americana*, *A. mitchilli*, and *D. cepedianum*.

Of the total retained reads for *M. saxatilis*, 33.85% were from soft-bodied prey and 66.15% were from hard-bodied prey.

Morone saxatilis diet had a diversity score in between that of *M. americana* and *A. mitchilli* (Shannon index of mean relative abundance= 2.13). Their overall diet was also generalist, with an emphasis on both *E. carolleeae* and *M. americana* (Fig. 3. 12). *Morone saxatilis* larvae also had a limited dietary niche breadth (Levin's measure, standardized= 0.39; calculated using frequency of occurrence).

Anchoa mitchilli

Twenty-six individual larvae were sampled to determine dietary gut content. Crustaceans made up 99% of the diet, followed by benthic taxa at 0.2%, rotifers at 0.2%, and diatoms at 0.1% (Fig. 3. 11). In descending order of their average relative abundance, the top individual prey taxa of *A. mitchilli* were: *A. tonsa*, *E. carolleeae*, *Synchaeta baltica* (rotifer), *Polydora cornuta* (annelid worm), and the aquatic snail *Biomphalaria*.

Of the total retained reads for *A. mitchilli*, 0.39% were from soft-bodied prey; 99.61% were from hard-bodied prey.

Anchoa mitchilli larvae had the least diverse diet compared to the other two larval fish species (Shannon index of mean relative abundance= 0.80), and they appeared to specialize on *Acartia tonsa*, occasionally consuming other prey (Fig. 3. 12). They also had a limited dietary niche breadth (Levin's measure, standardized= 0.37; calculated using frequency of occurrence).

Diet ontogeny

Morone americana

Eurytemora carolleeae was the dominant prey item across all size classes of *M. americana*. The 16 mm TL size class was a possible exception, but because the sample size was small (n= 1 *M. americana* larva 16-16.99 mm TL) this could represent an anomaly (Fig. 3.13). The second-most consumed prey was inconsistent, and there was a high diversity of prey in each size class.

There were apparent ontogenetic shifts in prey proportions in the diet with increasing size class (Fig. 3.16). The average relative abundance of *Diaphanosoma* increased in the diet with increasing larval body size. *Pleopsis polyphemoides*, *Polydora cornuta*, *Crassostrea virginica*, *Marenzelleria neglecta*, *Melosira varians*, *Minutocellus polymorphus*, *M. saxatilis*, *D. cepedianum*, *A. tonsa*, and *Bosmina liederi* all decreased in the diet with increasing larval fish body size (Table 3.4). All other taxa had no significant relationship with size class of larvae.

The smallest size classes (3-4.99 mm TL) had more opportunistic, generalist diets: the average relative abundance of the top five prey in the diets were fairly close, and Amundsen plots showed generalist diets with many rare prey and higher variation in diet between individual fish than within (Fig 3.19). Larger larvae (> 5 mm TL) had more specialist diets, where *E. carolleeae* average relative abundance was greater than even the next top four prey species

combined. Amundsen plots for these size classes show *E. carolleeae* as a dominant prey, with few other prey consumed and all at a low level.

Morone saxatilis

Eurytemora carolleeae was the dominant prey item across all size classes of *M. saxatilis*. The 8 mm TL size class was a possible exception, but because the sample size was small (n= 1 larva 8-8.99 mm TL) this could represent an anomaly (Fig. 3.14). The second-most consumed prey was generally *A. tonsa*, followed by fishes *M. americana* and *D. cepedianum*. There was a lower diversity of prey in each *M. saxatilis* size class when compared to *M. americana* larvae. The tertiary prey varied across size classes, but was generally *A. mitchilli*.

The only ontogenetic shift in prey prevalence in the diet was a decrease in *Acanthocyclops brevispinosus* average relative abundance with an increase in larval body size; all other taxa had no significant relationship with size class of larvae (Fig. 3.17 and Table 3.4).

The proportions of the average relative abundance of the top five prey taxa remained fairly consistent across size classes, and Amundsen plots for each size class reveal dietary specialization in size classes 3, 5, 9, 10, 12, and 13 but more generalist diets in classes 6, 7, 8 (Fig 3.20).

Anchoa mitchilli

Acartia. tonsa was the dominant prey item across all size classes of *A. mitchilli* larvae. The 17 mm TL size class was a possible exception, but it also had a small sample size (n= 1) and could be anomalous (Fig. 3.15). The second-most consumed prey was consistently *E. carolleeae*, and size class diet diversity was lowest compared to *M. americana* and *M. saxatilis* larvae. *Bosmina* was a consistent prey species for all sizes of *A. mitchilli* larvae; *Acanthocyclops* (copepod) and *Leptocheirus plumulosus* (amphipod) were also consumed by most size classes.

There was an apparent ontogenetic swap in prey prevalence in the diet, seen in the average relative abundance of *A. tonsa* and *E. carolleeae* with increasing larval body size. As the body size of *A. mitchilli* larvae increased, the proportion of the diet occupied by *A. tonsa* decreased and *E. carolleeae* increased (Fig. 3.18 and Table 3.4).

Anchoa mitchilli larvae of all size classes had specialist diets, mostly on *A. tonsa* (Fig 3.21). The lone exception was size class 17-17.99 mm TL, where the single larva caught in that size class consumed mostly *E. carolleeae*.

Spatiotemporal distribution of larvae

The moronid larvae co-occurred in spring samples (April, May; Fig. 3.22). *Morone americana* distribution was largely upriver at stations Jamaica Point, Buoy 45, and ET 5.1 in April (2018 only) and May (2018 and 2019), with two larvae sampled in the mid-Choptank at station ET 5.2 in April 2018. *Morone saxatilis* distribution was consistently limited to the oligohaline headwaters at Buoy 45 and ET 5.1.

Anchoa mitchilli only occurred in summer samples (June, August; Fig. 3.23). *Anchoa mitchilli* larvae were mostly caught at the mouth of the Choptank River at station EE 2.1 in June 2018, and at both the mouth (EE 2.1) and the oligohaline zone (Buoy 45) in August 2018.

Analysis of potential feeding selectivity

Only shared taxa were considered for these analyses. Shared taxa here refers to taxa which were found in both a fish gut sample and in the corresponding water column zooplankton sample. These came from paired samples taken at the same time and place as outlined in the methods of Chapter 2.

Some numerically important taxa are excluded from these analyses because they were not detected in paired samples of larval fish guts and the water column. Some important prey taxa were present in water column zooplankton samples from adjacent sites, but not the zooplankton samples corresponding with the sites where fish larvae were caught. This could indicate that the larvae had foraged from a different patch of plankton prior to capture in our net. In some cases, there was only one larva with a particular prey taxon within its gut so confidence intervals were impossible to calculate.

To assess potential feeding selectivity, larvae within each sample were aggregated into size classes in increments of 1 mm total length (TL); these groups will be referred to as "size-by-sample" hereafter. Average relative abundance and standard error of each prey taxon in the gut contents was calculated for each size class within each sample (i.e. the size-by-sample grouping). For simplicity, only the top 10 most abundant taxa in the stomach contents of each size class were examined. The abundance of each taxon was considered to be significantly different between the gut content and the water column if the proportion in the water column fell outside 95% confidence intervals of the average relative abundance within the guts of the larval fish.

Morone americana

All length classes had at least one prey taxa with significantly different proportions in the fish guts vs the water column (Table 3.5). Most of these prey taxa were in samples taken in May 2018 at station Buoy 45, where the bulk of *M. americana* larvae were sampled. The bulk of the prey taxa were crustaceans: *A. tonsa* (n= 13 *M. americana* size-by-sample groups), *E. carolleeae* (n= 12), *A. brevispinosus* (n= 8), *Bosmina liederi* (n= 6), *Diaphanosoma* (n= 5), *Pleopis polyphemoides* (n= 1), and *Amphibalanus improvisus* (n= 1). The other prey taxa were fish (*D.*

cepedianum [n= 8] and *M. saxatilis* [n= 2]), worms (*Marenzelleria neglecta* [n= 1] and *Polydora cornuta* [n= 1]), and diatoms (*Coscinodiscophyceae* [n= 1] and *Lithodesmium* [n= 1]).

The following taxa consistently had a significantly higher relative abundance in the water compared to their abundance in the *M. americana* larvae guts: *A. tonsa*, *A. brevispinosus*, *Diaphanosoma*, *A. improvisus*, *P. polyphemoides*, and *P. cornuta*. This implies possible selection against these taxa. The relative abundance in the gut was always significantly higher than the abundance in the river for *E. carolleeae*, *D. cepedianum*, *M. neglecta*, *M. saxatilis*, *Lithodesmium*, and *Coscinodiscophyceae*; this implies possible selection for these taxa. *Bosmina liederi* was generally significantly more abundant in the water than in the guts of larvae (n= 5 size-by-sample groups). However, for one size class (3-3.99 mm TL), *B. liederi* relative abundance was significantly higher in the guts than in the water.

There were some prey taxa that made up large proportions of the *M. americana* larvae gut contents, but their abundance in the water column was not significantly different from their abundance in the gut contents, implying no particular preference for or against these taxa (i.e. "neutrally selected"): *Bacillariophyta*, *Melosira ambiqua*, *Melosira varians*, *Minutocellus polymorphus*, *Spionidae*, *Synchaeta baltica* (Table 3.6).

Some taxa were only significantly different in abundance between the water column and the gut contents across select samples and length classes, rather than consistently across all. Of these, the following taxa were more often subject to potential selective pressures (for or against, as evidenced by a significant difference in abundance in the guts vs the water column) than neutrally selected: *A. tonsa* (n= 1 neutral selection vs n= 13 selection), *A. brevispinosus* (n= 1 vs n= 8), *B. liederi* (n= 3 vs n= 6), *D. cepedianum* (n= 5 vs n= 8), *E. carolleeae* (n= 5 vs n= 12).

There was no discernable pattern in consumption between sampling sites, sampling dates, and length classes.

The following taxa were more often neutrally selected and only occasionally subject to potential selective pressures: *Coscinodiscophyceae* (n= 2 neutral selection vs n= 1 selection), *Diaphanosoma* (n= 8 vs n= 5), *Lithodesmium* (n= 4 vs n= 1), *M. neglecta* (n= 3 vs n= 2), *P. cornuta* (n= 4 vs n= 1). Of these, there was no discernable pattern in consumption between sampling sites, sampling dates, and length classes except for *Lithodesmium* which was significantly more abundant in the guts of *M. americana* larvae 13-13.99 mm TL than in the water column (and for all other length classes was neutrally selected), and *M. neglecta* which was significantly more abundant in the guts of *M. americana* larvae 11-11.99 mm TL and 13-13.99 mm TL than in the water column (and for all other length classes was neutrally selected).

Morone saxatilis

All length classes (with more than one larva) had at least one prey taxon with significantly different proportions of abundance in the fish guts vs the water column (Table 3.7). All of these detections were in samples taken in May at Buoy 45 in both 2018 and 2019, where most of the *M. saxatilis* larvae were sampled. Most of the prey taxa with significant differences in abundance were crustaceans: *A. tonsa* (n= 5 size-by-sample groups), *A. brevispinosus* (n= 5), *E. carolleeae* (n= 4), *Bosmina liederi* (n= 4), *Diaphanosoma* (n= 1), *Pleopis polyphemoides* (n= 1), and *Leptodora kindtii* (n= 1). The other prey taxa were fish (*M. americana* [n= 5] and *D. cepedianum* [n= 1]).

The following taxa consistently had a significantly higher relative abundance in the water compared to their abundance in the *M. americana* larvae guts: *A. brevispinosus*, *B. liederi*, *Diaphanosoma*, *L. kindtii*, and *P. polyphemoides*. This implies possible selection against these

taxa. The relative abundance in the gut was always significantly higher than the abundance in the river for *E. carolleeae* and *D. cepedianum*; this implies possible selection for these taxa. *Acartia tonsa* was generally significantly more abundant in the water than in the guts of larvae (n= 3 size-by-sample groups); however, for two size classes in May 2019 at station Buoy 45 (5-5.99 and 10-10.99 mm TL), *A. tonsa* relative abundance was significantly higher in the guts than in the water. *Morone americana* was usually significantly more abundant in the guts than in the water (n= 4 size-by-sample groups). The size class where *M. americana* prey were more abundant in the water was 9-9.99 mm TL.

There were some prey taxa that made up large proportions of the *M. saxatilis* larvae gut contents, but their abundance in the water column was not significantly different from their abundance in the gut contents, implying "neutral" selection: *Lithodesmium*, *M. polymorphus*, *P. cornuta*, and *Synchaeta baltica* (Table 3.8).

Some taxa were only significantly different in abundance between the water column and the gut contents across select samples and length classes, rather than consistently across all. Of these, the following taxa were more often subject to potential selective pressures (for or against, as evidenced by a significant difference in abundance in the guts vs the water column) than neutrally selected: *A. tonsa* (n= 3 neutral selection vs n= 5 selection), and *M. americana* (n= 3 vs n= 5). There was no discernable pattern in consumption between sampling sites, sampling dates, and length classes.

Dorosoma cepedianum was more often neutrally selected and only occasionally subject to potential selective pressures (n= 7 neutral selection vs n= 1 selection). *Eurytemora carolleeae* was potentially selected or neutrally selected across an equal number of groups (n= 4 neutral

selection vs n= 4 selection). There was no discernable pattern in consumption between sampling sites, sampling dates, and length classes for these prey.

Anchoa mitchilli

All length classes (with more than one larva) had at least one prey taxon with significantly different proportions of abundance in the fish guts vs the water column (Table 3.9). All of these detections were in samples taken 2018 in June at EE 2.1 and August at Buoy 45, where most of the *A. mitchilli* larvae were sampled. Most of the prey taxa with significant differences in abundance were crustaceans: *A. tonsa* (n= 4 size-by-sample groups) and *E. carolleeae* (n= 3). There were also worms (*Alitta succinea* [n= 1] and *P. cornuta* [n= 1]), and the rotifer *Synchaeta baltica* (n= 1).

Alitta succinea and *P. cornuta* consistently had a significantly higher relative abundance in the water compared to their abundance in the *A. mitchilli* larvae guts, implying selection against these prey. The relative abundance in the gut was always significantly higher than the abundance in the river for *A. tonsa*, *E. carolleeae*, and *S. baltica*, implying possible selection for these prey.

The following prey taxa made up large proportions of the *A. mitchilli* larvae gut contents, but their abundance in the water column was not significantly different from their abundance in the gut contents, implying "neutral" selection: *A. improvisus*, *B. liederi*, and *P. polyphemoides* (Table 3.10).

Eurytemora carolleeae was more often subject to potential selective pressures (n= 3), except in one size-by-sample group where it was neutrally selected (n= 1, length class 6-6.99 mm TL).

Discussion

Blocking primer efficacy

Our blocking primer designs performed well from the perspective of species specificity and coblocking. A true coblocking test would involve sequencing replicates of the same zooplankton sample amplified with and without each blocking primer, then comparing the zooplankton species identified by each to ascertain whether any individual zooplankton species were being artificially excluded by the blocking primers. However, that work was beyond the scope of this study. It is worth noting that the zooplankton samples used in testing were the same mixed-species samples collected from the water column as part of this study, so we can be reasonably confident that any coblocking effects were minimal specifically for the zooplankton community we were studying.

Morone saxatilis had the highest percentage of predator DNA in the total reads at 49%. It is unclear why the percentage of predator DNA was so high, but it could have been a flaw in the design of the blocking primer. The blocking primer sequence had a 9 bp overlap with the universal primer instead of 10. On the surface this does not seem to be a major impediment, and the other metrics of the primer are sound (Tm= 72.6, length= 23 bp, CG%= 56.5, extinction coefficient= 201200, molecular weight= 6864.5 g/mol, and no self dimers). The PCR results with and without the blocking primer also indicate performance in alignment with the *M. americana* and *A. mitchilli* blocking primers (Fig. 3.2). However, the poor performance cannot be ignored. It is possible that there was an overwhelming amount of *M. saxatilis* DNA in each sample such that the blocking primer, even at 10x the concentration of the universal primer, could not prevent amplification of all sequences, but this seems less likely.

Feeding incidence

The *M. americana* and *A. mitchilli* larvae which did not amplify but also had no inhibition likely had empty or very nearly empty guts at the time they were sampled. Significantly reduced total reads indicates there was less DNA present for amplification overall, as one might expect from a fish with an empty gut. Unknown reads detected in full and empty gut larvae could have belonged to prey organisms which did not have a reference stored in the NCBI database, or could indicate the OTU sequence was too low quality to be confidently matched with the database. It is unlikely that the empty gut larvae would have both fewer overall sequences and a higher proportion of an unknown prey item in their guts compared to their peers; the empty gut larvae were caught in the same sampling effort with most of their peers so they were likely eating from the same prey field. Furthermore, the quality filters used on this data set were intentionally lowered in order to capture maximum species richness; some low quality reads are expected to have passed the filters. In this study, low quality sequence reads could be due to improper preservation and storage, or digestion by the larvae prior to preservation. DNA lingering in an otherwise empty gut is expected to be heavily digestion-degraded, and so likely accounts for the higher proportion of Unknown sequences in the guts of empty larvae. 13.8% of the *A. mitchilli* larvae and 14.9% of *M. americana* larvae sampled and amplified had this same "empty" gut pattern of amplification. Feeding incidence found in this study fell in between values recorded for larvae of these species so this tentative measure of feeding incidence is within expected parameters (Eldridge et al. 1982, Uphoff 1989, Auth 2003, Shoji et al. 2005, Campfield and Houde 2011, Shideler and Houde 2014a).

However, the size range of the larvae with "empty" guts was small, and close to the size where we expect to see first feeding (Setzler-Hamilton et al. 1982, Chesney 2008). *Morone americana* larvae with empty guts were in the size range 3.5-3.99 mm (n= 14); there were n= 39 *M. americana* larvae <4 mm TL in this study so 35.9% of these *M. americana* larvae had "empty" guts. *Anchoa mitchilli* with empty guts were in the size range 3.64-20.75 mm (n= 4; three out of the four were in the range 3-3.99 mm); there were n= 10 *A. mitchilli* larvae <4 mm TL in this study so 30% of these *A. mitchilli* larvae had "empty" guts. No *M. saxatilis* larvae showed this amplification pattern, but the smallest *M. saxatilis* larva was 3.98 mm TL and the only larva of that size; the next largest was 5.24 mm TL. The large proportion of small larvae without gut contents among *M. americana* and *A. mitchilli* might indicate delayed first feeding rather than empty guts of feeding larvae. The photographs of the fish did not seem to indicate this, however with tissue opacity caused by ethanol preservation it was difficult to distinguish full and empty stomachs (Fig. S3.2, Fig. S3.3).

Feeding incidence is an important measure of the health and potential success of a larval fish cohort and it is encouraging that metabarcoding might provide us with a version of this metric. However, more testing is required before these data can be used as a proxy for feeding incidence. Ideally, a laboratory experiment could be performed in which larvae of a given size range would be fed a known number and species of prey and sampled at various time points post-feeding to capture the timescale of prey digestion. Then a comparison could be made between the amplification patterns and sequence read proportions of the gut contents at those time points to ascertain whether metabarcoding really can inform us of feeding incidence.

Off-target detections

When considering fish species as prey, moronid juveniles and adults are piscivorous on larvae and eggs so fish detections were included in the prey analyses of *M. americana* and *M. saxatilis* (Chick and Avyle 2016, Pagenkopp Lohan et al. 2023). Both fish are also known to be cannibalistic, at least in later life stages, so there is a chance that the predator signal detected was not entirely from the larval predator but also from cannibalistic consumption of eggs or larvae of the same species. In order to determine this for certain, the gut contents would need to be morphologically identified, which was outside the scope of this study. All predator DNA sequences were considered to be from the larvae and excluded from downstream analyses.

Anchoa mitchilli larvae were noted in some studies to have consumed fish eggs, larvae, small fishes, and to be occasionally cannibalistic, however the larvae in those studies were much larger than the larvae in this study (> 30 mm SL) (Hildebrand and Schroeder 1927, Darnell 1958, Sheridan 1978). For this reason, all fish detections were excluded from the diets of *A. mitchilli* larvae in this study. However, fish detections made up a significant proportion of the total reads detected (6.6%, comprised in descending order of: *Morone saxatilis*, *Morone americana*, *Dorosoma cepedianum*, *Chasmodes bosquianus*, *Microgobius thalassinus*, *Membras martinica*). These species were also caught as larvae in the Choptank River during the sampling effort for this study, and recorded in the gut contents of *M. americana* and *M. saxatilis*. Because metabarcoding can detect even trace amounts of DNA, these reads could represent external contamination or incidental consumption by the *A. mitchilli* larvae of shed material from the "prey" fish species rather than intentional ingestion. However, the magnitude of the signal suggests otherwise, as does the percent presence of the prey fish in the *A. mitchilli* diet (these fish were found in the guts of 7.68-100% of *A. mitchilli* larvae, depending on the species of prey

fish). It is possible that these were legitimate detections of previously undocumented consumption of fish by smaller *A. mitchilli* larvae, whether intentionally or as an incidental catch from straining water for plankton. To know for certain, a simultaneous morphological study would need to be performed to confirm the physical presence of such prey.

Certain taxa were off-target but were consistently detected across multiple fish larvae species and had high percent occurrence within each species. Human detections were likely contamination from handling. Fungi like cladosporium were excluded on the basis that such detections may be spore DNA contamination from exposure of the samples to the air, however fungal detections could also be the result of larval fish consumption of decaying plant matter or detritus (Graça et al. 1993). With just DNA sequences, it is impossible to distinguish between fungal contamination and intentional or incidental consumption, so fungi were excluded. As single-celled algae, Chlorellaceae are likely too small to be intentionally targeted prey, so were probably secondary prey consumed by the organisms which were in turn consumed by the fish larvae. *Meleagris gallopavo* (turkey), while present in the Choptank watershed, was likely not a prey item of *M. saxatilis* and *A. mitchilli* larvae. However larvae could have intentionally or incidentally consumed fecal matter from *M. gallopavo* washed into the river. *Megathylacoides* (fish-specific tapeworm) detections were likely real detections of infection in all three larval species, however as parasites they were excluded from analyses.

Length vs. gape width

Gape width measures from this study do not match those of the literature; it is unclear if this is a function of the method used here (i.e. measured from photographs, after long-term

ethanol preservation), the small sample size available, or a function of natural larval growth and development. However, gape and prey sizes with ontogeny also do not agree in the literature. Detwyler and Houde (1970) predict that *M. americana* larvae in the size ranges collected in this study (3-18 mm TL) would accommodate average prey lengths 117.4-453.2 µm, implying larvae can only accommodate zooplankton ≥200 µm when they reach TL 9-10 mm, whereas Shoji et al. (2005) predict those same larvae accommodate average prey lengths 327.0-1229.0 µm, implying larvae can accommodate ≥200 µm at all body sizes and life stages. The values from our regression predict gape widths of 348.2-1216.7 µm. Only the regression was given in Detwyler and Houde (1970), fish body lengths and life stages being studied were not recorded, so we proceeded with the understanding that all *M. americana* larvae can consume zooplankton prey of all sizes captured in this study.

For *M. saxatilis*, data from this study and from the literature suggest that all body sizes of larvae surveyed in this study can accommodate zooplankton ≥200 µm (Dennerline and Van Den Avyle 2000, Campfield and Houde 2011, Sullivan et al. 2016, Vanalderweireldt et al. 2019). The smallest gape width was a measurement from this study at 320 µm for a larva 3.98 mm TL; all other studies predicted via linear regression or directly measured larger gape widths and average prey sizes for the same size larva. Therefore, we proceeded with the understanding that all *M. saxatilis* larvae can consume zooplankton prey of all sizes captured in this study.

Diets

Eurytemora carolleeae and *A. tonsa* dominated the diets of all three species of larval fish. These are spatially and seasonally dominant zooplankton species in the Choptank River and are

known prey of these larval fish (Bridgewater and Schmidt 1993, Limburg et al. 1997, Martino and Houde 2010, Campfield and Houde 2011), adding support to the genetic findings.

Close runners up were other crustaceans (*Bosmina*), also reported by the literature, followed by an abundance of fish (*M. americana*, *M. saxatilis*, *A. mitchilli*, *D. cepedianum*, *Membras martinica*). The magnitude of the signal from fishes in the diets of all three larvae suggest piscivory as a main feeding strategy, particularly for *M. saxatilis* for which fish made up 33% of the overall diet. There is likely also cannibalism among these larvae, however the sequences from predator and prey of the same species are indistinguishable with metabarcoding.

The percentage of diatoms in the diets of the moronids was higher than expected. They were likely secondary prey detections, particularly given that *E. carolleeae*, the dominant prey of both moronid larvae, is primarily herbivorous and likely had guts full of phytoplankton when they were in turn consumed by larvae.

Cnidarians were a novel addition to the diets of larval moronids, particularly the taxa: *Hydra vulgaris*, *Hydra oligactis*, *Anthoathecata*, and *Rathkea octopunctata*. This indicates the larvae of these three species are taking advantage of a previously undocumented food source, and has implications for the flow of energy and resources through the ecosystem.

Benthic taxa detected in the diets of the larvae could be the outcome of several scenarios. Fish larvae in the water column could have directly consumed pelagic eggs or larvae of benthic species, consumed any life stage of benthic species off the bottom, or consumed benthic species which were temporarily transiting through the pelagic either by choice (swimming) or by physical properties of the environment (turbulence).

Some of the benthic species detected in the larval guts such as *Amphibalanus* barnacles and spionid polychaetes have a planktonic larval stage which falls within the size fraction

consumed by the larvae. In addition, these benthic taxa also spawn around the same time the larvae hatch and feed, increasing the probability of fish larvae encountering the eggs and larvae of benthic species while foraging (Dauer et al. 1980). The fish larvae examined in this study were swimming in the upper half of the water column at the time of capture, but could have foraged on the benthos prior to capture, potentially accounting for the presence of DNA from benthic taxa in their guts. All of the prey taxa examined in the analysis of potential feeding selectivity were detected in both the fish guts and in the zooplankton nets, which were towed sequentially and at the same depths. Benthic taxa found in both the larval fish guts and the zooplankton nets are therefore likely to have been either pelagic eggs or larvae, or possibly any stage of a benthic taxa which happened to be swimming or caught in strong turbulence. Indeed, one of the stations most often sampled (Buoy 45) was highly turbid, with waters clouded by plant material and sediments that were also retained in the zooplankton nets (*anecdotal observation during morphological analysis of zooplankton samples in Chapter 2*). Benthic prey taxa consumed at this station may have been caught in turbulence and suspended in the pelagic, available for foraging by the larvae fish.

Rotifers made up a surprisingly small portion of the overall diets of the fish larvae. When they appeared, they were almost entirely *Synchaeta* spp. which are soft-bodied, rather than the more abundant *Brachionus* or *Keratella*. However, both *Brachionus* and *Keratella* are shelled and in some cases have spines, indicating the soft *Synchaeta* may be a more attractive meal for fish larvae.

It seems that metabarcoding did indeed reveal previously unrecorded diversity in larval fish diets, specifically with soft, quickly-digested organisms which would be difficult to identify

with traditional methods. Soft-bodied prey made up a significant proportion of *M. americana* larval diets, and the organisms identified as soft-bodied were generally novel observations of taxa such as hydra (*Hydra vulgaris*, *H. oligactis*), worms (*Marenzellaria neglecta*, *Polydora cornuta*, *Nais communis*), athecate rotifers (*Synchaeta baltica*), and hydroids (*Anthoathecata*). Other fish also made up a large proportion of the soft bodied detections (*M. saxatilis*, *Dorosoma cepedianum*, *Membras martinica*, *A. mitchilli*, *Perca flavescens*).

Soft-bodied prey made up an even larger portion of *M. saxatilis* larval diets, and the organisms identified as soft-bodied were generally novel observations of taxa such as hydra (*Hydra vulgaris*), worms (*Polydora cornuta*, *Spionidae*, *Boccardiella hamata*, *Aglaophamus dibranchis*), and athecate rotifers (*Synchaeta baltica*). Other fish also made up a large proportion of the soft bodied detections (*M. americana*, *A. mitchilli*, *D. cepedianum*, *Perca flavescens*, *Membras martinica*,).

For *A. mitchilli*, soft-bodied prey made up only a small portion of the diet: <1%. Their overwhelming consumption of the copepod *A. tonsa* and narrow dietary breadth focused on just this one species of zooplankton account for the tiny proportion of soft-bodied prey in their diets. It is important to note, however, that the soft-bodied prey these larvae were consuming were worms (*Aglaophamus dibranchis*, *Alitta succinea*, *Boccardiella hamata*, *Polydora cornuta*, *Spionidae*), hydra (*H. vulgaris*, *H. oligactis*), and rotifers (*Synchaeta*), just as with the moronids. It is also important to note the 6.6% of total reads detected in *A. mitchilli* guts which were fish sequence reads; if these detections were intentionally consumed prey, they also constitute soft-bodied prey.

Morone americana

Morone americana larvae were all collected in oligohaline-freshwater zones of the river and fed from similar zooplankton communities. Therefore, the apparent shift in their diets from more generalist to more specialist on *E. carolleeae* implies an ontogenetic change in feeding strategy. This is corroborated by the decline in average relative abundance and even removal of most taxa in *M. americana* diets as their body size increases, concomitant with an increase in *E. carolleeae* average relative abundance in their diets. These larvae may begin life by eating opportunistically from whatever they can find, and later in their lives when they have enough hunting ability and energy stores to be selective about what they eat, perhaps they choose only the most calorically-rich or nutritious prey available to them.

Size classes 12-12.99 mm and 16-16.99 mm broke the pattern of > 5 mm TL M. americana larvae specializing on *E. carolleeae*. Size class 12 had high consumption of both *E. carolleeae* and *M. saxatilis*, and 16 had equal consumption of both *E. carolleeae* and *Apocorophium lacustre*, an amphipod. All *M. americana* of size 12-12.99 mm were caught in May 2018 at Buoy 45, where they co-occurred alongside our largest catch of *M. saxatilis*; this might suggest size-constrained opportunistic feeding on *M. saxatilis* eggs or larvae, except that all *M. americana* of size classes 11, 13, 14, 16, and 17 were also caught in the same sampling effort and did not show the same specialization. Size bin 16 is represented by a single larva; this fish may have simply consumed an amphipod prior to sampling, accounting for the high representation of amphipod DNA in its diet.

Morone saxatilis

There was no apparent ontogenetic change in dietary strategy for *M. saxatilis*, except for the decline in *A. brevispinosus* with increasing body size. All of the larvae in size classes 6, 7, and 8 were caught in May 2019 at Buoy 45; the change to generalist dietary strategy in these size classes may reflect a response to a more even, less dominant prey field rather than ontogenetic flip-flopping between specialist and generalist feeding with growth.

Specialization, in the size classes where it occurred, was usually on *E. carolleeae* with the exception of size class 10 where it was on *M. americana*. Three out of the five larvae in size class 10 were caught in May 2018 at Buoy 45, where they co-occurred with our largest catch of *M. americana* larvae. All of the *M. saxatilis* larvae in classes 12 and 13 were also caught in the same sampling effort and while they did not show the same strong preference, the larvae in class 12 consumed *M. americana* as a strong second to *E. carolleeae*, possibly indicating size-constrained opportunistic feeding on *M. americana* eggs or larvae as a top prey when available.

Anchoa mitchilli

There was likely no ontogenetic shift in predation from *A. tonsa* to *E. carolleeae*. All the large larvae (bins 8, 15, 17) were caught in the same sample and show a gradual increase in the proportion of *E. carolleeae* in their diets with increasing body length, driving the plots in Fig. 3.18. The water column zooplankton samples collected alongside the larvae however indicate *A. tonsa* dominated the community, with *E. carolleeae* as a close second, and that the larger larvae were not consuming *E. carolleeae* in a proportion different to their proportion found in the environment. These fish were likely not switching prey affinity to a larger copepod as they grew, but rather feeding from what was available to them.

Spatiotemporal distribution of larvae

Morone americana spatial distribution seems to suggest three spawning events during the study years: the tail end of a spawning event in April 2018, the beginning of a spawn event in April 2018, and the start of another in May 2019. *Morone americana* larvae are 2-3 mm TL when they hatch; larvae of this size were caught at the freshwater station ET 5.1 in April 2018. One month later in May, there were larger larvae caught downriver at site Jamaica Point (Jam Pt), suggesting possible movement downriver of larvae from the cohort hatched in April; it is important to note that if they were migrating, they did not leave the oligohaline zone. Downriver movement is expected of moronids, which hatch in freshwater and migrate into higher salinity water as they mature into juveniles. The cohort at Buoy 45 in May 2018 was much larger, with larvae ranging from 3-18 mm TL, suggesting that the larvae remain in the oligohaline zone of the Choptank during the earliest stages of their lives. This is supported by observations of moronid larvae being retained in estuarine turbidity maximums, where saltwater and freshwater meet, mix, and create a turbulent zone rich in food resources i.e. zooplankton (North and Houde 2001). This pattern also appears to hold true for *M. saxatilis* larvae, which were only found in the oligohaline region of the Choptank.

Morone saxatilis distribution also suggests two spawn events: one in May 2018 and another in May 2019. Based on the number and size distribution of larvae, the May *M. saxatilis* spawn events were perhaps more synchronous with *M. americana* in 2018 than 2019. Given the low number and small body size (< 4 mm TL) of *M. americana*, *M. saxatilis* appears to have spawned earlier or grown faster than *M. americana* in May 2019.

Anchoa mitchilli distribution was counter-intuitive, with large numbers of small larvae at the mouth of the Choptank in June and a few large larvae in oligohaline waters in August.

However, *A. mitchilli* may follow a pattern opposite to moronids where they spawn in saltier water, with their larvae swimming upstream into fresher water (Mercer 1989, Campfield and Houde 2011). The presence of *A. mitchilli* larvae in June and August is in line with prior findings (Auth et al. 2020).

The moronids (*M. americana*, *M. saxatilis*) were separated from *A. mitchilli* in time; there was no competition between them for prey. However, based on the diet metabarcoding data, the moronids consumed *A. mitchilli*. There are three possible explanations for this finding: there were anchovy larvae present which evaded our sampling equipment, the moronids were feeding from patches containing *A. mitchilli* which were outside our immediate sampling site, or moronids were consuming mostly *A. mitchilli* eggs. Based on prior research in *A. mitchilli* spawning, it is most likely that the moronids were consuming early eggs (Mercer 1989). However, this is impossible to know for sure without a simultaneous morphological identification of gut contents.

The moronids co-occurred in both time and space and fed primarily on the same narrow niche of prey, so they could have been competing with each other for the same food resources. However, the high density of zooplankton in the Choptank River during this study makes such competition unlikely (Houde 1987, 2008). Competition is only likely to occur between these species when the zooplankton bloom is mismatched in time and space with the fish spawns, resulting in a more sparse prey field (Cushing 1990, Durant et al. 2007). There was an increase in moronid predation on moronids when they co-occurred in high numbers, possibly suggesting opportunistic predation on prey which is periodically abundant in the system and also a potential competitor for crustacean prey.

The sparse number of *M. saxatilis* larvae lends support to the observations of low recruitment in recent years, and suggests that the low recruitment originates in either low egg numbers or low larval success. Low larval success could be due to low hatch rates or heavy predation of the *M. saxatilis* eggs and larvae, but likely is not due to starvation as no "empty gut" *M. saxatilis* were sampled during this study; note that their absence from the study could also be due to our sampling method or the unsuitability of metabarcoding for measuring feeding incidence as previously discussed. Low numbers of *M. saxatilis* larvae are likely also not due to advection out of the study site, as *M. americana* larvae of the same size distributions co-occurred in the same spaces at the same time, and in much greater numbers.

Analysis of potential feeding selectivity

Some major prey taxa were not captured in the zooplankton nets used to sample the prey field. Among these, the most notable were the ichthyoplankton (larval fish). Ichthyoplankton are known to evade zooplankton nets, and this is most likely why they were not a major part of the zooplankton samples. This may be the case here because these samples were taken with a fine mesh net (64 um) in an estuary with high turbidity; the net likely filled quickly and produced a pressure wave which alerted any swimming larvae to its presence, allowing them to avoid capture (Gartz 1999).

A significant difference in proportion should be taken with a healthy grain of salt; this data does not, in isolation, suggest preference or rejection by the larval fish of a particular prey. Further work would be necessary to determine true feeding preference or selectivity.

Morone americana

Eurytemora carolleeae, the main prey consumed by *M. americana* larvae, was over-represented in their diets compared to the water column for all *M. americana* larvae, and the taxa which had the most significant differences between the proportions in the gut and the water column followed the same order as the major classes of taxa in the overall diets of *M. americana*. This result was expected based on prior work and lends support to the validity of CO1 metabarcoding.

Marenzelleria neglecta, when there was a significant difference in proportions, was also consistently over-represented in the larval diets, implying intentional targeting of this prey. Adults of this annelid worm have been observed with gametes in early spring, indicating that the worm larvae were likely the prey of larval *M. americana* (Dauer et al. 1980). Larvae of benthic species which spend part of their life cycle as plankton are not usually thought of as major contributors to the diets of fish larvae; this presents a new and important direction for further study.

Lithodesmium and *Coscinodiscophyceae* followed a similar pattern of over-representation. They are both diatoms, and likely consumed either incidentally alongside intentional prey, or are actually representative of secondary predation. It is very likely that the large proportion of *E. carolleeae* consumed by *M. americana* larvae had at least some of these two diatom species in their guts at the time they were predated, perhaps allowing for the over-representation in some guts but neutral representation in others. *Dorosoma cepedianum* and *M. saxatilis* were consistently over-represented; however as noted above, ichthyoplankton were artificially under-represented in the water column samples, so their over-representation in the larval diets is to be approached with healthy skepticism. Though the moronid larvae did consume

one another (or at least eggs) when they co-occured in large numbers, we cannot tell from this data whether they were doing so in an intentional or opportunistic manner.

Taxa which always appeared in roughly the same proportions in the water column as in larval diets could have been consumed opportunistically whenever they were encountered, however as the largest proportion of the diet was usually made up of *E. carolleeae*, some suppression of representation of other taxa is expected. These taxa may have actually been consumed with more intention, but with just proportional data this cannot be determined.

Given the importance of *B. liederi* and its congeners as prey for *M. americana* in prior literature, it was surprising that they were usually under-represented in the diets of the larvae compared to the water column (Setzler-Hamilton et al. 1982, Bridgewater and Schmidt 1993, Limburg and Pace 1999, Shoji et al. 2005, Martino and Houde 2010, Shideler and Houde 2014a, Chick and Avyle 2016). This could be a function of using proportional data: *E. carolleeae* detections took up a large portion of the total reads per gut and likely drove down the relative proportion of sequences allocated to *B. liederi*. However, it is worth noting that 2018-2019 were unusually wet years, which may have affected the prevalence and therefore relative abundance of prey in the water column. It is entirely possible that under more normal hydrological conditions, *B. liederi* are more available as prey and occupy a larger proportion of gut contents.

Morone saxatilis

Eurytemora carolleeae, the main prey of *M. saxatilis* larvae, was only over-represented in their diets for about half the size-by-sample groups; for the other half, the proportion of *E. carolleeae* was not significantly different from the proportion in the water column. This is unexpected given the heavy emphasis of *E. carolleeae* in the diets of all size classes of *M. saxatilis* larvae.

Morone americana and *D. cepedianum* were also over-represented, however as noted above, their over-representation in the larval diets is to be approached with healthy skepticism. Again, *B. liederi* was under-represented; this was a surprise given prior literature, and could be a result of using proportional data or the unusual environmental conditions during the study.

The lack of clear patterns in *M. saxatilis* is disappointing. It could be that the large proportion of reads taken up by predator sequences (49% of total reads) combined with the smaller sample size (further divided into the size-by-sample groups) compared to *M. americana* masks patterns in prey consumption we might otherwise see. Certainly, dividing relatively few samples into further groups resulted in fewer sample pairs which had enough data to calculate 95% CI for each of the top 10 prey taxa.

Anchoa mitchilli

Acartia tonsa, the main prey of *A. mitchilli* larvae, was over-represented in their diets compared to the water column for all *A. mitchilli* larvae.

Synchaeta baltica was also over-represented in the diets of one size-by-sample group and otherwise neutral, implying a low-level of intentional targeting. That group had the largest sample size, suggesting *S. baltica* predation by *A. mitchilli* may be more prominent in a similar study performed with more samples.

Eurytemora carolleeae was generally over-represented in *A. mitchilli* diets except in one sample. In that same sample, smaller larvae had a significantly larger proportion of *E. carolleeae* in their diet compared to the proportion in the water column, and the water column itself had relatively few *E. carolleeae* compared to *A. tonsa*. All larvae in the sample ate *A. tonsa* at a higher proportion than in the water, and the smaller larvae ate *E. carolleeae* at a higher proportion than in the water, but the larger larvae did not. This may suggest a size-based swap:

A. mitchilli larvae in this study were all feeding from the 64-200 µm size fraction, so they were consuming primarily copepod eggs, nauplii, and small copepodites. Detwyler and Houde (1970) noted that larger *A. mitchilli* larvae (~ 6mm TL) did not consume copepod nauplii anymore once they could consume copepodites. Therefore, the 6-6.99 mm TL size class larvae in this study may have swapped to consuming the more readily available, larger *A. tonsa* copepodites over *E. carolleeae* nauplii. Or, this could suggest a change in feeding styles. At some point in their growth and development, *A. mitchilli* swap from striking at prey to straining the water for prey (Darnell 1958). This would account for the neutrality of *E. carolleeae* and the maintained over-representation of *A. tonsa*.

Despite the smaller sample size compared to *M. saxatilis*, patterns in prey consumption for *A. mitchilli* were easier to discern. Perhaps this is due to the narrower niche breadth and specialist diet throughout ontogeny for this species. Perhaps this data is indeed missing patterns which would be otherwise clear with more samples.

Conclusions

Metabarcoding confirmed that larval *M. americana*, *M. saxatilis*, and *A. mitchilli* were generally consuming prey in alignment with prior studies. However, additional dietary diversity was revealed, particularly the larvae of benthic organisms (meroplankton) and cnidarians. These under-studied taxa deserve much more attention from future work in zooplankton ecology and habitat assessment.

Metabarcoding is a powerful tool for investigating dietary studies, but ultimately most useful when used in conjunction with traditional techniques. Genetic data captured high species

richness and diversity, particularly with soft-bodied prey which otherwise may be too degraded to be detected by morphological identification. However, for some of the novel detections such as the fish in the anchovy diets or the diatoms in the moronid diets, without a morphological verification of prey presence/absence in the gut, that diversity could have been a passive ingestion or secondary predation rather than an intentional consumption of prey. Metabarcoding might also be able to tell us about feeding incidence or onset of first feeding, but more testing is required.

Acknowledgements

Particular thanks to Ben Lee, who performed the zooplankton metabarcoding. Special thanks also to Ben Gregory and Alex Burns for consultation on laboratory technique, Dr. Allison Barba and Dr. Heather Cunningham for partnering on the Chesapeake Community College internship program with Horn Point Laboratory, and Stephanie D'Elia, Miles Bateson, and Lauren Ervin for assisting in fish sample processing and designing laboratory protocol. This project was supported by the Maryland Sea Grant project "*Novel Genomic Tools to Assess Fish Diet and Prey Quality in the Choptank River*" and grants from the Izaak Walton League of America Mid-Shore Chapter, and the Mid-Shore Fishing Club of Maryland.

References

Amundsen, P.-A., H.-M. Gabler, and F. J. Staldvik. 1996. A new approach to graphical analysis of feeding strategy from stomach contents data-modification of the Costello (1990) method. Journal of Fish Biology 48:607–614.

Auth, T., T. Arula, E. Houde, and R. Woodland. 2020. Spatial ecology and growth in early life stages of bay anchovy Anchoa mitchilli in Chesapeake Bay (USA). Marine Ecology Progress Series 651:125–143.

Auth, T. D. 2003. INTERANNUAL AND REGIONAL PATTERNS OF ABUNDANCE, GROWTH, AND FEEDING ECOLOGY OF LARVAL BAY ANCHOVY (ANCHOA MITCHILLI) IN CHESAPEAKE BAY. University of Maryland College Park.

Baldwin, Carole C., Mounts, Julie H., Smith, David G., and Weigt, Lee A. 2009. Genetic identification and color descriptions of early life-history stages of Belizean Phaeoptyx and Astrapogon (Teleostei: Apogonidae) with comments on identification of adult Phaeoptyx.

Beaugrand, G., K. M. Brander, J. Alistair Lindley, S. Souissi, and P. C. Reid. 2003. Plankton effect on cod recruitment in the North Sea. Nature 426:661–664.

Bridgewater, R., and R. E. Schmidt. 1993. Diets of larval white perch and striped bass in the Kingston region of the Hudson River estuary with comments on the significance of the Bosmina bloom.

Cabrol, J., G. Winkler, and R. Tremblay. 2015. Physiological condition and differential feeding behaviour in the cryptic species complex Eurytemora affinis in the St Lawrence estuary. Journal of Plankton Research 37:372–387.

Callahan, B. J., P. J. McMurdie, M. J. Rosen, A. W. Han, A. J. A. Johnson, and S. P. Holmes. 2016. DADA2: High-resolution sample inference from Illumina amplicon data. Nature Methods 13:581–583.

Campfield, P. A., and E. D. Houde. 2011. Ichthyoplankton community structure and comparative trophodynamics in an estuarine transition zone. Fishery Bulletin 109:1–19.

Chesney, E. J. 2008. Foraging behavior of bay anchovy larvae, Anchoa mitchilli. Journal of Experimental Marine Biology and Ecology 362:117–124.

Chick, J. H., and M. J. V. A. N. D. E. N. Avyle. 2016. Zooplankton Variability and Larval Striped Bass Foraging: Evaluating Potential Match / Mismatch Regulation 9:320–334.

Contreras, T., M. P. Olivar, P. A. Hulley, and M. L. Fernández De Puelles. 2019. Feeding ecology of early life stages of mesopelagic fishes in the equatorial and tropical Atlantic. ICES Journal of Marine Science 76:673–689.

Cushing, D. H. 1990. Plankton Production and Year-class Strength in Fish Populations: an Update of the Match/Mismatch Hypothesis. Advances in Marine Biology 26:249–293.

Darnell, R. M. 1958. Food Habits of Fishes and Larger Invertebrates of Lake Pontchartrain, Louisiana, an Estuarine Community. Pages 353–413 Institute of Marine Science.

Dauer, D. M., R. M. Ewing, G. H. Tourtellotte, and H. R. Barker. 1980. Nocturnal Swimming of Scolecolepides viridis (Polychaeta: Spionidae). Estuaries 3:148.

Dennerline, D. E., and M. J. Van Den Avyle. 2000. Sizes of prey consumed by two pelagic predators in US reservoirs: implications for quantifying biomass of available prey. Fisheries Research 45:147–154.

Detwyler, R., and E. D. Houde. 1970. Food selection by laboratory-reared larvae of the scaled sardine Harengula pensacolae (Pisces, Clupeidae) and the bay anchovy Anchoa mitchilli (Pisces, Engraulidae). Marine Biology 7:214–222.

Durant, J., D. Hjermann, G. Ottersen, and N. Stenseth. 2007. Climate and the match or mismatch between predator requirements and resource availability. Climate Research 33:271–283.

Eldridge, M. B., J. A. Whipple, and M. J. Bowers. 1982. BIOENERGETICS AND GROWTH OF STRIPED BASS, MORONE SAXATILIS, EMBRYOS AND LARVAE. Fishery Bulletin 80:461–474.

Fernando, A. V., K. B. Hecke, and M. A. Eggleton. 2018. Length, Body Depth, and Gape Relationships and Inference on Piscivory Among Common North American Centrarchids. Southeastern Naturalist 17:309–326.

Folmer, O., M. Black, W. Hoeh, R. Lutz, and R. Vrijenhoek. 1994. DNA primers for amplification of mitochondrial cytochrome c oxidase subunit I from diverse metazoan invertebrates. Molecular Marine Biology and Biotechnology:6.

Fraser, A. J., J. R. Sargent, and J. C. Gamble. 1989. Lipid class and fatty acid composition of Calanus finmarchicus (Gunnerus), Pseudocalanus sp. and Temora longicornis Muller from a nutrient-enriched seawater enclosure. Journal of Experimental Marine Biology and Ecology 130:81–92.

Frøslev, T. G., R. Kjøller, H. H. Bruun, R. Ejrnæs, A. K. Brunbjerg, C. Pietroni, and A. J. Hansen. 2017. Algorithm for post-clustering curation of DNA amplicon data yields reliable biodiversity estimates. Nature Communications 8:1188.

Gao, X., H. Lin, K. Revanna, and Q. Dong. 2017. A Bayesian taxonomic classification method for 16S rRNA gene sequences with improved species-level accuracy. BMC Bioinformatics 18:247.

Gartz, R. 1999. Measurement of larval striped bass (Morone saxatilis) net avoidance using evasion radius estimation to improve estimates of abundance and mortality. Journal of Plankton Research 21:561–580.

Govoni, J. J. 2005. Fisheries oceanography and the ecology of early life histories of fishes: a perspective over fifty years. Scientia Marina 69:125–137.

Graça, M. A. S., L. Maltby, and P. Calow. 1993. Importance of fungi in the diet of Gammarus pulex and Asellus aquaticus I: feeding strategies. Oecologia 93:139–144.

Graeve, M., W. Hagen, and G. Kattner. 1994. Herbivorous or omnivorous? On the significance of lipid compositions as trophic markers in Antarctic copepods. Deep Sea Research Part I: Oceanographic Research Papers 41:915–924.

Harding, J. 1999. Selective feeding behavior of larval naked gobies Gobiosoma bosc and blennies Chasmodes bosquianus and Hypsoblennius hentzi:preferences for bivalve veligers. Marine Ecology Progress Series 179:145–153.

Hare, J. A. 2014. The future of fisheries oceanography lies in the pursuit of multiple hypotheses. ICES Journal of Marine Science 71:2343–2356.

Hildebrand, S. F., and Wi. C. Schroeder. 1927. The Fishes of Chesapeake Bay. Bulletin of the US Bureau of Fisheries 43:1–366.

Hjort, J. 1914. Fluctuations in the great fisheries of northern Europe viewed in light of biological research. Rapports et procès-verbaux 20:237.

Houde, E. D. 1987. Fish Early Life Dynamics and Recruitment Variability. American Fisheries Society Symposium 2:17–29.

Houde, E. D. 2008. Emerging from Hjort's Shadow. Journal of Northwest Atlantic Fishery Science 41:53–70.

Hunt, G. L., K. O. Coyle, L. B. Eisner, E. V. Farley, R. A. Heintz, F. Mueter, J. M. Napp, J. E. Overland, P. H. Ressler, S. Salo, and P. J. Stabeno. 2011. Climate impacts on eastern

Bering Sea foodwebs: A synthesis of new data and an assessment of the Oscillating Control Hypothesis. ICES Journal of Marine Science 68:1230–1243.

Kattner, G., H. J. Hirche, and M. Krause. 1989. Spatial variability in lipid composition of calanoid copepods from Fram Strait, the Arctic. Marine Biology 102:473–480.

Leray, M., N. Agudelo, S. C. Mills, and C. P. Meyer. 2013a. Effectiveness of Annealing Blocking Primers versus Restriction Enzymes for Characterization of Generalist Diets: Unexpected Prey Revealed in the Gut Contents of Two Coral Reef Fish Species. PLoS ONE 8:e58076.

Leray, M., N. Knowlton, and R. J. Machida. 2022. MIDORI2: A collection of quality controlled, preformatted, and regularly updated reference databases for taxonomic assignment of eukaryotic mitochondrial sequences. Environmental DNA 4:894–907.

Leray, M., J. Y. Yang, C. P. Meyer, S. C. Mills, N. Agudelo, V. Ranwez, J. T. Boehm, and R. J. Machida. 2013b. A new versatile primer set targeting a short fragment of the mitochondrial COI region for metabarcoding metazoan diversity: Application for characterizing coral reef fish gut contents. Frontiers in Zoology 10:1–14.

Limburg, K. E., and M. L. Pace. 1999. Growth, mortality, and recruitment of larval Morone spp. in relation to food availability and temperature in the Hudson River. Fisheries Bulletin 97:80–91.

Limburg, K. E., M. L. Pace, D. Fischer, and K. K. Arend. 1997. Consumption, Selectivity, and Use of Zooplankton by Larval Striped Bass and White Perch in a Seasonally Pulsed Estuary:15.

Martino, E. J., and E. D. Houde. 2010. Recruitment of striped bass in Chesapeake Bay: Spatial and temporal environmental variability and availability of zooplankton prey. Marine Ecology Progress Series 409:213–228.

Mercer, L. 1989. Species profiles: Life histories and environmental requirements of coastal fishes and invertebrates (Mid-Atlantic). Page BR-82(11.109), TR-EL--82-4/82(11.109), 5479645.

Murphy, H. M., G. P. Jenkins, P. A. Hamer, S. E. Swearer, and M.-J. Rochet. 2012. Interannual variation in larval survival of snapper (*Chrysophrys auratus* , Sparidae) is linked to diet breadth and prey availability. Canadian Journal of Fisheries and Aquatic Sciences 69:1340–1351.

North, E. W., and E. D. Houde. 2001. Retention of White Perch and Striped Bass Larvae: Biological-Physical Interactions in Chesapeake Bay Estuarine Turbidity Maximum. Estuaries 24:756.

O'Donnell, J. L., R. P. Kelly, N. C. Lowell, and J. A. Port. 2016. Indexed PCR primers induce template- Specific bias in Large-Scale DNA sequencing studies. PLoS ONE 11:1–11.

Pagenkopp Lohan, K. M., R. Aguilar, R. DiMaria, K. Heggie, T. D. Tuckey, M. C. Fabrizio, and M. B. Ogburn. 2023. Juvenile Striped Bass consume diverse prey in Chesapeake Bay tributaries. Marine and Coastal Fisheries 15:e210259.

Perplexity. 2024. Perplexity.ai (versions from January 2024 until January 2025) [Large language model]. https://www.perplexity.ai/

Piñol, J., G. Mir, P. Gomez-Polo, and N. Agustí. 2015. Universal and blocking primer mismatches limit the use of high-throughput DNA sequencing for the quantitative metabarcoding of arthropods. Molecular Ecology Resources 15:819–830.

Rilling, G. C., and E. D. Houde. 1999. Regional and temporal variability in distribution and abundance of Bay Anchovy (Anchoa mitchilli) eggs, larvae, and adult biomass in the Chesapeake Bay. Estuaries 22:1096–1109.

Robert, D., H. M. Murphy, G. P. Jenkins, and L. Fortier. 2014. Poor taxonomical knowledge of larval fish prey preference is impeding our ability to assess the existence of a "critical period" driving year-class strength. ICES Journal of Marine Science 71:2042–2052.

Sargent, J. R., H. C. Eilertsen, S. Falk-Petersen, and J. P. Taasen. 1985. Carbon assimilation and lipid production in phytoplankton in northern Norwegian fjords. Marine Biology 85:109–116.

Setzler-Hamilton, E. M., P. W. Jones, G. E. Drewry, F. D. Martin, K. L. Ripple, M. Beaven, and J. A. Mihursky. 1982. A comparison of larval feeding habits among striped bass, white perch and clupeidae in the Potomac estuary. University of Maryland Center for Environmental and Estuarine Studies Chesapeake Biological Laboratory.

Sheridan, P. F. 1978. Food Habits of the Bay Anchovy, Anchoa mitchilli, in Apalachicola Bay, Florida. Northeast Gulf Science 2.

Shideler, A. C., and E. D. Houde. 2014. Spatio-temporal variability in larval-stage feeding and nutritional sources as factors influencing striped bass (Morone saxatilis) recruitment success. Estuaries and Coasts 37:561–575.

Shoji, J., E. W. North, and E. D. Houde. 2005. The feeding ecology of Morone americana larvae in the Chesapeake Bay estuarine turbidity maximum: the influence of physical conditions and prey concentrations. Journal of Fish Biology 66:1328–1341.

Su, M., H. Liu, X. Liang, L. Gui, and J. Zhang. 2018. Dietary Analysis of Marine Fish Species: Enhancing the Detection of Prey-Specific DNA Sequences via High-Throughput Sequencing Using Blocking Primers. Estuaries and Coasts 41:560–571.

Sullivan, L. J., T. R. Ignoffo, B. Baskerville-Bridges, D. J. Ostrach, and W. J. Kimmerer. 2016. Prey selection of larval and juvenile planktivorous fish: impacts of introduced prey. Environmental Biology of Fishes 99:633–646.

Uphoff, J. H. 1989. Environmental Effects on Survival of Eggs, Larvae, and Juveniles of Striped Bass in the Choptank River, Maryland. Transactions of the American Fisheries Society 118:251–263.

Vanalderweireldt, L., G. Winkler, M. Mingelbier, and P. Sirois. 2019. Early growth, mortality, and partial migration of striped bass (Morone saxatilis) larvae and juveniles in the St. Lawrence estuary, Canada. ICES Journal of Marine Science 76:2235–2246.

Vestheim, H., and S. N. Jarman. 2008. Blocking primers to enhance PCR amplification of rare sequences in mixed samples – a case study on prey DNA in Antarctic krill stomachs. Frontiers in Zoology 5:12.

Tables

Universal primers	Folmer jgHCO2198	R	5' TAIACYTCIGGRTGICCRAARAAYCA 3'
	Leray mICOIintF	F	5' GGWACWGGWTGAACWGTWTAYCCYCC 3'
Blocking primers	*M. americana*	F	5' **TCTATCCCCC**ACTTGCAAGTAACCT 3'
	M. saxatilis	F	5' **TTACCCCCC**TCTTGCAAGCAACC 3'
	A. mitchilli	F	5' **TTTACCCCCC**TCTAGCAGGAAATT 3'
Zooplankton sequences	*Acartia tonsa*		5' GGAACAGGATGAACAGTTTACCCTCCTTTGTCAAGTAATAT 3'
	Eurytemora carolleeae		5' GGCACGGGGTGAACAGTTTACCCCCCCCTGTCTAGAAATA 3'
	Marenzelleria neglecta		5' GGAACAGGATGAACCGTATATCCTCCTCTAGCAGGCAACCT 3'
	Diaphanosoma		5' GGAACCGGATGAACAGTTTATCCACCTCTTTCGGGCCCTA 3'
	Bosmina liederi		5' GGAACGGGTTGAACTGTTTACCCGCCGTTATCCTCCGGC 3'

Table 3.1: Table showing primer sequences used in the fish gut amplifications. Bold areas in the blocking primer sequences indicate areas of overlap with the universal primer. Blocking primer sequences are an exact pairing for each fish species; this greater affinity and concentration compared to the universal primer ensure more complete annealing to the larval fish DNA. A C3 spacer at the 3' end of each blocking primer prevents elongation. Each zooplankton sequence has five or more mismatches with the blocking primer sequence, ensuring low annealing efficacy with the blocking primer and allowing the universal primer to bind instead.

	M. americana	*A. mitchilli*
Full gut 95% CI	16,176- 23,764	9,105-47,186
Empty gut	**10,169**	**3,118**

Table 3.2: Table with the total sequence reads detected in each of two groups: "empty" gut larvae (larvae with no PCR amplification or inhibition) and their peers (same species, same length class, normal amplification). "Empty gut" indicates the total reads detected for each larva with an empty gut (n= 1 *M. americana*, n= 1 *A. mitchilli*), "Full gut 95% CI" indicates the 95% confidence interval range of the total reads detected for peers (n= 24 *M. americana*, n= 7 *A. mitchilli*). Values which fall outside confidence intervals and are therefore significantly different are in bold.

	M. americana			*A. mitchilli*		
	Predator	**Unknown**	**Other**	**Predator**	**Unknown**	**Other**
Full gut 95% CI	8-12	26-40	49-65	8-28	1-5	66-90
Empty gut	9	**43**	**48**	14	**7**	79

Table 3.3: Table comparing the percentages of total sequence reads divided into classifications between groups of fish larvae. Larvae are divided into two groups: "Empty gut" indicates the reads detected for each larva with an empty gut (larvae with no PCR amplification or inhibition; n= 1 *M. americana*, n= 1 *A. mitchilli*), "Full gut 95% CI" indicates the 95% confidence interval range of the reads detected for peers (same species, same length class, normal amplification; n= 24 *M. americana*, n= 7 *A. mitchilli*). Sequence reads for each group are divided into classifications: predator (sequence reads matching the larval fish species being tested), unknown (sequence reads with no taxonomic identification), and other (sequence reads with a taxonomic identification other than that of the larva being tested). Values which fall outside confidence intervals and are therefore significantly different are in bold.

Fish species	Prey taxa	Linear regression			Spearman correlation		Number of observations
		slope	r^2	p value	rho	p value	
Morone americana	*Diaphanosoma*	0.0129	0.270	0.057	0.538	0.050	14
	Pleopis polyphemoides	-0.0002	0.629	0.033	-0.857	0.024	7
	Polydora cornuta	-0.0009	0.419	0.043	-0.648	0.049	10
	Crassostrea virginica	-0.0009	0.944	0.006	-0.900	0.083	5
	Marenzelleria neglecta	-0.0022	0.208	0.137	-0.615	0.037	12
	Melosira varians	-0.0028	0.387	0.041	-0.455	0.163	11
	Minutocellus polymorphus	-0.0029	0.252	0.096	-0.678	0.019	12
	Morone saxatilis	-0.0038	0.049	0.448	-0.631	0.018	14
	Dorosoma cepedianum	-0.0043	0.212	0.098	-0.552	0.044	14
	Acartia tonsa	-0.0057	0.209	0.100	-0.697	0.007	14
	Bosmina liederi	-0.0116	0.472	0.019	-0.655	0.034	11
Morone saxatilis	*Acanthocyclops brevispinosus*	-0.0015	0.730	0.007	-0.857	0.011	8
Anchoa mitchilli	*Acartia tonsa*	-0.0407	0.729	0.007	-0.524	0.197	8
	Eurytemora carolleeae	0.0388	0.723	0.007	0.524	0.197	8

Table 3.4: Table showing linear regression and Spearman's correlation results for average relative abundance of prey taxa vs. size classes (TL, mm) of larvae for all three fish species. Significant relationships only.

Sample	Larvae size class	Taxa	Taxa proportion in gut		Taxa proportion in water column	Proportion higher in water	Proportion higher in gut
			95% CI, lower	95% CI, upper			
April18.51	3	*Bosmina liederi*	0.2292	0.6099	0.1375		*
		Morone saxatilis	0.0370	0.1421	0.0001		*
		Acanthocyclops brevispinosus	0.0029	0.0170	0.0840	*	
	4	*Morone saxatilis*	0.0108	0.0562	0.0001		*
		Acartia tonsa	-0.0023	0.0329	0.0434	*	
		Amphibalanus improvisus	0.0013	0.0049	0.0705	*	
April18.52	4	*Eurytemora carolleeae*	0.2782	0.7049	0.0846		*
		Polydora cornuta	-0.0088	0.0319	0.0965	*	
May18.B45	3	*Eurytemora carolleeae*	0.2830	0.4986	0.2622		*
		Dorosoma cepedianum	0.1249	0.2423	0.0015		*
		Acartia tonsa	0.1024	0.1788	0.2826	*	
	4	*Eurytemora carolleeae*	0.5238	0.8502	0.2622		*
		Acartia tonsa	0.0200	0.1479	0.2826	*	
		Dorosoma cepedianum	0.0174	0.0818	0.0015		*
		Coscinodiscophyceae	0.0050	0.0101	0.0033		*
	5	*Eurytemora carolleeae*	0.8835	1.0067	0.2622		*
		Acartia tonsa	0.0009	0.0202	0.2826	*	
		Bosmina liederi	0.0054	0.0149	0.0248	*	
		Diaphanosoma	-0.0006	0.0097	0.0151	*	
		Acanthocyclops brevispinosus	0.0011	0.0013	0.1112	*	
	6	*Eurytemora carolleeae*	0.8546	0.9744	0.2622		*
		Acartia tonsa	0.0132	0.0694	0.2826	*	
		Dorosoma cepedianum	0.0025	0.0060	0.0015		*
		Pleopis polyphemoides	0.0001	0.0015	0.0251	*	
	7	*Eurytemora carolleeae*	0.7685	1.0161	0.2622		*
		Acartia tonsa	-0.0057	0.0530	0.2826	*	
		Diaphanosoma	-0.0018	0.0101	0.0151	*	
		Acanthocyclops brevispinosus	-0.0024	0.0102	0.1112	*	
	8	*Dorosoma cepedianum*	0.0707	0.1520	0.0015		*
		Acartia tonsa	-0.0218	0.2401	0.2826	*	
	9	*Acartia tonsa*	-0.0267	0.1935	0.2826	*	
	10	*Eurytemora carolleeae*	0.7451	1.0051	0.2622		*
		Acartia tonsa	-0.0494	0.2170	0.2826	*	
		Dorosoma cepedianum	0.0034	0.0172	0.0015		*
		Bosmina liederi	-0.0021	0.0108	0.0248	*	
		Diaphanosoma	0.0015	0.0066	0.0151	*	
	11	*Eurytemora carolleeae*	0.9664	0.9788	0.2622		*
		Acanthocyclops brevispinosus	0.0007	0.0092	0.1112	*	
		Diaphanosoma	0.0005	0.0093	0.0151	*	
		Bosmina liederi	0.0015	0.0065	0.0248	*	
		Dorosoma cepedianum	0.0018	0.0046	0.0015		*
		Acartia tonsa	0.0020	0.0043	0.2826	*	
		Marenzelleria neglecta	0.0006	0.0030	0.0006		*
	12	*Eurytemora carolleeae*	0.3798	0.9613	0.2622		*
		Acartia tonsa	0.0047	0.0339	0.2826	*	
		Dorosoma cepedianum	0.0030	0.0076	0.0015		*
		Acanthocyclops brevispinosus	-0.0002	0.0097	0.1112	*	
	13	*Eurytemora carolleeae*	0.9154	0.9700	0.2622		*
		Dorosoma cepedianum	0.0017	0.0130	0.0015		*
		Acartia tonsa	0.0035	0.0109	0.2826	*	
		Bosmina liederi	0.0025	0.0082	0.0248	*	
		Acanthocyclops brevispinosus	0.0005	0.0056	0.1112	*	
		Marenzelleria neglecta	0.0009	0.0036	0.0006		*
		Lithodesmium	0.0008	0.0033	0.0006		*
	14	*Eurytemora carolleeae*	0.8574	1.0142	0.2622		*
		Bosmina liederi	0.0005	0.0126	0.0248	*	
		Acanthocyclops brevispinosus	-0.0022	0.0108	0.1112	*	
		Acartia tonsa	-0.0009	0.0090	0.2826	*	
May19.B45	3	*Eurytemora carolleeae*	0.2440	0.7138	0.2149		*
		Diaphanosoma	0.0198	0.0405	0.0655	*	
		Acanthocyclops brevispinosus	0.0091	0.0095	0.0591	*	

Table 3.5: Table showing only the taxa with a significant difference between their relative abundance in the water column vs *M. americana* gut contents. "*" denotes which abundance is significantly higher than the other.

Sample	Larvae size class	Taxa	Taxa proportion in gut		Taxa proportion in water column	Proportions significantly different
			95% CI, lower	95% CI, upper		
April18.51	3	*Eurytemora carolleeae*	0.0717	0.5601	0.1524	no
		Melosira varians	-0.1053	0.3646	0.0001	no
		Acartia tonsa	-0.0033	0.0531	0.0434	no
		Marenzelleria neglecta	-0.0022	0.0177	0.0014	no
	4	*Acanthocyclops brevispinosus*	0.0058	0.7936	0.0840	no
		Bosmina liederi	-0.2113	0.8745	0.1375	no
		Eurytemora carolleeae	-0.0008	0.3280	0.1524	no
		Melosira varians	-0.0357	0.1117	0.0001	no
April18.52	4	*Acartia tonsa*	0.1157	0.3409	0.2711	no
		Marenzelleria neglecta	-0.0924	0.3388	0.0007	no
May18.B45	3	*Minutocellus polymorphus*	-0.0583	0.2049	0.0004	no
		Lithodesmium	-0.0216	0.1090	0.0006	no
		Diaphanosoma	0.0081	0.0346	0.0151	no
	4	*Lithodesmium*	-0.0061	0.0491	0.0006	no
		Polydora cornuta	0.0022	0.0265	0.0053	no
		Diaphanosoma	0.0025	0.0199	0.0151	no
		Synchaeta baltica	0.0007	0.0150	0.0032	no
	5	*Dorosoma cepedianum*	-0.0055	0.0378	0.0015	no
		Coscinodiscophyceae	-0.0016	0.0053	0.0033	no
	6	*Polydora cornuta*	0.0031	0.0092	0.0053	no
		Synchaeta baltica	0.0007	0.0086	0.0032	no
		Minutocellus polymorphus	0.0000	0.0047	0.0004	no
		Spionidae	0.0006	0.0024	0.0006	no
		Lithodesmium	0.0001	0.0015	0.0006	no
	7	*Dorosoma cepedianum*	-0.0228	0.0925	0.0015	no
	8	*Eurytemora carolleeae*	0.1957	0.8505	0.2622	no
		Diaphanosoma	-0.0072	0.0612	0.0151	no
		Polydora cornuta	-0.0073	0.0286	0.0053	no
		Melosira ambiqua	0.0001	0.0123	0.0002	no
	9	*Eurytemora carolleeae*	0.0352	1.1784	0.2622	no
		Dorosoma cepedianum	-0.0666	0.3151	0.0015	no
		Melosira ambiqua	-0.0127	0.0564	0.0002	no
		Diaphanosoma	0.0083	0.0186	0.0151	no
	10	*Lithodesmium*	-0.0008	0.0115	0.0006	no
		Melosira ambiqua	-0.0007	0.0054	0.0002	no
		Bacillariophyta	0.0001	0.0026	0.0009	no
	12	*Diaphanosoma*	-0.0241	0.0983	0.0151	no
		Bosmina liederi	0.0013	0.0281	0.0248	no
		Polydora cornuta	-0.0016	0.0068	0.0053	no
	13	*Diaphanosoma*	0.0019	0.0404	0.0151	no
		Coscinodiscophyceae	-0.0022	0.0079	0.0033	no
	14	*Dorosoma cepedianum*	-0.0155	0.0798	0.0015	no
		Diaphanosoma	-0.0038	0.0191	0.0151	no
		Marenzelleria neglecta	-0.0004	0.0040	0.0006	no
		Minutocellus polymorphus	-0.0002	0.0018	0.0004	no
May18.JP	10	*Acartia tonsa*	0.2942	0.4876	0.3674	no
		Eurytemora carolleeae	0.1713	0.5097	0.1938	no
		Diaphanosoma	-0.1762	0.5824	0.0169	no
May19.B45	3	*Acartia tonsa*	-0.0072	0.2087	0.1838	no
		Dorosoma cepedianum	-0.0461	0.1835	0.0002	no
		Bosmina liederi	-0.0024	0.0720	0.0556	no
		Melosira varians	-0.0034	0.0240	0.0028	no

Table 3.6: Table showing only the taxa without a significant difference in their relative abundance in the water column vs *M. americana* gut contents.

Sample	Larvae size class	Taxa	Taxa proportion in gut		Taxa proportion in water column	Proportion higher in water	Proportion higher in gut
			95% CI, lower	95% CI, upper			
May18.B45	5	*Acartia tonsa*	-0.0412	0.1524	0.2623	*	
	9	*Eurytemora carolleeae*	0.8637	0.9543	0.2434		*
		Acartia tonsa	0.0171	0.1000	0.2623	*	
		Morone americana	0.0095	0.0387	0.0718	*	
		Acanthocyclops brevispinosus	0.0026	0.0027	0.1032	*	
		Bosmina liederi	0.0013	0.0015	0.0230	*	
	10	*Pleopis polyphemoides*	-0.0028	0.0088	0.0233	*	
	12	*Eurytemora carolleeae*	0.3438	1.0190	0.2434		*
		Acartia tonsa	-0.0146	0.2143	0.2623	*	
		Acanthocyclops brevispinosus	0.0025	0.0117	0.1032	*	
		Bosmina liederi	0.0001	0.0050	0.0230	*	
		Diaphanosoma	-0.0001	0.0011	0.0140	*	
May19.B45	5	*Acartia tonsa*	0.3651	0.4377	0.1837		*
		Eurytemora carolleeae	0.2273	0.4694	0.2148		*
		Morone americana	0.0659	0.1936	0.0007		*
		Acanthocyclops brevispinosus	0.0146	0.0283	0.0591	*	
		Leptodora kindtii	-0.0024	0.0239	0.0517	*	
	6	*Morone americana*	0.0430	0.1075	0.0007		*
		Acanthocyclops brevispinosus	-0.0015	0.0259	0.0591	*	
		Bosmina liederi	0.0090	0.0124	0.0556	*	
	7	*Morone americana*	0.0295	0.1110	0.0007		*
		Acanthocyclops brevispinosus	0.0098	0.0243	0.0591	*	
		Bosmina liederi	-0.0066	0.0264	0.0556	*	
	10	*Eurytemora carolleeae*	0.4599	0.5605	0.2148		*
		Acartia tonsa	0.2607	0.4227	0.1837		*
		Morone americana	0.0795	0.1166	0.0007		*
		Dorosoma cepedianum	0.0063	0.0635	0.0002		*

Table 3.7: Table showing only the taxa with a significant difference in their relative abundance in the water column vs *M. saxatilis* gut contents. "*" denotes which abundance is significantly higher than the other.

Sample	Larvae size class	Taxa	Taxa proportion in gut		Taxa proportion in water column	Proportions significantly different
			95% CI, lower	95% CI, upper		
May18.B45	5	*Eurytemora carolleeae*	-0.1120	1.3396	0.2434	no
		Minutocellus polymorphus	-0.1406	0.4344	0.0003	no
		Morone americana	-0.1233	0.4045	0.0718	no
		Dorosoma cepedianum	-0.0295	0.0971	0.0014	no
		Synchaeta baltica	-0.0030	0.0122	0.0030	no
		Lithodesmium	-0.0007	0.0026	0.0006	no
	9	*Dorosoma cepedianum*	0.0011	0.0033	0.0014	no
		Lithodesmium	0.0004	0.0013	0.0006	no
		Minutocellus polymorphus	-0.0003	0.0014	0.0003	no
	10	*Eurytemora carolleeae*	0.1102	0.7643	0.2434	no
		Morone americana	-0.2160	0.8566	0.0718	no
		Acartia tonsa	0.0009	0.4072	0.2623	no
		Synchaeta baltica	-0.0122	0.0389	0.0030	no
		Polydora cornuta	-0.0116	0.0363	0.0049	no
		Dorosoma cepedianum	-0.0040	0.0212	0.0014	no
	12	*Morone americana*	-0.1573	0.5737	0.0718	no
		Dorosoma cepedianum	0.0003	0.0028	0.0014	no
		Lithodesmium	0.0002	0.0011	0.0006	no
May19.B45	5	*Dorosoma cepedianum*	-0.0015	0.0996	0.0002	no
	6	*Eurytemora carolleeae*	0.0346	0.8625	0.2148	no
		Acartia tonsa	0.1625	0.5051	0.1837	no
		Dorosoma cepedianum	-0.0317	0.1645	0.0002	no
	7	*Eurytemora carolleeae*	0.1032	0.5569	0.2148	no
		Acartia tonsa	0.1329	0.3937	0.1837	no
		Dorosoma cepedianum	-0.0605	0.4116	0.0002	no

Table 3.8: Table showing only the taxa without a significant difference in their abundance in the water column vs *M. saxatilis* gut contents.

Sample	Larvae size class	Taxa	Taxa proportion in gut		Taxa proportion in water column	Proportion higher in water	Proportion higher in gut
			95% CI, lower	95% CI, upper			
August18.B45	15	*Acartia tonsa*	0.5270	0.7439	0.4829		*
		Eurytemora carolleeae	0.2545	0.4581	0.2234		*
June18.21	3	*Acartia tonsa*	0.9144	0.9741	0.2865		*
		Eurytemora carolleeae	0.0255	0.0830	0.0157		*
	4	*Acartia tonsa*	0.8614	0.9748	0.2865		*
		Eurytemora carolleeae	0.0239	0.1142	0.0157		*
		Synchaeta baltica	0.0032	0.0221	0.0003		*
		Polydora cornuta	0.0043	0.0203	0.0470	*	
		Alitta succinea	0.0004	0.0006	0.1659	*	
	6	*Acartia tonsa*	0.9663	0.9955	0.2865		*

Table 3.9: Table showing only the taxa with a significant difference in their relative abundance in the water column vs *A. mitchilli* gut contents. "*" denotes which abundance is significantly higher than the other.

Sample	Larvae size class	Taxa	Taxa proportion in gut		Taxa proportion in water column	Proportions significantly different
			95% CI, lower	95% CI, upper		
August18.B45	15	*Bosmina liederi*	0.0017	0.0150	0.0041	no
June18.21	4	*Pleopis polyphemoides*	-0.0005	0.0030	0.0004	no
		Amphibalanus improvisus	0.0001	0.0010	0.0005	no
	6	*Eurytemora carolleeae*	0.0037	0.0336	0.0157	no

Table 3.10: Table showing only the taxa without a significant difference in their abundance in the water column vs *A. mitchilli* gut contents.

Figures

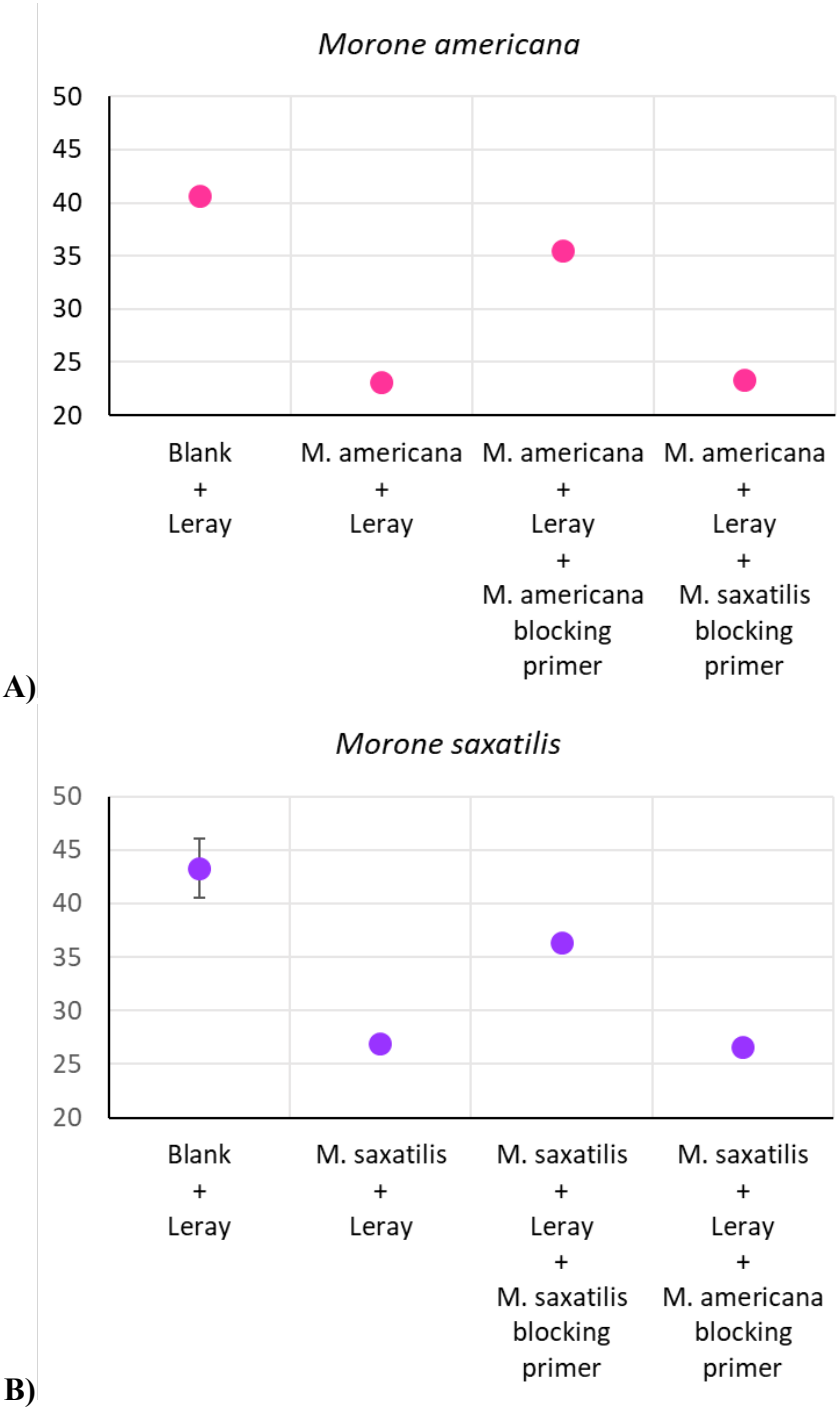

Fig. 3.1: Scatter plots demonstrating the species specificity of the blocking primers for A) *Morone americana* and B) *Morone saxatilis*. X-axes list the combinations of amplified DNA and primers in each test, y-axes list the Cq fluorescence value detected by qPCR. Error bars show standard error of Cq values; most testing did not produce enough error to appear beyond the margins of the points themselves.

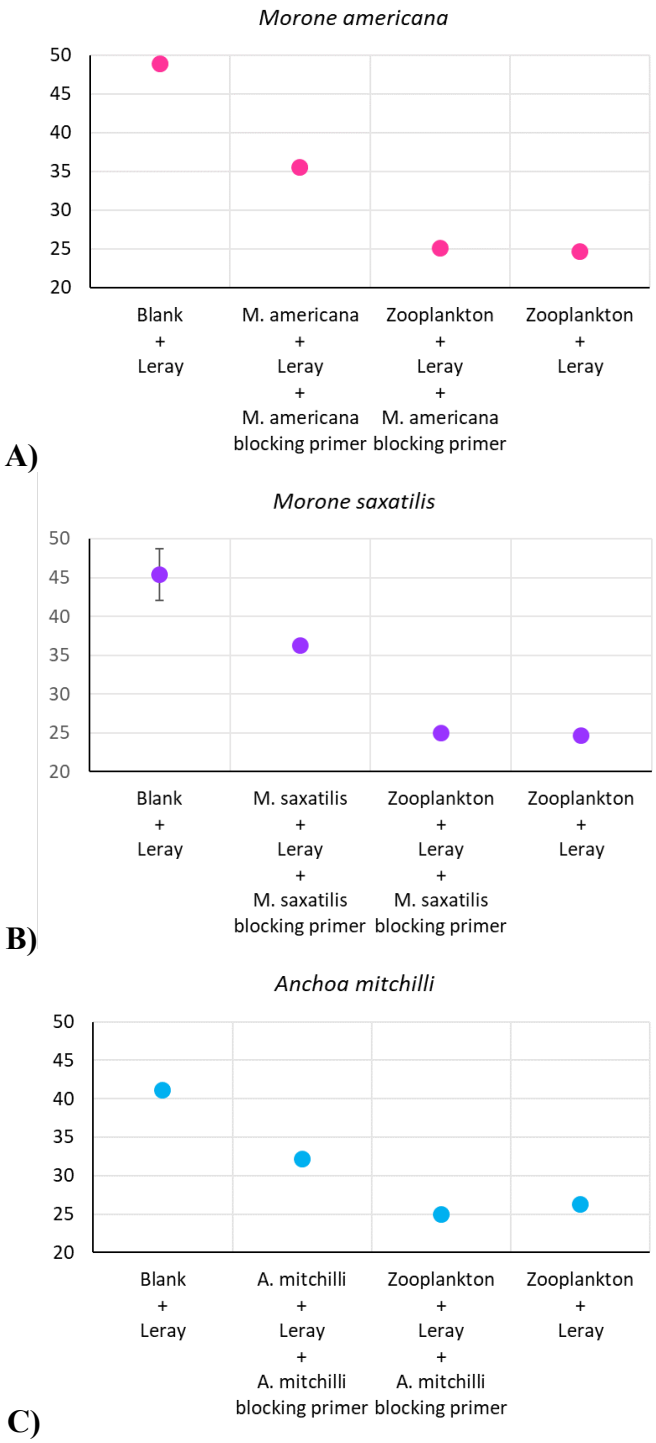

Fig. 3.2: Scatter plots demonstrating the coblocking capacity of the blocking primers for A) *Morone americana*, B) *Morone saxatilis*, C) *Anchoa mitchilli*. X-axes list the combinations of amplified DNA and primers in each test, y-axes list the Cq fluorescence value detected by qPCR. Error bars show standard error of Cq values; most testing did not produce enough error to appear beyond the margins of the points themselves.

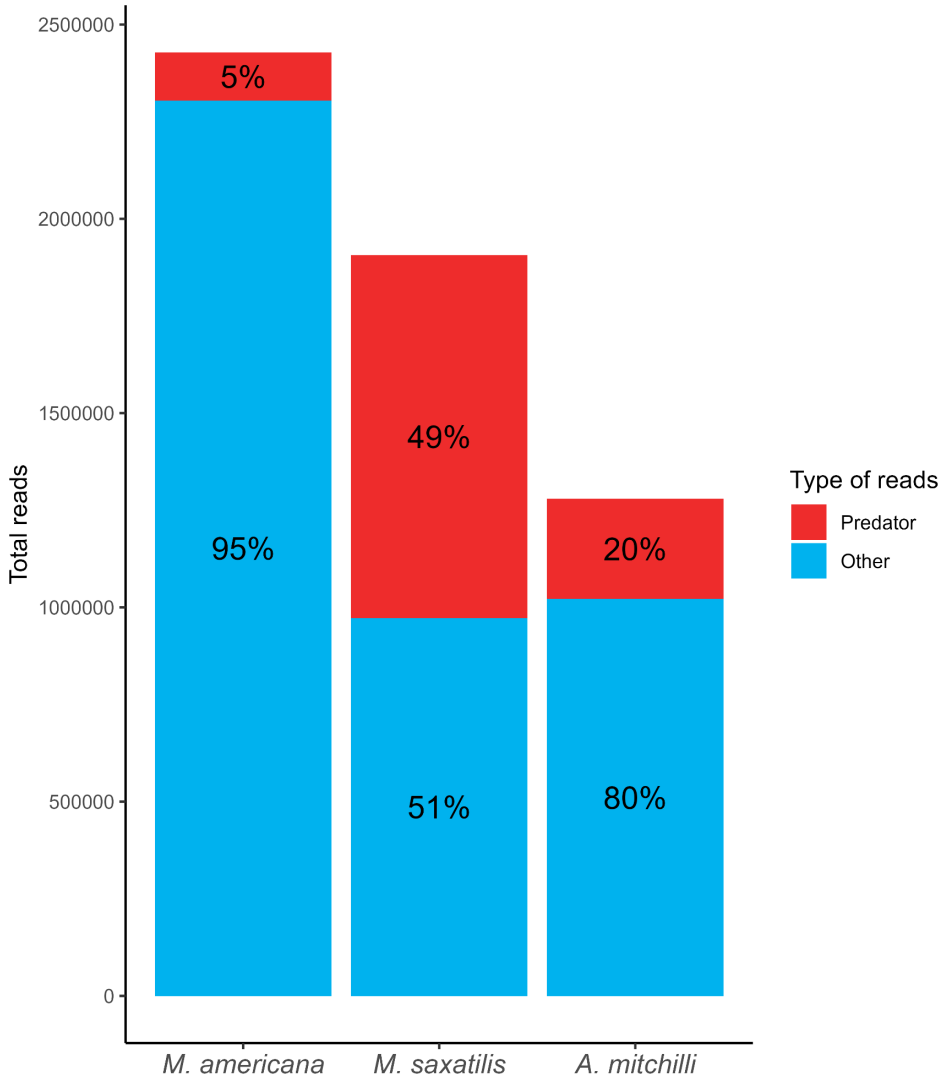

Fig. 3.3: Bar graph showing the total number of sequence reads for each fish species. Colors indicate reads from the same fish species (red: presumably predator reads), and all other species (blue: presumably prey and off-target reads). The data used were post-bioinformatics and filtering but included all taxa regardless of whether they were discarded from downstream analyses as off-target.

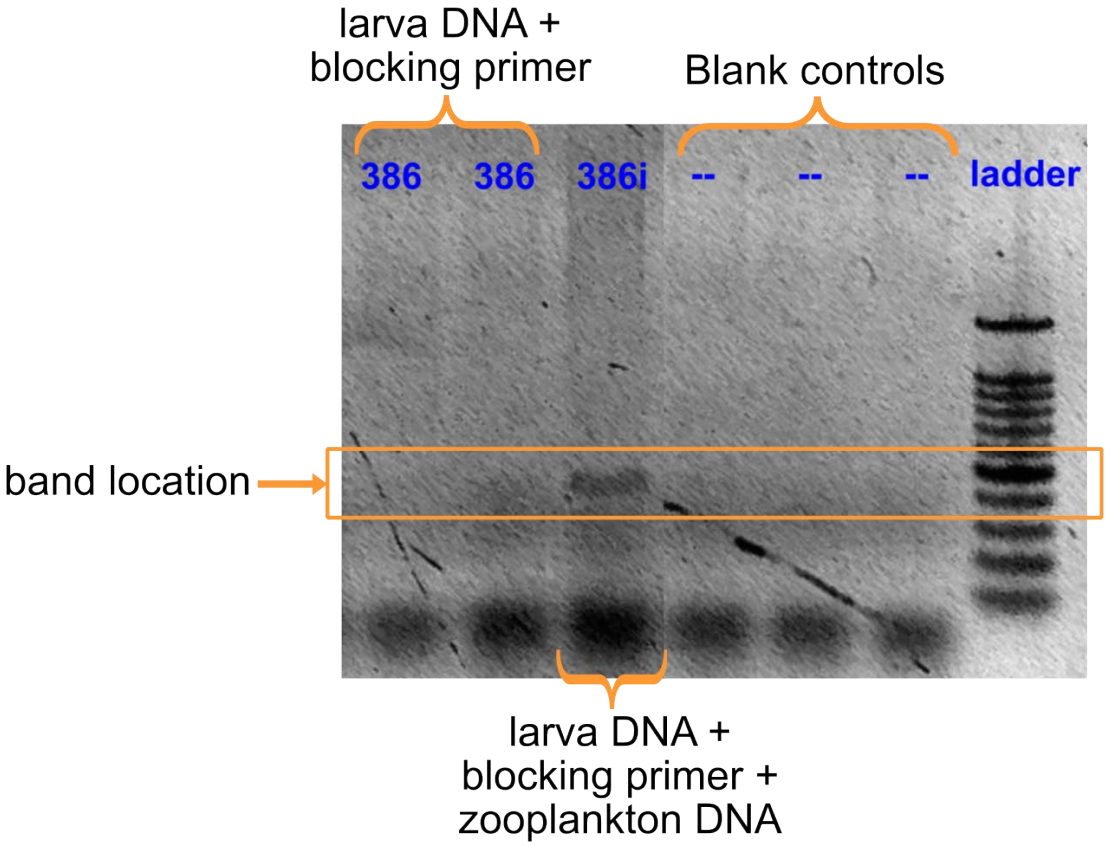

Fig. 3.4: Gel showing no amplification of 4 uL DNA from an *A. mitchilli* larva (lanes labeled 386), but successful amplification of 4 uL fish larva DNA plus 2 uL zooplankton DNA to test for inhibition (lane labeled 386i).

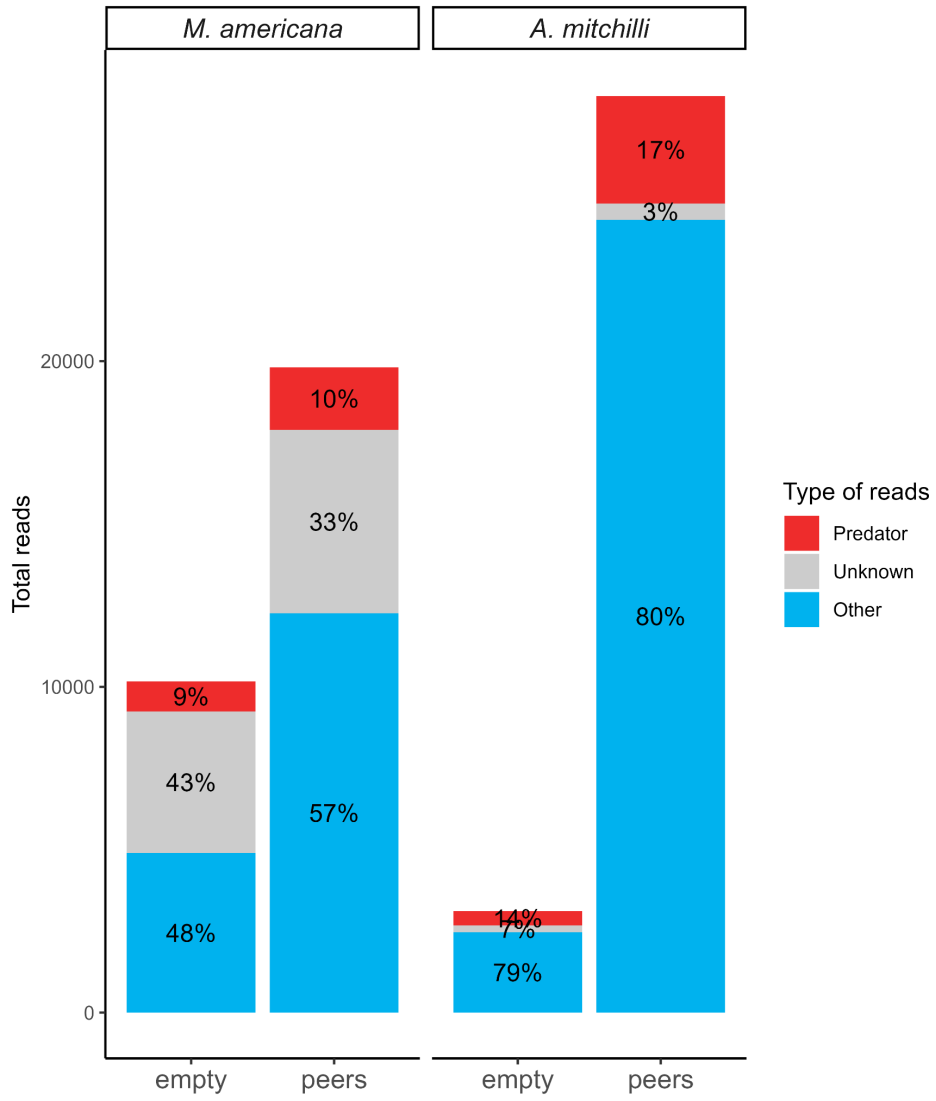

Fig. 3.5: Bar graph showing the total number of sequence reads for the fish with "empty" guts and their peers. Colors indicate reads from the same fish species (red: presumably predator reads), reads without a taxonomic identification (grey), and all other taxonomic identifications (blue: prey and off-target reads). The data used were post-processing but included all taxa, regardless of whether they were discarded from downstream analyses. Each empty fish is a single individual; peers are fish of the same species and length class as the "empty" larvae (3-3.99 mm TL for both species) which amplified and were sequenced as expected.

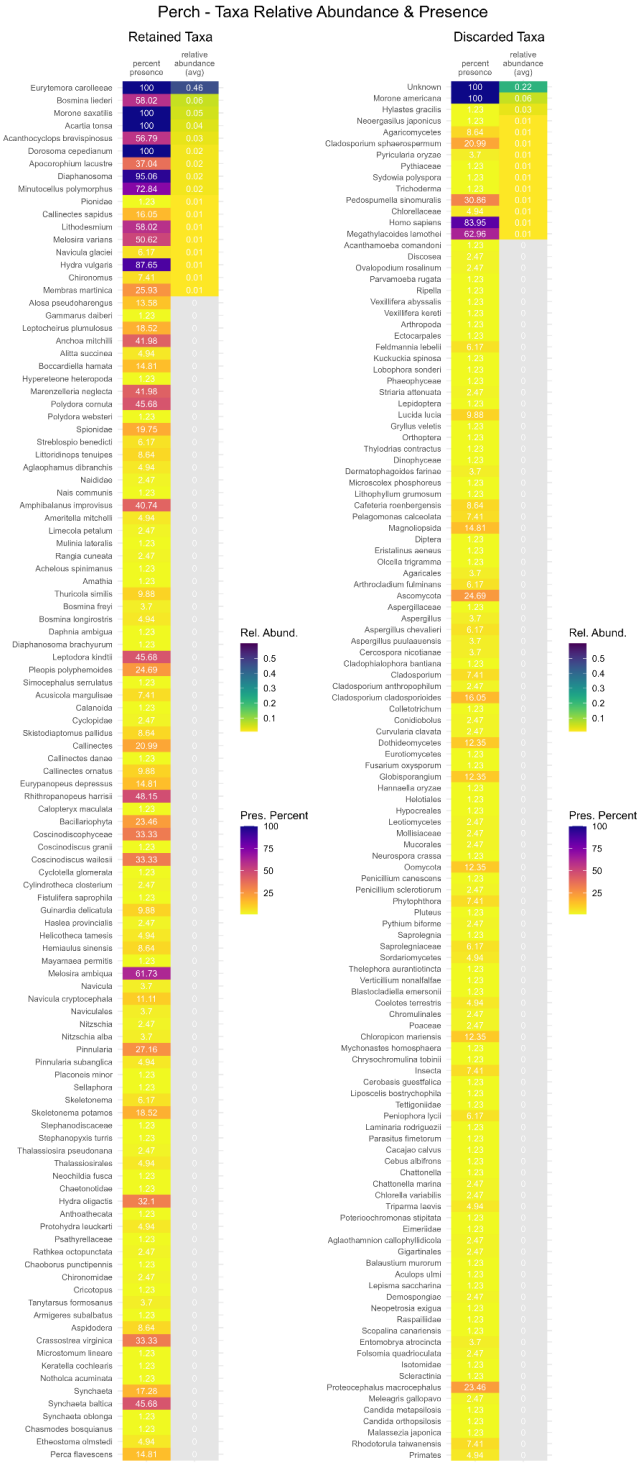

Fig. 3.6: Heatmaps showing retained and discarded taxa detected in *Morone americana* larval gut samples. Each column pair has percent presence on the left (number of larvae with these taxa in their gut, expressed as a percent), average relative abundance (average proportion of gut contents made up by each taxon) on the right. Column pairs are sorted vertically by decreasing average relative abundance; taxa having <0.01 average relative abundance greyed out.

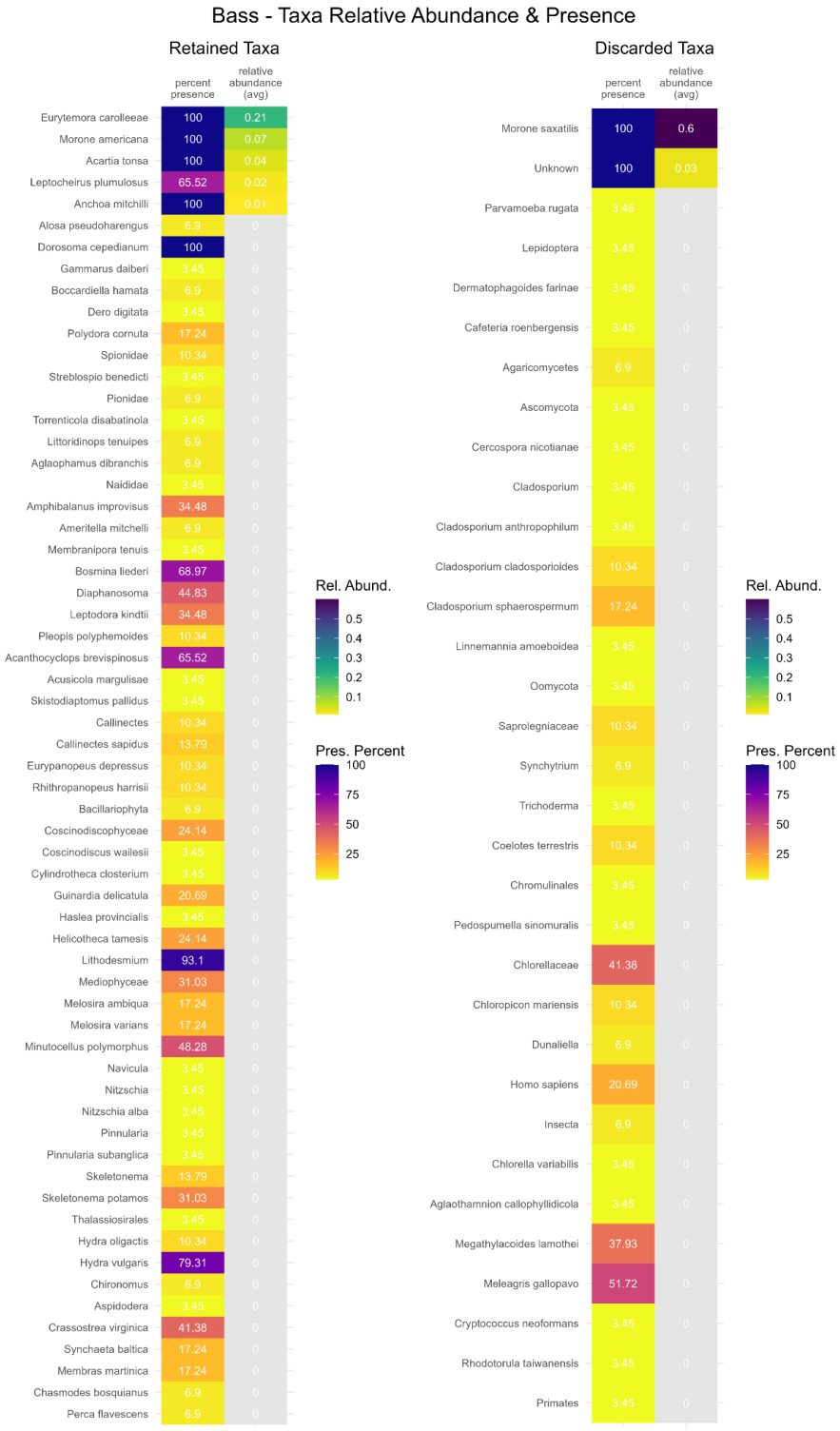

Fig. 3.7: Heatmaps showing retained and discarded taxa detected in *Morone saxatilis* larval gut samples. Each column pair has percent presence on the left (number of larvae with these taxa in their gut, expressed as a percent), average relative abundance (average proportion of gut contents made up by each taxon) on the right. Column pairs are sorted vertically by decreasing average relative abundance; taxa having <0.01 average relative abundance greyed out.

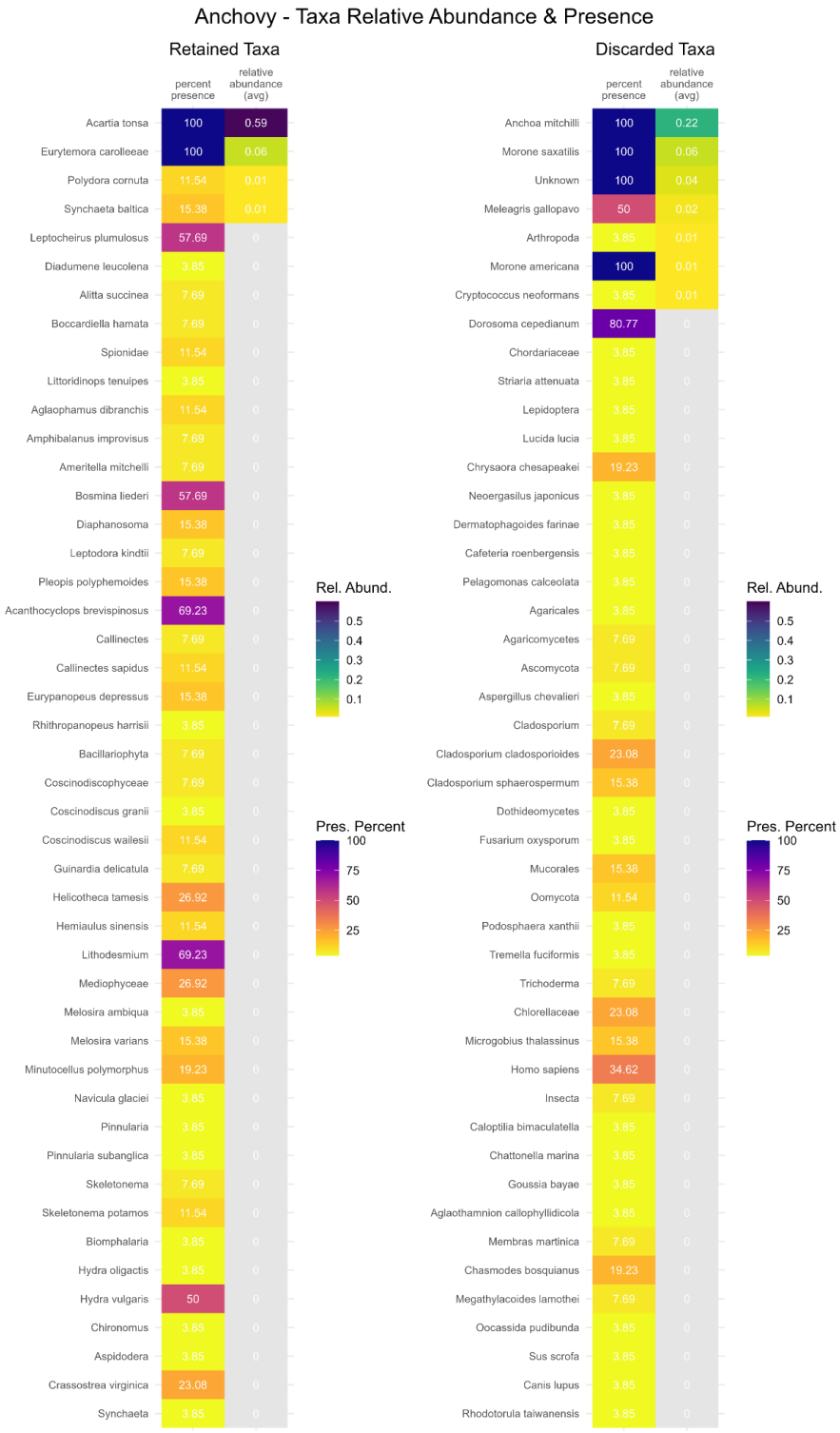

Fig. 3.8: Heatmaps showing retained and discarded taxa detected in *Anchoa mitchilli* larval gut samples. Each column pair has percent presence on the left (number of larvae with these taxa in their gut, expressed as a percent), average relative abundance (average proportion of gut contents made up by each taxon) on the right. Column pairs are sorted vertically by decreasing average relative abundance; taxa having <0.01 average relative abundance greyed out.

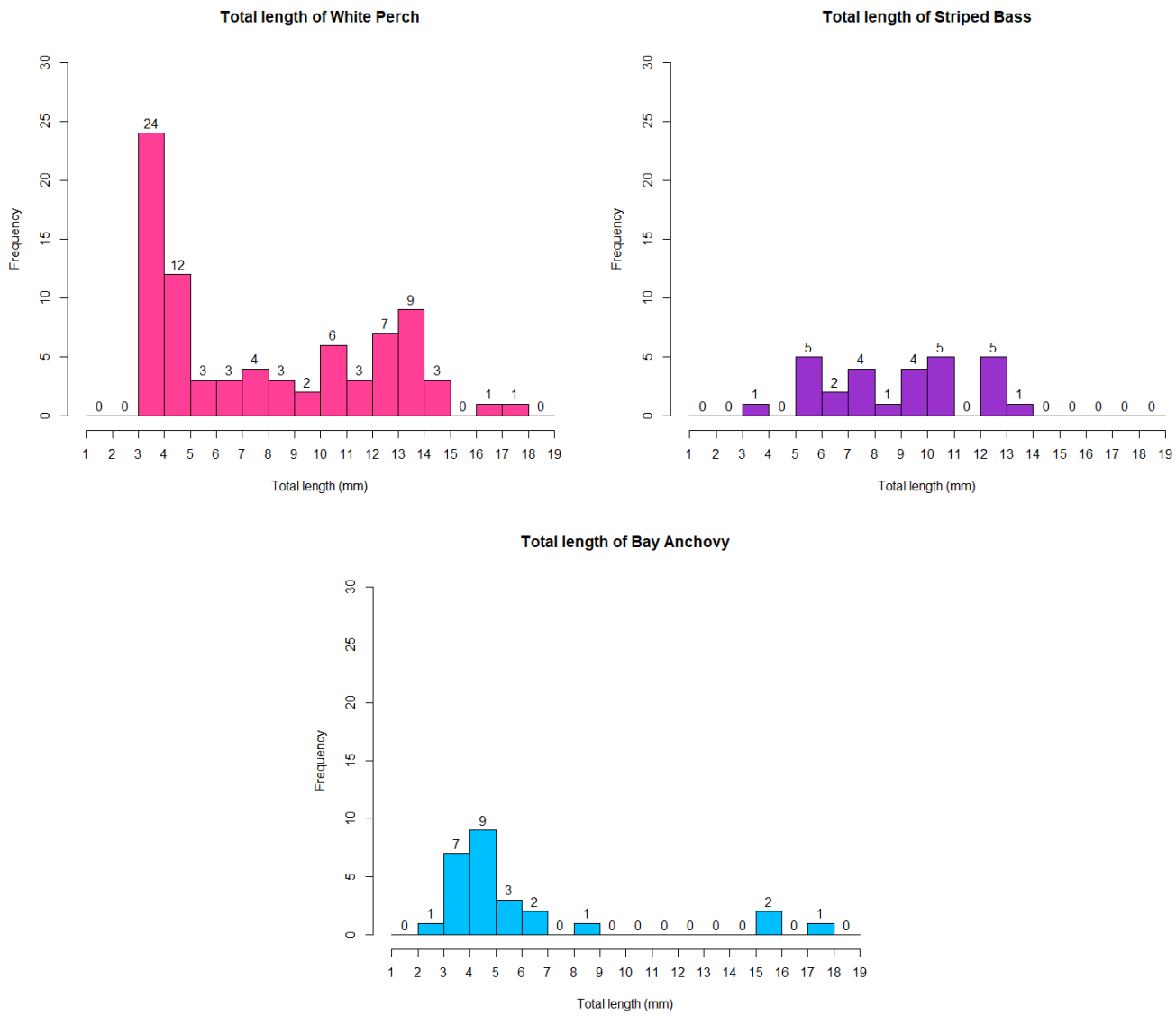

Fig. 3.9: Histograms depicting the frequency of body lengths (total length, in mm) recorded for each larval fish species.

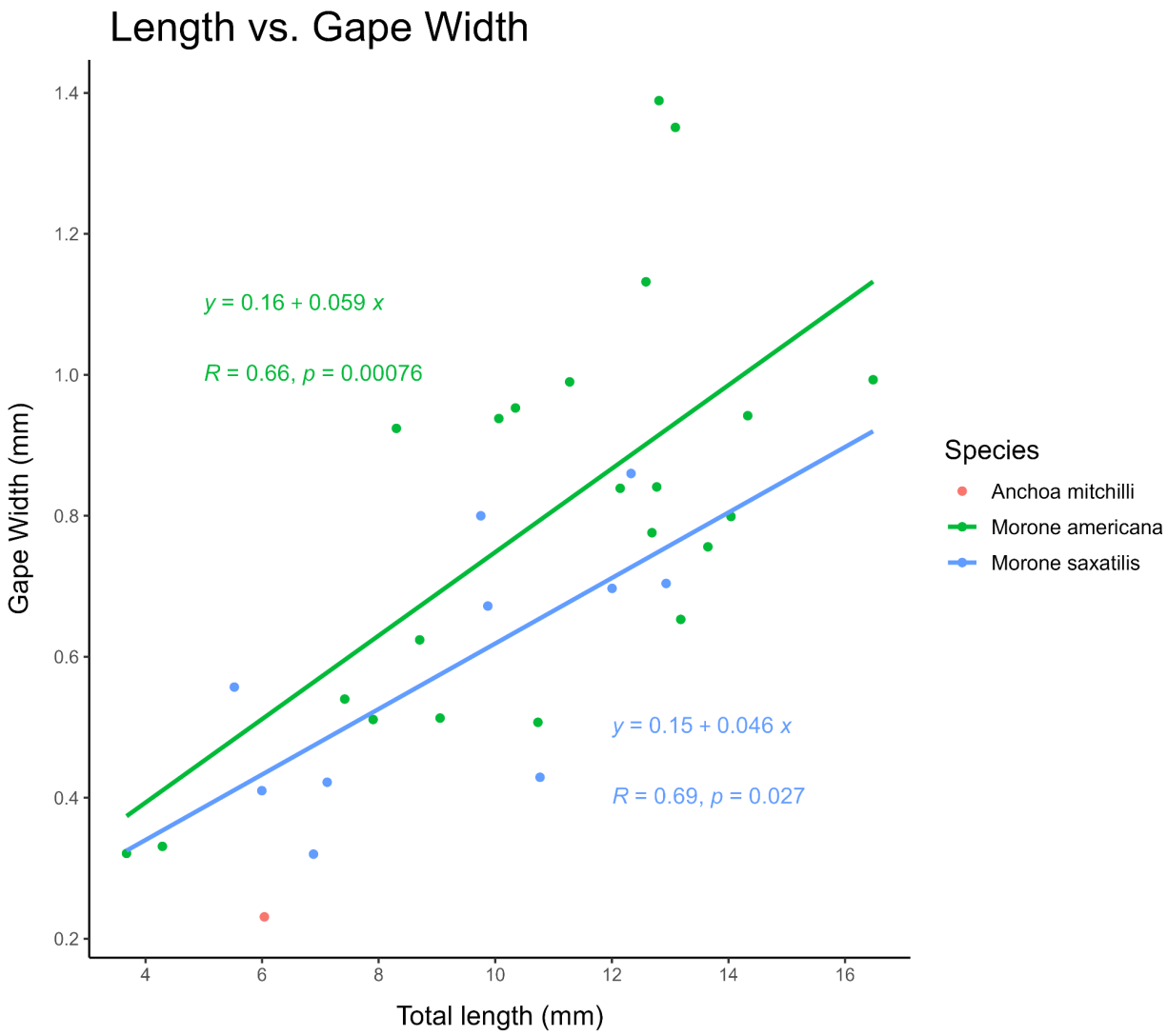

Fig. 3.10: Total length (mm) vs. gape width (mm) for each species of fish larvae measured in this study, with regression lines where possible (not possible for *A. mitchilli*).

Fig. 3.11: Relative abundance (percent of sequences from all sequences retained for each species of fish larvae surveyed) of each major prey group associated with each species of fish larvae. Data square root transformed for ease of viewing (note that the relative abundances no longer sum to 1 due to transformation).

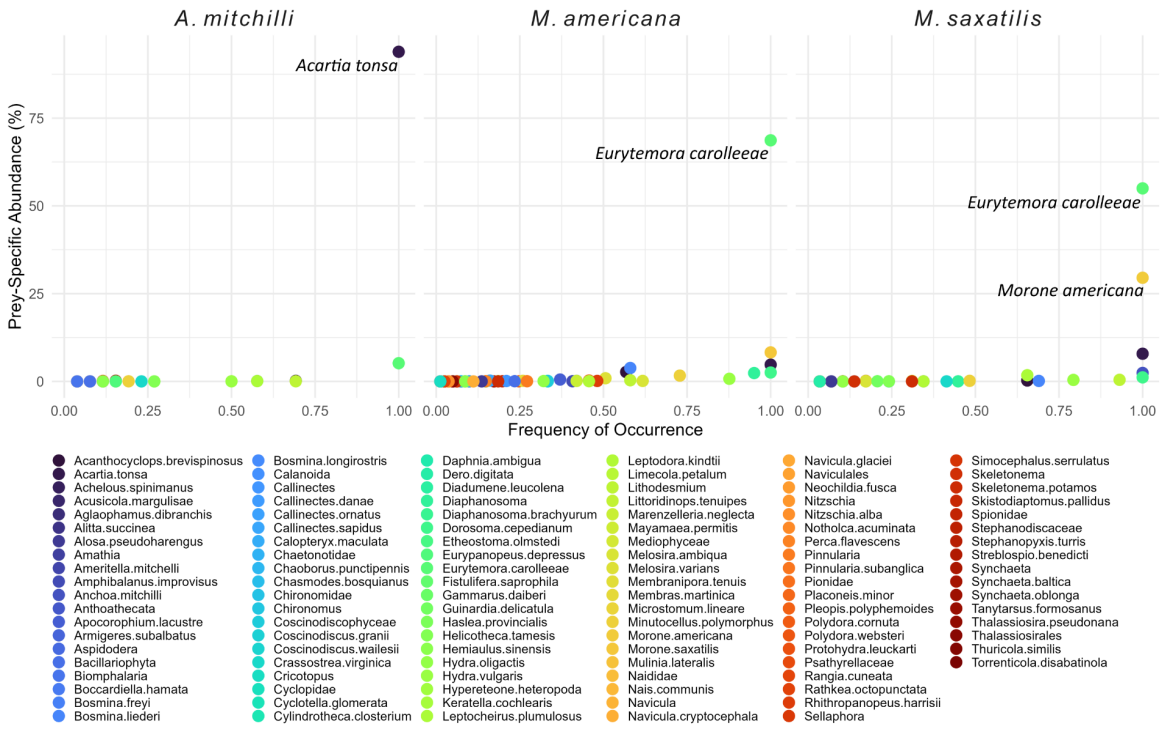

Fig. 3.12: Amundsen plots of *M. americana*, *M. saxatilis*, and *A. mitchilli* overall diets.

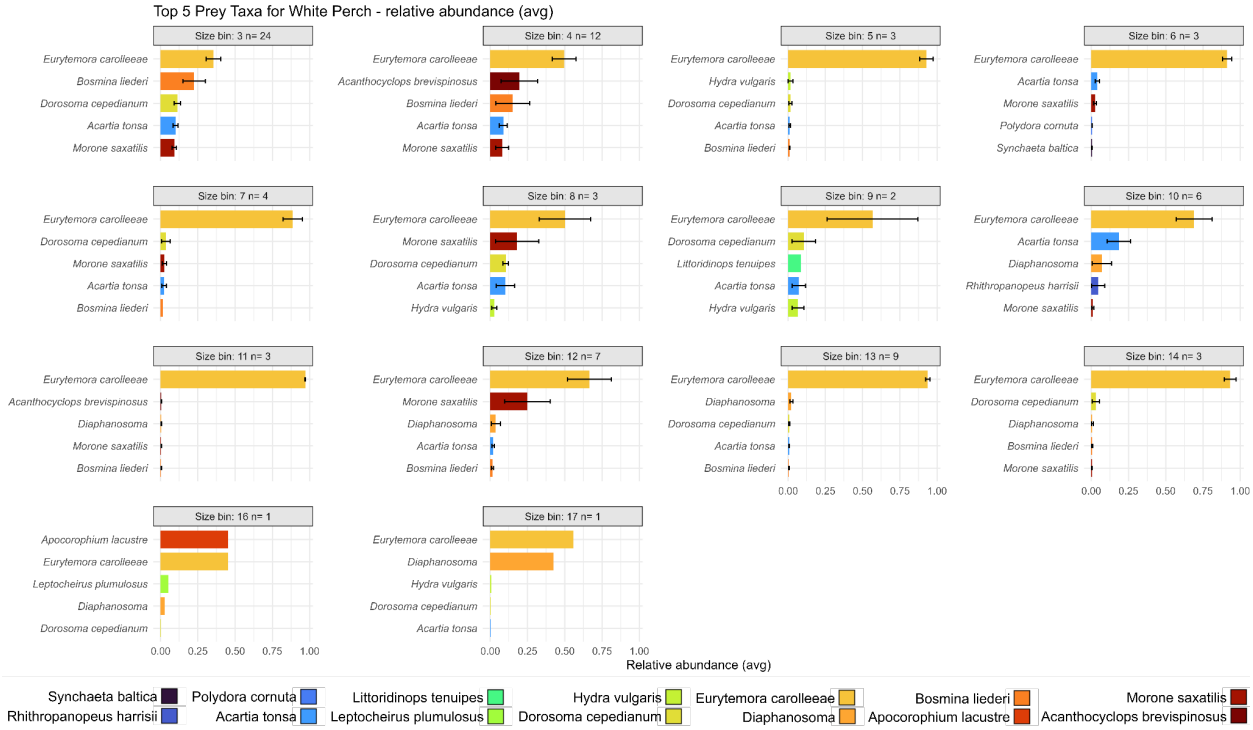

Fig. 3.13: Composite graph showing the average relative abundance of the top five prey taxa in *M. americana* larvae stomachs. Each sub-plot represents a larval size-class in increasing order (e.g. Size bin 3 represents larvae with TL 3-3.99 mm long, Size bin 4 represents larvae with TL 4-4.99 mm long, etc.). The colors identifying prey are consistent identifiers across all such graphs.

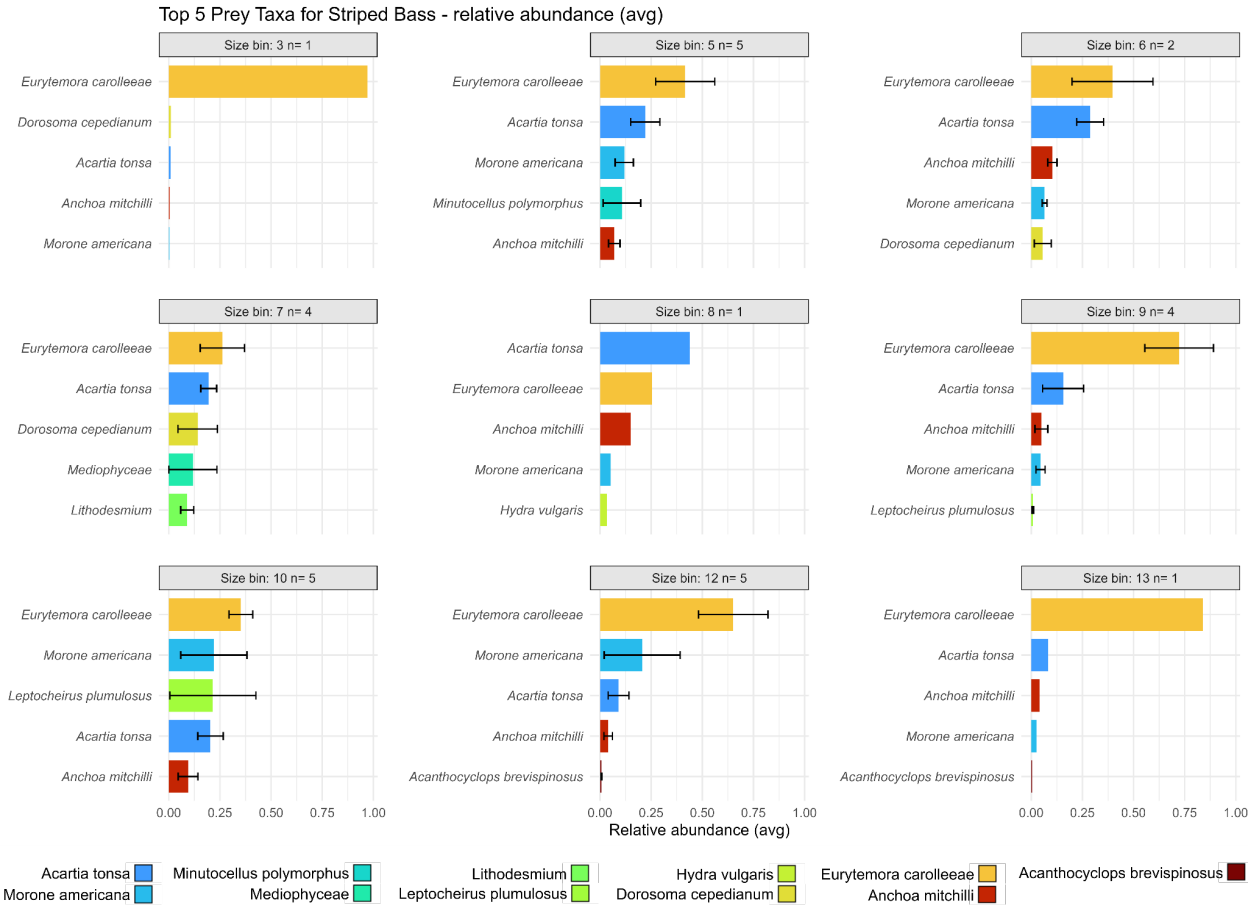

Fig. 3.14: Composite graph showing the average relative abundance of the top five prey taxa in *M. saxatilis* larvae stomachs. Each sub-plot represents a larval size-class in increasing order (e.g. Size bin 3 represents larvae with TL 3-3.99 mm long, Size bin 4 represents larvae with TL 4-4.99 mm long, etc.). The colors identifying prey are consistent identifiers across all such graphs.

Fig. 3.15: Composite graph showing the average relative abundance of the top five prey taxa in *A. mitchilli* larvae stomachs. Each sub-plot represents a larval size-class in increasing order (e.g. Size bin 3 represents larvae with TL 3-3.99 mm long, Size bin 4 represents larvae with TL 4-4.99 mm long, etc.). The colors identifying prey are consistent identifiers across all such graphs.

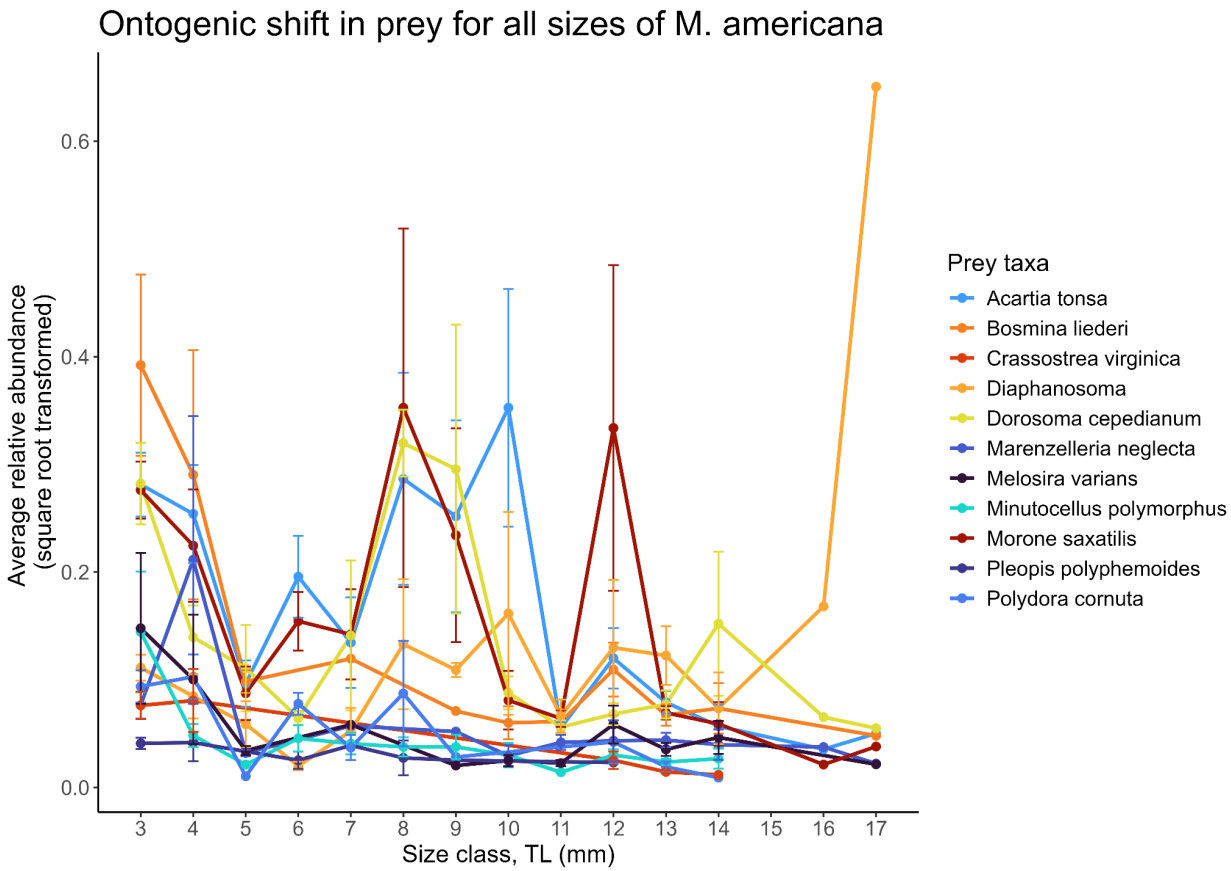

Fig. 3.16: Line graph showing the average relative abundance (square root transformed) of all of the prey taxa in the diets of *M. americana*, vs. the size classes of *M. americana* larvae surveyed (note that the relative abundances will no longer sum to 1 due to transformation). All prey displayed here had a significant ($p < 0.05$ for linear regression and/or Spearman's correlation) increase or decrease across the size classes of larvae; prey taxa without a trend across size classes are not shown.

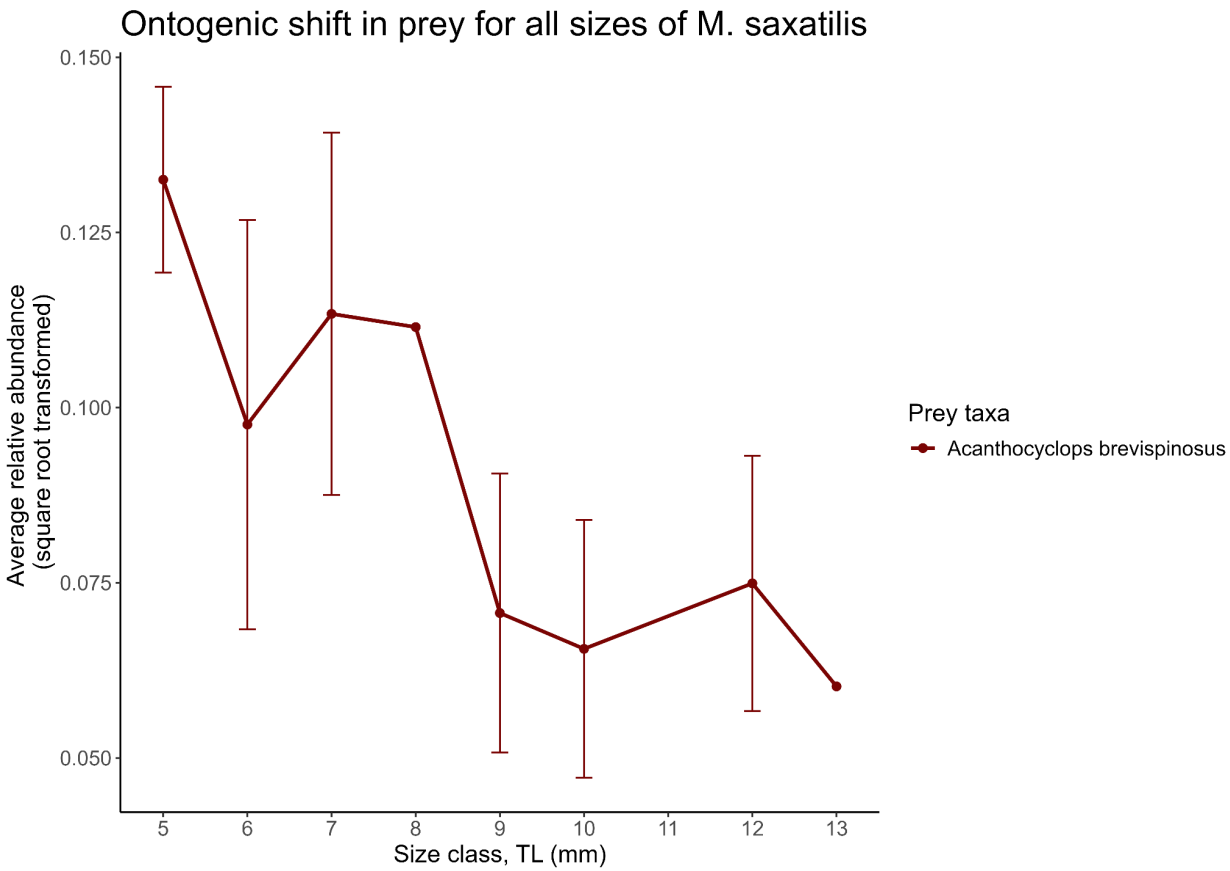

Fig. 3.17: Line graph showing the average relative abundance (square root transformed) of all of the prey taxa in the diets of *M. saxatilis*, vs. the size classes of *M. saxatilis* larvae surveyed (note that the relative abundances will no longer sum to 1 due to transformation). All prey displayed here showed a significant ($p < 0.05$ for linear regression and/or Spearman's correlation) increase or decrease across the size classes of larvae; prey taxa without a trend across size classes are not shown.

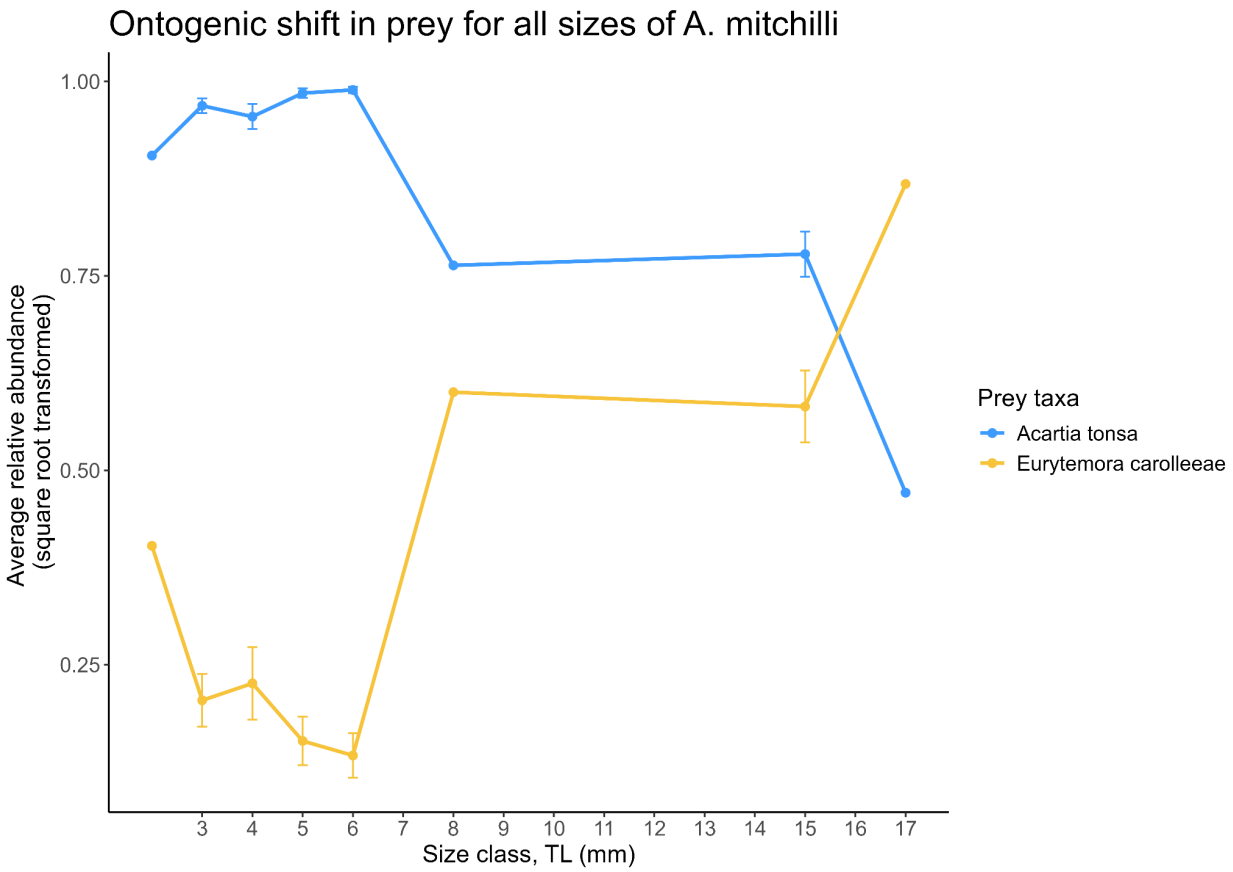

Fig. 3.18: Line graph showing the average relative abundance (square root transformed) of all of the prey taxa in the diets of *A. mitchilli*, vs. the size classes of *A. mitchilli* larvae surveyed (note that the relative abundances will no longer sum to 1 due to transformation). All prey displayed here showed a significant ($p < 0.05$ for linear regression and/or Spearman's correlation) increase or decrease across the size classes of larvae; prey taxa without a trend across size classes are not shown.

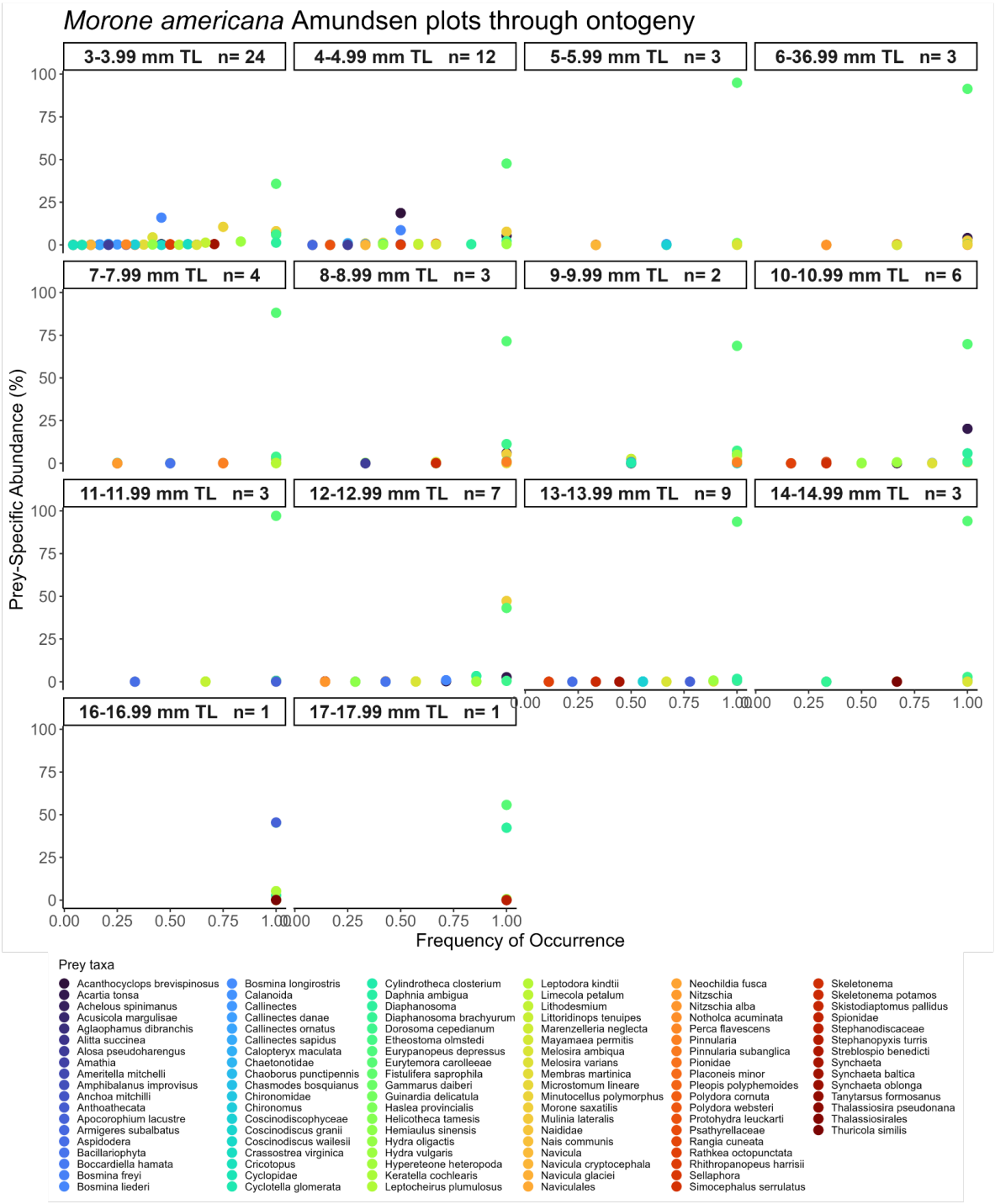

Fig. 3.19: Amundsen plots of *M. americana* by size class, showing the number of larvae in each class (n= xx).

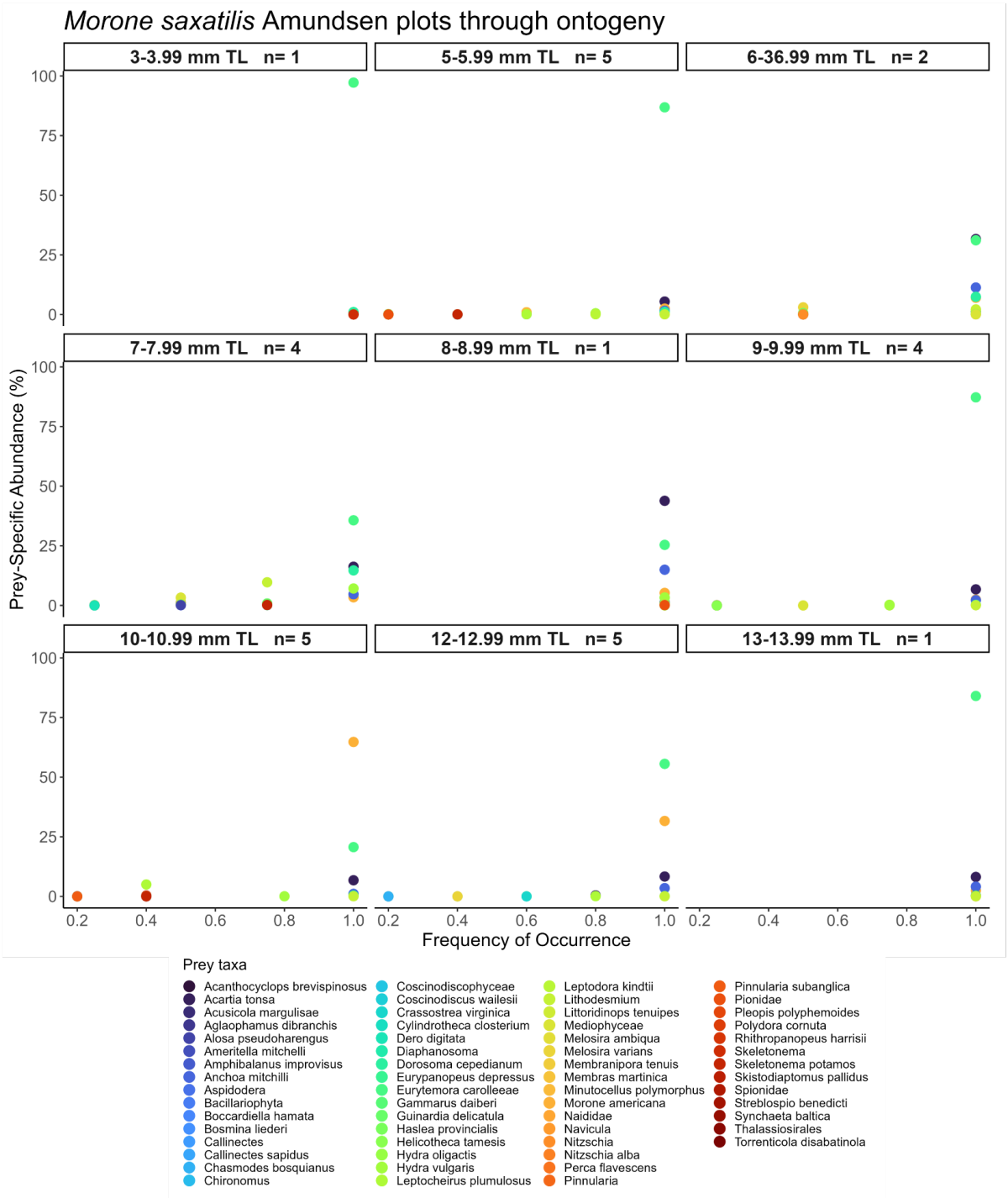

Fig. 3.20: Amundsen plots of *M. saxatilis* by size class, showing the number of larvae in each class (n= xx).

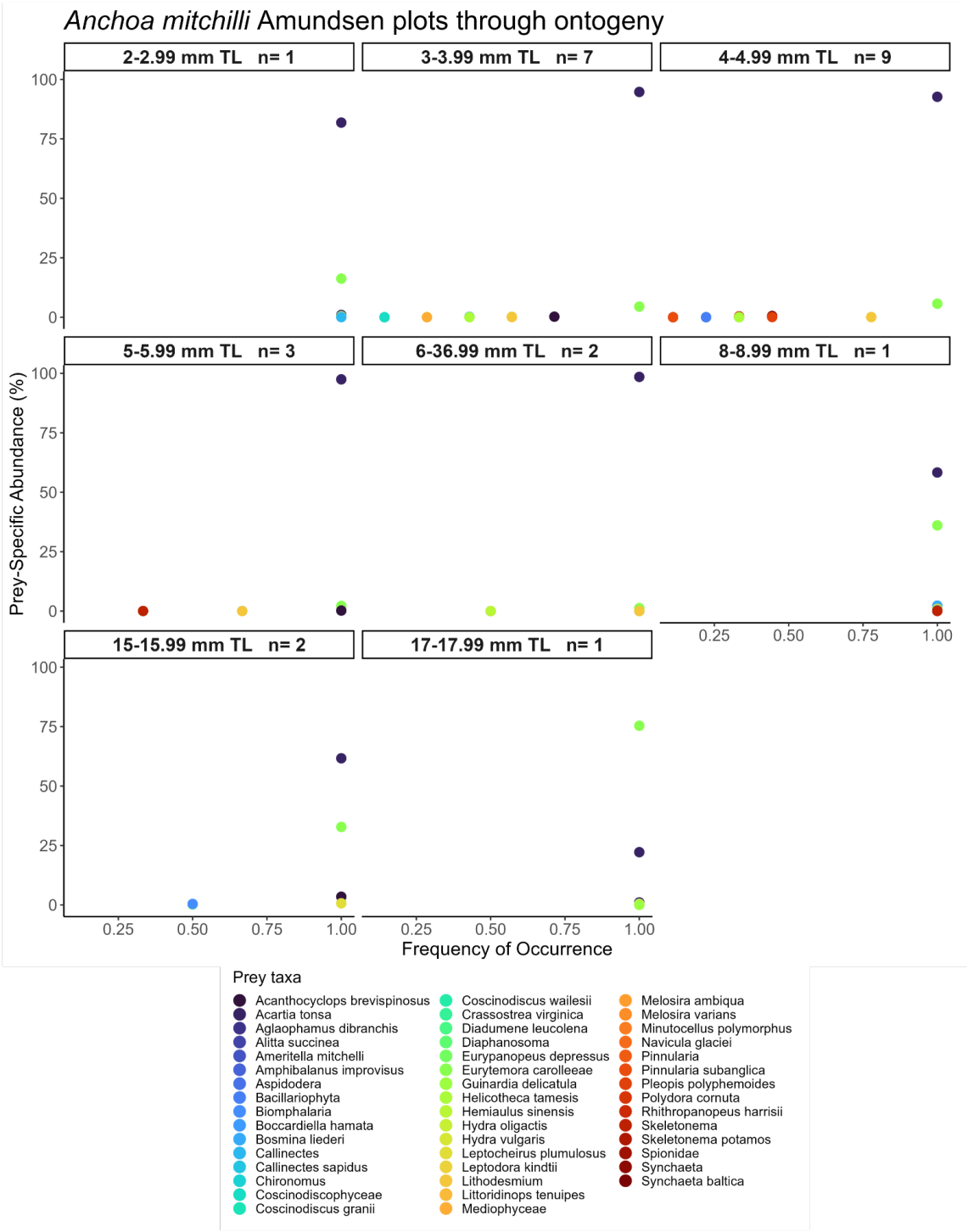

Fig. 3.21: Amundsen plots of *A. mitchilli* by size class, showing the number of larvae in each class (n= xx).

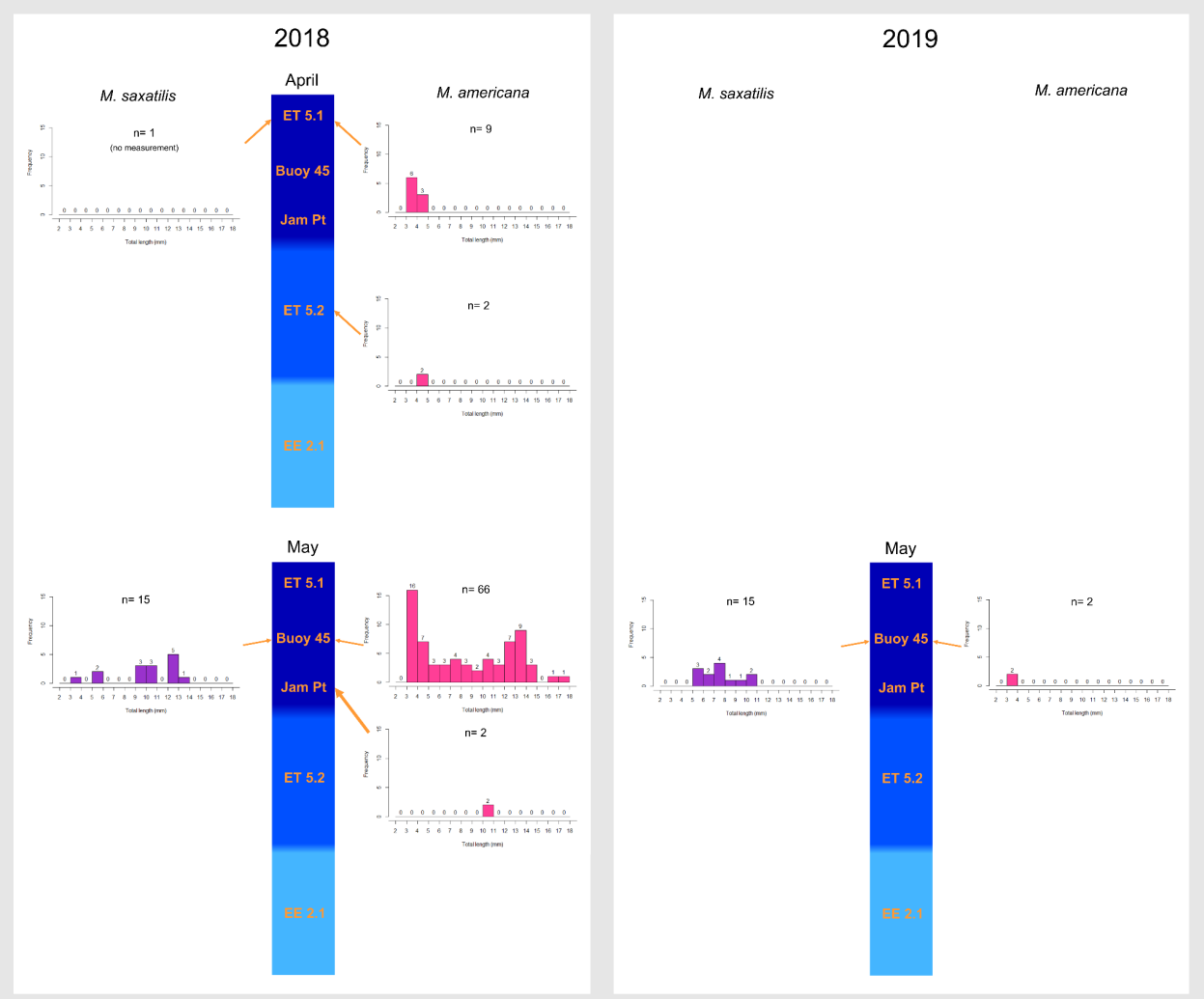

Fig. 3.22: Diagram showing spatiotemporal distribution of moronid (*M. americana, M. saxatilis*) size classes. Study year 2018 in the left column, 2019 in the right column. Within each year column, data for *M. saxatilis* is shown on the left in purple, *M. americana* on the right in pink. The central blue column shows the arrangement of stations from the headwaters of the Choptank (top, dark blue) to the mouth (bottom, light blue). Shades of blue indicate salinity zones: darkest blue= zone 1 (0-4 psu), mid blue= zone 2 (8-10 psu), light blue= zone 3 (10-14 psu). Each histogram lists the total number of larvae (n= xx) from the respective fish species sampled at that site and time, and shows the number of larvae within each 1 mm TL size bin.

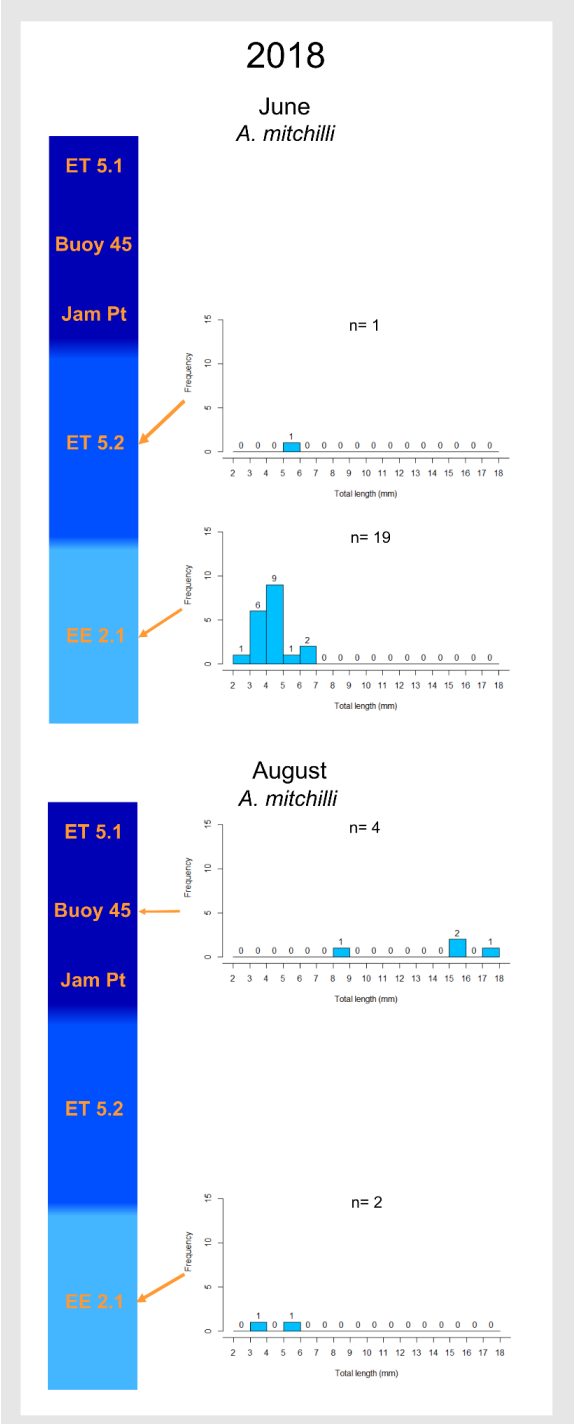

Fig. 3.23: Diagram showing spatiotemporal distribution of *A. mitchilli* size classes (data in blue histograms). Lefthand blue column shows the arrangement of stations from the headwaters of the Choptank (top, dark blue) to the mouth (bottom, light blue). Shades of blue indicate salinity zones: darkest blue= zone 1 (0-4 psu), mid blue= zone 2 (8-10 psu), light blue= zone 3 (10-14 psu). Each histogram lists the total number of larvae (n= xx) from the respective fish species sampled at that site and time, and shows the number of larvae within each 1 mm TL size bin.

Chapter 4: Zooplankton ecology in the Choptank River: then and now

Introduction

Zooplankton communities in the Chesapeake Bay and Choptank River are tied to hydrographic conditions. In particular, salinity, temperature, and dissolved oxygen values and zonation in the water column influence the geographic range, abundance, composition, and life cycle of zooplankton species (Ikeda et al. 2006, Reaugh et al. 2007, Martino and Houde 2010, Salcedo-Bauza 2017). As prevailing weather patterns shift in the Chesapeake Bay region, the already complex distribution and life cycles of zooplankton species also change (Reaugh et al. 2007, Kimmel et al. 2009).

Due to species-specific tolerances, zooplankton species abundances tend to correlate with parcels of water possessing particular physical parameters. The Choptank River is generally well-mixed but seasonally vertically stratified, with bottom water dissolved oxygen only occasionally falling below 3 mg/L in 1999-2010 and consistently above 3 mg/L 2010-2014 (Maryland DNR 2012, 2014). The primary physical parameter determining zooplankton species distribution in the Choptank River is the salinity gradient along the length of the river. The salinity gradient ranges from freshwater at the headwaters to mesohaline at the mouth (~Δ15 ppt). This range is large, only tolerated in its entirety by the most euryhaline zooplankton, and accounts for a matching gradient in zooplankton species distribution. The most common mesozooplankton species in the Chesapeake Bay and Choptank River, *Acartia tonsa* and *Eurytemora carolleeae* (prev. *Eurytemora affinis*), are distributed largely based on their salinity

tolerances: *A. tonsa* in oligohaline to polyhaline waters and *E. carolleeae* in fresh to oligohaline waters (Kimmel and Roman 2004). *Acartia tonsa* is further divided into potential cryptic species: genetically distinct lineages which are largely morphologically indistinguishable yet cannot interbreed. The *A. tonsa* cryptic species have different salinity tolerances, and generally occupy overlapping but distinct distributions (Chen and Hare 2008, Plough et al. 2018). The position of the salinity gradient varies temporally: daily with the tides, and seasonally with inputs of freshwater from spring rains and snowmelt. High river discharge in the spring brings an influx of fresh water which extends the freshwater front downstream, changing the position of the salinity gradient and the associated distribution and abundance of zooplankton species (Kimmel and Roman 2004). Conversely, in years with low springtime river discharge the freshwater front is shifted further upriver.

Species composition and abundance of mesozooplankton in the Chesapeake Bay and Choptank River are also influenced by trophic relationships. *Acartia tonsa* dominates the mesozooplankton in spring through early fall and gives way to *E. carolleeae* in the late fall through early spring (Kimmel and Roman 2004); they are also spatially distributed by salinity tolerances as discussed above. This seasonal succession of copepod species is determined by temperature influencing reproductive rates and styles (diapause/quiescent vs. subitaneous eggs) (Devreker et al. 2009, Jørgensen et al. 2019), but the abundance of each species is also influenced by the occurrence of spring and fall phytoplankton and microzooplankton blooms which are in turn cued by day length, temperature, water column mixing, and nutrient inputs (Kimmel et al. 2009). High river discharge brings with it an influx of terrestrial nutrients; consequently, years with high river discharge have larger spring phytoplankton blooms,

positioned towards the mouth of the estuary (Kimmel et al. 2009, Fisher et al. 2014). These large phytoplankton blooms are generally followed by large increases in the mesozooplankton population, including *A. tonsa* and *E. carolleeae*, though *A. tonsa* populations are generally controlled by top-down effects of predation (Reaugh et al. 2007, Kimmel et al. 2009).

The complexity in the timing of physical cues, reproductive cycles, and abundance peaks of predators and prey can lead to phenological mismatch in time and space. For example, phytoplankton and microzooplankton can bloom out of sync (spatially or temporally) with mesozooplankton, causing unexpectedly low abundances of seasonal zooplankton species (Cushing 1990). This mismatch can also occur between zooplankton and larval fish, reducing the foraging opportunities available to the larvae and increasing the probability of starvation-mediated predation (Martino and Houde 2010, Murphy et al. 2012, Siddon et al. 2013). As physical and biological parameters become more variable with increasing variability and intensity of weather patterns, the distribution, abundance, and composition of zooplankton assemblages will change; these bottom-up effects likely move through the food web, effecting the successful recruitment of zooplanktivorous larval fish.

The Chesapeake Bay Program performed zooplankton monitoring in the Chesapeake Bay and its tributaries (including the Choptank River) from 1984-2002. Many valuable products were produced by the monitoring project, such as the Zooplankton Index of Biological Integrity (ZIBI) and Food Availability Index (FAI), and zooplankton data were incorporated into water quality and fisheries models (Olson and Sellner 2005). However, zooplankton monitoring has not begun again in order to provide these indices and models with updated information in the face of a

changing climate; zooplankton were in fact removed from the Chesapeake Bay Water Quality model in 2019 in part due to the information becoming outdated (Cerco and Noel 2019). Comparing the zooplankton assemblages in the historic monitoring data with assemblages collected in 2018-2019 will likely reveal shifts in the zooplankton community which should be accounted for in modeling efforts.

Methods

2018-2019 data

Zooplankton samples were collected in 2018-2019 and processed as part of the Maryland Sea Grant project as detailed in Chapter 2; hereafter referred to as the SG study. The data from the samples identified via morphology under dissecting scope were used in this study. The morphological data used in Chapter 2 was a subset of the total data collected: paired morphological and metabarcoding samples were only possible for 45 out of 51 morphological samples. The full morphological data set was used here, and abundance units used were individuals/m^3.

Historical and additional environmental data

Environmental parameter data (salinity, water temperature, dissolved oxygen, chlorophyll a, and Secchi depth) for 1984-2001 were provided by the Maryland Department of Natural Resources Tidewater Ecosystem Assessment Division, Eyes on the Bay program (www.eyesonthebay.net). This monitoring program took monthly measures from stations in the Choptank River and the Chesapeake Bay. River flow data for 1984-2002 and 2018-2019 were

provided by the United States Geological Survey National Water Information System, and were gathered from the gauge at Greensboro, MD (site number: 01491000) using the dataRetrieval R package (De Cicco et al 2023). Zooplankton data for 1984-2002 were provided by the Chesapeake Bay Program (CBP) Zooplankton Monitoring Survey; both mesozooplankton (>202 μm) and microzooplankton (44-200 μm) data sets were used in this study. Chlorophyll a and Secchi depth data for 2018-2019 were provided by the Eyes on the Bay program and ShoreRivers Inc.

Missing values for chlorophyll a and Secchi depth at stations Dock, Jamaica Point, and Buoy 45 were interpolated with inverse distance weighting, performed in R using function idw from the gstat package.

Data analysis

All data curation and analyses were performed in R and Microsoft Excel. Code for select R analyses was written with drafting support from Perplexity.ai (Perplexity).

Each study sampled slightly different sites spanning the full salinity gradient of the Choptank River: SG sampled EE 2.1, Dock, ET 5.2, Jamaica Point, Buoy 45 and ET 5.1; and CBP sampled CB4.3C, EE 2.1, ET 5.2, and ET 5.1. For ease of comparison, the Choptank was split into three zones based on the mean salinity recorded at each site during each study: Fresh (zone 1, 0-4 psu; ET 5.1, Buoy 45, Jamaica Point), Median (zone 2, 6-10 psu; ET 5.2, Dock), and Salt (zone 3, 10-14 psu; EE 2.1, CB4.3C) (Fig. 4.1). Each zone includes at least one site which was heavily sampled by each study.

The environmental parameters considered in this study were: temperature, salinity, dissolved oxygen, chlorophyll a, Secchi depth, river flow on the day of sampling, average river

flow for the month of sampling, and average river flow for the month prior to sampling. Chlorophyll a was used as a proxy for phytoplankton abundance. Average river flow for the month prior to sampling was used to account for time-lagged effects of river flow rate on zooplankton.

The CBP mesozooplankton enumeration methods for Maryland waters changed slightly during the monitoring time period, creating three "bins" of time: 1984-1990 (MZ101A), 1990-2001 (MZ101B), and 1998-2002 (MZ101C). Samples enumerated with the MZ101C method were excluded entirely from this study as their focus was on larger organisms. There was no way to compensate for differences in MZ101A vs MZ101B and use of the methods did not overlap in time. Likewise, the CBP microzooplankton enumeration methods MI101 and MI103 were different; samples enumerated with MI103 were excluded from this study as they were biased towards smaller organisms. Units of zooplankton abundance for historic analyses were concentration (individuals/m^3).

When sample replicates were present, the mean abundance value for each taxon was calculated and used in downstream analyses. Taxa found in one replicate but not the other were included in the sample as recorded; zeros were not recorded in any data set. Only whole water column samples were considered, so for samples taken at discrete depths rather than through the entire water column the abundance for each taxon was summed across all depths and used in downstream analyses. When multiple life stages were recorded for a given taxon within a sample, the abundance of each life stage was summed to produce one total abundance per taxon, per sample.

Analyses focused on five zooplankton taxa which were dominant in the system and important prey for larval fishes: the copepods *Acartia tonsa* and *Eurytemora carolleeae* (prev.

Eurytemora affinis), the cladocerans *Bosmina* and *Diaphanosoma*, and the rotifer *Synchaeta*. While there are other zooplankton which are more important components of larval fish diets as discussed in Chapter 3, these five taxa were the only taxa out of the top 15 prey for *M. americana*, *M. saxatilis*, and *A. mitchilli* which were quantitatively sampled by both CBP and SG studies. Where analyses considered all zooplankton, in total or as a community, taxonomic assignments were backed out to the highest common resolution between the two studies (CBP and SG) to avoid artificially inflating differences in the time points resulting from classification nuance. After reassigning taxonomy, abundance data within each taxon in the same sample was summed to retain data.

Taxa not quantitatively sampled by both sampling methods for the SG study and the CBP sampling methods were excluded from their respective data sets; see supplemental Table S4.1 for a complete description. In the CBP microzooplankton data, there was a gap of 12 years where *Acartia tonsa* and *Eurytemora carolleeae* nauplii were not recorded (June 1986-April 1998); this was not due to methodological differences noted during this time. They were not recorded in the CBP mesozooplankton data set either, except perhaps as general copepod nauplii which were removed from the data set because they were not quantitatively sampled by the gear used. This limited the possible time points of focus for this study.

Time points of focus represent the beginning (1984-1985) and end (2000-2001) of the CBP zooplankton monitoring data, and SG study years (2018-2019). An additional year-pair (1999-2000) was selected based on the results of an rCCA test on the environmental parameters between our study years and historic year-pairs where all five zooplankton taxa of interest were quantified (rho= 0.99). Due to record high rainfalls, 2018-2019 had unusually high river flow rates, low salinity, low Secchi depth, and high water temperature compared to conditions during

1984-2001. These parameters, plus dissolved oxygen and chlorphyll a, were used to select the year-pair which was most similar to 2018-2019. This was done in order to compare zooplankton communities across distant time points, but with similar conditions, for long-term shifts in community structure over time. Year-pairs were chosen to best match the sampling structure of our study and account for interannual variation.

PERMANOVA testing on zooplankton community differences between year-pairs accounted for repeated sampling by using the salinity zones as blocks within which to run permutations. Salinity zones were selected rather than sites due to the use of different sites between studies.

Results

Zooplankton abundance over time

Total zooplankton

Linear regressions were run on log10 transformed total zooplankton abundance (individuals/m^3) over historic time points (1984-2001). Abundance significantly decreased for the microzooplankton size fraction; there was no significant pattern for the mesozooplankton fraction (Table 4.1). When the data were separated into salinity zones, mesozooplankton decreased over time in zone 1 (0-4 psu), and microzooplankton decreased in zone 2 (8-10 psu).

Select zooplankton taxa

Abundance of each select zooplankton taxon was analyzed using linear regression vs. time across 1984-2002. There was a clear seasonal signal in both CBP and our study data, in both size fractions (Figures 4.2, 4.3). To avoid confounding results with this seasonal signal (raw

abundance data showed no significant trends), a 12-month running mean of abundance was calculated for each taxon and used in downstream analyses.

In the mesozooplankton fraction (Fig. 4.4), *A. tonsa* showed a significant decrease with time, however *E. carolleeae, Bosmina,* and *Diaphanosoma* significantly increased in abundance (Table 4.2). In the microzooplankton fraction (Fig. 4.5), *A. tonsa* and *Synchaeta* both showed a significant increase over time.

Abundance of each target taxon within each salinity zone was examined separately across historic time points to tease out spatial effects. In salinity zone 1 mesozooplankton (Fig. 4.6), *Diaphanosoma* and *Bosmina* showed a significant increase with time (Table 4.2). *Acartia tonsa*, however, decreased. In the microzooplankton of salinity zone 1, *Synchaeta* showed a significant, linear decrease with time (Fig. 4.7). In salinity zone 2 mesozooplankton, *A. tonsa*, *E. carolleeae*, and *Bosmina* abundance increased significantly with time. In the microzooplankton fraction, only *A. tonsa* had a significant increase with time. In salinity zone 3 mesozooplankton, *A. tonsa* showed a significant decrease with time while *E. carolleeae* had a significant increase. In the microzooplankton, *A. tonsa* showed a significant decrease with time, and *Synchaeta* showed a significant increase over time.

Predicting abundance over time

Linear models were created using running means of select zooplankton taxa from CBP historic data (1984-2001); significant linear relationships were then used to predict the abundance of each taxon of interest in SG study years (2018-2019) with 95% confidence intervals.

In the mesozooplankton size fraction of the CBP data, *A. tonsa* adults showed a significant, linear ($p= 0.00002$, adj $r2= 0.16$), decrease over time (Table 4.2). *Acartia tonsa*

abundance measured in 2018-2019 was generally above the 95% CI of the predicted abundance (Fig. 4.8). *E. carolleeae* however showed a significant, linear (p= 0.00000025, adj r2= 0.24), increase over time. Their abundance in 2018-2019 was well below the 95% CI of their predicted abundance (Fig. 4.9). *Bosmina* also had a significant, linear (p= 0.047, adj r2= 0.033) increase over time with abundance in 2018-2019 below the predicted CI (Fig. 4.10). *Diaphanosoma* showed a significant, linear (p= 0.0082, adj r2= 0.076) increase over time. Their abundance in SG study years was below that predicted by the model, but only about half the timeframe (Fig. 4.11).

In the microzooplankton size fraction of the CBP data, in contrast to the adults, *A. tonsa* nauplii showed a significant, linear (p= 0.0024, adj r2= 0.23) increase over time. However, abundance of *A. tonsa* nauplii measured in 2018-12019 was below the 95% CI on the predicted abundance had this trend continued (Fig. 4.12). *Synchaeta* showed a significant, linear (p= 0.0017, adj r2= 0.084) increase over time. Running mean data in 2018-2019 was limited to a single point, which fell well below the predicted 95% CI (Fig. 4.13).

Relative abundance over time

Relative abundances of the select taxa and other zooplankton were plotted for each of the four time periods of interest. Among the mesozooplankton, results emphasized *Bosmina*, *Diaphanosoma*, and *Synchaeta* as primarily freshwater species, and showed a possibly more diverse freshwater community in 2018-2019 compared to the other three time points (Fig. 4.14). Among the microzooplankton, *Synchaeta* made up a surprising amount of the salt and median community in the historic data, and switched to dominating the fresh community in 2018-2019 (Fig. 4.15).

Years 1999-2000 were selected because the environmental conditions (temperature, salinity, dissolved oxygen, chlorophyll a, Secchi depth, and river discharge rates) most closely matched those of 2018-2019, but despite this it was clear that the zooplankton community structure was very different in these two time points, particularly in the fresh and median salinity zones for mesozooplankton and in all salinity zones for the microzooplankton.

Rank-dominance over time

Rank-dominance plots were constructed to examine patterns in the relative abundances of select taxa vs. other zooplankton in the community more closely. In the mesozooplankton fraction, the fresh zone (zone 1) showed the most radical dominance shifts: *A. tonsa* dominated the community, declined for two middling time points, then dominated again in 2018-2019 (Fig. 4.16). *Bosmina* followed the inverse pattern, with *E. carolleeae* and *Diaphanosoma* remaining the most stable in rank. Median salinity communities (zone 2) had some dominance shifts: *Bosmina* disappeared from this salinity zone in 2018-2019 and *A. tonsa* and *E. carolleeae* briefly swapped ranks in 2000-2001. Salt samples (zone 3) were stable, with *A. tonsa* strongly dominating all years and Bosmina appearing only in 1999-2001.

In the microzooplankton fraction, dominance shifts occurred in all salinity zones (Fig. 4.17). In the fresh zone, *Synchaeta* dominated in 2018-2019 and *E. carolleae* rose in the ranks across all time points; *Bosmina* only appeared in 2018-2019. At median salinity, *Synchaeta* dominated all but 2018-2019, which was dominated by *A. tonsa*, which steadily rose through the ranks across all time points. *E. carolleeae* also moved up through the ranks until 2018-2019. Salt samples were dominated by *A. tonsa* in 1984-1985 and 2018-2019, then *Synchaeta* in 1999-2000 and 2000-2001. *Eurytemora carolleeae* ranked relatively low in these samples.

There were some taxa which were highly ranked in the dominance curves but were not part of the five target taxa. These taxa were mostly copepods, rotifers, molluscs, and ciliates, and they made up on average 5.7% of the community (range 0.012 - 30.3%). Highly ranked non-target taxa were more likely to occur in the fresh samples, as opposed to the salt and median: of the non-target taxa which made up 10% or more of their community (n= 26), 12 occurred in fresh samples, 7 in median, and 7 in salt. Non-target taxa which made up ≥ 10% of their community also tended to come from the microzooplankton fraction rather than the mesozooplankton fraction.

Drivers of abundance

To investigate potential drivers of abundance patterns, simple (Table 4.3) and multiple (Table 4.4) linear regressions were performed on the log10 transformed abundances of the select taxa vs eight environmental parameters: salinity, temperature, chlorophyll a concentration, dissolved oxygen, Secchi depth, daily river flow, monthly river flow, and monthly river flow from the month prior to sampling. Testing used abundance data from both studies, split into size fractions (meso- and micro- zooplankton). Most environmental parameters were correlated with each other to varying degrees by nature of the Choptank River system, so multiple linear regressions were necessary to identify individual effects of parameters where influence could be confounded.

Simple and multiple linear regressions showed that *Diaphanosoma*, *Bosmina*, *E. carolleeae* (adults nauplii), and *A. tonsa* (adults and nauplii) all increased in abundance with increasing concentration of chlorophyll a.

Secchi depth appeared as significant in simple linear regressions for *Diaphanosoma*, *Bosmina*, and *E. carolleeae* (adults) where their abundance declined as secchi depth increased, but was not significant in any of the multiple linear regressions. This measure correlated with chlorophyll a; it was likely masking chlorophyll a effects in simple linear regression, which then appeared in multiple linear regression.

Increasing salinity drove a decrease in *Diaphanosoma*, *Bosmina*, and *E. carolleeae* (adults and nauplii), but drove an increase in *A. tonsa* (adults and nauplii). This is as we expect based on the salinity tolerances of the respective taxa and their appearance in the relative abundance and rank-dominance plots.

Temperature only appeared as a significant driver in multiple regression, where increasing temperature drove a decrease in *E. carolleeae* (adults and nauplii) and an increase in *A. tonsa* (adults and nauplii). Again, this is as expected based on recorded seasonal succession of these regionally dominant taxa (Kimmel and Roman 2004, Devreker et al. 2009).

Dissolved oxygen also only appeared in multiple regression, where an increase in oxygen drove a decline in *E. carolleeae* (adults) abundance and an increase in *A. tonsa* (adults) abundance.

Monthly average river discharge for the month each sample was taken only appeared as significant in multiple regression, where it drove a decrease in the abundance of *A. tonsa* (nauplii only) as discharge increased.

There were no significant relationships between *Synchaeta* abundance and any environmental parameters, and the rest of the environmental parameters had no significant linear relationship to the abundance of our taxa.

Community structure over time

Time points for these analyses were limited to three year-pairs due to the statistically problematic nature of including the same year (2000) in two consecutive year-pairs.

PERMANOVA testing on the zooplankton community at three time points (1984-1985, 2000-2001, 2018-2019) revealed significant differences between the year-pairs for both mesozooplankton and microzooplankton communities ($p= 0.001$, $F= 3.09$; $p= 0.001$, $F= 10.36$ respectively). For the mesozooplankton community, differences between year-pairs 1984-1985 vs. 2018-2019, and 2000-2001 vs. 2018-2019 were significant ($p= 0.006$, $p= 0.003$ respectively; post Bonferroni adjustment); there was no significant difference between year-pairs 1984-1985 vs. 2000-2001. Communities were visualized with NMDS run on a Bray-Curtis dissimilarity matrix of mesozooplankton abundance data (stress= 0.127) (Fig. 4.18). For the microzooplankton community, differences between all year-pairs were significant ($p= 0.003$ for each; post Bonferroni adjustment). Communities were visualized with NMDS run on a Bray-Curtis dissimilarity matrix of microzooplankton abundance data (stress= 0.176) (Fig. 4.19).

SIMPER testing on the zooplankton communities between year-pairs revealed the taxa which contributed the most to dissimilarities between communities. For the mesozooplankton, all four of the select taxa which appeared in that size fraction had large influences on community dissimilarity (*A. tonsa, E. carolleeae, Bosmina, Diaphanosoma*), however only *A. tonsa*'s influence was significant (likely their contribution to dissimilarity was not by chance) (permutation $p= 0.002$ for 1984-1985 vs. 2018-2019) (Table 4.5). The following taxa also had significant contributions to community dissimilarity for 1984-1985 vs. 2018-2019: Calanoida,

Cladocera, *Oithona colcarva*, Mollusca, and Crustacea. For 2000-2001 vs. 2018-2019, Cyclopoida, Annelida, and Harpacticoida had the only significant, if small, contributions to community dissimilarity.

In the microzooplankton community, three out of four of our taxa of interest which appeared in that size fraction had large influences on community dissimilarity (*A. tonsa, E. carolleeae, Synchaeta*), and their influence was significant (permutation p= 0.001, 0.009, 0.049 respectively for 2000-2001 vs 2018-2019) (Table 4.6). Rotifera and Annelida also had significant contributions to community dissimilarity for 2000-2001 vs 2018-2019. *Brachionus angularis* had a significant, if small, contribution to dissimilarity between 1984-1985 vs 2000-2001. Crustacea, *Brachionus angularis*, Bivalvia, Foraminifera, Nematoda, and Arachnida (mites) all had significant contributions to community dissimilarities between 1984-1985 vs 2018-2019.

BIOENV testing followed by Mantel testing on the Bray-Curtis dissimilarity matrices of zooplankton community data for all three year-pairs indicate that date (proxy for season), salinity, and temperature were the environmental variables best correlated with the dissimilarities between the year-pairs for both mesozooplankton (rho= 0.31, Mantel p= 0.001) and microzooplankton (rho= 0.44, Mantel p= 0.001). When date was excluded as a parameter, mesozooplankton community differences were most strongly associated with changes in chlorophyll a, salinity, and temperature (rho= 0.30, Mantel p= 0.001), and microzooplankton community changes were most strongly associated with changes in salinity, temperature, and monthly average river discharge (rho= 0.24, Mantel p= 0.001).

Discussion

Zooplankton abundance over time

Total zooplankton

The consistent decline in total microzooplankton in the entire Choptank over 1984-2001 was driven by their decline in zone 2 (8-10 psu), and for mesozooplankton in just the fresh headwaters of the Choptank River. This is potentially bad news for the food web; the main areas of the Choptank which are affected are the places fish larvae use as nursery grounds to feed on zooplankton and grow (North and Houde 2001, 2003). This is particularly concerning given the disparity between the predicted and actual abundances of select taxa which are important prey for larval fishes.

Predicting abundance over time

These results should be approached with healthy skepticism. Models were made using running means, which by nature are inseparable from time (violating linear regression assumptions of independent measures) and smooth variation in the underlying data. In addition, any linear trend, sufficiently extrapolated out, will run to infinitely high or low depending on the direction of the slope. However, both the predicted abundances and the measures of abundance in the SG study (with the possible exception of *A. tonsa* nauplii) are within the 95% CI of the running means calculated from the CBP study data. They are within the expected range of variation, so the predictions made would likely be considered reasonable.

None of the abundance predictions for the select taxa agreed well with the measured values. All models overestimated the abundance of each taxon with the exception of *A. tonsa* adults, which were underestimated. *Acartia tonsa* had the largest difference between measured

and predicted abundance for both micro- and mesozooplankton, and also the most angled slopes of the CBP models. Their historic trends were strong: the adult model had p= $1.99e^{-5}$, slope= $-8.83e^{-6}$, adj. r^2= 0.16; the model for the nauplii had p= 0.0024, slope= $9.091e^{-5}$, adj. r^2= 0.23. The large disparity between what those strong trends predict vs. the actual measures of 2018-2019 are concerning; something big happened to cause this change. The absence of zooplankton monitoring data in the intervening time between studies makes it difficult to ascertain exactly what occurred and when. However, we can use established relationships between environmental drivers of zooplankton abundance to suggest what might have occurred.

Drivers of abundance

The drivers of select taxa abundance were largely as expected, with the exception of chlorophyll a and dissolved oxygen. Assuming my reasoning in Chapter 2 was sound, the patterns observed here are counter-intuitive. However, Chapter 2 analyses did not include the Chesapeake Bay station CB4.3C. The inclusion of this station in analyses for this chapter may have produced the pattern of decreasing abundances of *A. tonsa* adults and nauplii in zone 3 by capturing hypoxia effects. This relationship could be strong enough to overpower the seasonal collinearity between oxygen and *A. tonsa* abundance I proposed in Chapter 2. *Eurytemora carolleeae* is a brood spawner rather than a broadcast spawner (Devreker et al. 2009), so even though they also appear in zone 3 (and presumably at the station CB4.3C) their hatch rates would not be affected by seasonal hypoxia in the same way as *A. tonsa* so the seasonal collinear relationships would still apply.

Similarly, Chapter 2 analyses frequently excluded station ET5.1 because it was only sampled once and each station was considered individually. In this chapter, station data were

aggregated by salinity zone, so the abundance and environmental measures from this station were included. Again, perhaps the inclusion of this data revealed a relationship between chlorophyll a and select taxa abundance which was stronger than the collinear seasonal relationships.

The historical decrease in *A. tonsa* was driven by decreases in the abundance of adults in zones 1 and 3 of the Choptank (headwaters and mouth, respectively). Being mostly freshwater, zone 1 is generally considered outside *A. tonsa*'s salinity tolerance range (Chen and Hare 2011). So it is possible they were being outcompeted by other species, or that the salinity in zone 1 declined over time and shifted their range downstream. *Acartia tonsa* nauplii increased in zone 2, possibly supporting the range shift hypothesis, but decreased in zone 3 along with the adults; whatever factor is acting on the adults in zone 3 may also be acting on the nauplii. Zone 3 includes a station from the CBP data which is near the channel of the mainstem Chesapeake Bay: CB4.3C. *Acartia tonsa* is a broadcast spawner which drops its eggs throughout the day; they then sink through the water until they hatch (Roman et al. 1993). The abundances of *A. tonsa* in zone 3 could be affected by their eggs dropping into the hypoxic zone of station CB4.3C during the summer, decreasing the local hatch rate and therefore the abundances of nauplii and adults in the seasonal timeframe considered by this study (Roman et al. 1993, Elliott et al. 2013). This is supported by the observations of Kimmel et al (2012), who saw a long-term decline in *A. tonsa* when examining the CBP data (1966-2002) for the mainstem of the Chesapeake Bay due to hypoxia effects and increasing water temperature.

The abundance of *E. carolleeae* increased over time in zones 2 and 3 which could indicate range expansion for this species due to an increase in salinity tolerance or overall decline in salinity of the Choptank over time; this aligns with the negative association between *E.*

carolleeae abundance and salinity. It is possible that increased river flow over time caused a flushing effect, however this is less likely as river flow was not significantly associated with *E. carolleeae* abundance.

The increase in *Bosmina* in zones 1 and 2 over time was no surprise as those zones fall within their salinity tolerances. As *Bosmina* abundance was also negatively associated with salinity, this also supports the idea of a decrease in Choptank salinity over time. The larger increase in zone 1 vs. zone 2 could correspond to spatial increases in food availability; *Bosmina* abundance was positively associated with chlorophyll a concentrations. If this is the case, this could indicate the headwaters of the Choptank are becoming more eutrophic and supporting a larger abundance of specific zooplankton species, but fewer total zooplankton overall.

Diaphanosoma increased in zone 1 only. As they were also positively associated with chlorophyll a concentrations, this could indicate a range expansion to take advantage of a possibly more eutrophic system.

Synchaeta abundance decreased in zone 1, but increased in zone 3. This could indicate a range shift, but because *Synchaeta* was not significantly associated with any environmental driver it is difficult to say what could influence their distribution and abundance.

Community structure over time

Even after compensating for nuances in assigning taxonomic resolution, both size fractions of the zooplankton community were significantly different at the start and end of the CBP study compared to the SG study. There are three possible explanations for this. The first is that differences in the sampling and sample processing methods between the studies created artificial differences in the communities. While the SG study was not designed with this specific

investigation in mind, the sample collection and processing methods were very similar. For the community analyses the taxonomic identifications were backed out to a common level to remove bias introduced by having different workers assign taxonomy, so the major differences between the studies are in the mesh sizes used to separate the micro- and mesozooplankton: CBP used 202 μm mesh for the mesozooplankton and 44-200 μm for the microzooplankton, whereas we used 200 μm mesh for the mesozooplankton and 64-200 μm for the microzooplankton. If this gear were used to sample from the exact same community, one would reasonably expect the mesozooplankton communities to be basically the same and the microzooplankton communities to be different; certainly the microzooplankton would be more diverse because the gear samples a larger size fraction of the community. However, even microzooplankton communities sampled with the same gear at the start and end of CBP monitoring demonstrated a significant shift in composition. This indicates that the microzooplankton community differences between CBP and SG are not entirely caused by differences in sampling method, and there are other factors at play.

The second explanation is that the community shift could be caused by the unusually wet conditions during 2018-2019. Determining the impact of this anomaly was the idea behind including another year-pair with conditions similar to 2018-2019, however with the limitations imposed by the inconsistent recording of *A. tonsa* and *E. carolleeae* nauplii there were few non-overlapping year-pairs to choose from in the rCCA.

The third is that something happened in the time between the two studies which significantly altered the zooplankton community from the baseline established in 1984-2001. Given that the abundances of the select taxa were influenced by several environmental parameters, it is likely that significant change in some combination of these parameters caused the community shift. The environmental drivers identified by BIOENV with the greatest

correlations with community shifts were as we expected to see: salinity, temperature, chlorophyll a concentration, and river flow rate were all identified as significant drivers of the abundances of our select taxa. It follows that these variables would also explain variance in the zooplankton community as a whole. Date was not included in the testing of our select taxa abundances due to high correlation with the other environmental variables, so of course it was not identified as a significant driver. However, it is unsurprising that date correlated significantly with differences in the zooplankton community; date was used as a proxy for season, and the zooplankton community of the Choptank River has a demonstrated seasonality (Kimmel and Roman 2004, Devreker et al. 2009, Millette et al. 2015). None of this, however, tells us exactly which variables initiated the change and how they themselves have changed over time.

Large-scale weather patterns such as El Niño/La Niña (ENSO), the North Atlantic Oscillation (NAO), and Atlantic Multidecadal Oscillation (AMO) might be at play here. Briefly, El Niño causes warmer temperatures and decreased precipitation on the Mid-Atlantic coast of the US on the timescale of months to a year; La Niña causes cooler temperatures and increased precipitation in this region on the timescale of years (Physical Sciences Laboratory, 2025). ENSO was in neutral phase in 1984-1985, briefly negative (La Niña) in 2000 then back to neutral for the rest of 2000-2001, and largely positive (El Niño) in 2018-2019 (NOAA, 2025). Positive NAO causes warmer temperatures and increased precipitation in this region, and negative NAO causes cooler temperatures and decreased precipitation on the timescale of months to years (National Centers for Environmental Information, 2025). NAO was briefly positive in early 1984 and briefly negative in early 1985, positive in early 2000 but neutral for the rest of 2000-2001, and largely positive for 2018 and negative for 2019 (NOAA, 2025). Positive AMO causes warmer temperatures and decreased precipitation; negative AMO causes

cooler temperatures and increased precipitation on the timescale of decades (Nye et al. 2014). AMO was in negative phase in 1984-1985 and neutral phase in 2000-2001 and 2018-2019 (NOAA, 2025). Some combination of these weather patterns could have had an effect on the environmental conditions and therefore the zooplankton communities during the study time periods, however determining the exact influence of each requires investigation beyond the scope of this study.

The mesozooplankton community at the start and end of the CBP study was significantly different from the SG study, but not within the CBP timeseries. This further cements the idea that an unknown event or rising pressure crossed a threshold between the baseline established in 1984-2001 and 2018-2019. All year-pairs in the microzooplankton community were significantly different, but based on the NMDS and SIMPER results the SG year-pair was more different than the CBP years were to each other. The microzooplankton community at the start of the CBP monitoring was particularly different compared to the SG study. Whatever factors caused the zooplankton community shifts acted more strongly on the microzooplankton than the mesozooplankton, causing a higher degree of change, faster. The zooplankton community shift has implications for the Choptank and Chesapeake Bay food web. Zooplankton are the primary prey of first-feeding fish larvae, and so support the health of fisheries (Bridgewater and Schmidt 1993, Limburg et al. 1997, Martino and Houde 2010, Campfield and Houde 2011). Zooplankton community structure and trophic interactions also control the flow of energy through the pelagic environment from primary producers to higher trophic level consumers (Bi and Sommer 2020), and effect the transfer of matter and energy between the pelagic and benthos in the form of passive descent of carcasses and fecal pellets and active transport from migrating zooplankters

such as mysids (Urrere and Knauer 1981, Kiljunen et al. 2020). It is important to know what the structure of the zooplankton community is, and to what degree it is performing its ecological functions.

Changes in the abundances of the select taxa helped drive shifts in the zooplankton community of the Choptank River, but other taxa also played a significant role. A significant contribution here indicates one of two scenarios: the taxon had a variable contribution to dissimilarity between year-pair zooplankton communities (i.e. unusually high standard deviation), or the taxon had a consistent contribution to dissimilarity (i.e. unusually low standard deviation). In the first scenario, the taxon's abundance fluctuated largely between groups; in the second, it was unusually constant.

Acartia tonsa influenced the mesozooplankton community by remaining constant in 1984-1985 vs. 2018-2019; Calanoida, Cladocera, *Oithona colcarva*, Mollusca, and Crustacea all fluctuated. In 2000-2001 vs. 2018-2019 Cyclopoida, Annelida, and Harpacticoida all fluctuated. In 1984-1985 vs. 2018-2019, Crustacea influenced the microzooplankton community by remaining constant; *Brachionus angularis*, Bivalvia, Foraminifera, Nematoda, and Mites fluctuated. In 2000-2001 vs. 2018-2019 *Synchaeta* and *A. tonsa* remained constant; Rotifera, *E. carolleeae*, and Annelida fluctuated. in 1984-1985 vs. 2000-2001 *Brachionus angularis* fluctuated. A deep dive into the ecology of these respective groups would be required in order to understand why the contribution of some of these groups to dissimilarity remained consistent and others fluctuated.

Conclusions

The exclusion of outdated zooplankton data from the Chesapeake Bay Water Quality model was likely correct. It is always important to have up-to-date information for predictive model accuracy, however in addition to this good practice we have demonstrated that the zooplankton community is significantly different from what would be expected based on the community characteristics revealed in the CBP monitoring data.

Observed shifts in the zooplankton community were likely driven by all the usual environmental suspects, but there were some anomalous patterns that we could not untangle that deserve further investigation.

It is important that the drivers behind the change in zooplankton community structure are investigated: the areas of the Choptank which saw significant declines in overall zooplankton abundance and the largest shifts in zooplankton community over time were the fish nursery grounds, which potentially impact recruitment. The salt fronts where fish larvae tend to gather are by nature variable areas, however the degree of change in the zooplankton communities is unusually large. Perhaps the decline in *Morone americana* recruitment over recent years has something to do with these shifts in their prey. The Choptank River does not exist in isolation; it is possible the pattern we observed here has occurred in other Chesapeake Bay tributaries and nursery grounds as well; this also warrants further investigation.

Because of the potentially outsized impact of zooplankton communities on fisheries health, Bay-wide monitoring of zooplankton should not have ceased. Indeed, in an era of anthropogenic climate change this is when we need monitoring the most in order to notice unexpected environmental changes as they occur and adapt rapidly to their onset.

Acknowledgements

This project was supported by the Maryland Sea Grant "*Novel Genomic Tools to Assess Fish Diet and Prey Quality in the Choptank River*" (https://www.mdsg.umd.edu/research-projects/2018/rfish-109).

References

Bi, R., and U. Sommer. 2020. Food Quantity and Quality Interactions at Phytoplankton–Zooplankton Interface: Chemical and Reproductive Responses in a Calanoid Copepod. Frontiers in Marine Science 7:15.

Bridgewater, R., and R. E. Schmidt. 1993. Diets of larval white perch and striped bass in the Kingston region of the Hudson River estuary with comments on the significance of the Bosmina bloom.

Campfield, P. A., and E. D. Houde. 2011. Ichthyoplankton community structure and comparative trophodynamics in an estuarine transition zone. Fishery Bulletin 109:1–19.

Cerco, C. F., and M. R. Noel. 2017. 2017 Chesapeake Bay Water Quality and Sediment Transport Model:580.

Chen, G., and M. P. Hare. 2008. Cryptic ecological diversification of a planktonic estuarine copepod, Acartia tonsa. Molecular Ecology 17:1451–1468.

Chen, G., and M. P. Hare. 2011. Cryptic diversity and comparative phylogeography of the estuarine copepod Acartia tonsa on the US Atlantic coast. Molecular Ecology 20:2425–2441.

Cushing, D. H. 1990. Plankton Production and Year-class Strength in Fish Populations: an Update of the Match/Mismatch Hypothesis. Advances in Marine Biology 26:249–293.

Devreker, D., S. Souissi, G. Winkler, J. Forget-Leray, and F. Leboulenger. 2009. Effects of salinity, temperature and individual variability on the reproduction of Eurytemora affinis (Copepoda; Calanoida) from the Seine estuary: A laboratory study. Journal of Experimental Marine Biology and Ecology 368:113–123.

Elliott, D. T., J. J. Pierson, and M. R. Roman. 2013. Predicting the Effects of Coastal Hypoxia on Vital Rates of the Planktonic Copepod Acartia tonsa Dana. PLoS ONE 8.

Fisher, T. R., G. Breeze, and W. R. Boynton. 2014. Cultural eutrophication in the Choptank and Patuxent estuaries of Chesapeake Bay 51:435–447.

Ikeda, T., A. Yamaguchi, and T. Matsuishi. 2006. Chemical composition and energy content of deep-sea calanoid copepods in the western North Pacific.

Jørgensen, T. S., P. M. Jepsen, H. C. B. Petersen, D. S. Friis, and B. W. Hansen. 2019. Eggs of the copepod Acartia tonsa Dana require hypoxic conditions to tolerate prolonged embryonic development arrest. BMC Ecology 19:1.

Kiljunen, M., H. Peltonen, M. Lehtiniemi, L. Uusitalo, T. Sinisalo, J. Norkko, M. Kunnasranta, J. Torniainen, A. J. Rissanen, and J. Karjalainen. 2020. Benthic-pelagic coupling and trophic relationships in northern Baltic Sea food webs. Limnology and Oceanography 65:1706–1722.

Kimmel, D. G., W. D. Miller, L. W. Harding, E. D. Houde, and M. R. Roman. 2009. Estuarine Ecosystem Response Captured Using a Synoptic Climatology. Estuaries and Coasts 32:403–409.

Kimmel, D., and M. Roman. 2004. Long-term trends in mesozooplankton abundance in Chesapeake Bay, USA: influence of freshwater input. Marine Ecology Progress Series 267:71–83.

Limburg, K. E., M. L. Pace, D. Fischer, and K. K. Arend. 1997. Consumption, Selectivity, and Use of Zooplankton by Larval Striped Bass and White Perch in a Seasonally Pulsed Estuary:15.

Martino, E. J., and E. D. Houde. 2010. Recruitment of striped bass in Chesapeake Bay: Spatial and temporal environmental variability and availability of zooplankton prey. Marine Ecology Progress Series 409:213–228.

Millette, N. C., D. K. Stoecker, and J. J. Pierson. 2015. Top-down control by micro- and mesozooplankton on winter dinoflagellate blooms of Heterocapsa rotundata. Aquatic Microbial Ecology 76:15–25.

Murphy, H. M., G. P. Jenkins, P. A. Hamer, S. E. Swearer, and M.-J. Rochet. 2012. Interannual variation in larval survival of snapper (*Chrysophrys auratus* , Sparidae) is linked to diet breadth and prey availability. Canadian Journal of Fisheries and Aquatic Sciences 69:1340–1351.

North, E. W., and E. D. Houde. 2001. Retention of White Perch and Striped Bass Larvae: Biological-Physical Interactions in Chesapeake Bay Estuarine Turbidity Maximum. Estuaries 24:756.

North, E. W., and E. D. Houde. 2003. Linking ETM physics, zooplankton prey, and fish early-life histories to striped bass Morone saxatilis and white perch M. americana recruitment. Marine Ecology Progress Series 260:219–236.

Nye, J. A., M. R. Baker, R. Bell, A. Kenny, K. H. Kilbourne, K. D. Friedland, E. Martino, M. M. Stachura, K. S. Van Houtan, and R. Wood. 2014. Ecosystem effects of the Atlantic Multidecadal Oscillation. Journal of Marine Systems 133:103–116.

Olson, M. M., and K. G. Sellner. 2005. Zooplankton/Food Web Monitoring for Adaptive Multi-Species Management Near-term Recommendations. Page 85. Workshop report, Smithsonian Environmental Research Center.

Perplexity. 2024. Perplexity.ai (versions from January 2024 until January 2025) [Large language model]. https://www.perplexity.ai/

Plough, L. V., C. Fitzgerald, A. Plummer, and J. J. Pierson. 2018. Reproductive isolation and morphological divergence between cryptic lineages of the copepod Acartia tonsa in Chesapeake Bay. Marine Ecology Progress Series 597:99–113.

Reaugh, M. L., M. R. Roman, and D. K. Stoecker. 2007. Changes in plankton community structure and function in response to variable freshwater flow in two tributaries of the Chesapeake Bay. Estuaries and Coasts 30:403–417.

Roman, M. R., A. L. Gauzens, W. K. Rhinehart, and J. R. White. 1993. Effects of low oxygen waters on Chesapeake Bay zooplankton. Limnology and Oceanography 38:1603–1614.

Salcedo-Bauza, A. 2017, May. Zooplankton composition in Hampton Roads Virginia: spatio-temporal variability and DNA barcoding of COI gene. Hampton University.

Siddon, E. C., T. Kristiansen, F. J. Mueter, K. K. Holsman, R. A. Heintz, and E. V. Farley. 2013. Spatial match-mismatch between juvenile fish and prey provides a mechanism for recruitment variability across contrasting climate conditions in the eastern Bering Sea. PLoS ONE 8.

The Maryland Department of Natural Resources, Tidewater Ecosystem Assessment Division. Eyes on the Bay (www.eyesonthebay.net)

Urrere, M. A., and G. A. Knauer. 1981. Zooplankton fecal pellet fluxes and vertical transport of particulate organic material in the pelagic environment. Journal of Plankton Research 3:369–387.

U.S. Geological Survey, 2016, National Water Information System data available on the World Wide Web (USGS Water Data for the Nation), accessed June 24, 2023, at http://waterdata.usgs.gov/nwis/

Tables

Salinity zone	Size fraction	Linear regression		
		slope	p	adjusted r^2
All combined	Microzooplankton	-0.010	1.59E-02	0.015
1	Microzooplankton	-0.028	7.54E-05	0.13
2	Mesozooplankton	0.029	6.73E-03	0.061

Table 4.1: Linear regression results on CBP historic data. Log10 transformed total zooplankton abundance vs. time; significant results only. Results shown for the entire Choptank River, and with the river separated into salinity zones (1= 0-4 psu, 2= 8-10 psu, and 3= 10-14 psu). Slope units are individuals/m^3/year.

Salinity zone	Size fraction	Taxon	Linear regression			Spearman-rank correlation	
			slope	p	adjusted r^2	p	rho
All combined	Mesozooplankton	*A. tonsa*	-277.552	2.00E-05	0.16	2.00E-03	-0.31
		E. carolleeae	567.72	2.50E-07	0.24	8.60E-07	0.52
		Bosmina	1103.9	0.047	0.033	2.30E-04	0.38
		Diaphanosoma	151.392	8.20E-03	0.076	5.90E-03	0.31
	Microzooplankton	*A. tonsa*	2870.14	0.0024	0.23		
		Synchaeta	3154	1.70E-03	0.084	3.50E-02	0.21
1	Mesozooplankton	*A. tonsa*	-441.56	4.30E-04	0.14	3.20E-02	-0.24
		Bosmina				1.90E-05	0.45
		Diaphanosoma	170.316	4.70E-03	0.09	2.90E-03	0.34
	Microzooplankton	*Synchaeta*	-2775.52	2.00E-04	0.13	3.40E-05	-0.42
2	Mesozooplankton	*A. tonsa*	346.94	9.00E-04	0.10	2.50E-03	0.30
		E. carolleeae	1987.02	5.90E-03	0.15	4.00E-04	0.52
		Bosmina				2.00E-02	0.38
	Microzooplankton	*A. tonsa*	5992.6	5.20E-07	0.57	2.00E-06	0.76
3	Mesozooplankton	*A. tonsa*	-756.96	< 2.2e-16	0.57	< 2.2e-16	-0.73
		E. carolleeae				8.60E-04	0.55
	Microzooplankton	*A. tonsa*	-23970.4	7.00E-05	0.42	1.30E-03	-0.57
		Synchaeta	15770	2.50E-07	0.23	5.90E-04	0.34

Table 4.2: Linear regression and Spearman-rank correlation results on CBP historic data. 12-month running means of select taxa abundance vs. time; significant results only. Results shown for the entire Choptank River, and with the river separated into salinity zones (1= 0-4 psu, 2= 8-10 psu, and 3= 10-14 psu). Slope units are individuals/m^3/year.

Size fraction	Taxon	Environmental parameter	slope	p	adjusted r^2
Mesozooplankton	*Diaphanosoma*	salinity	-0.28	5.55E-09	0.31
		chlorophyll a	0.025	1.99E-02	0.049
		secchi	-2.48	7.45E-04	0.11
	Bosmina	chlorophyll a	0.060	2.76E-09	0.21
		secchi	-1.84	1.49E-15	0.34
	E. carolleeae	secchi	-0.88	5.36E-11	0.19
Microzooplankton	*E. carolleeae*	salinity	-0.065	4.36E-03	0.1300
		chlorophyll a	0.027	1.93E-02	0.084

Table 4.3: Table of simple linear regression results for concentration (individuals/m^3) of select taxa vs environmental parameters. Significant results only.

Size fraction	Taxon	model p	adjusted r^2	Environmental parameter	slope	p
Mesozooplankton	*Bosmina*	1.04E-09	0.57	salinity	-0.23	1.04E-09
				chlorophyll a	0.03	1.20E-02
	E. carolleeae	1.86E-08	0.44	salinity	-0.14	1.86E-08
				temperature	-0.12	1.50E-06
				chlorophyll a	0.024	3.10E-03
				dissolved oxygen	-0.16	2.30E-02
	A. tonsa	9.02E-17	0.34	salinity	0.12	< 2e-16
				temperature	0.055	1.37E-04
				chlorophyll a	0.015	4.10E-03
				dissolved oxygen	0.075	4.60E-02
Microzooplankton	*E. carolleeae*	1.41E-03	0.23	salinity	-0.10	1.40E-03
				temperature	-0.086	2.80E-02
				chlorophyll a	0.031	1.50E-02
	A. tonsa	1.57E-03	0.35	salinity	0.060	1.60E-03
				temperature	0.044	2.10E-02
				chlorophyll a	0.019	1.40E-02
				monthly mean rive	-0.0016	2.70E-02

Table 4.4: Table of multiple linear regression results for concentration (individuals/m^3) of select taxa vs environmental parameters. Significant results only.

1984-1985 vs 2018-2019				2000-2001 vs 2018-2019			
species	average	p		species	average	p	
Acartia tonsa	0.452815	0.002	*	*Acartia tonsa*	0.390185	0.161	
Eurytemora carolleeae	0.089642	0.704		Bosmina	0.171191	0.135	
Bosmina	0.060317	0.999		*Eurytemora carolleeae*	0.099312	0.588	
Balanomorpha	0.057196	0.141		Balanomorpha	0.035139	0.806	
Rotifera	0.024744	0.285		Cyclopoida	0.028465	0.009	*
Gastropoda	0.022935	0.093		Annelida	0.025181	0.047	*
Diaphanosoma	0.020663	0.56		Rotifera	0.023582	0.141	
Calanoida	0.017512	0.008	*	Gastropoda	0.020891	0.114	
Cladocera	0.017001	0.003	*	*Diaphanosoma*	0.020584	0.512	
Annelida	0.016074	0.785		Bivalvia	0.006743	0.195	
Ostracoda	0.011114	0.073		Cladocera	0.005355	0.866	
Cyclopoida	0.008091	0.998		Ostracoda	0.005117	0.894	
Bivalvia	0.006902	0.368		Harpacticoida	0.004553	0.033	*
Oithona colcarva	0.00351	0.019	*	Calanoida	0.003961	0.816	
Brachionus calyciflorus	0.002441	0.555		*Brachionus calyciflorus*	0.002311	0.477	
Mollusca	0.002203	0.001	*	Ergasilus	0.001884	0.381	
Ergasilus	0.001992	0.381		*Oithona colcarva*	0.001816	0.675	
Harpacticoida	0.001051	0.961		*Synchaeta*	0.000545	0.477	
Crustacea	0.000915	0.001	*	*Brachionus angularis*	0.000374	0.429	
Hydrozoan	0.000705	0.063		Hydrozoan	0.000307	0.832	
Synchaeta	0.000577	0.556		Animalia	0.000261	0.682	
Animalia	0.000437	0.072		Mite	0.000204	0.199	
Brachionus angularis	0.000285	0.545		Crustacea	0.000201	0.994	
Mite	0.000213	0.242		*Rhithropanopeus harrisii*	0.000183	0.279	
Nematoda	0.00019	0.339		Nematoda	0.00018	0.26	
Amphipod	0.000176	0.596		Amphipod	0.000175	0.64	
Rhithropanopeus harrisii	0.000155	0.469		*Brachionus rubens*	0.000158	0.309	
Brachionus rubens	0.000137	0.458		Brachionus	0.000115	0.477	
Brachionus	0.000121	0.556		Unknown	0.000109	0.443	
Unknown	0.000116	0.543		Keratella	2.87E-05	0.475	
Keratella	3.04E-05	0.556		Mollusca	0		

Table 4.5: Results of SIMPER pairwise testing on mesozooplankton community data from three year-pairs: 1984-1985, 2000-2001, and 2018-2019. Only significant pairwise test results are shown. Average indicates the average contribution of each taxon to the dissimilarity, * indicates taxa with significant permutation p values.

1984-1985 vs 2000-2001			1984-1985 vs 2018-2019			2000-2001 vs 2018-2019		
species	**average**	**p**	**species**	**average**	**p**	**species**	**average**	**p**
Synchaeta	0.236618	0.472	Crustacea	0.359681	0.001 *	Synchaeta	0.277362	0.049 *
Crustacea	0.175745	0.346	Synchaeta	0.256222	0.251	*Acartia tonsa*	0.213531	0.001 *
Acartia tonsa	0.09722	0.999	*Acartia tonsa*	0.115594	0.959	Crustacea	0.135312	0.976
Rotifera	0.070373	0.811	*Brachionus angularis*	0.058509	0.001 *	Rotifera	0.112039	0.004 *
Brachionus angularis	0.04861	0.031 *	Rotifera	0.032609	1	*Eurytemora carolleeae*	0.050703	0.009 *
Keratella	0.047774	0.182	Keratella	0.031941	0.84	Keratella	0.046565	0.218
Eurytemora carolleeae	0.022523	0.879	Bivalvia	0.017981	0.001 *	Filinia	0.023573	0.129
Filinia	0.020271	0.42	Cyclopoida	0.01779	0.566	Cyclopoida	0.019808	0.439
Brachionus	0.01492	0.264	*Eurytemora carolleeae*	0.017329	0.92	*Brachionus angularis*	0.011764	0.993
Bivalvia	0.00995	0.83	Brachionus	0.014717	0.307	Brachionus	0.009302	0.773
Gastropoda	0.006434	0.872	Gastropoda	0.014292	0.428	Gastropoda	0.009179	0.728
Brachionus calyciflorus	0.003658	0.542	Filinia	0.009301	0.959	Bivalvia	0.008235	0.97
Annelida	0.001922	0.984	*Brachionus calyciflorus*	0.004102	0.383	Annelida	0.006441	0.033 *
Unknown	0.001081	0.276	Annelida	0.002117	0.949	*Brachionus calyciflorus*	0.003331	0.662
Foraminifera	0.000512	0.203	*Brachionus caudatus*	0.00163	0.573	*Brachionus caudatus*	0.001623	0.416
Brachionus caudatus	0.0005	0.836	Unknown	0.001106	0.303	Unknown	0.000893	0.607
Brachionus rubens	0.000468	0.528	Foraminifera	0.000759	0.008 *	Balanomorpha	0.000298	0.766
Nematoda	0.000402	0.649	Nematoda	0.000672	0.023 *	Nematoda	0.000253	0.985
Mite	0.0001	0.191	*Brachionus rubens*	0.000633	0.258	Animalia	0.000149	0.569
Animalia	2.42E-05	0.973	Balanomorpha	0.000254	0.798	Calanoida	0.000123	0.726
Brachionus urceolaris	0		Mite	0.000175	0.001 *	Bosmina	0.000117	0.72
Bosmina	0		Calanoida	9.69E-05	0.58	*Brachionus rubens*	7.88E-05	0.975
Cyclopoida	0		Bosmina	8.28E-05	0.599	Mollusca	4.05E-05	0.713
Balanomorpha	0		Animalia	7.66E-05	0.797	Foraminifera	3.91E-05	0.994
Calanoida	0		Mollusca	3.52E-05	0.583	*Brachionus urceolaris*	1.02E-06	0.699
Mollusca	0		*Brachionus urceolaris*	7.14E-07	0.579	Mite	0	

Table 4.6: Results of SIMPER pairwise testing on microzooplankton community data from three year-pairs: 1984-1985, 2000-2001, and 2018-2019. Only significant pairwise test results are shown. Average indicates the average contribution of each taxon to the dissimilarity, * indicates taxa with significant permutation p values.

Figures

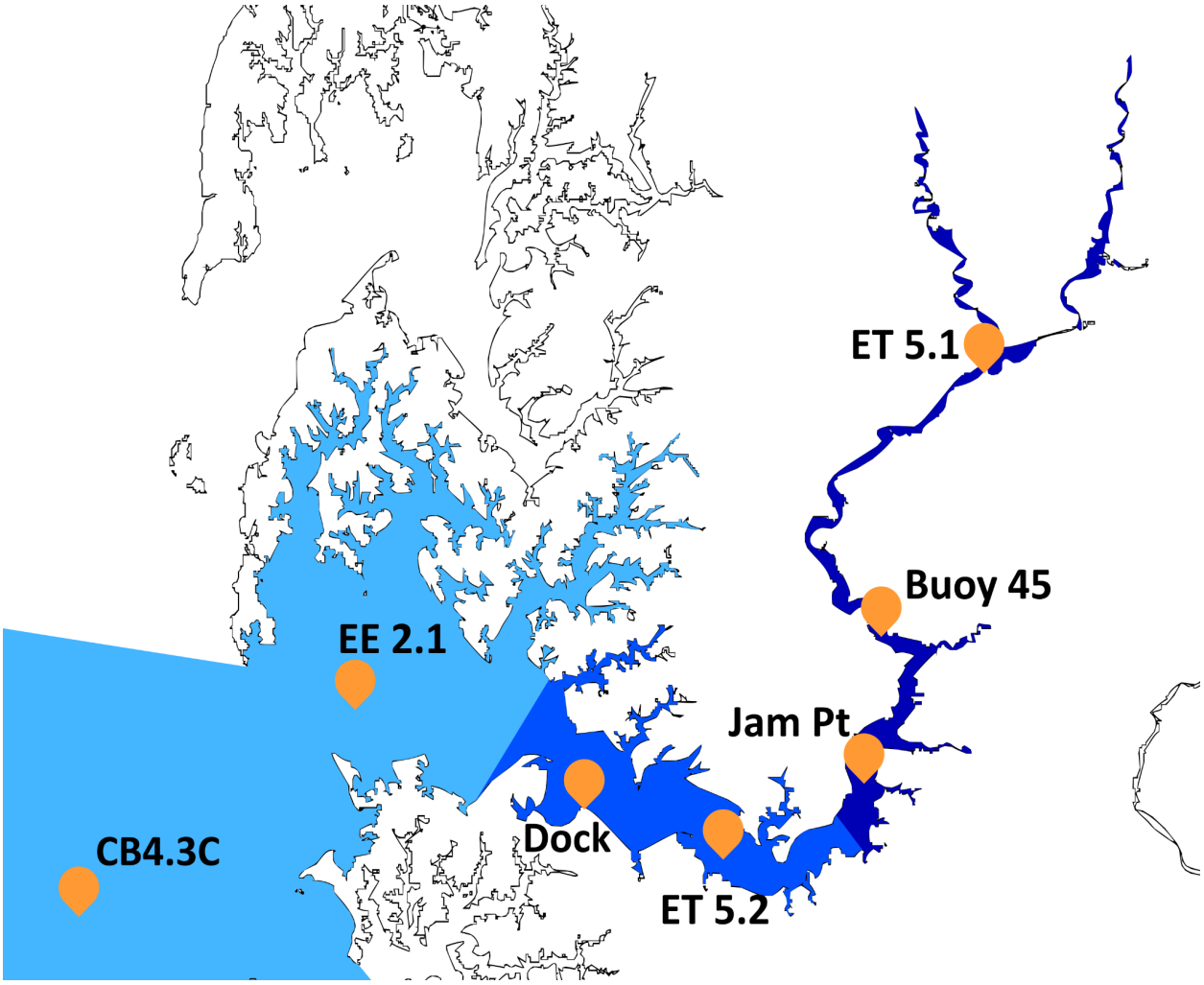

Fig. 4.1: Map of the Choptank River with all sites used to examine zooplankton ecology. Hues of blue represent salinity zones: dark blue= fresh (zone 1, 0-4 psu), blue= median (zone 2, 6-10 psu), and light blue= salt (zone 3, 10-14 psu).

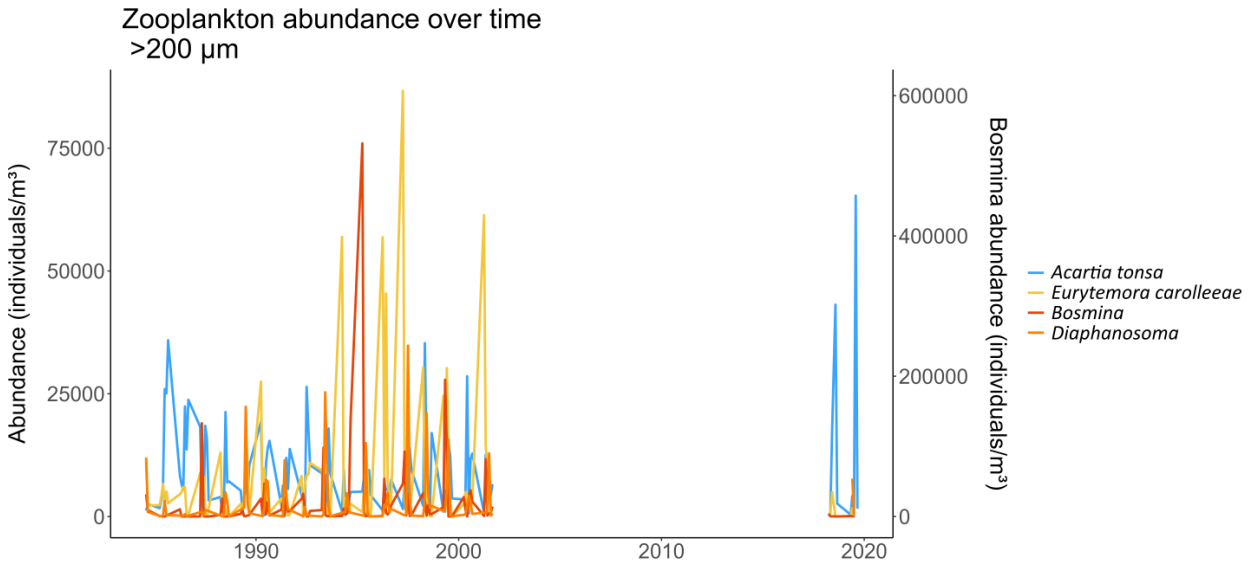

Fig. 4.2: Abundance (individuals/m³) of select mesozooplankton taxa over time. *Bosmina* scaled for clarity; dedicated y-axis on the right.

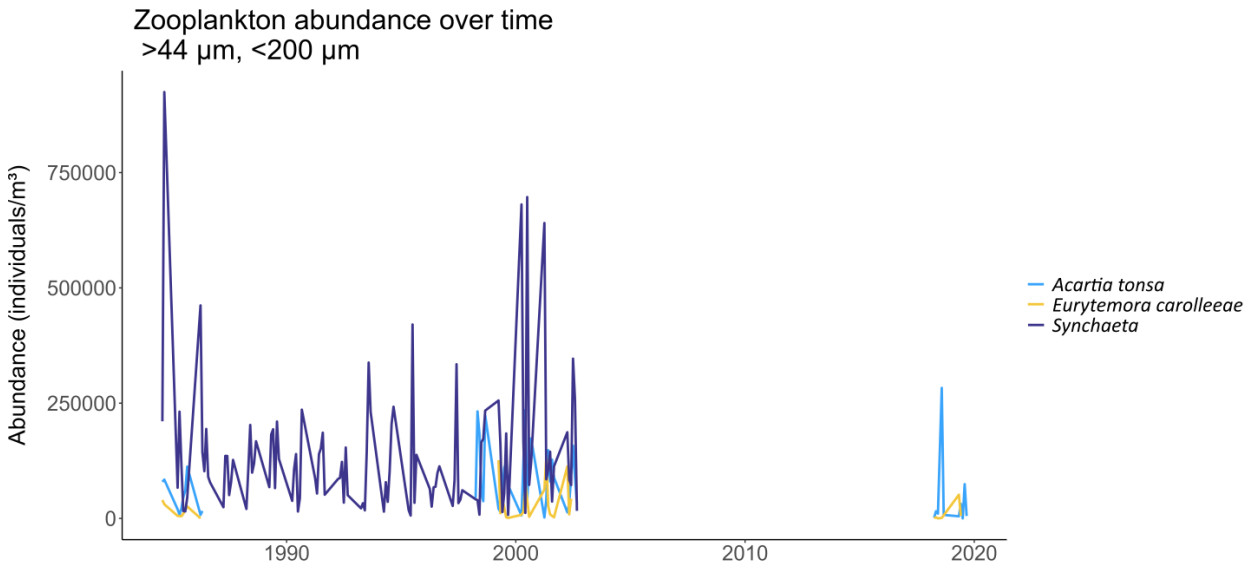

Fig. 4.3: Abundance (individuals/m³) of select microzooplankton taxa over time.

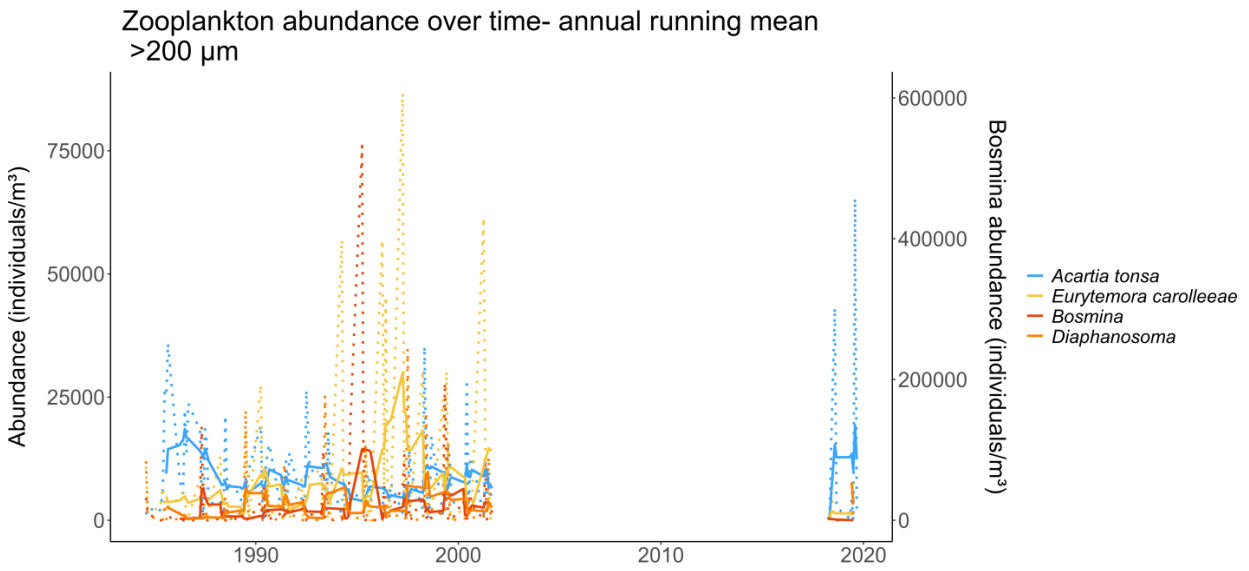

Fig. 4.4: 12-month running mean of abundance (individuals/m³) (solid lines) and raw abundance (dotted lines) of select mesozooplankton taxa over time. *Bosmina* scaled for clarity; dedicated y-axis on the right.

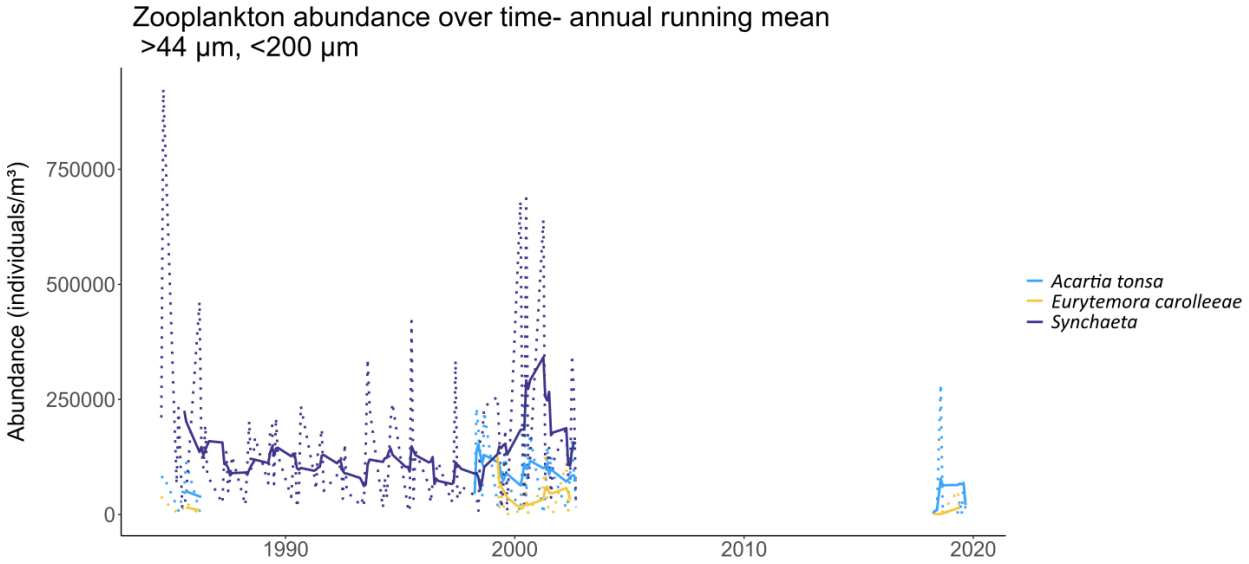

Fig. 4.5: 12-month running mean of abundance (individuals/m³) (solid lines) and raw abundance (dotted lines) of select microzooplankton taxa over time.

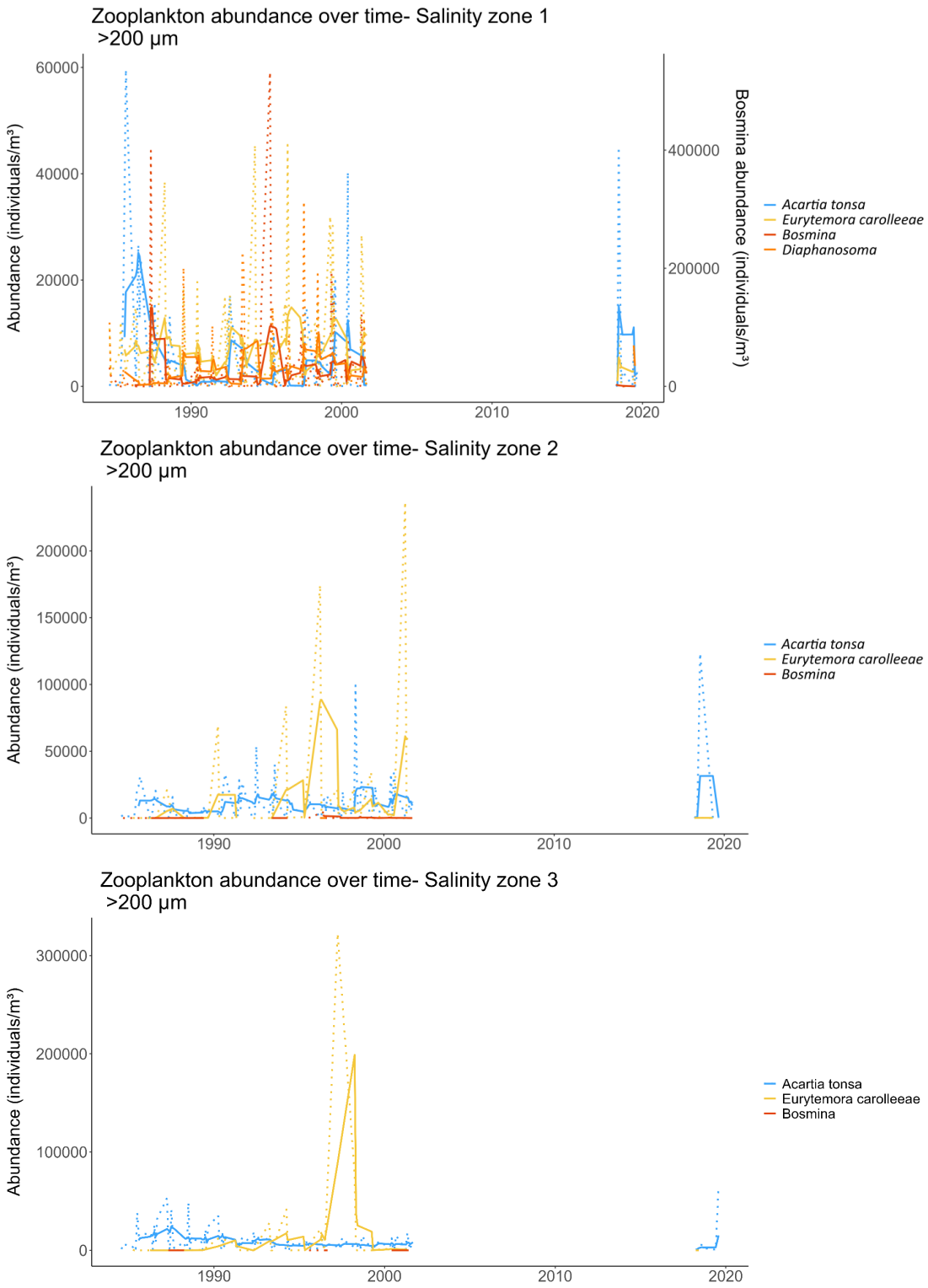

Fig. 4.6: 12-month running mean of abundance (individuals/m³) (solid lines) and raw abundance (dotted lines) of select mesozooplankton taxa over time in salinity zones zone 1 (0-4 psu), 2 (8-10 psu), and 3 (10-14 psu).

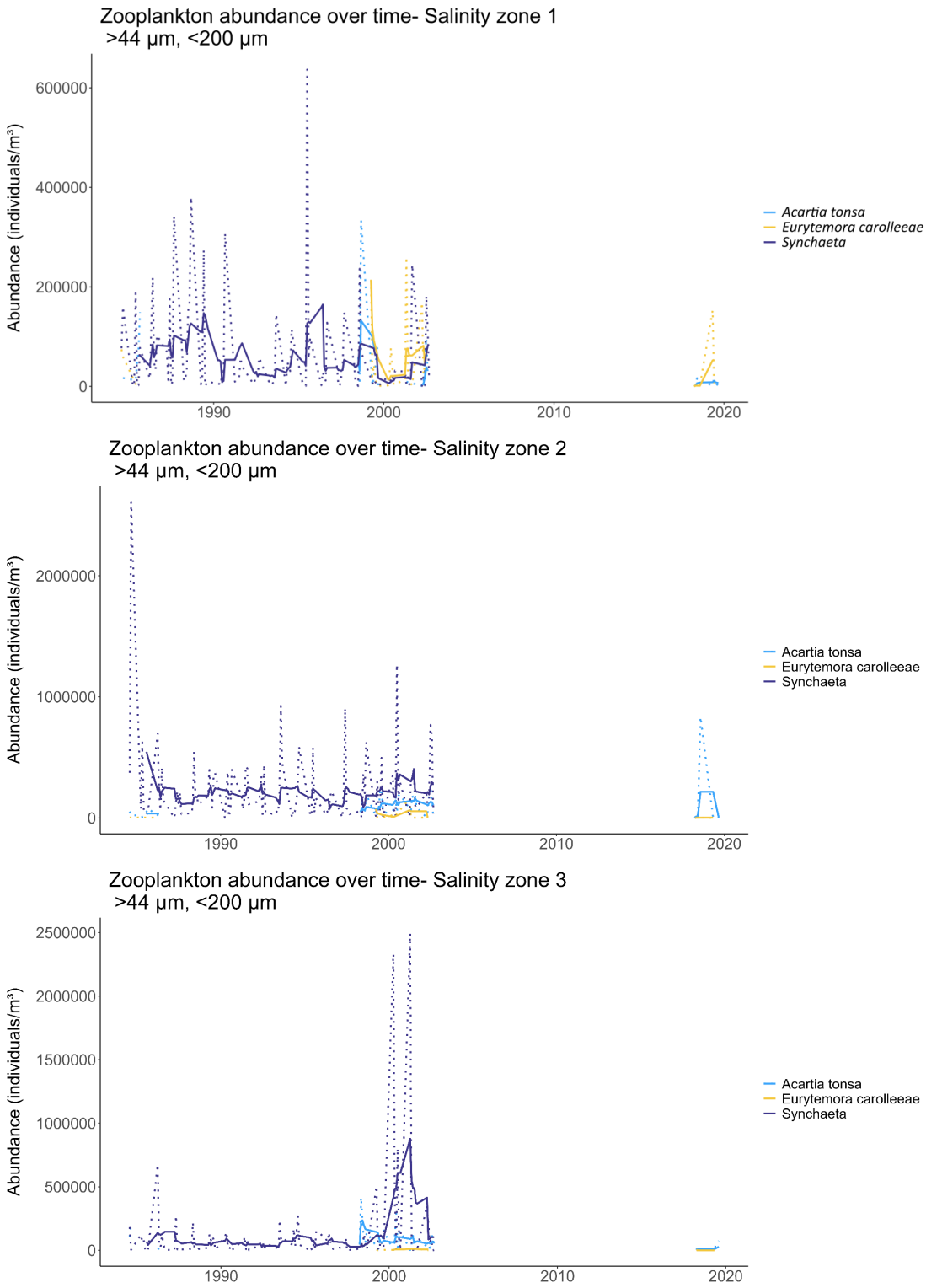

Fig. 4.7: 12-month running mean of abundance (individuals/m³) (solid lines) and raw abundance (dotted lines) of select microzooplankton taxa over time in salinity zones zone 1 (0-4 psu), 2 (8-10 psu), and 3 (10-14 psu).

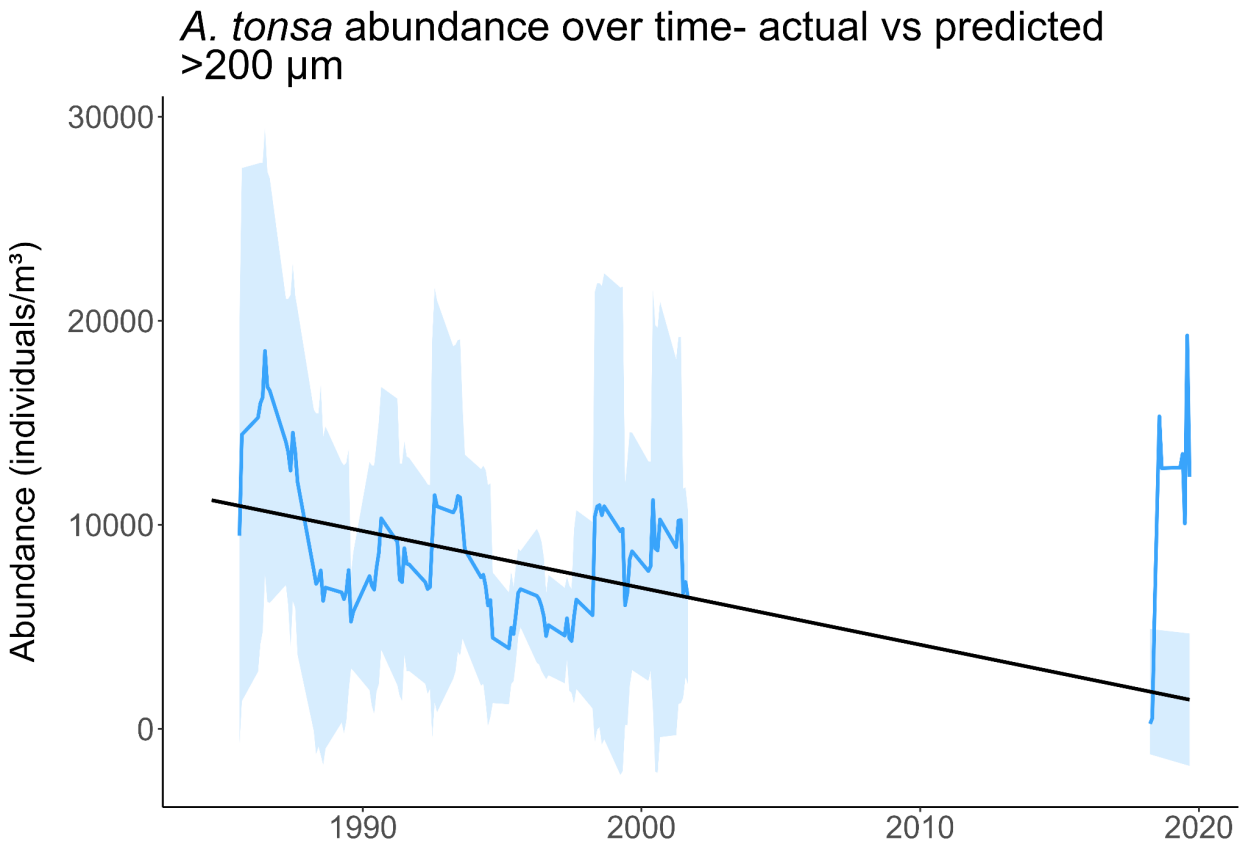

Fig. 4.8: *Acartia tonsa* mesozooplankton (adults) abundance over time as predicted by CBP data vs SG study measures. Abundance shown is the 12-month running mean of CBP data (1984-2001) and SG data (2018-2019). The black line is a linear regression generated by modeling CBP *A. tonsa* running mean abundance over time, extrapolated across the full timeline. The shaded area represents 95% confidence intervals of CBP data as measured (1984-2001), and as predicted based on the regression (2018-2019).

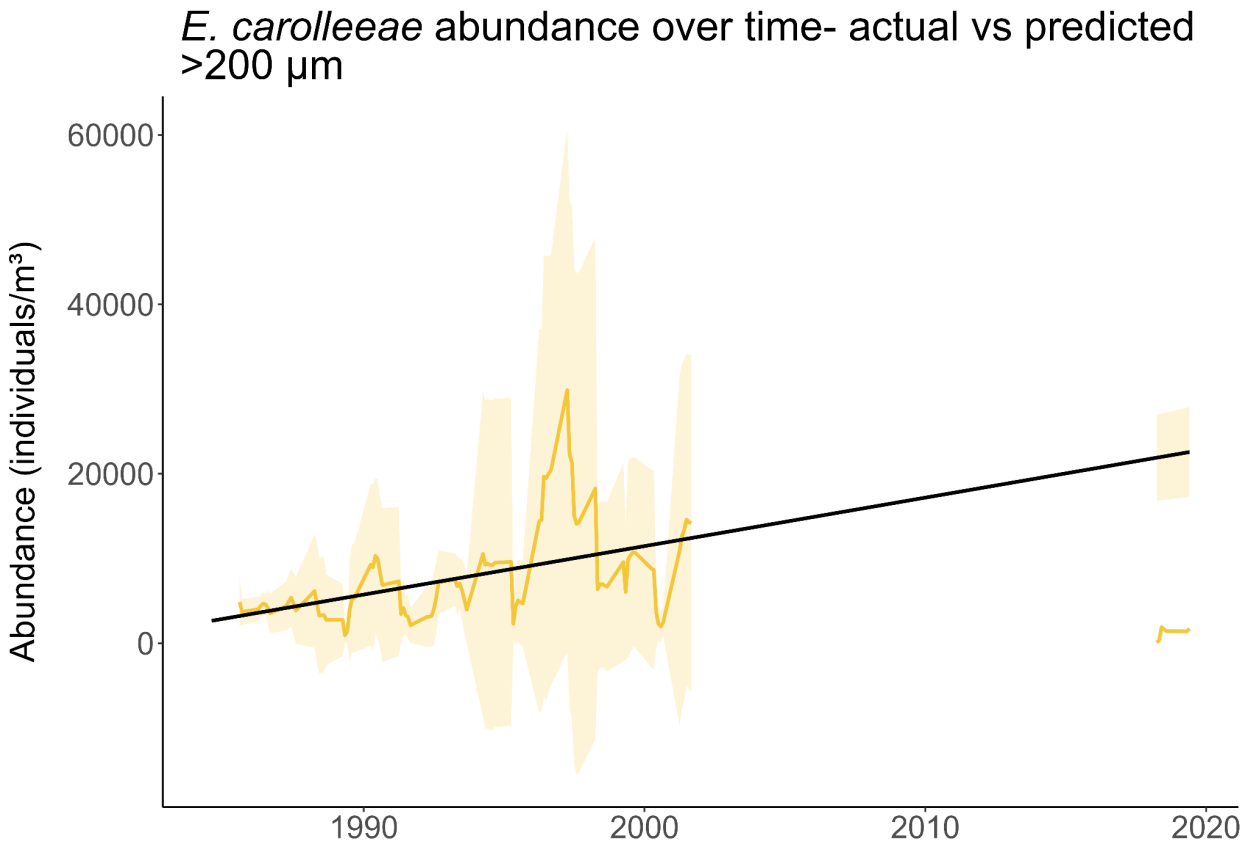

Fig. 4.9: *Eurytemora carolleeae* mesozooplankton (adults) abundance over time as predicted by CBP data vs SG study measures. Abundance shown is the 12-month running mean of CBP data (1984-2001) and SG data (2018-2019). The black line is a linear regression generated by modeling CBP *E. carolleeae* running mean abundance over time, extrapolated across the full timeline. The shaded area represents 95% confidence intervals of CBP data as measured (1984-2001), and as predicted based on the regression (2018-2019).

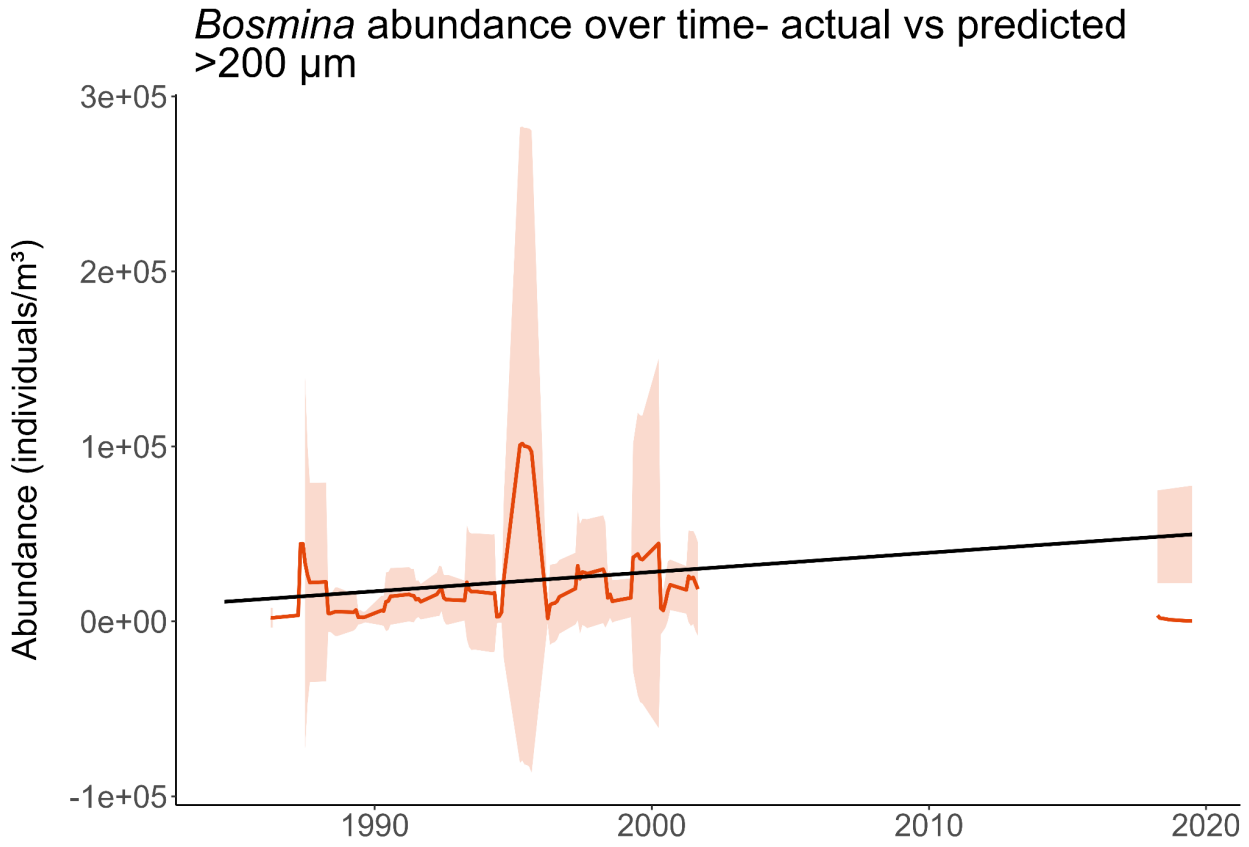

Fig. 4.10: *Bosmina* mesozooplankton abundance over time as predicted by CBP data vs SG study measures. Abundance shown is the 12-month running mean of CBP data (1984-2001) and SG data (2018-2019). The black line is a linear regression generated by modeling CBP *Bosmina* running mean abundance over time, extrapolated across the full timeline. The shaded area represents 95% confidence intervals of CBP data as measured (1984-2001), and as predicted based on the regression (2018-2019).

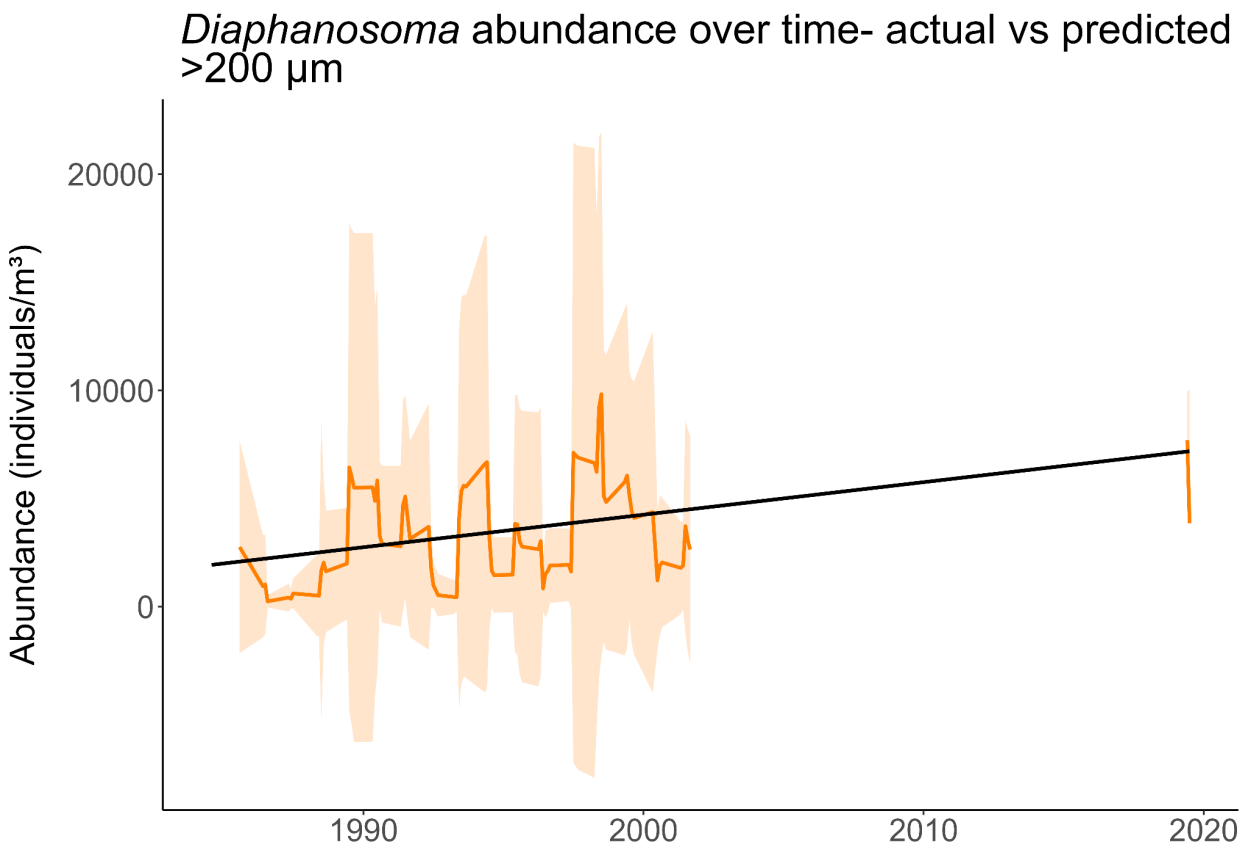

Fig. 4.11: *Diaphanosoma* mesozooplankton abundance over time as predicted by CBP data vs SG study measures. Abundance shown is the 12-month running mean of CBP data (1984-2001) and SG data (2018-2019). The black line is a linear regression generated by modeling CBP *Diaphanosoma* running mean abundance over time, extrapolated across the full timeline. The shaded area represents 95% confidence intervals of CBP data as measured (1984-2001), and as predicted based on the regression (2018-2019).

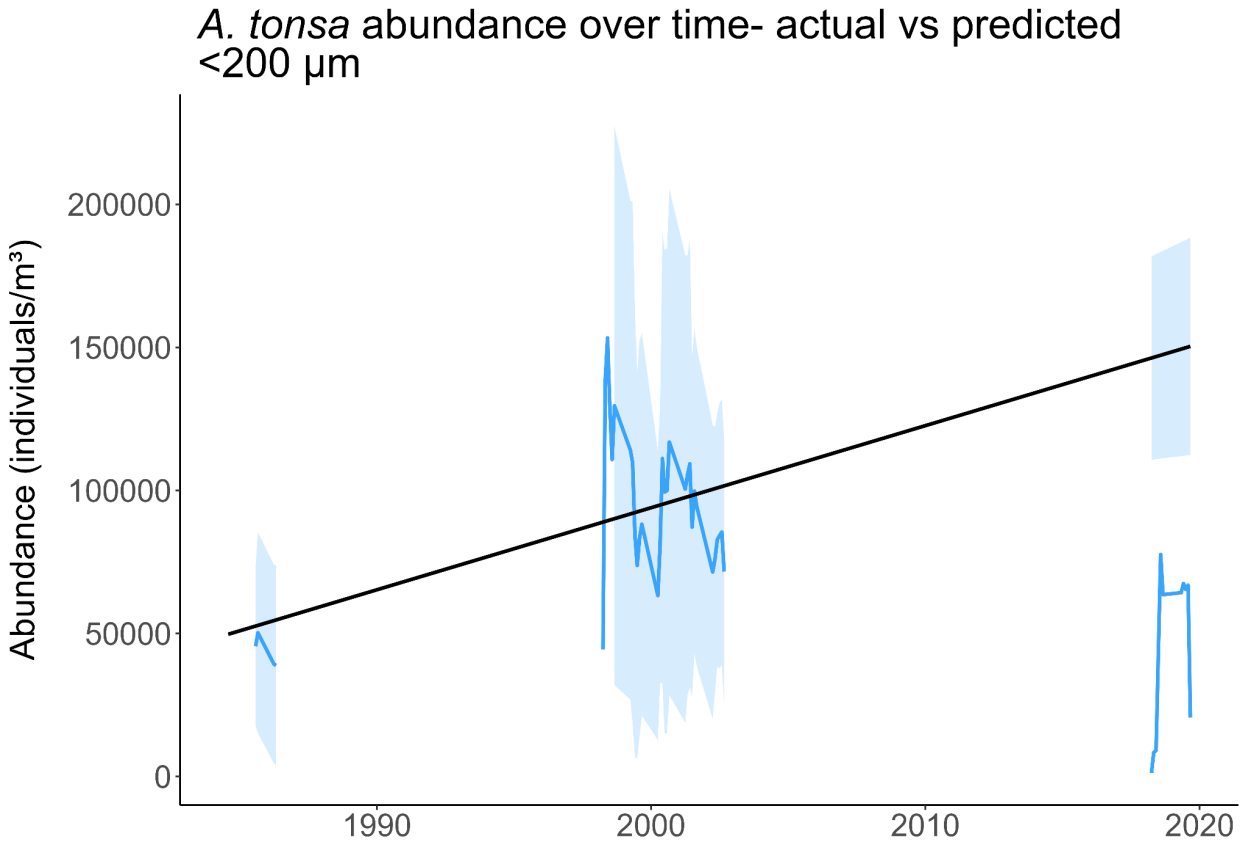

Fig 4.12: *Acartia tonsa* microzooplankton (nauplii) abundance over time as predicted by CBP data vs our study measures. Abundance shown is the 12-month running mean of CBP data (1984-2002) and our study (2018-2019). The black line is a linear regression generated by modeling CBP *A. tonsa* running mean abundance over time, extrapolated across the full timeline. The shaded area represents 95% confidence intervals of CBP data as measured (1984-2002), and as predicted based on the regression (2018-2019).

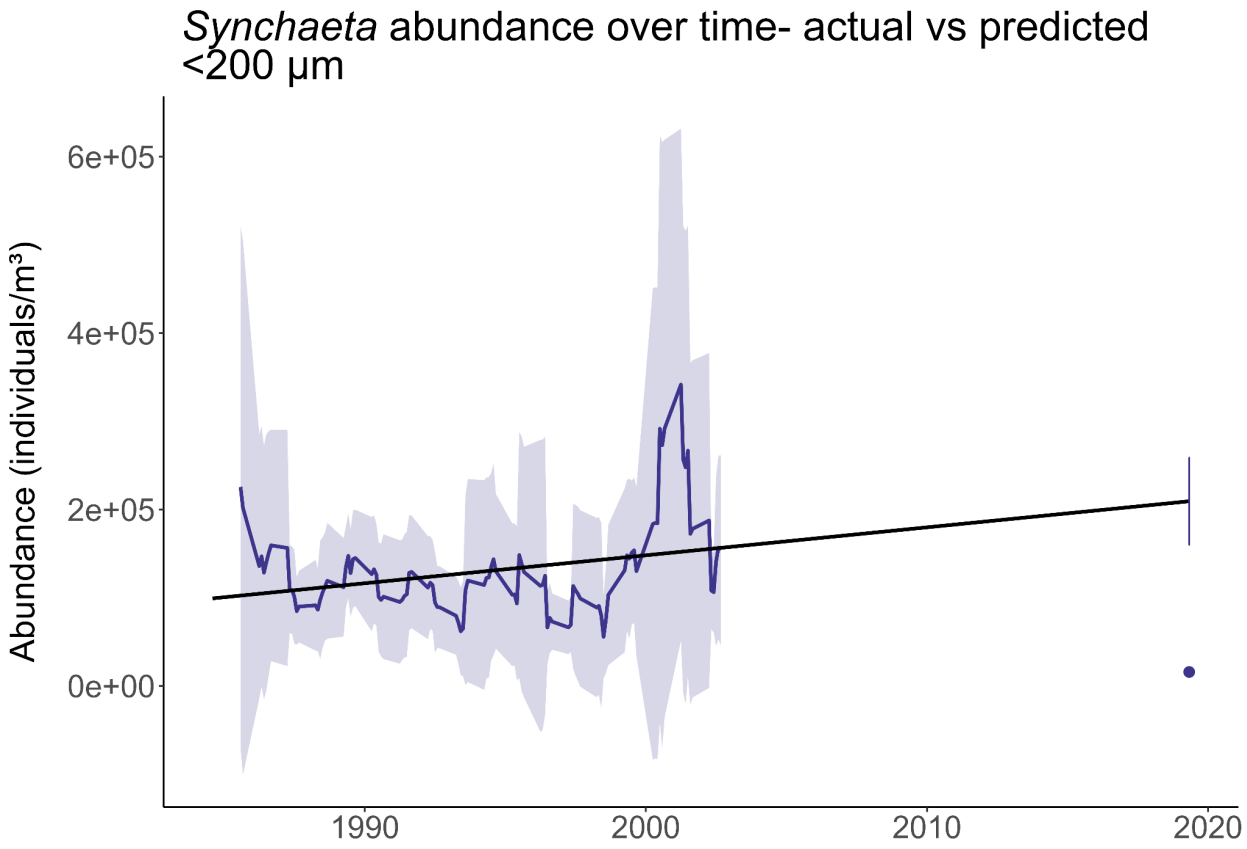

Fig. 4.13: *Synchaeta* microzooplankton abundance over time as predicted by CBP data vs our study measures. Abundance shown is the 12-month running mean of CBP data (1984-2002) and our study (2018-2019; here appearing as a single point due to limited data). The black line is a linear regression generated by modeling CBP *Synchaeta* running mean abundance over time, extrapolated across the full timeline. The shaded area represents 95% confidence intervals of CBP data as measured (1984-2002), and as predicted based on the regression (2018-2019; here appearing as a line due to limited data).

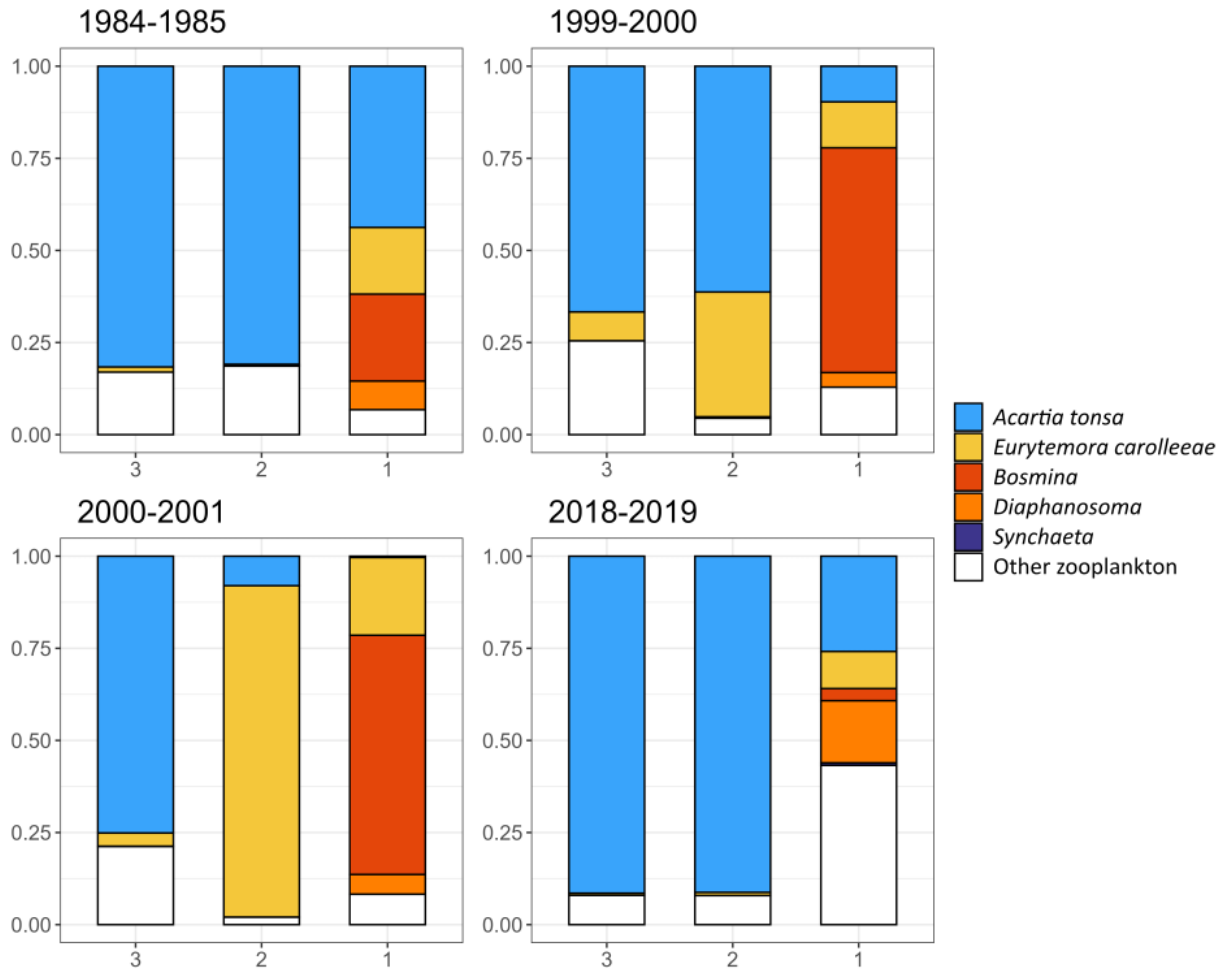

Fig. 4.14: Relative abundance of select mesozooplankton taxa at four time points and three salinity zones. The beginning (1984-1985) and end (2000-2001) of the CBP zooplankton monitoring data, two years which were most like SG study years in terms of environmental conditions (1999-2000), and SG study years (2018-2019). Fresh (zone 1, 0-4 psu), Median (zone 2, 6-10 psu), and Salt (zone 3, 10-14 psu).

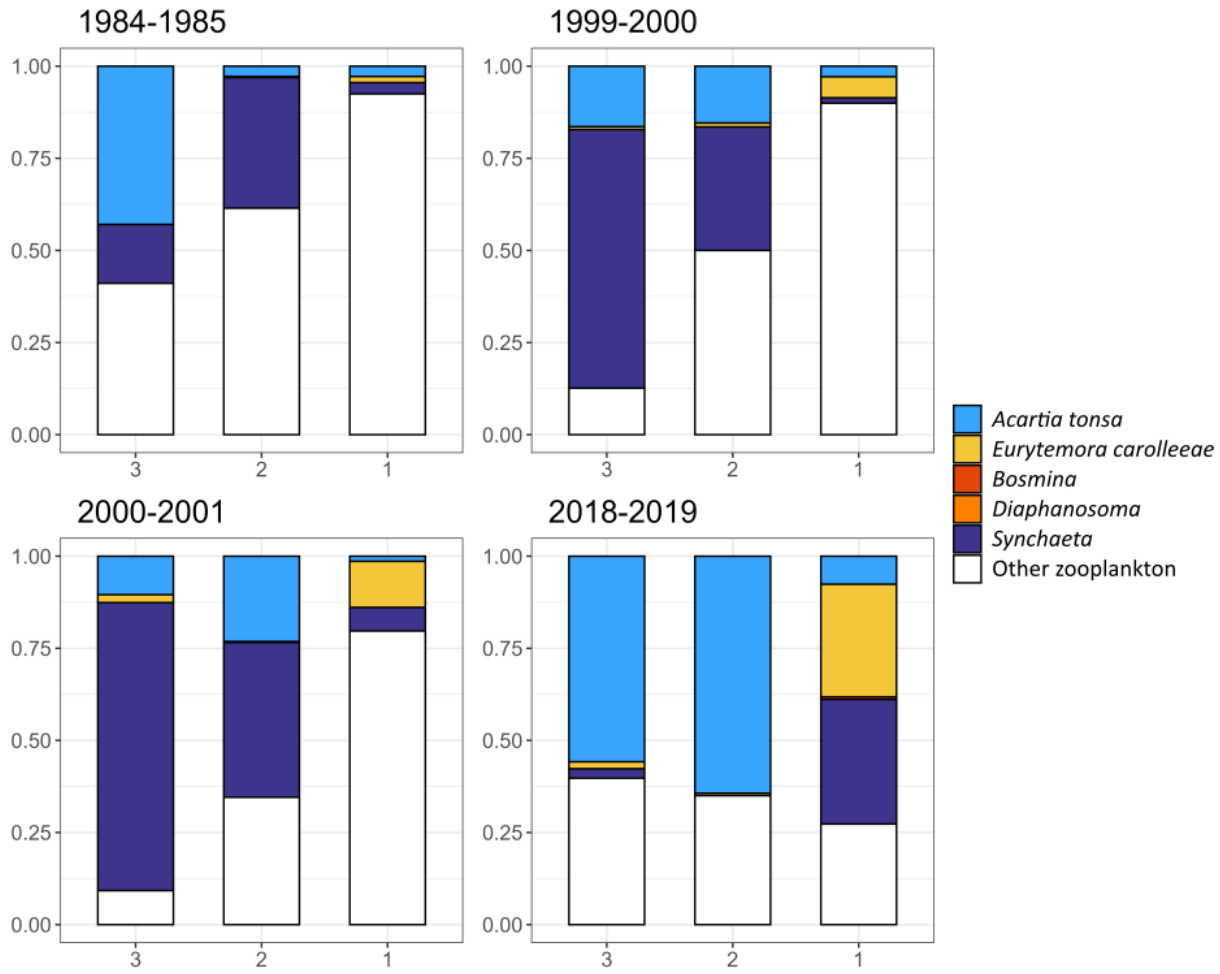

Fig. 4.15: Relative abundance of select microzooplankton taxa at four time points and three salinity zones. The beginning (1984-1985) and end (2000-2001) of the CBP zooplankton monitoring data, two years which were most like SG study years in terms of environmental conditions (1999-2000), and SG study years (2018-2019). Fresh (zone 1, 0-4 psu), Median (zone 2, 6-10 psu), and Salt (zone 3, 10-14 psu).

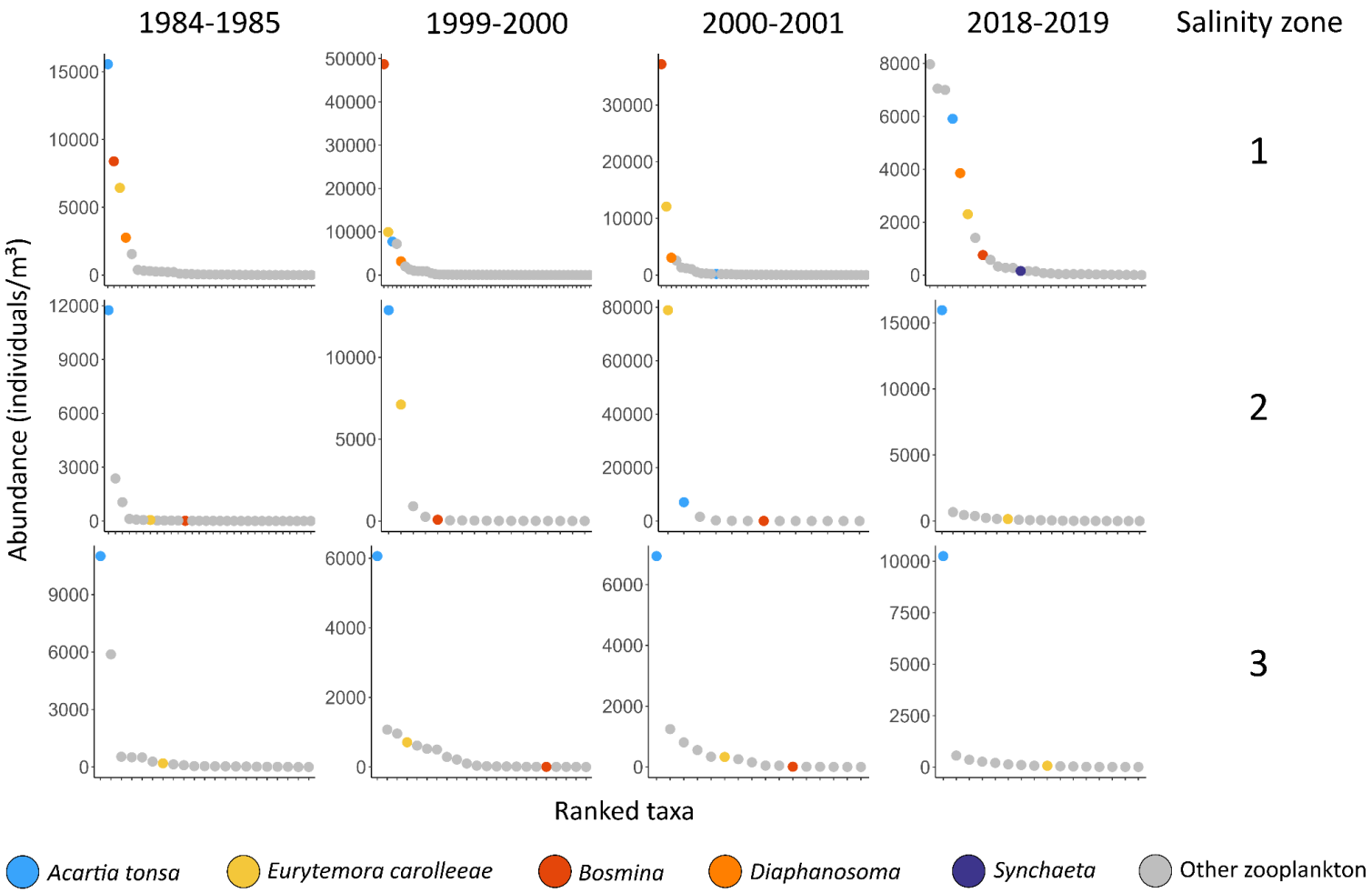

Fig. 4.16: Rank-dominance of select mesozooplankton taxa at four time points and three salinity zones. The beginning (1984-1985) and end (2000-2001) of the CBP zooplankton monitoring data, two years which were most like our study years in terms of environmental conditions (1999-2000), and our study years (2018-2019). Fresh (zone 1, 0-4 psu), Median (zone 2, 6-10 psu), and Salt (zone 3, 10-14 psu).

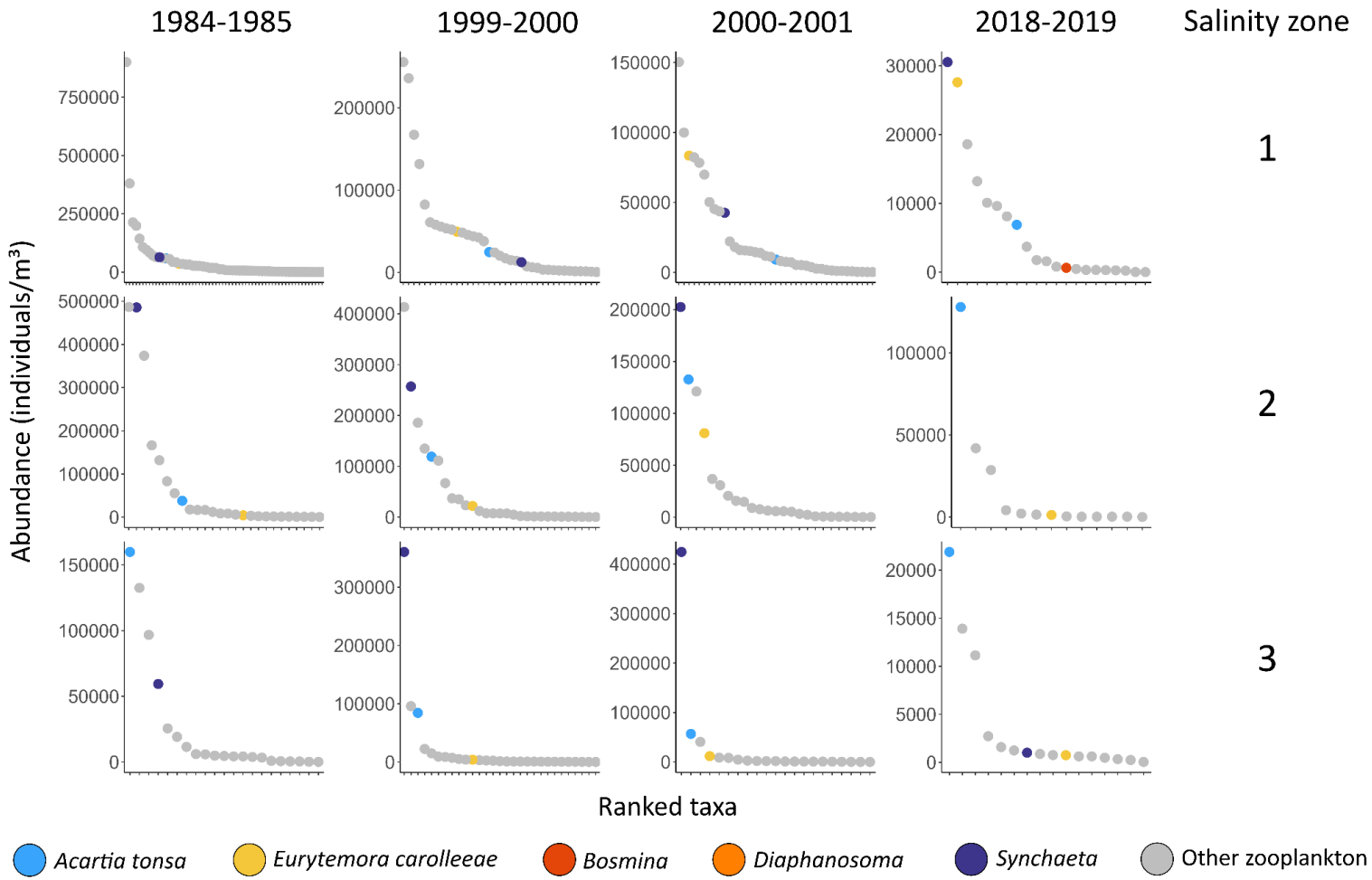

Fig. 4.17: Rank dominance of select microzooplankton taxa at four time points and three salinity zones. The beginning (1984-1985) and end (2000-2001) of the CBP zooplankton monitoring data, two years which were most like our study years in terms of environmental conditions (1999-2000), and our study years (2018-2019). Fresh (zone 1, 0-4 psu), Median (zone 2, 6-10 psu), and Salt (zone 3, 10-14 psu).

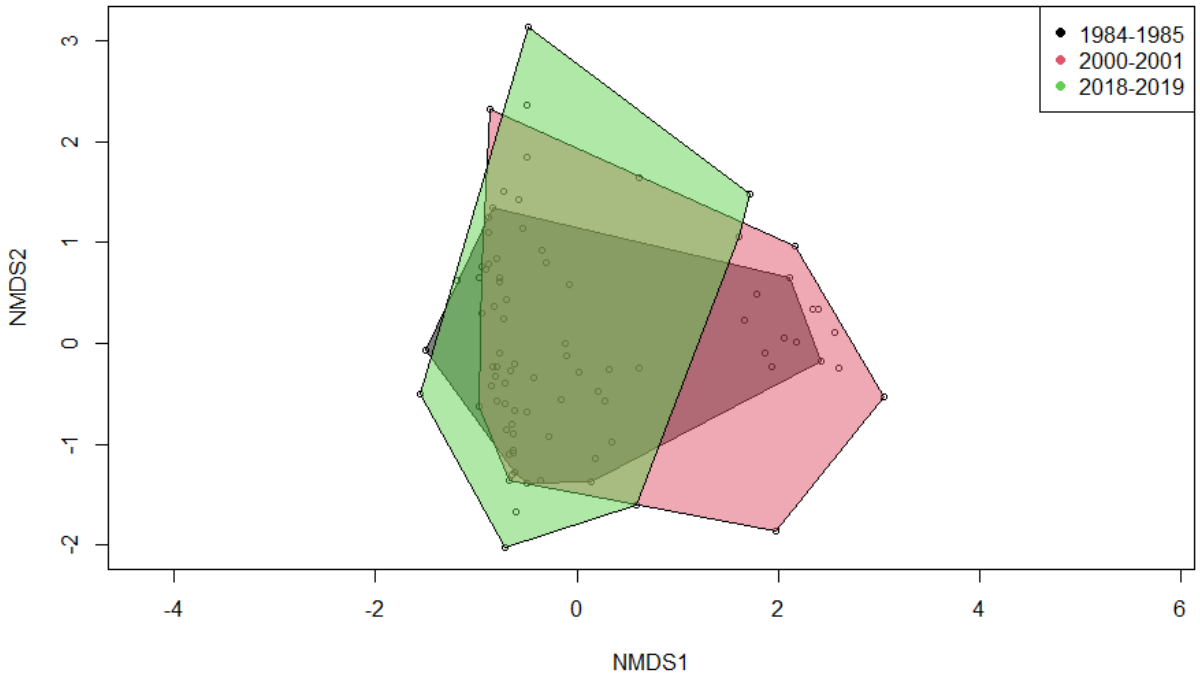

Fig. 4.18: NMDS on mesozooplankton community data from three year-pairs: 1984-1985, 2000-2001, and 2018-2019. Significant differences between 1984-1985 and 2018-2019, and 2000-2001 and 2018-2019 only.

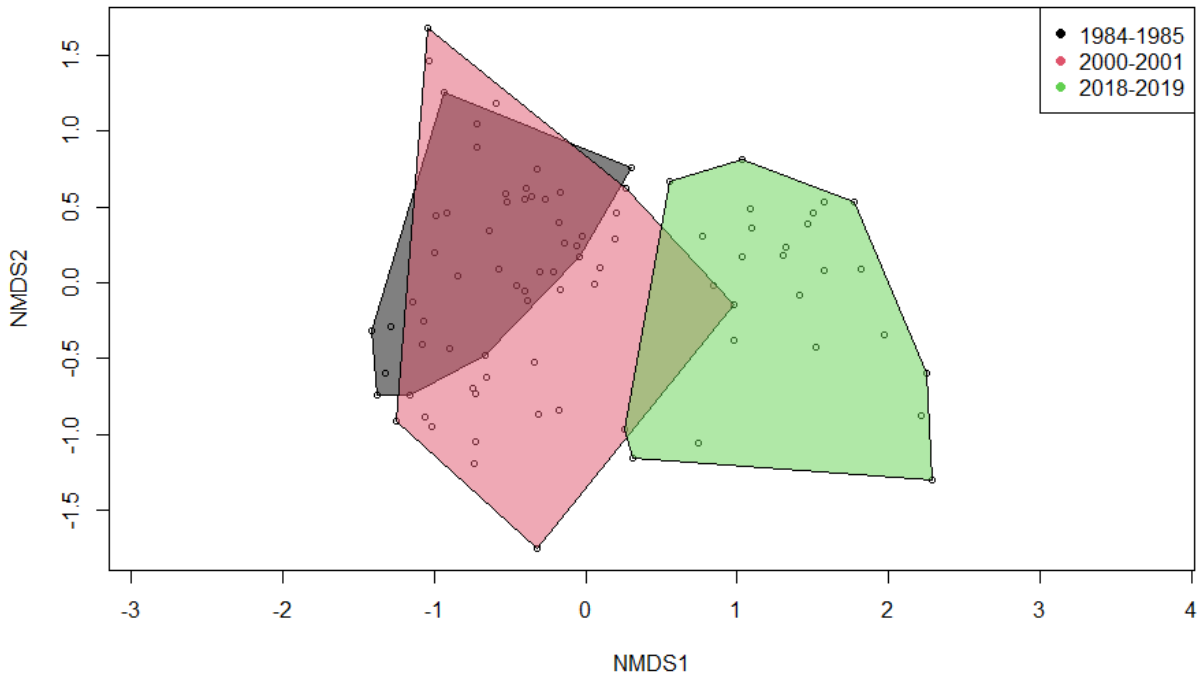

Fig. 4.19: NMDS on microzooplankton community data from three year-pairs: 1984-1985, 2000-2001, and 2018-2019. All year-pairs were significantly different from one another.

Chapter 5: Conclusion

This dissertation has demonstrated that CO1 metabarcoding is a cost-effective, efficient, powerful tool for uncovering biodiversity in zooplankton and in larval fish diets. However, it is a powerful tool to wield cautiously when applying to ecological questions. Metabarcoding will lead to misleading conclusions if used in isolation; it must be paired with traditional morphological techniques to gain a complete understanding of zooplankton and larval fish feeding ecology. When designing bioinformatics pipelines for questions of community and dietary ecology, it is important not to use strict quality filtering protocols; they exclude too much data and present an artificially narrow view of factors impacting the study subject. Issues caused by strict filtering could also be amended by expansion of reference databases to include estuarine zooplankton species, particularly understudied species such as annelids and freshwater species which experience genetic divergence more rapidly, so that matches between reference databases and study data are strong enough to pass strict filtering.

Through CO1 metabarcoding, the larval stages (2-20 mm TL) of *Morone americana*, *Morone saxatilis*, and *Anchoa mitchilli* were found to consume zooplankton prey in alignment with prior studies, with the addition of cnidarians and the larvae of benthic organisms, and for *A. mitchilli* specifically, other fishes. This is largely due to the ability of metabarcoding to identify digestion-degraded soft tissues and make use of trace DNA, however because this study was not performed in tandem with morphological identification there is still more work to be done to verify some of the results presented here; particularly to resolve the question of how *A. mitchilli* larvae were ingesting DNA of other fishes. Metabarcoding might also be able to tell us about feeding incidence or onset of first feeding, but more testing is required.

There was heavy emphasis on the following select zooplankton taxa in the diets of larval fishes: *Eurytemora carolleeae, Acartia tonsa, Bosmina, Diaphanosoma, Synchaeta*. Given the link between prey abundance and larval fish mortality, it is important to understand the ecology of these taxa and of the zooplankton community as a whole through time. The zooplankton community in the Choptank River was significantly different in 2018-2019 from what we would expect based on community structure and trends in select taxa abundance as recorded in the Chesapeake Bay Program zooplankton monitoring data (1985-2002). Environmental drivers of the observed shifts were as expected: chlorophyll a concentration, salinity, temperature, dissolved oxygen, and monthly average river flow. However, we do not know when these parameters changed or exactly how they altered the zooplankton communities in the years between 2002 and 2018.

Crucially, the areas of the Choptank River with significant declines in overall zooplankton abundance and the largest changes in the zooplankton community over time were the larval fish nursery grounds. These unexpected shifts may be in part responsible for observed reductions in recruitment of *M. saxatilis* (Martino and Houde 2010, Shideler and Houde 2014b, Uphoff 2023). *Morone saxatilis* and *M. americana* larvae co-occurred in time and space and consumed mostly *E. carolleeae* which was unexpectedly low in 2018-2019; *M. saxatilis* specialized on *E. carolleeae* whereas *M. americana* were more generalist, at least in their first feeding stage. The moronid larvae may have been competing locally for a food resource which was unexpectedly limited, but the *M. americana* larvae were able to diversify their diets to a

higher degree than *M. saxatilis* in order to compensate. Future work in larval fish ecology should use the expanded dietary information from this work to examine relationships between prey populations and fish recruitment success. Equipped with more knowledge of larval fish dietary habits, we may be able to produce more accurate predictions of recruitment success.

Monitoring and surveys of zooplankton should be expanded to include cnidarians, meroplankton, and ichthyoplankton: taxa which make up significant portions of larval fish diets and are generally not the taxa of focus in zooplankton survey efforts. The CBP zooplankton monitoring program did a good job of this; they recorded cnidarians, hydrozoans, and hydra as part of their data set. However, our SG study did not in part because we assumed larvae were focusing their diets on crustaceans; had we known these taxa were important prey, we might have quantified additional aliquots intentionally scanning for cnidarians. Metabarcoding can help with zooplankton monitoring as far as detecting species presence/absence, but the method needs work in order to become quantitative; to have the highest impact, the data produced needs to be comparable with historic data and useful to modelers. In order to do this, we will need to expand databases as discussed previously and also quantify species- and marker-specific amplification biases. Those relationships can be used to generate correction factors to convert reads to counts.

Because of the potentially outsized impact of zooplankton communities on fisheries health, Bay-wide monitoring of zooplankton should not have ceased. Indeed, in an era of anthropogenic climate change this is when we need monitoring the most in order to observe unexpected environmental changes as they occur and adapt rapidly to their onset. As weather patterns become more variable, scattershot sampling efforts during increasingly anomalous

conditions might not be enough to predict future changes.

References

Martino, E. J., and E. D. Houde. 2010. Recruitment of striped bass in Chesapeake Bay: Spatial and temporal environmental variability and availability of zooplankton prey. Marine Ecology Progress Series 409:213–228.

Shideler, A. C., and E. D. Houde. 2014. Spatio-temporal Variability in Larval-Stage Feeding and Nutritional Sources as Factors Influencing Striped Bass (Morone saxatilis) Recruitment Success. Estuaries and Coasts 37:561–575.

Uphoff, J. H. 2023. Perspective comes with time: What do long-term egg and juvenile indices say about Chesapeake Bay Striped Bass productivity? Marine and Coastal Fisheries 15.

2) Added 500 µL AL buffer to sample, vortexed, then incubated at 56°C for 10 minutes
3) Added 500 µL 100% ethanol to sample
4) Pipetted all of the sample from the 2ml tube into the spin column and centrifuged at ≥ 8,000 rpm for 1 min
8) Used elution buffer warmed to 65°C to elute DNA in two aliquots of 40ul and 30ul and incubated the elution buffer on the column prior to centrifugation for 10 min at 65°C

Fig. S2.1: Modified steps of Qiagen DNeasy blood and tissue DNA extraction kit. All other steps were followed as written in the kit protocol.

Sequence Name	**Sequence**
Components of Oligos:	pad - **barcode** - Leray F
Leray CO1-F_m1IntF	GGW ACW GGW TGA ACW GTW TAY CCY CC
Leray CO1-R_ jgHC0	TAN ACY TCN GGR TGN CCR AAR AAY CA
Leray F Tag-1-AACAAC	NNN **AAC AAC** GGW ACW GGW TGA ACW GTW TAY CCY CC
Leray F Tag-2-TCACTC	NNN TCA CTC GGW ACW GGW TGA ACW GTW TAY CCY CC
Leray F Tag-3-TTGAGT	NNN TTG AGT GGW ACW GGW TGA ACW GTW TAY CCY CC
Leray F Tag-4-CTTGGT	NNN CTT GGT GGW ACW GGW TGA ACW GTW TAY CCY CC
Leray F Tag-5-AAGGTC	NNN AAG GTC GGW ACW GGW TGA ACW GTW TAY CCY CC
Leray F Tag-6-GTAACA	NNN GTA ACA GGW ACW GGW TGA ACW GTW TAY CCY CC
Leray F Tag-7-TTCGGA	NNN TTC GGA GGW ACW GGW TGA ACW GTW TAY CCY CC
Leray F Tag-8-GCGGTT	NNN GCG GTT GGW ACW GGW TGA ACW GTW TAY CCY CC
Leray F Tag-9-TCGTTA	NNN TCG TTA GGW ACW GGW TGA ACW GTW TAY CCY CC
Leray F Tag-10-GAAGCT	NNN GAA GCT GGW ACW GGW TGA ACW GTW TAY CCY CC
Leray F Tag-11-GTCTTA	NNN GTC TTA GGW ACW GGW TGA ACW GTW TAY CCY CC
Leray F Tag-12-TATCTG	NNN TAT CTG GGW ACW GGW TGA ACW GTW TAY CCY CC
Leray F Tag-13-AACCGA	NNN AAC CGA GGW ACW GGW TGA ACW GTW TAY CCY CC
Leray F Tag-14-GAACTA	NNN GAA CTA GGW ACW GGW TGA ACW GTW TAY CCY CC
Leray F Tag-15-AAGCAG	NNN AAG CAG GGW ACW GGW TGA ACW GTW TAY CCY CC
Leray F Tag-16-TCCAGC	NNN TCC AGC GGW ACW GGW TGA ACW GTW TAY CCY CC
Leray F Tag-17-GGCGCA	NNN GGC GCA GGW ACW GGW TGA ACW GTW TAY CCY CC
Leray F Tag-18-AATCCT	NNN AAT CCT GGW ACW GGW TGA ACW GTW TAY CCY CC
Leray F Tag-19-CGACGT	NNN CGA CGT GGW ACW GGW TGA ACW GTW TAY CCY CC
Leray F Tag-20-ACACAA	NNN ACA CAA GGW ACW GGW TGA ACW GTW TAY CCY CC
Leray F Tag-21-TGTGGC	NNN TGT GGC GGW ACW GGW TGA ACW GTW TAY CCY CC
Leray F Tag-22-GATATT	NNN GAT ATT GGW ACW GGW TGA ACW GTW TAY CCY CC
Leray F Tag-23-TATACC	NNN TAT ACC GGW ACW GGW TGA ACW GTW TAY CCY CC
Leray F Tag-24-CGGCCA	NNN CGG CCA GGW ACW GGW TGA ACW GTW TAY CCY CC
Leray F Tag-25-CCGGAA	NNN CCG GAA GGW ACW GGW TGA ACW GTW TAY CCY CC
Leray F Tag-26-CCGTCC	NNN CCG TCC GGW ACW GGW TGA ACW GTW TAY CCY CC
Leray F Tag-27-TTGCAA	NNN TTG CAA GGW ACW GGW TGA ACW GTW TAY CCY CC
Leray F Tag-28-ACTTCA	NNN ACT TCA GGW ACW GGW TGA ACW GTW TAY CCY CC
Leray F Tag-29-TCGACG	NNN TCG ACG GGW ACW GGW TGA ACW GTW TAY CCY CC
Leray F Tag-30-AGACCG	NNN AGA CCG GGW ACW GGW TGA ACW GTW TAY CCY CC
Leray F Tag-31-CTCATG	NNN CTC ATG GGW ACW GGW TGA ACW GTW TAY CCY CC
Leray F Tag-32-GCTCCG	NNN GCT CCG GGW ACW GGW TGA ACW GTW TAY CCY CC
Leray F Tag-33-CTCTGC	NNN CTC TGC GGW ACW GGW TGA ACW GTW TAY CCY CC
Leray F Tag-34-AGCTGG	NNN AGC TGG GGW ACW GGW TGA ACW GTW TAY CCY CC
Leray F Tag-35-ACCTAT	NNN ACC TAT GGW ACW GGW TGA ACW GTW TAY CCY CC
Leray F Tag-36-CCTAAT	NNN CCT AAT GGW ACW GGW TGA ACW GTW TAY CCY CC
Leray F Tag-37-AGTGTT	NNN AGT GTT GGW ACW GGW TGA ACW GTW TAY CCY CC
Leray F Tag-38-AAGACA	NNN AAG ACA GGW ACW GGW TGA ACW GTW TAY CCY CC
Leray F Tag-39-CACGTA	NNN CAC GTA GGW ACW GGW TGA ACW GTW TAY CCY CC
Leray F Tag-40-GCGAGA	NNN GCG AGA GGW ACW GGW TGA ACW GTW TAY CCY CC
Leray F Tag-41-CCTGTC	NNN CCT GTC GGW ACW GGW TGA ACW GTW TAY CCY CC
Leray F Tag-42-TGGCGG	NNN TGG CGG GGW ACW GGW TGA ACW GTW TAY CCY CC
Leray F Tag-43-TGTATA	NNN TGT ATA GGW ACW GGW TGA ACW GTW TAY CCY CC
Leray F Tag-44-TACTTC	NNN TAC TTC GGW ACW GGW TGA ACW GTW TAY CCY CC
Leray F Tag-45-ATGGAT	NNN ATG GAT GGW ACW GGW TGA ACW GTW TAY CCY CC
Leray F Tag-46-CGCGAT	NNN CGC GAT GGW ACW GGW TGA ACW GTW TAY CCY CC
Leray F Tag-47-AGGTAA	NNN AGG TAA GGW ACW GGW TGA ACW GTW TAY CCY CC
Leray F Tag-48-ACGCGC	NNN ACG CGC GGW ACW GGW TGA ACW GTW TAY CCY CC

Table S2.2: Table of forward barcode and primer sequences for metabarcoding of zooplankton samples.

Sequence Name	**Sequence**
Components of Oligos	pad - **barcode** - Leray F
Leray R Tag-1-AACAAC	NNN AAC AAC TAN ACY TCN GGR TGN CCR AAR AAY CA
Leray R Tag-2-TCACTC	NNN TCA CTC TAN ACY TCN GGR TGN CCR AAR AAY CA
Leray R Tag-3-TTGAGT	NNN TTG AGT TAN ACY TCN GGR TGN CCR AAR AAY CA
Leray R Tag-4-CTTGGT	NNN CTT GGT TAN ACY TCN GGR TGN CCR AAR AAY CA
Leray R Tag-5-AAGGTC	NNN AAG GTC TAN ACY TCN GGR TGN CCR AAR AAY CA
Leray R Tag-6-GTAACA	NNN GTA ACA TAN ACY TCN GGR TGN CCR AAR AAY CA
Leray R Tag-7-TTCGGA	NNN TTC GGA TAN ACY TCN GGR TGN CCR AAR AAY CA
Leray R Tag-8-GCGGTT	NNN GCG GTT TAN ACY TCN GGR TGN CCR AAR AAY CA
Leray R Tag-9-TCGTTA	NNN TCG TTA TAN ACY TCN GGR TGN CCR AAR AAY CA
Leray R Tag-10-GAAGCT	NNN GAA GCT TAN ACY TCN GGR TGN CCR AAR AAY CA
Leray R Tag-11-GTCTTA	NNN GTC TTA TAN ACY TCN GGR TGN CCR AAR AAY CA
Leray R Tag-12-TATCTG	NNN TAT CTG TAN ACY TCN GGR TGN CCR AAR AAY CA
Leray R Tag-13-AACCGA	NNN AAC CGA TAN ACY TCN GGR TGN CCR AAR AAY CA
Leray R Tag-14-GAACTA	NNN GAA CTA TAN ACY TCN GGR TGN CCR AAR AAY CA
Leray R Tag-15-AAGCAG	NNN AAG CAG TAN ACY TCN GGR TGN CCR AAR AAY CA
Leray R Tag-16-TCCAGC	NNN TCC AGC TAN ACY TCN GGR TGN CCR AAR AAY CA
Leray R Tag-17-GGCGCA	NNN GGC GCA TAN ACY TCN GGR TGN CCR AAR AAY CA
Leray R Tag-18-AATCCT	NNN AAT CCT TAN ACY TCN GGR TGN CCR AAR AAY CA
Leray R Tag-19-CGACGT	NNN CGA CGT TAN ACY TCN GGR TGN CCR AAR AAY CA
Leray R Tag-20-ACACAA	NNN ACA CAA TAN ACY TCN GGR TGN CCR AAR AAY CA
Leray R Tag-21-TGTGGC	NNN TGT GGC TAN ACY TCN GGR TGN CCR AAR AAY CA
Leray R Tag-22-GATATT	NNN GAT ATT TAN ACY TCN GGR TGN CCR AAR AAY CA
Leray R Tag-23-TATACC	NNN TAT ACC TAN ACY TCN GGR TGN CCR AAR AAY CA
Leray R Tag-24-CGGCCA	NNN CGG CCA TAN ACY TCN GGR TGN CCR AAR AAY CA
Leray R Tag-25-CCGGAA	NNN CCG GAA TAN ACY TCN GGR TGN CCR AAR AAY CA
Leray R Tag-26-CCGTCC	NNN CCG TCC TAN ACY TCN GGR TGN CCR AAR AAY CA
Leray R Tag-27-TTGCAA	NNN TTG CAA TAN ACY TCN GGR TGN CCR AAR AAY CA
Leray R Tag-28-ACTTCA	NNN ACT TCA TAN ACY TCN GGR TGN CCR AAR AAY CA
Leray R Tag-29-TCGACG	NNN TCG ACG TAN ACY TCN GGR TGN CCR AAR AAY CA
Leray R Tag-30-AGACCG	NNN AGA CCG TAN ACY TCN GGR TGN CCR AAR AAY CA
Leray R Tag-31-CTCATG	NNN CTC ATG TAN ACY TCN GGR TGN CCR AAR AAY CA
Leray R Tag-32-GCTCCG	NNN GCT CCG TAN ACY TCN GGR TGN CCR AAR AAY CA
Leray R Tag-33-CTCTGC	NNN CTC TGC TAN ACY TCN GGR TGN CCR AAR AAY CA
Leray R Tag-34-AGCTGG	NNN AGC TGG TAN ACY TCN GGR TGN CCR AAR AAY CA
Leray R Tag-35-ACCTAT	NNN ACC TAT TAN ACY TCN GGR TGN CCR AAR AAY CA
Leray R Tag-36-CCTAAT	NNN CCT AAT TAN ACY TCN GGR TGN CCR AAR AAY CA
Leray R Tag-37-AGTGTT	NNN AGT GTT TAN ACY TCN GGR TGN CCR AAR AAY CA
Leray R Tag-38-AAGACA	NNN AAG ACA TAN ACY TCN GGR TGN CCR AAR AAY CA
Leray R Tag-39-CACGTA	NNN CAC GTA TAN ACY TCN GGR TGN CCR AAR AAY CA
Leray R Tag-40-GCGAGA	NNN GCG AGA TAN ACY TCN GGR TGN CCR AAR AAY CA
Leray R Tag-41-CCTGTC	NNN CCT GTC TAN ACY TCN GGR TGN CCR AAR AAY CA
Leray R Tag-42-TGGCGG	NNN TGG CGG TAN ACY TCN GGR TGN CCR AAR AAY CA
Leray R Tag-43-TGTATA	NNN TGT ATA TAN ACY TCN GGR TGN CCR AAR AAY CA
Leray R Tag-44-TACTTC	NNN TAC TTC TAN ACY TCN GGR TGN CCR AAR AAY CA
Leray R Tag-45-ATGGAT	NNN ATG GAT TAN ACY TCN GGR TGN CCR AAR AAY CA
Leray R Tag-46-CGCGAT	NNN CGC GAT TAN ACY TCN GGR TGN CCR AAR AAY CA
Leray R Tag-47-AGGTAA	NNN AGG TAA TAN ACY TCN GGR TGN CCR AAR AAY CA
Leray R Tag-48-ACGCGC	NNN ACG CGC TAN ACY TCN GGR TGN CCR AAR AAY CA

Table S2.3: Table of reverse barcode and primer sequences for metabarcoding of zooplankton samples.

Annelida,Polychaeta,Unknown,Unknown,Unknown,Unknown
Arthropoda,Arachnida,Trombidiformes,Halacaridae,Unknown,Unknown
Arthropoda,Branchiopoda,Diplostraca,Bosminidae,Bosmina,longirostris
Arthropoda,Branchiopoda,Diplostraca,Podonidae,Pleopis,polyphemoides
Arthropoda,Branchiopoda,Diplostraca,Sididae,Diaphanosoma,Unknown
Arthropoda,Branchiopoda,Diplostraca,Sididae,Unknown,Unknown
Arthropoda,Hexanauplia,Calanoida,Acartiidae,Acartia,tonsa
Arthropoda,Hexanauplia,Calanoida,Temoridae,Eurytemora,carolleeae
Arthropoda,Hexanauplia,Calanoida,Unknown,Unknown,Unknown
Arthropoda,Hexanauplia,Cyclopoida,Cyclopidae,Tropocyclops,Unknown
Arthropoda,Hexanauplia,Cyclopoida,Oithonidae,Oithona,colcarva
Arthropoda,Hexanauplia,Cyclopoida,Unknown,Unknown,Unknown
Arthropoda,Hexanauplia,Harpacticoida,Ameiridae,Stygonitocrella,Unknown
Arthropoda,Hexanauplia,Harpacticoida,Unknown,Unknown,Unknown
Arthropoda,Hexanauplia,Poecilostomatoida,Ergasilidae,Ergasilus, Unknown
Arthropoda,Hexanauplia,Unknown,Unknown,Unknown,Unknown
Arthropoda,Malacostraca,Decapoda,Panopeidae,Rhithropanopeus,harrisii
Arthropoda,Thecostraca,Balanomorpha,Balanidae,Balanus,Unknown
Arthropoda,Thecostraca,Balanomorpha,Chthamalidae,Chthamalus,Unknown
Bryozoa,Unknown,Unknown,Unknown,Unknown,Unknown
Foraminifera,Unknown,Unknown,Unknown,Unknown,Unknown
Mollusca,Bivalvia,Unknown,Unknown,Unknown,Unknown
Mollusca,Gastropoda,Unknown,Unknown,Unknown,Unknown
Mollusca,Unknown,Unknown,Unknown,Unknown,Unknown
Nematoda,Unknown,Unknown,Unknown,Unknown,Unknown
Platyhelminthes,Unknown,Unknown,Unknown,Unknown,Unknown
Rotifera,Eurotatoria,Ploima,Brachionidae,Brachionus,angularis
Rotifera,Eurotatoria,Ploima,Brachionidae,Brachionus,calyciflorus
Rotifera,Eurotatoria,Ploima,Brachionidae,Brachionus,caudatus
Rotifera,Eurotatoria,Ploima,Brachionidae,Brachionus,rubens or plicatilis
Rotifera,Eurotatoria,Ploima,Brachionidae,Brachionus,Unknown
Rotifera,Eurotatoria,Ploima,Brachionidae,Brachionus,urceolaris
Rotifera,Eurotatoria,Ploima,Brachionidae,Keratella,gracilenta
Rotifera,Eurotatoria,Ploima,Brachionidae,Keratella,Unknown
Rotifera,Eurotatoria,Ploima,Notommatidae,Notommata,Unknown
Rotifera,Eurotatoria,Ploima,Synchaetidae,Synchaeta,Unknown
Rotifera,Unknown,Unknown,Unknown,Unknown,Unknown

Table S2.4: Table of taxa identified in the morphological data set, listed in alphabetical order by phylum. Full taxonomic identification is written out in the format: phylum,class,order,family,genus,species. Where a taxonomic level was unknown, “Unknown” is substituted.

Annelida,Clitellata,Crassiclitellata,Unknown,Unknown,Unknown
Annelida,Clitellata,Tubificida,Naididae,Unknown,Unknown
Annelida,Polychaeta,Capitellidae,Capitellidae,Heteromastus,filiformis
Annelida,Polychaeta,Capitellidae,Capitellidae,Mediomastus,ambiseta
Annelida,Polychaeta,Orbiniidae,Orbiniidae,Leitoscoloplos,robustus
Annelida,Polychaeta,Phyllodocida,Goniadidae,Glycinde,multidens
Annelida,Polychaeta,Phyllodocida,Nereididae,Alitta,succinea
Annelida,Polychaeta,Phyllodocida,Nereididae,Laeonereis,culveri
Annelida,Polychaeta,Phyllodocida,Phyllodocidae,Hypereteone,heteropoda
Annelida,Polychaeta,Phyllodocida,Phyllodocidae,Unknown,Unknown
Annelida,Polychaeta,Spionida,Spionidae,Marenzelleria,neglecta
Annelida,Polychaeta,Spionida,Spionidae,Polydora,cornuta
Annelida,Polychaeta,Spionida,Spionidae,Polydora,Unknown
Annelida,Polychaeta,Spionida,Spionidae,Polydora,websteri
Annelida,Polychaeta,Spionida,Spionidae,Streblospio,benedicti
Annelida,Polychaeta,Spionida,Spionidae,Streblospio,gynobranchiata
Annelida,Polychaeta,Spionida,Spionidae,Unknown,Unknown
Annelida,Polychaeta,Terebellida,Pectinariidae,Pectinaria,gouldii
Arthropoda,Arachnida,Trombidiformes,Limnesiidae,Limnesia,fulgida
Arthropoda,Arachnida,Trombidiformes,Unknown,Unknown,Unknown
Arthropoda,Branchiopoda,Diplostraca,Bosminidae,Bosmina,freyi
Arthropoda,Branchiopoda,Diplostraca,Bosminidae,Bosmina,liederi
Arthropoda,Branchiopoda,Diplostraca,Bosminidae,Bosmina,longirostris
Arthropoda,Branchiopoda,Diplostraca,Chydoridae,Alona,Unknown
Arthropoda,Branchiopoda,Diplostraca,Chydoridae,Chydorus,brevilabris
Arthropoda,Branchiopoda,Diplostraca,Chydoridae,Unknown,Unknown
Arthropoda,Branchiopoda,Diplostraca,Daphniidae,Daphnia,ambigua
Arthropoda,Branchiopoda,Diplostraca,Daphniidae,Daphnia,parvula
Arthropoda,Branchiopoda,Diplostraca,Leptodoridae,Leptodora,kindtii
Arthropoda,Branchiopoda,Diplostraca,Macrotrichidae,Ilyocryptus,agilis
Arthropoda,Branchiopoda,Diplostraca,Moinidae,Moina,micrura
Arthropoda,Branchiopoda,Diplostraca,Podonidae,Pleopis,polyphemoides
Arthropoda,Branchiopoda,Diplostraca,Sididae,Diaphanosoma,chankensis
Arthropoda,Branchiopoda,Diplostraca,Sididae,Diaphanosoma,Unknown
Arthropoda,Hexanauplia,Calanoida,Acartiidae,Acartia,tonsa
Arthropoda,Hexanauplia,Calanoida,Diaptomidae,Skistodiaptomus,pallidus
Arthropoda,Hexanauplia,Calanoida,Temoridae,Eurytemora,affinis
Arthropoda,Hexanauplia,Calanoida,Temoridae,Eurytemora,carolleeae
Arthropoda,Hexanauplia,Calanoida,Temoridae,Eurytemora,Unknown
Arthropoda,Hexanauplia,Calanoida,Unknown,Unknown,Unknown
Arthropoda,Hexanauplia,Cyclopoida,Cyclopidae,Acanthocyclops,americanus
Arthropoda,Hexanauplia,Cyclopoida,Cyclopidae,Acanthocyclops,brevispinosus
Arthropoda,Hexanauplia,Cyclopoida,Cyclopidae,Acanthocyclops,robustus
Arthropoda,Hexanauplia,Cyclopoida,Cyclopidae,Apocyclops,spartinus
Arthropoda,Hexanauplia,Cyclopoida,Cyclopidae,Macrocyclops,albidus
Arthropoda,Hexanauplia,Cyclopoida,Cyclopidae,Mesocyclops,edax
Arthropoda,Hexanauplia,Cyclopoida,Cyclopidae,Mesocyclops,pehpeiensis
Arthropoda,Hexanauplia,Cyclopoida,Cyclopidae,Tropocyclops,prasinus
Arthropoda,Hexanauplia,Cyclopoida,Unknown,Unknown,Unknown
Arthropoda,Hexanauplia,Harpacticoida,Ectinosomatidae,Pseudobradya,minor
Arthropoda,Hexanauplia,Harpacticoida,Miraciidae,Schizopera,knabeni
Arthropoda,Hexanauplia,Poecilostomatoida,Ergasilidae,Acusicola,margulisae
Arthropoda,Hexanauplia,Poecilostomatoida,Ergasilidae,Neoergasilus,japonicus
Arthropoda,Hexanauplia,Unknown,Unknown,Unknown,Unknown

Table S2.5: Table of taxa identified in the inclusive data set, listed in alphabetical order by phylum. Full taxonomic identification is written out in the format: phylum,class,order,family,genus,species. Where a taxonomic level was unknown, “Unknown” is substituted. Continued on next two pages.

Arthropoda,Insecta,Diptera,Chaoboridae,Chaoborus,punctipennis
Arthropoda,Insecta,Diptera,Chironomidae,Dicrotendipes,modestus
Arthropoda,Insecta,Diptera,Chironomidae,Procladius,Unknown
Arthropoda,Insecta,Diptera,Culicidae,Ochlerotatus,Unknown
Arthropoda,Insecta,Diptera,Tabanidae,Tabanus,par
Arthropoda,Insecta,Odonata,Calopterygidae,Calopteryx,maculata
Arthropoda,Insecta,Trichoptera,Hydroptilidae,Ochrotrichia,dactylophora
Arthropoda,Malacostraca,Decapoda,Palaemonidae,Palaemon,pugio
Arthropoda,Malacostraca,Decapoda,Panopeidae,Eurypanopeus,depressus
Arthropoda,Malacostraca,Decapoda,Panopeidae,Rhithropanopeus,harrisii
Arthropoda,Malacostraca,Decapoda,Portunidae,Callinectes,sapidus
Arthropoda,Malacostraca,Mysida,Mysidae,Michthyops,parvus
Arthropoda,Malacostraca,Mysida,Mysidae,Neomysis,americana
Arthropoda,Ostracoda,Podocopida,Cyprididae,Cypridopsis,vidua
Arthropoda,Ostracoda,Podocopida,Cyprididae,Unknown,Unknown
Arthropoda,Thecostraca,Balanomorpha,Balanidae,Amphibalanus,improvisus
Arthropoda,Thecostraca,Balanomorpha,Balanidae,Amphibalanus,subalbidus
Arthropoda,Unknown,Unknown,Unknown,Unknown,Unknown
Bryozoa,Gymnolaemata,Cheilostomatida,Electridae,Conopeum,chesapeakensis
Bryozoa,Gymnolaemata,Cheilostomatida,Electridae,Conopeum,tenuissimum
Bryozoa,Gymnolaemata,Cheilostomatida,Membraniporidae,Membranipora,tenuis
Bryozoa,Gymnolaemata,Ctenostomatida,Unknown,Unknown,Unknown
Bryozoa,Gymnolaemata,Ctenostomatida,Vesiculariidae,Amathia,brasiliensis
Bryozoa,Gymnolaemata,Ctenostomatida,Vesiculariidae,Amathia,distans
Bryozoa,Gymnolaemata,Ctenostomatida,Vesiculariidae,Amathia,evelinae
Bryozoa,Gymnolaemata,Ctenostomatida,Vesiculariidae,Amathia,Unknown
Chordata,Actinopteri,Atheriniformes,Atherinopsidae,Membras,martinica
Chordata,Actinopteri,Atheriniformes,Atherinopsidae,Menidia,beryllina
Chordata,Actinopteri,Atheriniformes,Atherinopsidae,Menidia,menidia
Chordata,Actinopteri,Blenniiformes,Blenniidae,Chasmodes,bosquianus
Chordata,Actinopteri,Clupeiformes,Clupeidae,Brevoortia,tyrannus
Chordata,Actinopteri,Clupeiformes,Clupeidae,Dorosoma,cepedianum
Chordata,Actinopteri,Clupeiformes,Engraulidae,Anchoa,mitchilli
Chordata,Actinopteri,Moronidae,Moronidae,Morone,americana
Chordata,Actinopteri,Moronidae,Moronidae,Morone,saxatilis
Cnidaria,Anthozoa,Actiniaria,Diadumenidae,Diadumene,leucolena
Cnidaria,Hydrozoa,Anthoathecata,Eudendriidae,Eudendrium,carneum
Cnidaria,Hydrozoa,Anthoathecata,Moerisiidae,Moerisia,inkermanica
Cnidaria,Hydrozoa,Anthoathecata,Unknown,Unknown,Unknown
Cnidaria,Hydrozoa,Leptothecata,Blackfordiidae,Blackfordia,virginica
Cnidaria,Hydrozoa,Limnomedusae,Geryoniidae,Liriope,tetraphylla
Cnidaria,Scyphozoa,Semaeostomeae,Pelagiidae,Chrysaora,chesapeakei
Ctenophora,Tentaculata,Lobata,Bolinopsidae,Mnemiopsis,leidyi
Gastrotricha,Chaetonotida,Chaetonotida,Chaetonotidae,Chaetonotus,jaceki
Gastrotricha,Chaetonotida,Chaetonotida,Chaetonotidae,Lepidodermella,Unknown
Gastrotricha,Chaetonotida,Chaetonotida,Chaetonotidae,Unknown,Unknown
Mollusca,Bivalvia,Cardiida,Tellinidae,Ameritella,mitchelli
Mollusca,Bivalvia,Cardiida,Tellinidae,Limecola,petalum
Mollusca,Bivalvia,Galeommatida,Montacutidae,Kurtiella,bidentata
Mollusca,Bivalvia,Myida,Dreissenidae,Mytilopsis,leucophaeata
Mollusca,Bivalvia,Myida,Teredinidae,Bankia,barthelowi
Mollusca,Bivalvia,Mytilida,Mytilidae,Ischadium,recurvum
Mollusca,Bivalvia,Mytilida,Mytilidae,Unknown,Unknown
Mollusca,Bivalvia,Venerida,Mactridae,Mulinia,lateralis
Mollusca,Bivalvia,Venerida,Mactridae,Rangia,cuneata

Mollusca,Gastropoda,Acteonidae,Acteonidae,Japonactaeon,punctostriatus
Mollusca,Gastropoda,Cephalaspidea,Cylichnidae,Acteocina,canaliculata
Mollusca,Gastropoda,Cephalaspidea,Haminoeidae,Haminoea,solitaria
Mollusca,Gastropoda,Ellobiida,Ellobiidae,Melampus,bidentatus
Mollusca,Gastropoda,Littorinimorpha,Cochliopidae,Littoridinops,tenuipes
Mollusca,Gastropoda,Littorinimorpha,Littorinidae,Littoraria,irrorata
Mollusca,Gastropoda,Neogastropoda,Muricidae,Scabrotrophon,inspiratus
Mollusca,Gastropoda,Nudibranchia,Facelinidae,Cratena,pilata
Mollusca,Gastropoda,Nudibranchia,Onchidorididae,Corambe,obscura
Mollusca,Gastropoda,Nudibranchia,Trinchesiidae,Tenellia,adspersa
Mollusca,Gastropoda,Systellommatophora,Onchidiidae,Peronia,verruculata
Nemertea,Enopla,Monostilifera,Amphiporidae,Unknown,Unknown
Nemertea,Palaeonemertea,Carinomiformes,Carinomidae,Carinoma,Unknown
Platyhelminthes,Cestoda,Rhinebothriidea,Rhinebothriidae,Rhinebothrium,Unknown
Platyhelminthes,Rhabditophora,Polycladida,Notoplanidae,Notoplana,australis
Platyhelminthes,Rhabditophora,Polycladida,Stylochidae,Stylochus,ellipticus
Rotifera,Eurotatoria,Ploima,Brachionidae,Keratella,cochlearis
Xenacoelomorpha,Acoela,Acoela,Anaperidae,Neochildia,fusca

Annelida,Polychaeta,Capitellidae,Capitellidae,Heteromastus,filiformis
Annelida,Polychaeta,Capitellidae,Capitellidae,Mediomastus,ambiseta
Annelida,Polychaeta,Orbiniidae,Orbiniidae,Leitoscoloplos,robustus
Annelida,Polychaeta,Phyllodocida,Goniadidae,Glycinde,multidens
Annelida,Polychaeta,Phyllodocida,Nereididae,Alitta,succinea
Annelida,Polychaeta,Phyllodocida,Nereididae,Laeonereis,culveri
Annelida,Polychaeta,Phyllodocida,Nereididae,Unknown,Unknown
Annelida,Polychaeta,Phyllodocida,Phyllodocidae,Hypereteone,heteropoda
Annelida,Polychaeta,Spionida,Spionidae,Marenzelleria,neglecta
Annelida,Polychaeta,Spionida,Spionidae,Polydora,cornuta
Annelida,Polychaeta,Spionida,Spionidae,Polydora,websteri
Annelida,Polychaeta,Spionida,Spionidae,Streblospio,benedicti
Annelida,Polychaeta,Terebellida,Pectinariidae,Pectinaria,gouldii
Arthropoda,Branchiopoda,Diplostraca,Bosminidae,Bosmina,freyi
Arthropoda,Branchiopoda,Diplostraca,Bosminidae,Bosmina,longirostris
Arthropoda,Branchiopoda,Diplostraca,Chydoridae,Chydorus,brevilabris
Arthropoda,Branchiopoda,Diplostraca,Daphniidae,Daphnia,ambigua
Arthropoda,Branchiopoda,Diplostraca,Daphniidae,Daphnia,parvula
Arthropoda,Branchiopoda,Diplostraca,Podonidae,Pleopis,polyphemoides
Arthropoda,Hexanauplia,Calanoida,Acartiidae,Acartia,tonsa
Arthropoda,Hexanauplia,Calanoida,Diaptomidae,Skistodiaptomus,pallidus
Arthropoda,Hexanauplia,Calanoida,Temoridae,Eurytemora,affinis
Arthropoda,Hexanauplia,Calanoida,Temoridae,Eurytemora,Unknown
Arthropoda,Hexanauplia,Cyclopoida,Cyclopidae,Acanthocyclops,americanus
Arthropoda,Hexanauplia,Cyclopoida,Cyclopidae,Acanthocyclops,brevispinosus
Arthropoda,Hexanauplia,Cyclopoida,Cyclopidae,Macrocyclops,albidus
Arthropoda,Hexanauplia,Cyclopoida,Cyclopidae,Mesocyclops,edax
Arthropoda,Hexanauplia,Cyclopoida,Cyclopidae,Mesocyclops,pehpeiensis
Arthropoda,Hexanauplia,Harpacticoida,Miraciidae,Schizopera,knabeni
Arthropoda,Insecta,Diptera,Chaoboridae,Chaoborus,punctipennis
Arthropoda,Insecta,Diptera,Chironomidae,Dicrotendipes,modestus
Arthropoda,Insecta,Diptera,Culicidae,Ochlerotatus,Unknown
Arthropoda,Insecta,Odonata,Calopterygidae,Calopteryx,maculata
Arthropoda,Malacostraca,Decapoda,Palaemonidae,Palaemon,pugio
Arthropoda,Malacostraca,Decapoda,Panopeidae,Eurypanopeus,depressus
Arthropoda,Malacostraca,Decapoda,Panopeidae,Rhithropanopeus,harrisii
Arthropoda,Malacostraca,Decapoda,Portunidae,Callinectes,sapidus
Arthropoda,Malacostraca,Mysida,Mysidae,Neomysis,americana
Arthropoda,Thecostraca,Balanomorpha,Balanidae,Amphibalanus,improvisus
Arthropoda,Thecostraca,Balanomorpha,Balanidae,Amphibalanus,subalbidus
Bryozoa,Gymnolaemata,Cheilostomatida,Electridae,Conopeum,chesapeakensis
Bryozoa,Gymnolaemata,Cheilostomatida,Electridae,Conopeum,tenuissimum
Bryozoa,Gymnolaemata,Cheilostomatida,Membraniporidae,Membranipora,tenuis

Table S2.6: Table of taxa identified in the exclusive data set, listed in alphabetical order by phylum. Full taxonomic identification is written out in the format: phylum,class,order,family,genus,species. Where a taxonomic level was unknown, “Unknown” is substituted. Continued on next page.

Chordata,Actinopteri,Atheriniformes,Atherinopsidae,Membras,martinica
Chordata,Actinopteri,Atheriniformes,Atherinopsidae,Menidia,beryllina
Chordata,Actinopteri,Atheriniformes,Atherinopsidae,Menidia,menidia
Chordata,Actinopteri,Blenniiformes,Blenniidae,Chasmodes,bosquianus
Chordata,Actinopteri,Clupeiformes,Clupeidae,Brevoortia,Unknown
Chordata,Actinopteri,Clupeiformes,Clupeidae,Dorosoma,cepedianum
Chordata,Actinopteri,Clupeiformes,Engraulidae,Anchoa,mitchilli
Chordata,Actinopteri,Moronidae,Moronidae,Morone,americana
Chordata,Actinopteri,Moronidae,Moronidae,Morone,saxatilis
Cnidaria,Anthozoa,Actiniaria,Diadumenidae,Diadumene,leucolena
Cnidaria,Hydrozoa,Anthoathecata,Moerisiidae,Moerisia,inkermanica
Cnidaria,Hydrozoa,Leptothecata,Blackfordiidae,Blackfordia,virginica
Cnidaria,Scyphozoa,Semaeostomeae,Pelagiidae,Chrysaora,Unknown
Mollusca,Bivalvia,Cardiida,Tellinidae,Ameritella,mitchelli
Mollusca,Bivalvia,Cardiida,Tellinidae,Limecola,petalum
Mollusca,Bivalvia,Myida,Dreissenidae,Mytilopsis,leucophaeata
Mollusca,Bivalvia,Mytilida,Mytilidae,Ischadium,recurvum
Mollusca,Bivalvia,Venerida,Mactridae,Mulinia,lateralis
Mollusca,Bivalvia,Venerida,Mactridae,Rangia,cuneata
Mollusca,Gastropoda,Acteonidae,Acteonidae,Japonactaeon,punctostriatus
Mollusca,Gastropoda,Cephalaspidea,Cylichnidae,Acteocina,canaliculata
Mollusca,Gastropoda,Cephalaspidea,Haminoeidae,Haminoea,solitaria
Mollusca,Gastropoda,Ellobiida,Ellobiidae,Melampus,bidentatus
Mollusca,Gastropoda,Littorinimorpha,Cochliopidae,Littoridinops,tenuipes
Mollusca,Gastropoda,Littorinimorpha,Littorinidae,Littoraria,irrorata
Mollusca,Gastropoda,Nudibranchia,Facelinidae,Cratena,pilata
Mollusca,Gastropoda,Nudibranchia,Onchidoridae,Corambe,obscura
Mollusca,Gastropoda,Nudibranchia,Trinchesiidae,Tenellia,adspersa
Platyhelminthes,Rhabditophora,Polycladida,Unknown,Unknown,Unknown
Rotifera,Eurotatoria,Ploima,Brachionidae,Keratella,cochlearis
Xenacoelomorpha,Acoela,Acoela,Anaperidae,Neochildia,fusca

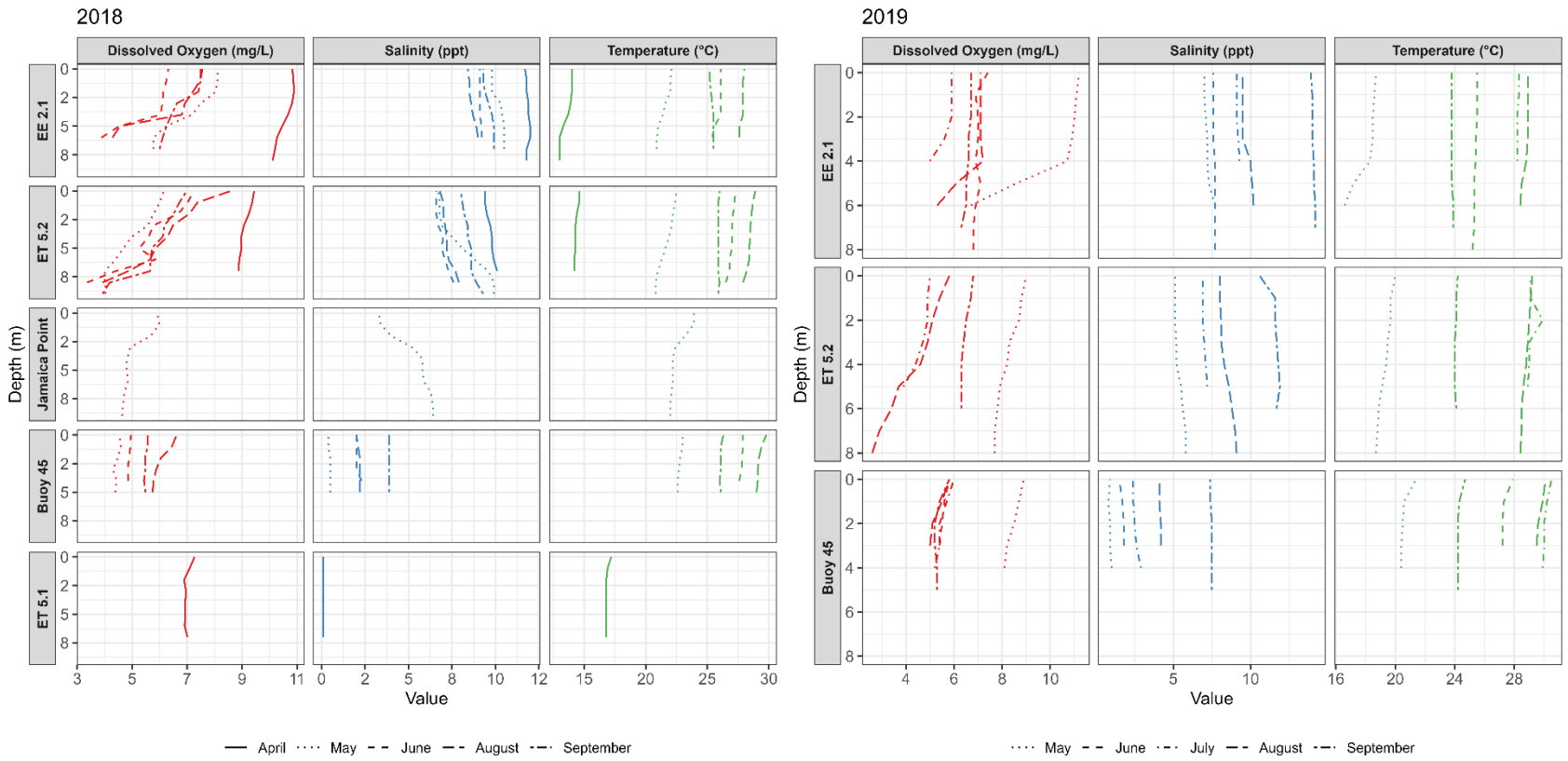

Fig S2.7: Grids of line graphs showing water column profiles from surface to within 1m of the bottom for select hydrographic data at all stations sampled in 2018 (left grid) and 2019 (right grid). Each row represents data from a station, in order top to bottom from the headwaters to the mouth of the Choptank River. Each column represents Dissolved oxygen (mg/L, red), Salinity (ppt, blue), or Temperature (°C, green). Line textures indicate the month of sampling.

4) Incubate at 55°C in a shaking incubator (speed= 210) for 3 hours (or overnight)
8) Incubate at 65°C for 10 minutes
9) Add 200 µl 100% ethanol and vortex to mix
20) Add 50 µl Elution Buffer heated to 65°C. Incubate at 65°C for 10 minutes. Centrifuge at maximum speed for 1 minute
For fish gut content samples, use 75 µl Elution Buffer and incubate for 15 min

Fig S3.1: Modified steps of Omega EZNA tissue DNA extraction kit. All other steps were followed as written in the kit protocol.

Soft-bodied taxa		Hard-bodied taxa	
Acanthamoeba comandoni	Kuckuckia spinosa	Acanthocyclops brevispinosus	Mayamaea permitis
Agaricales	Laminaria rodriguezii	Acartia tonsa	Mediophyceae
Agaricomycetes	Leotiomycetes	Achelous spinimanus	Meleagris gallopavo
Aglaophamus dibranchis	Linnemannia amoeboidea	Aculops ulmi	Melosira ambiqua
Aglaothamnion callophyllidicola	Lobophora sonderi	Acusicola margulisae	Melosira varians
Alitta succinea	Malassezia japonica	Ameritella mitchelli	Minutocellus polymorphus
Alosa pseudoharengus	Marenzelleria neglecta	Amphibalanus improvisus	Mulinia lateralis
Amathia	Megathylacoides lamothei	Apocorophium lacustre	Navicula
Anchoa mitchilli	Membranipora tenuis	Armigeres subalbatus	Navicula cryptocephala
Anthoathecata	Membras martinica	Arthropoda	Navicula glaciei
Arthrocladium fulminans	Microgobius thalassinus	Bacillariophyta	Naviculales
Ascomycota	Microscolex phosphoreus	Balaustium murorum	Neoergasilus japonicus
Aspergillaceae	Microstomum lineare	Biomphalaria	Nitzschia
Aspergillus	Mollisiaceae	Bosmina freyi	Nitzschia alba
Aspergillus chevalieri	Morone americana	Bosmina liederi	Notholca acuminata
Aspergillus puulaauensis	Morone saxatilis	Bosmina longirostris	Olcella trigramma
Aspidodera	Mucorales	Calanoida	Oocassida pudibunda
Blastocladiella emersonii	Mychonastes homosphaera	Callinectes	Orthoptera
Boccardiella hamata	Naididae	Callinectes danae	Parasitus fimetorum
Cacajao calvus	Nais communis	Callinectes ornatus	Pinnularia
Cafeteria roenbergensis	Neochildia fusca	Callinectes sapidus	Pinnularia subanglica
Candida metapsilosis	Neopetrosia exigua	Calopteryx maculata	Pionidae
Candida orthopsilosis	Neurospora crassa	Caloptilia bimaculatella	Placoneis minor
Cebus albifrons	Oomycota	Canis lupus	Pleopis polyphemoides
Cercospora nicotianae	Ovalopodium rosalinum	Cerobasis guestfalica	Poaceae
Chaetonotidae	Parvamoeba rugata	Chaoborus punctipennis	Rangia cuneata
Chasmodes bosquianus	Pedospumella sinomuralis	Chironomidae	Rhithropanopeus harrisii
Chattonella	Pelagomonas calceolata	Chironomus	Scleractinia
Chattonella marina	Penicillium canescens	Coelotes terrestris	Sellaphora
Chlorella variabilis	Penicillium sclerotiorum	Coscinodiscophyceae	Simocephalus serrulatus
Chlorellaceae	Peniophora lycii	Coscinodiscus granii	Skeletonema
Chloropicon mariensis	Perca flavescens	Coscinodiscus wailesii	Skeletonema potamos
Chordariaceae	Phaeophyceae	Crassostrea virginica	Skistodiaptomus pallidus
Chromulinales	Phytophthora	Cricotopus	Stephanodiscaceae
Chrysaora chesapeakei	Pluteus	Cyclopidae	Stephanopyxis turris
Chrysochromulina tobinii	Podosphaera xanthii	Cyclotella glomerata	Sus scrofa
Cladophialophora bantiana	Polydora cornuta	Cylindrotheca closterium	Tanytarsus formosanus
Cladosporium	Polydora websteri	Daphnia ambigua	Tettigoniidae
Cladosporium anthropophilum	Poterioochromonas stipitata	Dermatophagoides farinae	Thalassiosira pseudonana
Cladosporium cladosporioides	Primates	Diaphanosoma	Thalassiosirales
Cladosporium sphaerospermum	Proteocephalus macrocephalus	Diaphanosoma brachyurum	Thylodrias contractus
Colletotrichum	Protohydra leuckarti	Diptera	Torrenticola disabatinola
Conidiobolus	Psathyrellaceae	Entomobrya atrocincta	Triparma laevis
Cryptococcus neoformans	Pyricularia oryzae	Eristalinus aeneus	Unknown
Curvularia clavata	Pythiaceae	Eurypanopeus depressus	
Demospongiae	Pythium biforme	Eurytemora carolleeae	
Dero digitata	Raspailiidae	Fistulifera saprophila	
Diadumene leucolena	Rathkea octopunctata	Folsomia quadrioculata	
Dinophyceae	Rhodotorula taiwanensis	Gammarus daiberi	
Discosea	Ripella	Gryllus veletis	
Dorosoma cepedianum	Saprolegnia	Guinardia delicatula	
Dothideomycetes	Saprolegniaceae	Haslea provincialis	
Dunaliella	Scopalina canariensis	Helicotheca tamesis	
Ectocarpales	Sordariomycetes	Hemiaulus sinensis	
Eimeriidae	Spionidae	Hylastes gracilis	
Etheostoma olmstedi	Streblospio benedicti	Insecta	
Eurotiomycetes	Striaria attenuata	Isotomidae	
Feldmannia lebelii	Sydowia polyspora	Keratella cochlearis	
Fusarium oxysporum	Synchaeta	Lepidoptera	
Gigartinales	Synchaeta baltica	Lepisma saccharina	
Globisporangium	Synchaeta oblonga	Leptocheirus plumulosus	
Goussia bayae	Synchytrium	Leptodora kindtii	
Hannaella oryzae	Thelephora aurantiotincta	Limecola petalum	
Helotiales	Thuricola similis	Liposcelis bostrychophila	
Homo sapiens	Tremella fuciformis	Lithodesmium	
Hydra oligactis	Trichoderma	Lithophyllum grumosum	
Hydra vulgaris	Verticillium nonalfalfae	Littoridinops tenuipes	
Hypereteone heteropoda	Vexillifera abyssalis	Lucida lucia	
Hypocreales	Vexillifera kereti	Magnoliopsida	

Table S3.2: Table describing which taxa were classified as hard-bodied and soft-bodied prey. Bryozoans were classified as soft bodied on the assumption that fish larvae were consuming free-swimming bryozoan larvae (generally without shells) rather than feeding from benthic bryozoan colonies (generally with encrusting type shells).

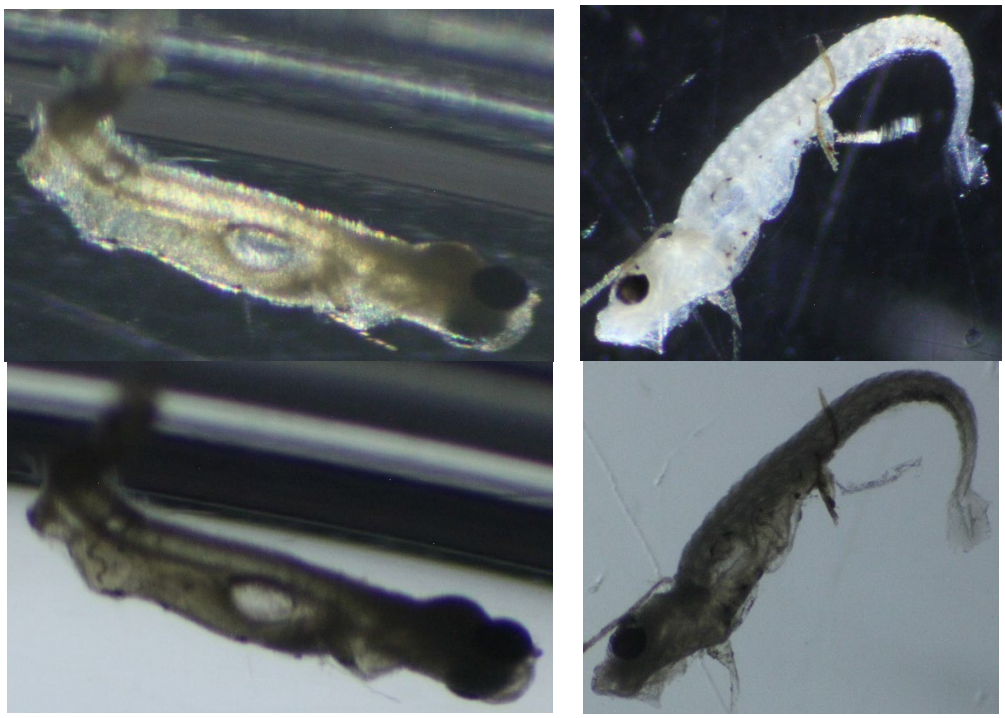

Fig S3.3: Photographs of empty (left column) and full (right column) larvae of *Morone americana*.

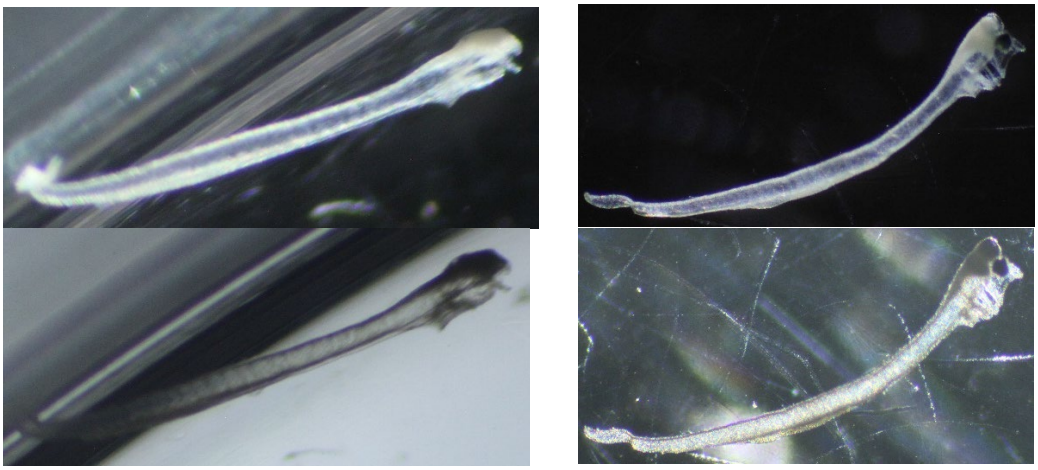

Fig S3.4: Photographs of empty (left column) and full (right column) larvae of *Anchoa mitchilli*.

Taxon	Life stage	Data set excluded from	Reason
Jellyfish	all	CBP mesozooplankton	not enumerated in SG data set
Copepod	nauplii		not caught quantitatively
All	eggs	SG mesozooplankton	not caught quantitatively
Copepod	nauplii		
All	eggs	SG microzooplankton	not enumerated in CBP data set
Copepod	copepodites		
Copepod	copepodites	CBP microzooplankton	not consistently enumerated within data set

Table S.4.1: List of taxa and life stages excluded from each data set, and why they were omitted.

List of combined references

Ahlstrom, E. H., and J. R. Thrailkill. 1963. Plankton volume loss with time of preservation. Pages 57–73.

Amundsen, P.-A., H.-M. Gabler, and F. J. Staldvik. 1996. A new approach to graphical analysis of feeding strategy from stomach contents data-modification of the Costello (1990) method. Journal of Fish Biology 48:607–614.

Andries, J.-C. 2001. Endocrine and environmental control of reproduction in Polychaeta. Canadian Journal of Zoology 79:254–270.

Auth, T., T. Arula, E. Houde, and R. Woodland. 2020. Spatial ecology and growth in early life stages of bay anchovy Anchoa mitchilli in Chesapeake Bay (USA). Marine Ecology Progress Series 651:125–143.

Auth, T. D. 2003. INTERANNUAL AND REGIONAL PATTERNS OF ABUNDANCE, GROWTH, AND FEEDING ECOLOGY OF LARVAL BAY ANCHOVY (ANCHOA MITCHILLI) IN CHESAPEAKE BAY. University of Maryland College Park.

Baldwin, Carole C., Mounts, Julie H., Smith, David G., and Weigt, Lee A. 2009. Genetic identification and color descriptions of early life-history stages of Belizean Phaeoptyx and Astrapogon (Teleostei: Apogonidae) with comments on identification of adult Phaeoptyx.

Balvay, P. G. 1987. Equivalence parameters to estimate total abundance of zooplankton 49.

Beaugrand, G., K. M. Brander, J. Alistair Lindley, S. Souissi, and P. C. Reid. 2003. Plankton effect on cod recruitment in the North Sea. Nature 426:661–664.

Bernard, I., J.-C. Massabuau, P. Ciret, M. Sow, A. Sottolichio, S. Pouvreau, and D. Tran. 2016. In situ spawning in a marine broadcast spawner, the Pacific oyster *C rassostrea gigas* :

Timing and environmental triggers: Spawning in Oysters. Limnology and Oceanography 61:635–647.

Bi, R., and U. Sommer. 2020. Food Quantity and Quality Interactions at Phytoplankton–Zooplankton Interface: Chemical and Reproductive Responses in a Calanoid Copepod. Frontiers in Marine Science 7:15.

Bridgewater, R., and R. E. Schmidt. 1993. Diets of larval white perch and striped bass in the Kingston region of the Hudson River estuary with comments on the significance of the Bosmina bloom.

Bucklin, A., P. K. Lindeque, N. Rodriguez-Ezpeleta, A. Albaina, and M. Lehtiniemi. 2016. Metabarcoding of marine zooplankton: prospects, progress and pitfalls. Journal of Plankton Research 38:393–400.

Bucklin, A., K. T. C. A. Peijnenburg, K. N. Kosobokova, T. D. O'Brien, L. Blanco-Bercial, A. Cornils, T. Falkenhaug, R. R. Hopcroft, A. Hosia, S. Laakmann, C. Li, L. Martell, J. M. Questel, D. Wall-Palmer, M. Wang, P. H. Wiebe, and A. Weydmann-Zwolicka. 2021. Toward a global reference database of COI barcodes for marine zooplankton. Marine Biology 168:78.

Bucklin, A., D. Steinke, and L. Blanco-Bercial. 2011. DNA Barcoding of Marine Metazoa. Annual Review of Marine Science 3:471–508.

Bucklin, A., H. D. Yeh, J. M. Questel, D. E. Richardson, B. Reese, N. J. Copley, and P. H. Wiebe. 2019. Time-series metabarcoding analysis of zooplankton diversity of the NW Atlantic continental shelf. ICES Journal of Marine Science 76:1162–1176.

Butowski, N., and R. Morin. 2015. 2014 Fishery Managemant Plans. Report to the Legislative Committees, Maryland Department of Natural Resources Fisheries Service, Annapolis, MD.

Cabrol, J., G. Winkler, and R. Tremblay. 2015. Physiological condition and differential feeding behaviour in the cryptic species complex Eurytemora affinis in the St Lawrence estuary. Journal of Plankton Research 37:372–387.

Callahan, B. J., P. J. McMurdie, M. J. Rosen, A. W. Han, A. J. A. Johnson, and S. P. Holmes. 2016. DADA2: High-resolution sample inference from Illumina amplicon data. Nature Methods 13:581–583.

Campfield, P. A., and E. D. Houde. 2011. Ichthyoplankton community structure and comparative trophodynamics in an estuarine transition zone. Fishery Bulletin 109:1–19.

Cerco, C. F., and M. R. Noel. 2019. 2017 Chesapeake Bay Water Quality and Sediment Transport Model:580.

Chen, G., and M. P. Hare. 2008. Cryptic ecological diversification of a planktonic estuarine copepod, Acartia tonsa. Molecular Ecology 17:1451–1468.

Chen, G., and M. P. Hare. 2011. Cryptic diversity and comparative phylogeography of the estuarine copepod Acartia tonsa on the US Atlantic coast. Molecular Ecology 20:2425–2441.

Chesney, E. J. 2008. Foraging behavior of bay anchovy larvae, Anchoa mitchilli. Journal of Experimental Marine Biology and Ecology 362:117–124.

Chick, J. H., and M. J. V. A. N. D. E. N. Avyle. 2016. Zooplankton Variability and Larval Striped Bass Foraging : Evaluating Potential Match / Mismatch Regulation 9:320–334.

Childress, J. J., and B. A. Seibel. 1998. Life at Stable low Oxygen Levels: Adaptations of Animals to Oceanic Oxygen Minimum Layers. Journal of Experimental Biology 201:1223–1232.

Compson, Z. G., B. McClenaghan, G. A. C. Singer, N. A. Fahner, and M. Hajibabaei. 2020. Metabarcoding From Microbes to Mammals: Comprehensive Bioassessment on a Global Scale. Frontiers in Ecology and Evolution 8:581835.

Contreras, T., M. P. Olivar, P. A. Hulley, and M. L. Fernández De Puelles. 2019. Feeding ecology of early life stages of mesopelagic fishes in the equatorial and tropical Atlantic. ICES Journal of Marine Science 76:673–689.

Cushing, D. H. 1990. Plankton Production and Year-class Strength in Fish Populations: an Update of the Match/Mismatch Hypothesis. Advances in Marine Biology 26:249–293.

Darnell, R. M. 1958. Food Habits of Fishes and Larger Invertebrates of Lake Pontchartrain, Louisiana, an Estuarine Community. Pages 353–413 Institute of Marine Science.

Dauer, D. M., R. M. Ewing, G. H. Tourtellotte, and H. R. Barker. 1980. Nocturnal Swimming of Scolecolepides viridis (Polychaeta: Spionidae). Estuaries 3:148.

DeBoyd, S. L. 1977. A guide to marine coastal plankton and marine invertebrate larvae. Kendall/Hunt Publishing Company, Dubuque, Iowa, USA.

Dennerline, D. E., and M. J. Van Den Avyle. 2000. Sizes of prey consumed by two pelagic predators in US reservoirs: implications for quantifying biomass of available prey. Fisheries Research 45:147–154.

Detwyler, R., and E. D. Houde. 1970. Food selection by laboratory-reared larvae of the scaled sardine Harengula pensacolae (Pisces, Clupeidae) and the bay anchovy Anchoa mitchilli (Pisces, Engraulidae). Marine Biology 7:214–222.

Devreker, D., S. Souissi, G. Winkler, J. Forget-Leray, and F. Leboulenger. 2009. Effects of salinity, temperature and individual variability on the reproduction of Eurytemora affinis (Copepoda; Calanoida) from the Seine estuary: A laboratory study. Journal of Experimental Marine Biology and Ecology 368:113–123.

Dorfman, D., A. Mabrouk, L. Bauer, C. Clement, D. M. Nelson, and L. Claflin. 2016. Choptank Ecological Assessment: Digital Atlas- Baseline Status Report.

Downie, A. T., W. W. Bennett, S. Wilkinson, M. De Bruyn, and J. D. DiBattista. 2024. From land to sea: Environmental DNA is correlated with long-term water quality indicators in an urbanized estuary. Marine Pollution Bulletin 207:116887.

Durant, J., D. Hjermann, G. Ottersen, and N. Stenseth. 2007. Climate and the match or mismatch between predator requirements and resource availability. Climate Research 33:271–283.

Eldridge, M. B., J. A. Whipple, and M. J. Bowers. 1982. BIOENERGETICS AND GROWTH OF STRIPED BASS, MORONE SAXATILIS, EMBRYOS AND LARVAE. Fishery Bulletin 80:461–474.

Elliott, D. T., J. J. Pierson, and M. R. Roman. 2012. Relationship between environmental conditions and zooplankton community structure during summer hypoxia in the northern Gulf of Mexico. Journal of Plankton Research 34:602–613.

Elliott, D. T., J. J. Pierson, and M. R. Roman. 2013. Predicting the Effects of Coastal Hypoxia on Vital Rates of the Planktonic Copepod Acartia tonsa Dana. PLoS ONE 8.

Ershova, E. A., O. S. Wangensteen, R. Descoteaux, C. Barth-Jensen, and K. Præbel. 2021. Metabarcoding as a quantitative tool for estimating biodiversity and relative biomass of marine zooplankton. ICES Journal of Marine Science.

Favier, J.-B., and G. Winkler. 2014. Coexistence, distribution patterns and habitat utilization of the sibling species complex Eurytemora affinis in the St Lawrence estuarine transition zone. Journal of Plankton Research 36:1247–1261.

Fernando, A. V., K. B. Hecke, and M. A. Eggleton. 2018. Length, Body Depth, and Gape Relationships and Inference on Piscivory Among Common North American Centrarchids. Southeastern Naturalist 17:309–326.

Fisher, T. R., G. Breeze, and W. R. Boynton. 2014. Cultural eutrophication in the Choptank and Patuxent estuaries of Chesapeake Bay 51:435–447.

Folmer, O., M. Black, W. Hoeh, R. Lutz, and R. Vrijenhoek. 1994. DNA primers for amplification of mitochondrial cytochrome c oxidase subunit I from diverse metazoan invertebrates. Molecular Marine Biology and Biotechnology:6.

Fraser, A. J., J. R. Sargent, and J. C. Gamble. 1989. Lipid class and fatty acid composition of Calanus finmarchicus (Gunnerus), Pseudocalanus sp. and Temora longicornis Muller from a nutrient-enriched seawater enclosure. Journal of Experimental Marine Biology and Ecology 130:81–92.

Frøslev, T. G., R. Kjøller, H. H. Bruun, R. Ejrnæs, A. K. Brunbjerg, C. Pietroni, and A. J. Hansen. 2017. Algorithm for post-clustering curation of DNA amplicon data yields reliable biodiversity estimates. Nature Communications 8:1188.

Gao, X., H. Lin, K. Revanna, and Q. Dong. 2017. A Bayesian taxonomic classification method for 16S rRNA gene sequences with improved species-level accuracy. BMC Bioinformatics 18:247.

Gartz, R. 1999. Measurement of larval striped bass (Morone saxatilis) net avoidance using evasion radius estimation to improve estimates of abundance and mortality. Journal of Plankton Research 21:561–580.

Govoni, J. J. 2005. Fisheries oceanography and the ecology of early life histories of fishes: a perspective over fifty years. Scientia Marina 69:125–137.

Graça, M. A. S., L. Maltby, and P. Calow. 1993. Importance of fungi in the diet of Gammarus pulex and Asellus aquaticus I: feeding strategies. Oecologia 93:139–144.

Graeve, M., W. Hagen, and G. Kattner. 1994. Herbivorous or omnivorous? On the significance of lipid compositions as trophic markers in Antarctic copepods. Deep Sea Research Part I: Oceanographic Research Papers 41:915–924.

Harding, J. 1999. Selective feeding behavior of larval naked gobies Gobiosoma bosc and blennies Chasmodes bosquianus and Hypsoblennius hentzi:preferences for bivalve veligers. Marine Ecology Progress Series 179:145–153.

Hare, J. A. 2014. The future of fisheries oceanography lies in the pursuit of multiple hypotheses. ICES Journal of Marine Science 71:2343–2356.

Hartman, K. J., and S. B. Brandt. 1995. Predatory demand and impact of striped bass, bluefish, and weakfish in the Chesapeake Bay: applications of bioenergetics models. Canadian Journal of Fisheries and Aquatic Sciences 52:1667–1687.

Hensen. (n.d.). First reference to stempel pipette.

Hildebrand, S. F., and Wi. C. Schroeder. 1927. The Fishes of Chesapeake Bay. Bulletin of the US Bureau of Fisheries 43:1–366.

Hirai, J., K. Hidaka, S. Nagai, and Y. Shimizu. 2021. DNA/RNA metabarcoding and morphological analysis of epipelagic copepod communities in the Izu Ridge off the southern coast of Japan. ICES Journal of Marine Science:fsab064.

Hjort, J. 1914. Fluctuations in the great fisheries of northern Europe viewed in light of biological research. Rapports et procès-verbaux 20:237.

Houde, E. D. 1987. Fish Early Life Dynamics and Recruitment Variability. American Fisheries Society Symposium 2:17–29.

Houde, E. D. 2008. Emerging from Hjort's Shadow. Journal of Northwest Atlantic Fishery Science 41:53–70.

Hunt, G. L., K. O. Coyle, L. B. Eisner, E. V. Farley, R. A. Heintz, F. Mueter, J. M. Napp, J. E. Overland, P. H. Ressler, S. Salo, and P. J. Stabeno. 2011. Climate impacts on eastern Bering Sea foodwebs: A synthesis of new data and an assessment of the Oscillating Control Hypothesis. ICES Journal of Marine Science 68:1230–1243.

Ikeda, T., A. Yamaguchi, and T. Matsuishi. 2006. Chemical composition and energy content of deep-sea calanoid copepods in the western North Pacific.

Johnson, W. S., and D. M. Allen. 2012. Zooplankton of the Atlantic and Gulf coasts: a guide to their identification and ecology, second edition. Johns Hopkins University Press, Baltimore, Maryland USA.

Jørgensen, T. S., P. M. Jepsen, H. C. B. Petersen, D. S. Friis, and B. W. Hansen. 2019. Eggs of the copepod Acartia tonsa Dana require hypoxic conditions to tolerate prolonged embryonic development arrest. BMC Ecology 19:1.

Jung, S., and E. D. Houde. 2003. Spatial and temporal variabilities of pelagic fish community structure and distribution in Chesapeake Bay, USA. Estuarine, Coastal and Shelf Science 58:335–351.

Kattner, G., H. J. Hirche, and M. Krause. 1989. Spatial variability in lipid composition of calanoid copepods from Fram Strait, the Arctic. Marine Biology 102:473–480.

Kiljunen, M., H. Peltonen, M. Lehtiniemi, L. Uusitalo, T. Sinisalo, J. Norkko, M. Kunnasranta, J. Torniainen, A. J. Rissanen, and J. Karjalainen. 2020. Benthic-pelagic coupling and trophic relationships in northern Baltic Sea food webs. Limnology and Oceanography 65:1706–1722.

Kimmel, D. G., W. D. Miller, L. W. Harding, E. D. Houde, and M. R. Roman. 2009. Estuarine Ecosystem Response Captured Using a Synoptic Climatology. Estuaries and Coasts 32:403–409.

Kimmel, D., and M. Roman. 2004. Long-term trends in mesozooplankton abundance in Chesapeake Bay, USA: influence of freshwater input. Marine Ecology Progress Series 267:71–83.

Leray, M., N. Agudelo, S. C. Mills, and C. P. Meyer. 2013a. Effectiveness of Annealing Blocking Primers versus Restriction Enzymes for Characterization of Generalist Diets: Unexpected Prey Revealed in the Gut Contents of Two Coral Reef Fish Species. PLoS ONE 8:e58076.

Leray, M., N. Knowlton, and R. J. Machida. 2022. MIDORI2: A collection of quality controlled, preformatted, and regularly updated reference databases for taxonomic assignment of eukaryotic mitochondrial sequences. Environmental DNA 4:894–907.

Leray, M., J. Y. Yang, C. P. Meyer, S. C. Mills, N. Agudelo, V. Ranwez, J. T. Boehm, and R. J. Machida. 2013b. A new versatile primer set targeting a short fragment of the mitochondrial COI region for metabarcoding metazoan diversity: Application for characterizing coral reef fish gut contents. Frontiers in Zoology 10:1–14.

Limburg, K. E., and M. L. Pace. 1999. Growth, mortality, and recruitment of larval Morone spp. in relation to food availability and temperature in the Hudson River. Fisheries Bulletin 97:80–91.

Limburg, K. E., M. L. Pace, D. Fischer, and K. K. Arend. 1997. Consumption, Selectivity, and Use of Zooplankton by Larval Striped Bass and White Perch in a Seasonally Pulsed Estuary:15.

Lindeque, P. K., H. E. Parry, R. A. Harmer, P. J. Somerfield, and A. Atkinson. 2013. Next Generation Sequencing Reveals the Hidden Diversity of Zooplankton Assemblages. PLoS ONE 8:e81327.

Machida, R. J., H. Kurihara, R. Nakajima, T. Sakamaki, Y.-Y. Lin, and K. Furusawa. 2021. Comparative analysis of zooplankton diversities and compositions estimated from complement DNA and genomic DNA amplicons, metatranscriptomics, and morphological identifications. ICES Journal of Marine Science:fsab084.

Martino, E. J., and E. D. Houde. 2010. Recruitment of striped bass in Chesapeake Bay: Spatial and temporal environmental variability and availability of zooplankton prey. Marine Ecology Progress Series 409:213–228.

Mercer, L. 1989. Species profiles: Life histories and environmental requirements of coastal fishes and invertebrates (Mid-Atlantic). Page BR-82(11.109), TR-EL--82-4/82(11.109), 5479645.

Mercier, A., and J.-F. Hamel. 2010. Synchronized breeding events in sympatric marine invertebrates: role of behavior and fine temporal windows in maintaining reproductive isolation. Behavioral Ecology and Sociobiology 64:1749–1765.

Millette, N. C., D. K. Stoecker, and J. J. Pierson. 2015. Top-down control by micro- and mesozooplankton on winter dinoflagellate blooms of Heterocapsa rotundata. Aquatic Microbial Ecology 76:15–25.

Murphy, H. M., G. P. Jenkins, P. A. Hamer, S. E. Swearer, and M.-J. Rochet. 2012. Interannual variation in larval survival of snapper (*Chrysophrys auratus* , Sparidae) is linked to diet breadth and prey availability. Canadian Journal of Fisheries and Aquatic Sciences 69:1340–1351.

North, E. W., and E. D. Houde. 2001. Retention of White Perch and Striped Bass Larvae: Biological-Physical Interactions in Chesapeake Bay Estuarine Turbidity Maximum. Estuaries 24:756.

North, E. W., and E. D. Houde. 2003. Linking ETM physics, zooplankton prey, and fish early-life histories to striped bass Morone saxatilis and white perch M. americana recruitment. Marine Ecology Progress Series 260:219–236.

Nye, J. A., M. R. Baker, R. Bell, A. Kenny, K. H. Kilbourne, K. D. Friedland, E. Martino, M. M. Stachura, K. S. Van Houtan, and R. Wood. 2014. Ecosystem effects of the Atlantic Multidecadal Oscillation. Journal of Marine Systems 133:103–116.

O'Donnell, J. L., R. P. Kelly, N. C. Lowell, and J. A. Port. 2016. Indexed PCR primers induce template- Specific bias in Large-Scale DNA sequencing studies. PLoS ONE 11:1–11.

Olson, M. M., and K. G. Sellner. 2005. Zooplankton/Food Web Monitoring for Adaptive Multi-Species Management Near-term Recommendations. Page 85. Workshop report, Smithsonian Environmental Research Center.

Pagenkopp Lohan, K. M., R. Aguilar, R. DiMaria, K. Heggie, T. D. Tuckey, M. C. Fabrizio, and M. B. Ogburn. 2023. Juvenile Striped Bass consume diverse prey in Chesapeake Bay tributaries. Marine and Coastal Fisheries 15:e210259.

Pan, W., C. Qin, T. Zuo, G. Yu, W. Zhu, H. Ma, and S. Xi. 2021. Is Metagenomic Analysis an Effective Way to Analyze Fish Feeding Habits? A Case of the Yellowfin Sea Bream Acanthopagrus latus (Houttuyn) in Daya Bay. Frontiers in Marine Science 8:634651.

Pennak, R. W. 1953. Fresh-water invertebrates of the United States. The Ronald Press Company, New York, New York, USA.

Perplexity. 2024. Perplexity.ai (versions from January 2024 until January 2025) [Large language model]. https://www.perplexity.ai/

Piñol, J., G. Mir, P. Gomez-Polo, and N. Agustí. 2015. Universal and blocking primer mismatches limit the use of high-throughput DNA sequencing for the quantitative metabarcoding of arthropods. Molecular Ecology Resources 15:819–830.

Plough, L. V., C. Fitzgerald, A. Plummer, and J. J. Pierson. 2018. Reproductive isolation and morphological divergence between cryptic lineages of the copepod Acartia tonsa in Chesapeake Bay. Marine Ecology Progress Series 597:99–113.

Porter, T. M., and M. Hajibabaei. 2020. Putting COI Metabarcoding in Context: The Utility of Exact Sequence Variants (ESVs) in Biodiversity Analysis. Frontiers in Ecology and Evolution 8:248.

Questel, J. M., R. R. Hopcroft, H. M. DeHart, C. A. Smoot, K. N. Kosobokova, and A. Bucklin. 2021. Metabarcoding of zooplankton diversity within the Chukchi Borderland, Arctic Ocean: improved resolution from multi-gene markers and region-specific DNA databases. Marine Biodiversity 51:4.

Reaugh, M. L., M. R. Roman, and D. K. Stoecker. 2007. Changes in plankton community structure and function in response to variable freshwater flow in two tributaries of the Chesapeake Bay. Estuaries and Coasts 30:403–417.

Rilling, G. C., and E. D. Houde. 1999. Regional and temporal variability in distribution and abundance of Bay Anchovy (Anchoa mitchilli) eggs, larvae, and adult biomass in the Chesapeake Bay. Estuaries 22:1096–1109.

Robert, D., H. M. Murphy, G. P. Jenkins, and L. Fortier. 2014. Poor taxonomical knowledge of larval fish prey preference is impeding our ability to assess the existence of a “critical period” driving year-class strength. ICES Journal of Marine Science 71:2042–2052.

Roman, M. R., A. L. Gauzens, W. K. Rhinehart, and J. R. White. 1993. Effects of low oxygen waters on Chesapeake Bay zooplankton. Limnology and Oceanography 38:1603–1614.

Salcedo-Bauza, A. 2017, May. Zooplankton composition in Hampton Roads Virginia: spatio-temporal variability and DNA barcoding of COI gene. Hampton University.

Sargent, J. R., H. C. Eilertsen, S. Falk-Petersen, and J. P. Taasen. 1985. Carbon assimilation and lipid production in phytoplankton in northern Norwegian fjords. Marine Biology 85:109–116.

Schroeder, A., D. Stanković, A. Pallavicini, F. Gionechetti, M. Pansera, and E. Camatti. 2020. DNA metabarcoding and morphological analysis - Assessment of zooplankton biodiversity in transitional waters. Marine Environmental Research 160:104946.

Setzler, E. M., W. R. Boynton, K. V. Wood, H. H. Zion, L. Lubbers, N. K. Mountford, P. Frere, L. Tucker, and J. A. Mihursky. 1980. Synopsis of Biological Data on Striped Bass, Morone saxatilis (Walbaum). NOAA technical report NMFS circular, National Oceanic and Atmospheric Administration.

Setzler-Hamilton, E. M., P. W. Jones, G. E. Drewry, F. D. Martin, K. L. Ripple, M. Beaven, and J. A. Mihursky. 1982. A comparison of larval feeding habits among striped bass, white perch and clupeidae in the Potomac estuary. University of Maryland Center for Environmental and Estuarine Studies Chesapeake Biological Laboratory.

Sheridan, P. F. 1978. Food Habits of the Bay Anchovy, Anchoa mitchilli, in Apalachicola Bay, Florida. Northeast Gulf Science 2.

Shideler, A. C., and E. D. Houde. 2014a. Spatio-temporal variability in larval-stage feeding and nutritional sources as factors influencing striped bass (Morone saxatilis) recruitment success. Estuaries and Coasts 37:561–575.

Shideler, A. C., and E. D. Houde. 2014b. Spatio-temporal Variability in Larval-Stage Feeding and Nutritional Sources as Factors Influencing Striped Bass (Morone saxatilis) Recruitment Success. Estuaries and Coasts 37:561–575.

Shoji, J., E. W. North, and E. D. Houde. 2005. The feeding ecology of Morone americana larvae in the Chesapeake Bay estuarine turbidity maximum: the influence of physical conditions and prey concentrations. Journal of Fish Biology 66:1328–1341.

Siddon, E. C., T. Kristiansen, F. J. Mueter, K. K. Holsman, R. A. Heintz, and E. V. Farley. 2013. Spatial match-mismatch between juvenile fish and prey provides a mechanism for recruitment variability across contrasting climate conditions in the eastern Bering Sea. PLoS ONE 8.

Smithsonian Environmental Research Center. 2005. Zooplankton / Food-Web Monitoring for Adaptive Multi Species Management. Chesapeake Research Consortium.

Southwick Associates. 2019. The Economic Contributions of Recreational and Commercial Striped Bass Fishing. McGraw Center for Conservation Leadership, Fernandina Beach, FL.

Stribling, J. B., S. R. Moulton, and G. T. Lester. 2003. Determining the quality of taxonomic data. Journal of the North American Benthological Society 22:621–631.

Su, M., H. Liu, X. Liang, L. Gui, and J. Zhang. 2018. Dietary Analysis of Marine Fish Species: Enhancing the Detection of Prey-Specific DNA Sequences via High-Throughput Sequencing Using Blocking Primers. Estuaries and Coasts 41:560–571.

Sullivan, L. J., T. R. Ignoffo, B. Baskerville-Bridges, D. J. Ostrach, and W. J. Kimmerer. 2016. Prey selection of larval and juvenile planktivorous fish: impacts of introduced prey. Environmental Biology of Fishes 99:633–646.

The Maryland Department of Natural Resources, Tidewater Ecosystem Assessment Division. Eyes on the Bay (www.eyesonthebay.net)

Thorp, J. H. and A. P. Covich. 2001. Ecology and classification of North American freshwater invertebrates, second edition. Academic Press, San Diego, California, USA.

Uphoff, J. H. 1989. Environmental Effects on Survival of Eggs, Larvae, and Juveniles of Striped Bass in the Choptank River, Maryland. Transactions of the American Fisheries Society 118:251–263.

Uphoff, J. H. 2023. Perspective comes with time: What do long-term egg and juvenile indices say about Chesapeake Bay Striped Bass productivity? Marine and Coastal Fisheries 15.

Urrere, M. A., and G. A. Knauer. 1981. Zooplankton fecal pellet fluxes and vertical transport of particulate organic material in the pelagic environment. Journal of Plankton Research 3:369–387.

U.S. EPA. 2017. National Lakes Assessment 2017. Laboratory Operations Manual. V.1.1. EPA 841-B-16-004. U.S. Environmental Protection Agency, Washington, DC.

U.S. Geological Survey, 2016, National Water Information System data available on the World Wide Web (USGS Water Data for the Nation), accessed June 24, 2023, at http://waterdata.usgs.gov/nwis/

Vanalderweireldt, L., G. Winkler, M. Mingelbier, and P. Sirois. 2019. Early growth, mortality, and partial migration of striped bass (Morone saxatilis) larvae and juveniles in the St. Lawrence estuary, Canada. ICES Journal of Marine Science 76:2235–2246.

Vandeputte, D., G. Kathagen, K. D'hoe, S. Vieira-Silva, M. Valles-Colomer, J. Sabino, J. Wang, R. Y. Tito, L. De Commer, Y. Darzi, S. Vermeire, G. Falony, and J. Raes. 2017. Quantitative microbiome profiling links gut community variation to microbial load. Nature 551:507–511.

Verberk, W. C. E. P., D. T. Bilton, P. Calosi, and J. I. Spicer. 2011. Oxygen supply in aquatic ectotherms: Partial pressure and solubility together explain biodiversity and size patterns 92:1565–1572.

Vestheim, H., and S. N. Jarman. 2008. Blocking primers to enhance PCR amplification of rare sequences in mixed samples – a case study on prey DNA in Antarctic krill stomachs. Frontiers in Zoology 5:12.

Whitfield, A. K., M. Elliott, A. Basset, S. J. M. Blaber, and R. J. West. 2012. Paradigms in estuarine ecology – A review of the Remane diagram with a suggested revised model for estuaries. Estuarine, Coastal and Shelf Science 97:78–90.